Structural Connectivity of the Brain in Autism Spectrum Disorder

Clare Rachel Gibbard

Thesis submitted to University College London

in fulfilment of the requirements for the degree of

Doctor of Philosophy in Neuroscience

Developmental Imaging and Biophysics Section

UCL Institute of Child Health

2015

Declaration

The work presented in this thesis is the work of the author, Clare Rachel Gibbard. Where information has been derived from other sources, this has been indicated in the text.

Clare Rachel Gibbard

Abstract

Autism spectrum disorder (ASD) is a neurodevelopmental condition characterised by social communication deficits and restricted and repetitive interests. It mostly affects males, and has a range of severities and presentations. The causes of ASD are, as yet, unknown, though research indicates that a combination of genetic and environmental factors contribute to aberrant brain structure and function. The structure of the brain can be non-invasively assessed *in vivo* using magnetic resonance imaging (MRI). The MRI method diffusion tensor imaging (DTI) can be used to reconstruct the brain's white matter tracts and quantify their microstructural health.

The aim of this thesis is to investigate white matter microstructure in ASD, and comprises of four studies: an investigation of the association between white matter microstructure and the spectrum of ASD traits; a study of amygdala connections and their association with ASD symptomatology; a graph theory approach to investigate the structural networks of the brain; a study of sex-based differences in brain structure in ASD, and unaffected siblings of probands.

White matter microstructure was associated with ASD traits across a spectrum that incorporated healthy controls through to those with clinically-diagnosed autism. Associations between the microstructure of amygdala–cortical connections and ASD symptoms were dependent upon the brain region and ASD trait of interest. The ASD structural network was similar to that of controls, which indicates that the macromolecular arrangement of the ASD brain is relatively conserved. There were some sex-based differences in white matter microstructure in ASD, though fewer than anticipated.

In conclusion, DTI techniques provide evidence that brain microstructure is compromised in ASD, and that the severity of the structural deficits is correlated with symptom severity in a specific fashion. Brain topology is relatively conserved, indicating that ASD arises from deficits in the quality of brain connections, rather than their overall arrangement.

Acknowledgements

I would like to thank my supervisors Chris Clark, David Skuse, and Jonathan Clayden for their unwavering support and guidance throughout my studentship. I am very blessed to have had such an inspirational and generous supervisory team.

I am hugely indebted to UCL Grand Challenges for funding my studentship, and to the Yale-UCL Collaborative for financing my placement at Yale University. I am also very grateful to members of the ICH Postgraduate advisory and administrative teams for support and guidance during my studies.

Many thanks go to Juejing Ren, from the ICH Behavioural and Brain Sciences Unit, and research radiographer Tina Banks for participant scanning. I am grateful to everyone at the ICH Developmental Imaging and Biophysics Section for your advice and friendship over the past four years; it has been a great place to grow. Particular mentions are due to Kiran Seunarine and Fani Deligianni for their patience and expertise; Sally Dowsett for her joyfulness and kindness; and all my fellow PhD students for reassurance that we were in it together. Thank you also to Carla Startin and Sarah Osborne from the ICH Behavioural and Brain Sciences Unit.

I would also like to thank Kevin Pelphrey and his team - in particular Roger Jou, Brent Vander Wyk, Devon Oosting, and Charlotte Pretzsch - for so kindly welcoming me to Yale University. It was a brief, but truly enriching experience.

Lastly, but by no means least, thanks are due to my wonderful family and friends for their unstinting kindness, love, support, and encouragement. I have been a very lucky recipient of your companionship, and for that I will be eternally grateful.

'It is prosperity that gives us friends, adversity that proves them'

Proverb (source unknown)

Contents

List of Figures

List of Tables

Nomenclature

B_0 – static magnetic field

ω_0 – precessional frequency

γ – gyromagnetic ratio

ΔE – separation between energy levels

M_o – net magnetisation

X – magnetic susceptibility

B_1 – applied resonant magnetic field

t_p – duration of applied radiofrequency pulse

α - flip angle

J – flux. Net movement of molecules

D – diffusion coefficient

∇C – particle concentration gradient

G – diffusion gradient strength

δ – diffusion gradient duration

Δ – interval between diffusion gradients

b-value – degree of diffusion weighting

τ – diffusion time

ε_1, ε_2 and ε_3 – diffusion tensor eigenvectors

λ_1, λ_2 & λ_3 – diffusion tensor eigenvalues

mT – milliTesla

m – metre

mm – millimetre

ms – millisecond

Na^+ - sodium ion

K^+ - potassium ion

Ca^{2+} - calcium ion

Abbreviations

AAL – anatomical automatic labelling

AD – axial diffusivity

ADC – apparent diffusion coefficient

ADHD – attention deficit hyperactivity disorder

ADI – autism diagnostic inventory

ADOS – autism diagnostic observation schedule

APA – American Psychiatric Association

ASD – autism spectrum disorder

AQ – autism quotient

BA – Brodmann area

BBSU – Behavioural and Brain Sciences Unit

BRIEF – behaviour rating inventory of executive function

CARS – childhood autism rating scale

CC – corpus callosum

CDD – childhood disintegrative disorder

CELF – clinical evaluation of language fundamentals

CR – corona radiata

CSD – constrained spherical deconvolution

CSF – cerebrospinal fluid

DD – developmentally delayed

DI – developmentally impaired

DICOM – digital imaging and communications in medicine

DSI – diffusion spectrum imaging

DSM – Diagnostic and Statistical Manual of Mental Disorders

DTI – diffusion tensor imaging

EPI – echo planar imaging

FA – fractional anisotropy

FDR – false discovery rate

FID – free induction decay

FLASH – fast low angle shot

fMRI – functional magnetic resonance imaging

FOV – field of view

FSL – FMRIB software library

FT – Fourier transformation

FWE – family wise error

GABA - γ-aminobutanoic acid

GARS – Gilliam autism rating scale

GFA – generalised fractional anisotropy

G_{FE} – frequency-encoding gradient

GOSH – Great Ormond Street Hospital

G_{PE} – phase-encoding gradient

G_{RO} – readout gradient

G_{SS} – slice-selective gradient

HFA – high functioning autism

HR – high risk

IC – internal capsule

ICH – Institute of Child Health

ICD – International Classification of Diseases

IFOF – inferior fronto-occipital fasciculus

ILF – inferior longitudinal fasciculus

IQ – intelligence quotient

L - left

LFA – low functioning autism

LR – low risk

MD – mean diffusivity

MNI – Montreal Neurological Institute and Hospital

MR – magnetic resonance

MRI – magnetic resonance imaging

NIfTI – neuroimaging informatics technology initiative

NMR – nuclear magnetic resonance

PCA – principal component analysis

PDD – principal diffusion direction

PDD-NOS – pervasive developmental disorder not otherwise specified

PGSE – pulsed gradient spin echo

PTR – post thalamic radiation

R - right

RD – radial diffusivity

RF – radiofrequency

ROI – region of interest

SFOF – superior fronto-occipital fasciculus

SLF – superior longitudinal fasciculus

SLI – specific language impairment

SNR – signal-to-noise ratio

SPM – statistical parametric mapping

SRS – social responsiveness scale

SSRI – selective serotonin re-uptake inhibitor

T - Tesla

T_1 – spin-lattice relaxation time

T_2 – spin-spin relaxation time

TBSS – tract-based spatial statistics

TD – typically developing

TE – echo time

TFCE – threshold-free cluster enhancement

TI – inversion time

TR – repetition time

UCL – University College London

UF – uncinate fasciculus

VABS – Vineland adaptive behaviour scale

VBM – voxel-based morphometry

WASI – Wechsler abbreviated scale of intelligence

WHO – World Health Organisation

Chapter 1 Autism Spectrum Disorder and Brain Anatomy

This chapter provides an introduction to autism spectrum disorder (ASD), including symptoms, aetiology, and commonly used intervention strategies. ASD is thought to arise from altered neurological development, and the focus of this thesis is the investigation of brain structure in ASD, so an overview of brain anatomy and major theories regarding the brain in ASD are provided here.

1.1 Autism Spectrum Disorder

1.1.1 Brief History

The term autism (from the Greek *'autos'*, meaning *'self'*) was first used in 1910 to describe a subset of schizophrenia patients who were very withdrawn [1]. Autism was first recognised as a syndrome by Kanner in 1943 [2], who identified it as a behavioural condition that began in childhood and was characterised by a desire for solitude, and inflexibility. This was followed in 1944 by Asperger's description of a condition that shared the same features as autism [3], often referred to as Asperger's syndrome. However, autism wasn't entered into official manuals for the diagnosis of psychiatric conditions – the World Health Organization (WHO)'s international classification of diseases (ICD) and the American Psychiatric Association (APA)'s diagnostic and statistical manual of mental disorders (DSM) – until 1978 [4] and 1980 [5], respectively.

Subsequent to the first descriptions of autism and Asperger's syndrome, a spectrum of traits has been reported [6] that encompasses a wide range of symptoms and severities. A great deal of debate has surrounded the question of whether this autistic spectrum reflects one syndrome with a common pathology, or a collection of several different syndromes. Current consensus is that the autistic spectrum encompasses a group of related disorders that have an allied pathology and similar

presentations. A diagnosis of ASD amalgamates prior descriptions of autism and Asperger's syndrome into a core set of difficulties that may be associated with accompanying features, and has different tiers of severity.

1.1.2 Current Diagnostic Criteria

Current diagnostic criteria for ASD were defined in 1994 by the WHO in the 10th edition of the ICD manual (ICD-10) [7] (see Appendix A: ICD-10 Diagnostic Criteria), and in 2013 by the APA in the 5th edition of the DSM (DSM-V) [8] (see Appendix B: DSM-5). A revised version of the ICD (ICD-11) is anticipated in 2017 [9]. The diagnostic criteria outlined below are based on those of the DSM-V.

ASD is diagnosed upon presentation of a dyad of core symptoms: persistent deficits in social interaction and communication, in addition to repetitive and/or stereotyped behaviours. Symptoms must be present during early development, cause significant impairment in current functioning, and should not be better captured by a diagnosis of intellectual disability or developmental delay. A diagnosis of ASD is supplemented with a specification of current severity in each of the two symptom domains, and information stating whether the ASD is accompanied by: intellectual impairment; language impairment; a known medical/genetic condition or environmental factor; another neurodevelopmental, mental or behavioural disorder; and/or catatonia. There is a strong relationship between intellectual disorder and ASD, and many individuals diagnosed with ASD have accompanying intellectual difficulties.

Impairments in social communication include a) deficits in social and emotional reciprocity, such as difficulty maintaining back-and-forth conversation, and inappropriate responses during social interactions, including fewer person-directed social overtures; b) impairments in non-verbal communications used during social

interaction, for example gestures, eye contact, and person-directed facial expressions; and c) difficulties in the development, maintenance, and understanding of relationships.

The restricted and/or repetitive behaviours and interests that manifest in ASD are varied, but are typically: a) stereotyped or repetitive movements (including flapping), use of objects (e.g. lining objects up), or speech (such as echolalia – repeating other people's vocalisations – and idiosyncratic phrasing); b) Inflexible adherence to routines, insistence of sameness, and difficulty switching between tasks; c) highly restricted and fixated interests and patterns of thinking; d) hyper- or hypo-reactivity to sensory stimuli, and excessive interest in, or exploration of, sensory aspects of the environment (such as licking objects or fascination with lights or reflections).

Several other traits are regularly described in individuals with ASD. These include imagination deficits, physical clumsiness, abnormal prosody of speech, reduced cognitive processing speed (particularly in social situations), and disturbed sleep patterns. Difficulties with eating, mainly related to restricted food preferences and sensitivity to appearance, taste, texture, and smell, are often seen. Aggression and irritability can occur, often due to frustration, a lack of comprehension, or reduced inhibition when in a state of physiological arousal.

Many individuals diagnosed with ASD without accompanying intellectual impairment, often termed high-functioning ASD, have the mental acuity to live a relatively 'normal' life, with education and the ability to carry out some form of work within their grasp. This can disguise real difficulties with the core features of ASD, and raise questions regarding *how* and *when* the boundary between clinical

syndrome and 'eccentricities' of behaviour as part of normal variation should be delineated; ASD is a spectrum, but the breadth of the phenotype is often unclear.

Several conditions are sometimes included in the atypical ASD category. These include childhood disintegrative disorder (CDD), a very rare condition characterised by a sudden regression and loss of acquired skills, and Rett's syndrome, a condition similar to CDD found only in girls.

1.1.3 Diagnostic Tools

Several tools are employed clinically to help determine whether diagnostic criteria are met. The aim of each diagnostic tool is to explore the limits of an individual's capabilities in each of the main ASD traits, and thus expose any difficulties. A final diagnosis is usually only made after several interactions between clinical staff, including psychiatrists and psychologists, and the individual, in addition to discussion with caregivers and teachers. The most commonly used instruments are the autism diagnostic interview (ADI) [10], a semi-structured interview with the individual's primary care-givers, and the autism diagnostic observation schedule (ADOS) [11], a guided observation and interaction with the individual. The developmental, dimensional and diagnostic interview (3di) [12] is a computer-based tool used to assess ASD traits dimensionally (i.e. with reference to the spectrum) following interviews with primary care givers, and emulates ADI diagnostic algorithm scores.

1.1.4 Co-morbidities

The presence of co-existing conditions is common in ASD, and suggests that some of the causes of ASD correspond to those of other neurodevelopmental conditions, and that ASD confers vulnerability to these conditions and *vice versa*. Common co-morbidities are: epilepsy [13], depression, anxiety, attention deficit hyperactivity

disorder (ADHD), and conduct disorders [14]. Some of these co-morbid difficulties arise due to limitations in understanding social situations, feelings of isolation, and hypersensitivity/heightened arousal. Tourette's syndrome is also common in individuals with ASD [15]. Turner syndrome affects women and is associated with elevated incidence of ASD [16]. A sub-population of fewer than 10% of individuals diagnosed with ASD has exceptional memory or other remarkable but isolated abilities, known as savant skills, in disciplines such as mental arithmetic, art, and music [17][18].

1.1.5 Epidemiology

Recent studies suggest that ASD affects approximately 1% of the population, with prevalence rates of 1 in 63 [19], 1 in 102 [20], and 1 in 68 [21] reported in recent years. This is a huge increase compared to the first estimate of 0.045% (a prevalence rate of 1 in 2,222) in 1966 [22]. In 1999, Gillberg and Wing estimated that non-US prevalence rates had increased by 3.8% per year since 1966 [23]. Several explanations for the rise in ASD cases have been expounded: firstly, the diagnostic criteria for autism have expanded from the discrete condition described by Kanner to include a spectrum of cases. This has greatly increased the number of individuals encapsulated by a diagnosis of an ASD [24]. Advances in awareness and expert clinical support have also contributed to the rise in diagnosis rates. Advanced parental age has also been identified as a potential factor in the rising number of in ASD cases [25]. A contrasting theory is that the rise in cases is a reflection of increased opportunity for individuals with high-functioning ASD for employment [26] and procreation [27].

ASD is more common in males than females, with an average ratio of 4 males:1 female reported [28]. This sex ratio is higher for high-functioning ASD, with estimates rising to 8:1 [7]. The cause of the disparity in diagnosis rates between the sexes is not known for certain. It may be due to male susceptibility to X-linked

conditions (see section 1.1.6) or explained by the 'male brain' hypothesis [29] (see section 1.3.9), which states that ASD is a result of excessively male characteristics of behaviour, brain structure and function. Some studies suggest that for females to be diagnosed with ASD they must have experienced greater genetic anomalies, hence more severe neurodevelopmental impairment, than males diagnosed with ASD [30] (discussed in more detail in Chapter 8). However, a major proportion of the sex ratio is likely to reflect inadequacies in current diagnostic criteria [31], and difficulty identifying the different ways ASD presents in females; for example, females with an ASD often display different types of restricted and repetitive behaviours [32][33], greater ability to form friendships [34] in comparison with males with ASD.

1.1.6 Aetiology

ASD is a neurodevelopmental disorder, which means that symptoms are thought to arise as a result of abnormalities in brain structure and function during development. The cause of these brain modifications and the associated ASD phenotype is unknown. It is likely that a combination of genetic susceptibilities and environmental triggers contribute to its development. The heterogeneity observed in individual presentations of ASD symptoms and their severity may be due to differences in the underlying pathology; for example, the exact combination of over- or under-expressed genes may differ from case to case.

Recent twin studies estimate ASD heritability to range between 50% and 95% [35][36]. Increased likelihood of ASD or a 'broader autism phenotype' of ASD-related cognitive and/or social difficulties has been described in both twin [37][38] and family studies [39]. Children are more likely to have ASD if a sibling has already been diagnosed [40]. No single gene or chromosomal abnormality has been shown to selectively cause ASD. The range of autistic phenotypes and symptom severities, including traits in the general population, indicates that a certain proportion of autistic behaviours are triggered by genetic mutations (including

deletion, duplication, and replication errors) and another proportion by the complex interplay of single nucleotide polymorphisms that occur throughout the population as part of natural variation [41]. Genes involved in neural connectivity, social and emotional responsiveness, and sex hormone regulation are thought to be involved in ASD [42]. A particular area of interest is functional variation among genes involved in synaptic transmission [43][44], which affects the speed and coherence of information transfer within the brain. Genes involved in the regulation of transcription and post-translational modification have also been implicated in ASD [45], suggesting that, to some extent, the disorder can be associated with changes in the frequency with which certain genes are translated into proteins, and modifications following gene translation, in addition to mutations within the genetic code itself.

The increased prevalence of ASD in males relative to females is suggestive of a male vulnerability that may be conferred by X-chromosome abnormalities [46]. Males only have one copy of the X chromosome, which means that they are particularly vulnerable to any mutated or defective X-chromosome genes because they are homozygous for these genes, and therefore do not have a healthy reserve; hence the likelihood of X-linked disorders in males is increased. Genes on the X chromosome associated with ASD include those involved in neural connectivity and intracellular signalling pathways [47][48][49]. X-chromosome deletions in females are also associated with increased incidence of autistic traits [50].

Environmental risk factors for ASD are the subject of contentious debate. A great deal of anguish was caused by the early theory that ASD is caused by unemotional parenting [2][51], a concept that rapidly gained notoriety as the 'refrigerator mother' theory. Attention on environmental factors has since concentrated on foetal development, including prenatal exposure to high levels of testosterone [52], stress [53] and atmospheric pollutants [54]. It has been proposed that these early

exposures alter brain growth and neurochemistry, leading to the development of ASD. Epigenetic modifications of genes have also been implicated in ASD, which could be evidence that there is a link between environmental influences and genetic susceptibility [55].

1.1.7 Biological Markers

The search for biomarkers (variables associated with a condition that are measurable within the affected individual) and endophenotypes (heritable characteristics associated with a condition in the affected individual, but also observed to an extent in related family members) of ASD is important because findings have implications for diagnosis, identification of the origins of ASD, and for the assessment of potential treatments. Major concerns with biomarker research are the extent to which features are specific to ASD, easily measurable, and are representative of the severity of ASD. Findings are varied (for a recent review see [56]), although research suggests that impaired mitochondrial metabolism [57][58], abnormal concentrations of the neurotransmitter serotonin [59], melatonin (a hormone that regulates circadian rhythms) [60], and oxytocin (a bonding hormone) [61], and altered brain electrophysiology [62] are relatively consistent markers in ASD. Brain imaging techniques are beginning to identify neurological biomarkers of ASD (discussed in Chapter 3).

Macrocephaly has been reported in roughly a quarter of individuals with ASD [63][64][65]. Macrocephaly in individuals with ASD is more likely to occur in younger age groups than in adulthood [63][37]. Relatively large head sizes have also been measured in un-affected family members of autistic probands [65][66][67]. However, recent work suggests that the incidence of macrocephaly in ASD may have been exaggerated by inadequate reference measurements [68][69]. In addition, studies have suggested that the relationship between head circumference and

clinical outcome in ASD is complex [70], and that head circumference is more strongly related to genetic ancestry, height and age than with ASD status [71].

1.1.8 Management and Interventions

There is no cure for ASD, and it is usually a life-long condition. The prognosis is better for individuals with milder autistic symptoms and higher IQ [72][73]. Autistic symptoms can be improved by the consistent application of management practices, such as behavioural intervention, social skills training, and cognitive behavioural therapy [74]. Rapid improvements in response to behavioural intervention are correlated with positive treatment outcomes [75]. Behavioural training with family members and at school is beneficial in maintaining improvements outside of the clinic. Co-existing conditions, such as epilepsy, negatively impact on prognosis [76]. Therefore, the management of co-existing conditions using medication and cognitive therapies can provide a great deal of relief. Individuals with speech impairments often benefit from speech and language therapy. As an individual with ASD matures, appropriate guidance for safely navigating the adult world – including advice on relationships, use of social media, and looking after finances – can help to reduce vulnerability.

Presently there is no medication to treat the core social and communication deficits in ASD. Current pharmacotherapies typically focus on the alleviation of co-occurring conditions and the management of stereotypical behaviours: antipsychotics and tranquilisers are often effective against irritability, aggression and stereotypy, and selective serotonin re-uptake inhibitors (SSRIs) are often used in the management of anxiety and repetitive behaviours [77][78]; however, use of these medications is not often recommended, particularly in children. Oxytocin is emerging as a promising hormonal treatment for ASD [79][80], although caution has to be maintained in lieu of large-scale clinical trials [81]. Much interest has developed around the potential of alternative treatments for the alleviation of ASD

symptoms, including dietary restriction/supplementation, yeast treatment, osteopathy, dance and music therapy, holding therapy, and animal therapy. However, there is currently a lack of scientific evidence for the utility of such treatments in ASD.

It is important to consider the effects of ASD on those around the affected individual; parents are typically subject to high levels of emotional distress and upheaval, and un-affected siblings may feel marginalised by the attention their affected brother or sister receives. Professional and peer support is invaluable in providing outlets and coping strategies.

In a very small number of cases, autistic behaviours are completely ameliorated [82]. The causes of these rare recoveries from ASD are unknown; early misdiagnosis may be a factor as evidence indicates that diagnoses are relatively stable [74].

1.2 The Brain

As stated in section 1.1, ASD is a neurodevelopmental disorder and the brain is heavily implicated in both the development and maintenance of ASD. The brain is responsible for conscious thought, interpretation of sensory inputs, memory, the orchestration of movement, and numerous automatic responses. The work described in this thesis focuses on understanding the complex network of brain connections that are thought to underlie autistic behaviours. This section provides an overview of the brain, from its microstructure through to its macromolecular anatomy.

1.2.1 Neurons

The brain consists of several cell types, each specialised for a particular function. Glial cells make up the majority of cells in the brain, and play a variety of important roles in the maintenance of the brain. For example, astrocytes provide structural and metabolic support to neurons, and oligodendrocytes insulate the axons of neurons via the myelin sheath.

Neurons are responsible for the processing power of the brain, transmitting information in the form of nerve signals at high speeds. Most neurons in the brain are interneurons, which facilitate rapid information flow via circuits with other neurons. As shown in Figure 1, neurons consist of a cell body which houses the majority of the organelles, including the nucleus, and a long thin projection called the axon, which is insulated by the myelin sheath. The cell body is surrounded by dendrites which receive signals from neighbouring neurons, whilst the axon finishes in a set of terminal branches which relay incoming signals to other neurons across the synapse.

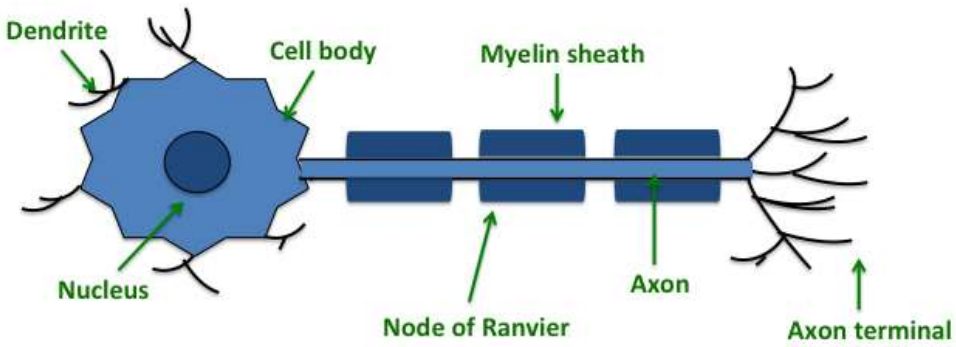

Figure 1 A neuron.

1.2.2 Information Relay

Signals, or impulses, pass along the axon of a neuron from the dendritic inputs through to the axon terminal outputs. This axonal information flow is mediated by rapid changes in the electrical potential of the cell, mediated by the movement of

electrically-charged ions across the semi-permeable membrane. This is known as an action potential. At rest, an axon's membrane is polarised – it has a negative charge on the inside and a positive charge on the outside – due to high levels of positively-charged sodium ions (Na^+) in the extracellular space and the movement of positively-charged potassium (K^+) ions out of the cell via leak channels. The incoming signal is a stimulus that causes voltage-gated sodium channels to open in the neighbouring portion of the axonal membrane. This allows the Na^+ ions to rush into that part of the cell (attracted by the negative charge), thus increasing the concentration of positively-charged ions inside and depolarising the membrane. Once the depolarisation has passed a threshold, the sodium channels close and voltage-gated potassium channels open allowing the K^+ ions to flow out of that section of the cell (repelled by the now-positive charge within), re-polarising the cell membrane. This action potential induces another action potential in the adjacent portion of the axon, thus relaying the impulse to the axon terminals. The process is accelerated via the presence of the myelin sheath, which insulates the axon membrane aside from regularly-spaced gaps called nodes of Ranvier. The myelin sheath causes the action potential to transit very quickly from node to node in a process called saltatory conduction, as shown in Figure 2.

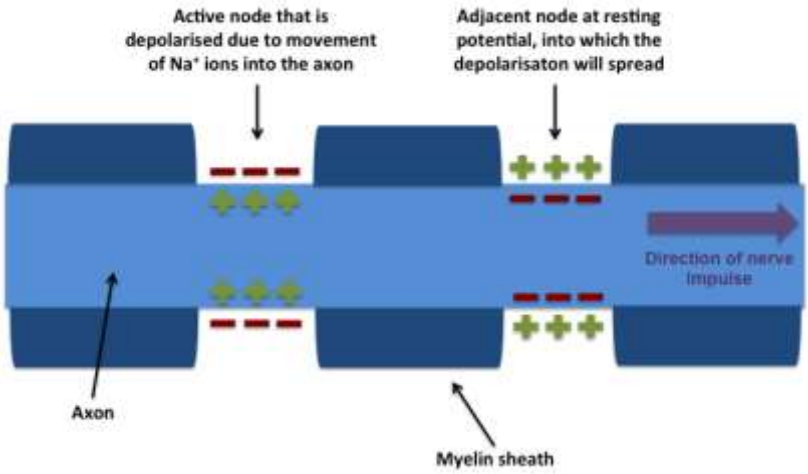

Figure 2 An action potential passing along an axon via saltatory conduction.

In order to relay the nerve impulse from the axon terminal to a neighbouring axon, the signal has to traverse the synapse. When the action potential arrives at the axon terminal, otherwise known as the pre-synaptic terminal, it stimulates voltage-gated calcium channels to open, allowing the influx of calcium (Ca^{2+}) ions. The Ca^{2+} ions stimulate the fusion of vesicles containing neurotransmitters to the pre-synaptic membrane followed by exocytosis, which releases the neurotransmitters into the synapse. The neurotransmitters bind to specific receptors on the membrane of the neighbouring axon, known as the post-synaptic membrane, thus relaying the impulse to the next neuron (see Figure 3). There are many different neurotransmitters including peptides, small molecules, amino acids, and soluble gases. The neurotransmitter employed by a neuron depends upon the action required. For example, γ-aminobutanoic acid (GABA) is used to send inhibitory messages, whilst dopamine is an excitatory neurotransmitter.

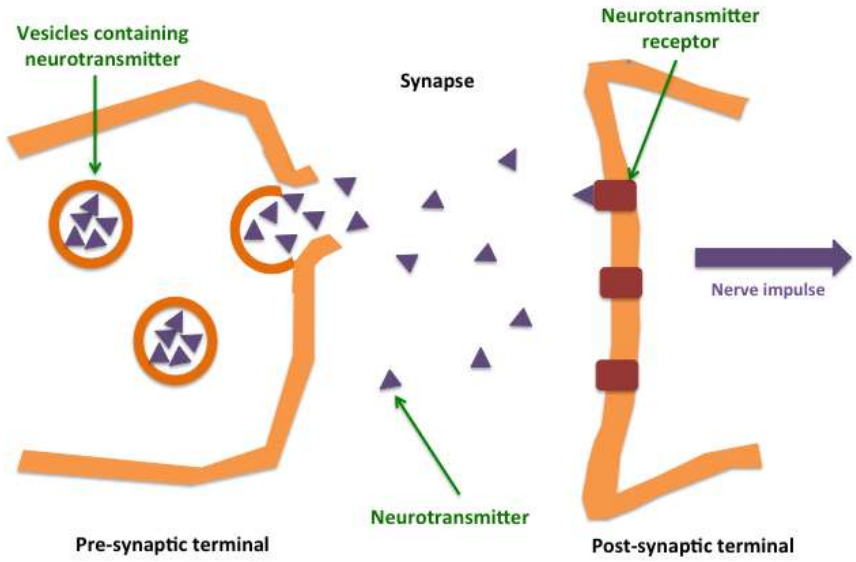

Figure 3 Synaptic transmission.

1.2.3 Brain Anatomy

As shown in Figure 4, the brain is divided into two hemispheres, and composed of three main parts: the cerebrum (or forebrain), the cerebellum (or hindbrain) which is involved in movement and balance, and the brainstem which connects to the spinal

cord and regulates many autonomic functions. Cerebrospinal fluid (CSF) resides in the spaces, or ventricles, of the brain, and provides multiple functions, including physical protection, pressure regulation, and waste clearance. The meninges and the skull further safeguard the brain, and the blood-brain barrier affords protection against infection by restricting the transfer of blood-borne particles into the brain.

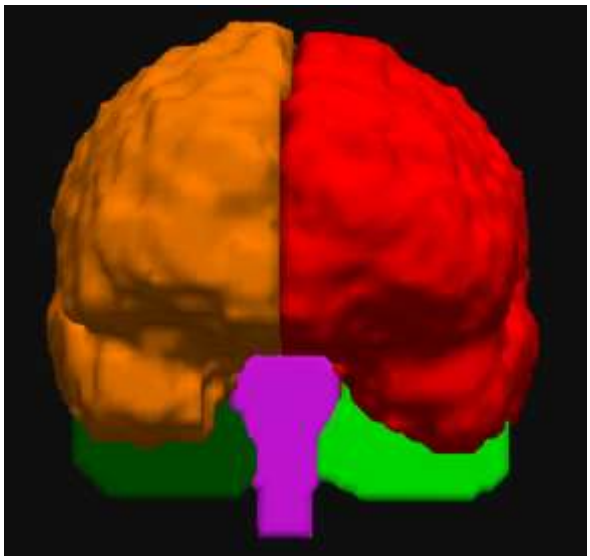

Figure 4 The human brain.

The cerebrum is shown in red/orange, the cerebellum in green/dark green, and the brainstem in magenta. Note the two hemispheres.

1.2.3.1 Cerebral Grey Matter

In the cerebrum, neurons in the brain are arranged in an ordered fashion, such that their cell bodies reside in the outer layer of the brain, known as the cerebral cortex, and in the central portion of the brain, known as the sub-cortex. The cerebral cortex is folded into gyrae and sulci, thus increasing the surface area and packing potential of the brain. Axons project from the brain's cortices. The cortices appear grey and the axons appear white due to the presence of myelin, hence the terms grey matter and white matter, respectively. The cell bodies in the grey matter group into cohesive regions, which are known to perform particular brain functions. As proposed by Brodmann [83], among others, the grey matter in the cerebral cortex (often called the cortical grey matter), can be sub-divided into many small

functional regions on the basis of their cytoarchitecture (see Figure 5). Cortical regions that are adjacent to one another have been grouped into lobes (see Figure 6). The frontal lobe is believed to engender impulse control and decision-making; the parietal lobe integrates sensory and motor functions; the occipital lobe processes visual stimuli; and the temporal lobe handles auditory, olfactory, and complex emotional stimuli. The insula cortex is often designated as a lobe, and is associated with several functions including perception.

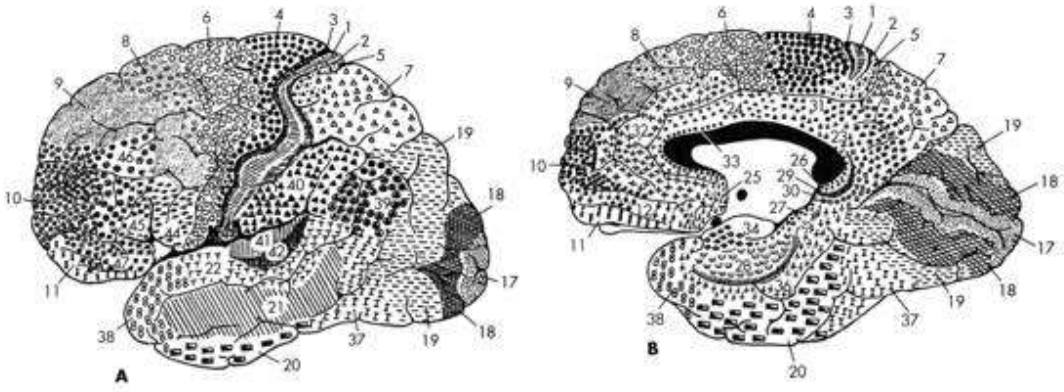

Figure 5 Regions of the cortex as identified by Brodmann.
Lateral (A) and medial (B) surfaces are shown (adapted from [83]**).**

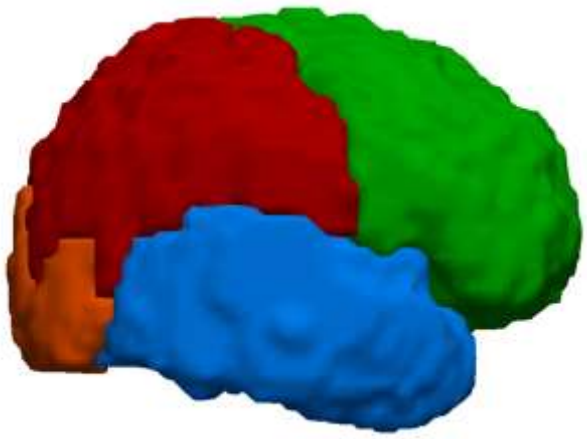

Figure 6 The lobes of the brain.
The frontal lobe is shown in green, the parietal lobe in red, the occipital lobe in orange, and temporal lobe in blue.

The subcortical grey matter regions are shown in Figure 7. The thalamus is a hub, mediating information transfer between brain regions. The caudate and the putamen together form the striatum which, along with the globus pallidus, is associated with fine motor control. The nucleus accumbens is thought to be involved in reward; the hippocampus is critical for spatial navigation and memory; and the amygdala is central to emotional processing.

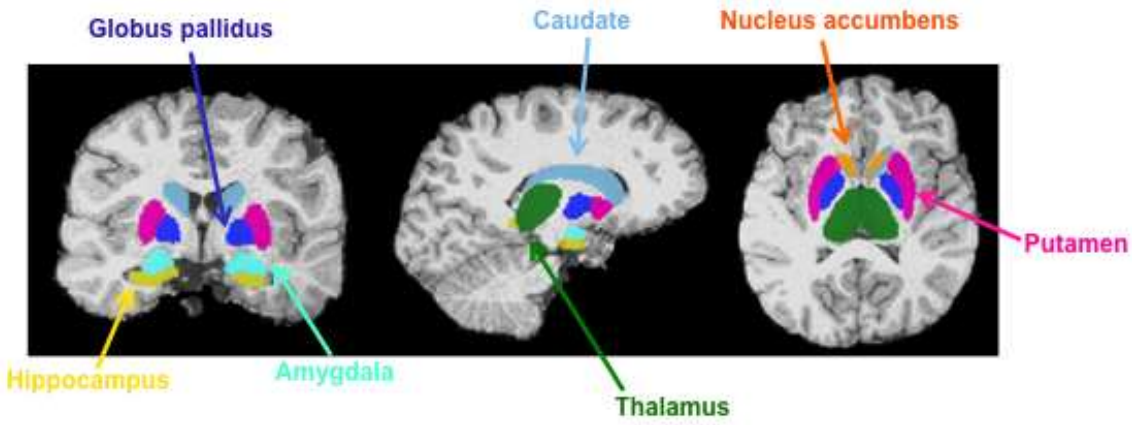

Figure 7 Subcortical grey matter regions of the brain.

The amygdala (cyan), caudate (light blue), globus pallidus (dark blue), hippocampus (yellow), nucleus accumbens (orange), putamen (magenta), and thalamus (green) are shown. The caudate and putamen form the striatum.

The limbic lobe is thought to be responsible for many emotional and olfactory functions. The exact complement of structures comprising the limbic lobe are subject to debate [84], although both cortical and subcortical grey matter structures are known to be involved (see Figure 8).

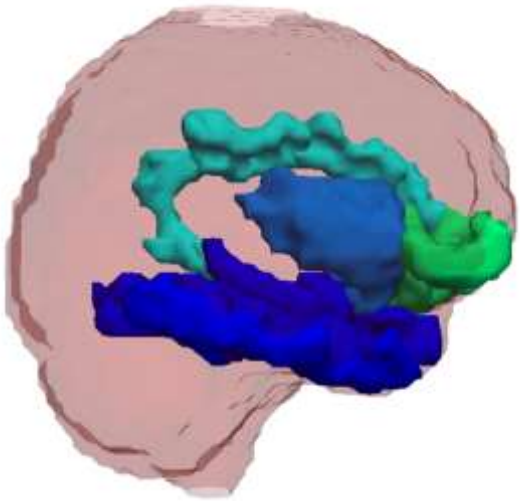

Figure 8 The limbic lobe.

The frontal lobe (green) and temporal lobe (dark blue) structures are shown in addition to the cingulum (turquoise), and the insula (mid blue).

1.2.3.2 Cerebral White Matter

Grey matter regions in the cerebrum are structurally linked by white matter tracts. White matter tracts consist of bundles of myelinated axons and are responsible for the flow of information via action potentials and synaptic transmission, as outlined in section 1.2.2. There are several major white matter tracts in the brain, each connecting different grey matter regions [85] as shown in Figure 9. The corpus callosum is the largest tract and connects the two hemispheres of the brain, along with the smaller anterior and posterior commissures. The cingulum is adjacent to the corpus callosum and curves between the frontal and temporal lobes; the arcuate fasciculus also connects frontal, parietal and temporal lobe structures. The inferior longitudinal fasciculus (ILF) and the inferior fronto-occipital fasciculus (IFOF) connect the occipital and temporal lobes. The uncinate fasciculus joins the anterior temporal lobe and the inferior frontal lobe. The corticospinal tract connects the motor regions of the cortex to the brain stem, whilst the corona radiata and internal capsule join subcortical structures to the frontal and parietal cortices, and the fornix links the medial temporal lobe with the hypothalamus.

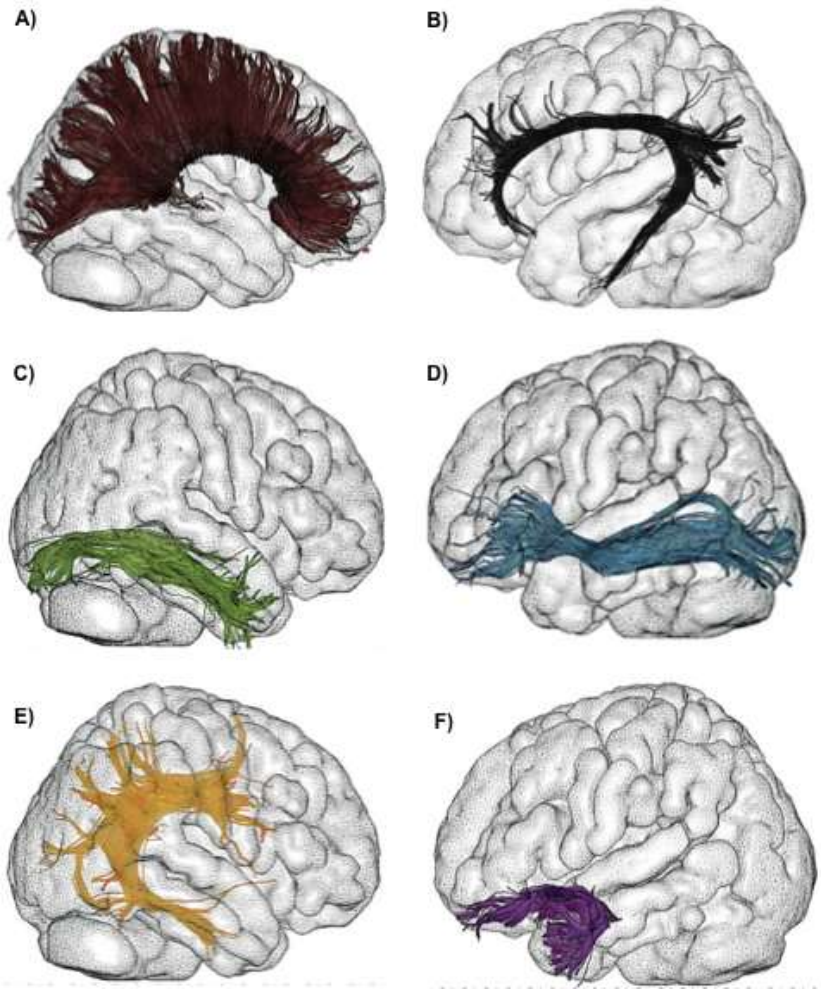

Figure 9 The major white matter tracts of the brain.

Adapted from [85]**, showing A) the corpus callosum, B) the cingulum, C) the inferior longitudinal fasciculus, D) the inferior fronto-occipital fasciculus, E) the arcuate fasciculus, and F) the uncinate fasciculus.**

1.2.4 Brain Development

ASD is thought to arise from abnormalities in the development of the brain. During the first few years of life, the brain grows rapidly. Much of this growth occurs due to the proliferation of glial cells, including those that myelinate the white matter [86]. The neurons in the brain make an increasing number of synaptic connections during early development. However this is followed by synaptic pruning which

takes place up until adolescence, in which the plethora of synaptic connections is trimmed back as a consequence of competitive selection; pruning results in the loss of connections that are weak and relatively under-utilised, and the reinforcement and strengthening of those connections that are regularly accessed. In ASD, research suggests that pruning is limited [87] and that brain connections develop atypically [88].

1.3 Theories of ASD

A plethora of theories have been published hypothesising the cognitive and neural processes that underpin ASD symptomatology. Several of the theories are described below. To date, no single concept provides a comprehensive and concrete explanation of ASD. It may emerge that a combination of these theories best describes the neural processes that predispose ASD; since there is heterogeneity in symptom presentation within the autistic spectrum, it is likely that there is a distribution of the severity and type of neural changes that are associated with these symptoms.

1.3.1 Disconnection - synaptic transmission

The synaptic transmission theory states that ASD is caused by a reduction in the efficiency of information transfer within the brain. It is thought that symptoms arise due to a combination of synapse malfunction (for example, imbalance of excitatory and inhibitory transmission; impaired vesicular transport; reduced plasticity) [88] and a reduction in synaptic pruning [87], both of which lead to inefficient, inappropriate, and/or unnecessary connections within the brain. Rapid value judgements need to be made in social situations – for example, whether another individual poses a threat – and it is thought that poor flow of information in the brain reduces the ability of individuals with ASD to process and integrate social stimuli. A recent study provided evidence for this theory: in a mouse model with

reduced synaptic pruning and ASD-like symptoms, activation of neuronal autophagy rectified synaptic pathology and reduced the incidence of ASD-like social behaviour deficits [87]. A recent review summarised the role of mutations in *synaptins* (genes involved in the regulation of synaptic transmission) in ASD pathology [89].

1.3.2 Disconnection - processing speed and integration

A model has been described proposing that ASD is a disorder affecting the processing of complex information, such as social communication and context, with sparing of the ability to process relatively uncomplicated information, such as facts and figures [90][91]. Social interactions are multisensory events, with a requirement for fast and accurate comprehension of a multitude of features, such as eye contact, gesture, and tone of voice, and a need to respond quickly and appropriately. Evidence indicates that individuals with ASD often report feeling overwhelmed and needing 'time to think' in social situations [92]. This theory suggests that the rapid integration of complex social information, and thus the networks of communication between brain regions, is impaired in ASD, leading to a lack of understanding and inappropriate social behaviour. This theory has links with the synaptic transmission hypothesis (section 1.3.1), because delays and/or a reduction in information transfer at the synapse will hamper the integration of complex data and impair understanding; however, this theory posits that processing deficits in ASD can arise from both structural and/or functional disconnections, and that there is relative sparing of non-social processing. There is both structural and functional evidence of elevated short-range connectivity and reduced long-range connectivity within the autistic brain [93][94][95][96], and for disconnection between brain regions [97]. This theory is related to the theory of mind (see section 1.3.5), in that it describes impairments in understanding social situations, but the emphasis in this disconnection theory is on the relative complexity of social stimuli.

1.3.3 Weak central coherence

The weak central coherence theory [98][99] hypothesises that ASD is caused by a cognitive style of processing that favours small details over the 'big picture'. An individual with a weak central coherence is more likely to disregard the overall meaning or significance of a situation, and instead focus on the separate details. This is very common in individuals with ASD who, for example, often describe how parts of a picture look rather than describing the overall significance of the scene. Recent evidence has led to the suggestion that weak central coherence is the product of a bias towards local processing, rather than a lack of ability to process global information [100]. There is evidence that weak central coherence in ASD is associated with disconnection across large-scale neural circuits [101], which is indicative of a disconnection syndrome, as outlined in sections 1.3.1 and 1.3.2.

1.3.4 Contextualisation

A theory that is highly related to the weak central coherence theory (section 1.3.3) is that ASD occurs as a result of deficits in contextualisation [102][103][104]. For example, hypersensitivity to sounds or changes in routine may be related to a reduced ability to contextualise what is occurring, rather than the stimulus or situation itself. This could lead to excessive arousal and anxiety or frustration, as is often observed in ASD (see section 1.3.10). Social interactions are heavily reliant on context – for example, the question "What are you looking at?" could pose a threat if it is asked by a stranger in an antagonising manner; conversely it could be a demonstration of friendly interest – which could explain the comparative impairments in social functions relative to other processes in ASD.

1.3.5 Theory of mind

The theory of mind (sometimes referred to as mind-blindness or mentalising) is the ability to attribute mental states to oneself and others, and to appreciate that people often differ from one another in their emotional state. It has been proposed that the

social shortfalls central to ASD are caused by impairments in theory of mind [105][106]. Structural and functional deficits in neural circuits involving the temporal lobe have been related to theory of mind difficulties in ASD [107], and reduced amygdala activation has been identified in ASD subjects during a task requiring theory of mind [108].

1.3.6 Mirror neurons

Mirror neurons are sometimes referred to as the basis of neurological empathy, and activate during imitation and passive viewing of other people's activities. The mirror neuron theory of ASD proposes that symptoms arise due to a deficit in the activation of mirror neurons in the brain [109][110]. In ASD, reduced mirror neuron activation has been observed in conjunction with reduced function of theory of mind (see section 1.3.5) networks, suggesting that deficits in imitation and empathy overlap with theory of mind difficulties [111][112].

1.3.7 Face processing and emotion recognition

Impairments in face processing, including recognition and memory, and in emotion recognition have been described in ASD, and are thought to arise from functional deficits in regions of the temporal lobe (see reviews [113][114]), and recruitment of atypical brain regions during face processing [115]. ASD is often characterised by avoidance of eye contact [116], thus removing the primary means of identifying and interpreting facial expressions. Reduced inclination for eye contact may arise as a result of elevated physiological arousal, which individuals with ASD tend to experience when making eye contact [117]; in this study, reduced emotion recognition accuracy was associated with greater physiological arousal. This may mean that eye contact is interpreted as a threat, which in turn reduces the ability or inclination of the individual to interpret emotions or generate directed social overtures. A recent study has indicated that a lack of social memory in ASD is not caused by a lack of eye contact *per se*, rather that aberrant post-processing is at fault

[118]. The theory of ASD as a face-processing disorder links strongly with the theory of mind (section 1.3.5) and disconnection (section 1.3.2) of social networks within the brain.

1.3.8 Social bonding

A further theory of ASD is that it arises from a deficit in early social bonding, which is predominately mediated by the hormones oxytocin and vasopressin [119]. It is thought that that this hormone-mediated bonding activates reward circuits in the brain during typical social bonding [120][121], and that deficits in this system in ASD reduce feelings of reward during social interaction and diminish the urge to connect socially. Skuse et al. [122] identified a link between social bonding and emotion recognition ability (section 1.3.7), suggesting that impairments in social bonding, as observed in ASD, adversely affect social functioning. Recent evidence has shown that administration of oxytocin to children with ASD can increase activation of the brain during social judgement tasks [123], and improve the quality of social interactions [124].

1.3.9 Extreme male brain

Baron-Cohen has posited the extreme male brain theory of ASD [29][125][126], suggesting that males and females have different cognitive profiles, with males typically better at 'systematising' and females at 'empathising', and that the cognitive profile of an individual with ASD is an amplification of the typical male profile. Systematising is the ability to construct or analyse rule-bound systems, including the ability to predict how the system will behave, whilst empathising represents the ability to identify another person's emotions and thoughts, predict their behaviours, and respond appropriately. The symptoms associated with ASD, such as lower empathy, reduced ability to read social cues and respond appropriately, rigidity, collecting and organising things, and restricted interests, are indicative of a hyper-systematising cognitive profile. In 2005 Baron-Cohen et al.

reviewed evidence for the neurological basis of the extreme male brain in ASD [127], and identified whole brain and amygdala enlargement in typical males compared to females that was more pronounced in ASD, in addition to regions of the brain, such as the corpus callosum and internal capsule, that were smaller in typical males than females, and even smaller in ASD. There is evidence that high levels of prenatal exposure to testosterone correlate with the incidence of autistic traits [128][129], thus indicating that the 'extreme male brain' is seeded before birth. The extreme male brain theory is similar to the weak central coherence theory (section 1.3.3), in that it describes the propensity of individuals with ASD for attention to detail and fact-based analysis, and to theory of mind (section 1.3.5), which describes impairments in the ability to imagine another person's thoughts or feelings in ASD. However, the extreme male brain theory takes this further by providing a hypothesis for the increased incidence of ASD in males relative to females.

1.3.10 Self-regulation

Self-regulation is the ability to manage one's own behaviour such that it adheres to core values – for example, completing a school assignment because of a commitment to gaining an education – and the capacity to regulate emotions, such as calming oneself down when upset. Difficulties with self-regulation are common in ASD, resulting in inappropriate behaviours and extremes of mood. It has been proposed that self-regulatory deficits in ASD are associated with orbitofrontal cortex–amygdala circuits [130]. Self-regulation abilities may overlap with theory of mind (section 1.3.5) and contextualisation (section 1.3.4), since a lack of awareness regarding other people's feelings and the nature of a situation could lead to a reduction in the drive or ability to manage oneself in a way that is appropriate [131].

1.3.11 Executive dysfunction

Executive functions regulate underlying cognitive processes, including working memory, the ability to make and execute plans, reasoning, and shifts in attention

(see review by [132]). This theory proposes that dysfunction in executive processing is central to ASD, rather than a symptom of it [133]. Executive dysfunction in ASD is associated with reduced flexibility and difficulty switching attention, in addition to impairments with planning and the adjustment of plans in response to change in circumstance [134]. Executive function deficits in ASD often relate to problems with self-regulation (section 1.3.10); for example, displays of great emotional distress following what may appear to be a trivial change in routine. Executive functions are predominately mediated by the frontal lobe and basal ganglia (reviewed by [135]), thus indicating that these regions and the connections between them are impaired in ASD.

1.3.12 Understanding and integrating theories of autism

It is likely that a comprehensive and accurate explanation of ASD requires a combination of those conceptualisations described above. For example, aberrant face processing networks may interact with theory of mind and mirror neuron deficits, resulting in reduced ability to identify the emotional status of others and empathise with them; weak central coherence and impairments in contextualisation may combine to render individuals 'blind' to social context, thus compounding their emotion recognition deficits; a propensity to systematise, coupled with reduced ability to self-regulate could exaggerate this by making an individual appear 'cold' or 'removed', and result in inappropriate social responses; and difficulties with executive functions will mean that a switch in focus towards someone who is displaying emotions (that the sufferer of ASD finds difficult to identify and empathise with) is unlikely. Integration of the many and diverse theories of ASD is complex, not least because the definition of ASD is indeterminate (based on the interpretation of observed and reported behaviours) and fluid, and cases are incredibly heterogeneous – no two cases of ASD are exactly alike. A combination of neurodevelopmental processes, genetics, and, to a certain extent, the environment, will contribute to the development and maintenance of symptoms in each case. Furthermore, ASD occurs at the intersection between behaviour and cognition,

which means that conceptualisations of ASD must combine an understanding of the ways in which neurological features influence, and are influenced by, both the thoughts and actions involved in social interactions.

An apparent consistency in the explanations of ASD presented above is that disordered or aberrant neural circuits are associated with its characteristic behaviours. Questions then remain: which neural circuits are affected in ASD? Are only social communication networks affected? What is the nature of the neurological anomalies observed in ASD? How do aberrations in neural circuits relate to particular ASD traits? Is there overlap? A great deal of research is currently in process to answer these important questions; the work presented in this thesis contributes towards this endeavour with the aim of improving understanding of neural connectivity in ASD, and the identification of associations between structural changes within the brain and symptomatology.

1.4 Conclusions

ASD is a neurodevelopmental condition characterised by impairments in social communication, and the presence of stereotypical behaviours. The cause of ASD is unknown, though there is evidence that it is highly heritable. The brain is a complex structure, with vastly interconnected regions that enable higher-level functions. Several theories of ASD have been proposed, the majority of which identify altered brain connectivity as a contributing factor to ASD symptoms. Much of the research examining the neural basis of ASD has investigated structural and functional brain changes *in vivo* using magnetic resonance imaging (MRI), and the work presented in this thesis builds on this body of knowledge. The theory behind MRI is given in Chapter 2, and findings from prior research investigating the ASD brain using MRI are presented in Chapter 3.

Chapter 2 Introduction to Magnetic Resonance Imaging

This chapter gives an overview of the development of magnetic resonance imaging (MRI), and an explanation of nuclear magnetic resonance (NMR) which underpins the technique. This is followed by an outline of T_1-weighted and diffusion-weighted MRI methods, which form the basis of the acquired imaging data covered in this thesis.

2.1 A brief history of MRI

In 1946 Bloch [136] and Purcell [137] independently discovered that certain atomic nuclei are able to absorb and subsequently re-emit radiofrequency (RF) energy when they are placed in a magnetic field. This phenomenon is called Nuclear Magnetic Resonance (NMR), and the time that it takes nuclei, on average, to return to the original resting state is called the relaxation time. In 1949 Hahn noticed that a second burst of RF energy could induce a repeat of this NMR signal, which was dubbed the spin echo [138]. Specific RF energies at the Larmour, or resonant, frequency are required to induce NMR in particular nuclei. The resonant frequency is also proportional to the strength of the magnetic field applied. The characteristic resonant frequency of different nuclei were demonstrated by Proctor and Yu [139] and Dickinson [140] who used this information to identify nuclei and calculate their concentration.

It wasn't until decades later that NMR was applied to medical imaging. In 1971 Damadian showed that mouse tumours had elevated relaxation times compared to normal tissues *in vitro* [141]. This observation reinforced the idea that NMR could be used in the identification and classification of different tissues and disease conditions *in vivo*. In 1973 Lauterbur [142] developed an alternative approach by employing smaller magnetic fields with linear gradients in order to induce

positionally-dependent nuclear resonances, in order to generate the first two-dimensional and three-dimensional NMR images. This was the beginning of MRI, and was followed in 1974 by the first living mouse MRI scan [143], and in 1977 by the first *in vivo* human body scan generated using MRI [144].

MRI has continued to develop from the first scans to its present-day form. Technological advances have greatly improved image quality and the development of novel MRI techniques have extended its applicability from structural analysis to functional assessment. MRI is now routinely employed in diagnosis and surgical planning for conditions ranging from cancer to ligament injuries, and its use as a research tool has been pivotal in informing our understanding of both anatomy and behaviour.

MRI scanners have a large cylindrical superconducting magnet, which has a central bore for the subject to lie in (see Figure 10). The scanner encircles the subject in order that the imaging magnetic field gradients can be applied over three dimensions and a three-dimensional image can be obtained. Transmit coils are used to generate RF pulses, and subsequent NMR signals are measured using receiver coils that are usually placed over the anatomy of interest.

Figure 10 An MRI Scanner.

[image courtesy of Jess Cooper].

2.2 Advantages of MRI

MRI is an incredibly useful imaging tool in both clinical and research settings. Its primary benefit is that it is non-invasive and low-risk. The magnetic fields and RF pulses do not alter or damage the biochemistry of the body, which is an advantage over other commonly used medical imaging tools, such as X-rays and computed tomography (CT), which use ionising radiation.

Another advantage of MRI is that a good level of detail and contrast can be easily and quickly generated in a great number of structures, thus widening its applicability. For example, MRI is unimpeded by bone, meaning that clear images of the brain can be acquired, unlike X-rays that are impeded by skull and cannot be used to visualise the underlying brain. An additional benefit of MRI is that, in addition to investigating anatomy, dynamic imaging can be employed in order to measure functional activity and blood flow over time. In the brain this can be used to probe cognition, and the impact of conditions such as cancer on blood delivery.

Both structural and functional MRI can be used to distinguish diseased tissue from healthy tissue, and clinically in order to facilitate surgical planning, or to monitor the success of drug-based interventions. MRI is a useful tool in the research setting, as it enables non-invasive observation of the causes and progression of diseases, as well as healthy developmental processes.

2.3 Limitations of MRI

One limitation of MRI is the expense and difficulty of installing and maintaining an MRI scanner; MRI scanners are expensive, and the scanning room must be encased in a Faraday cage in order to prevent external RF signals from affecting the measured MR signal.

Safety is an important consideration, as loose metallic objects can be drawn into the magnetic field, and some implanted metallic devices may heat up during scanning. For that reason all loose metal objects are removed prior to scanning, and implants are checked for MRI-compatibility. Since MRI scanning does not involve the use of ionising radiation it is unlikely to harm the foetus, but as a precaution pregnant women typically only have an MRI when it is a clinical necessity. The switching of magnetic field gradients in the MRI scanner is very loud so protective headgear is mandatory. The bore in which the patient lies is narrow and can induce feelings of claustrophobia. This is of particular concern in vulnerable patient groups, though an alarm is given to all patients so that they can be removed from the scanner at any time.

Artefacts sometimes form on an MRI scan and reduce its quality. There are many potential causes of artefact, though the most common are from patient motion, RF

interference, rapid changes in susceptibility, cardiac pulsation, and respiration. For this reason the patient is instructed to remain as still as possible in the scanner. MRI scans can show biology in great detail, particularly at high magnetic field strengths. However, MRI cannot currently provide the same level of spatial resolution as *ex-vivo* techniques such as histopathology or electron microscopy. This can result in partial volume effects, whereby a voxel (a single volume element of a scan) can contain more than one type of tissue.

2.4 NMR

As outlined in section 2.1, the basis of the MRI signal is NMR – the resonance of nuclei in the presence of a magnetic field and applied RF energy. This section will explain NMR in more detail and outline how it is captured in MRI. General references for this section include [145][146].

2.4.1 Nuclear spin

Atoms consist of a core nucleus, containing positively-charged protons and neutrons which do not possess a charge. The nucleus is surrounded by negatively-charged electrons. Atoms with an asymmetric arrangement of protons in the nucleus will spin spontaneously with a constant velocity around an axis perpendicular to the direction of rotation. This spinning asymmetric charge induces a local magnetic field, called a magnetic moment, around the nucleus. NMR only occurs in nuclei which spin and thus have this associated magnetic moment.

Hydrogen atoms (^{1}H), often referred to as protons, spin because their nucleus contains only one proton and no neutrons. This magnetic moment, coupled with their abundance in the human body – in water and organic compounds – means that protons have traditionally been selected as the optimum target for MRI. The high

quantity of protons in the body maximises the types of tissue that can be imaged using MRI and strengthens the NMR signal, which is relatively weak from a single proton but much stronger when it is measured from a collection of protons in the shared environment of a tissue.

2.4.2 Proton spin in a magnetic field

Under typical conditions, protons spin around their axes. However, these axes are oriented at random which means that there is no net magnetisation. During MRI, the protons are placed in a strong, static magnetic field called B_0. This field imparts a turning force on protons, causing their magnetic moment to align with B_0. This causes the proton spin to precess around the direction of B_0 (see Figure 11).

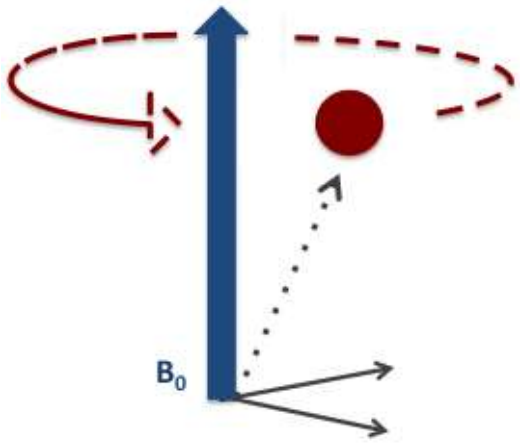

Figure 11 A proton precessing in the presence of magnetic field B_0.

Protons precess at a constant frequency, which is proportional to B_0. This is called the Larmor frequency, and is described by the Larmor equation (Equation 1) in which ω_0 is the precessional frequency in megahertz (MHz), γ is a constant called the gyromagnetic ratio (MHz T^{-1}) and B_0 is the magnetic field strength in Tesla (T).

Equation 1 $\omega_0 = \gamma B_0$

2.4.3 Net magnetisation in a magnetic field

The Zeeman interaction describes the coupling between the proton spin and B_0: with the proton spin either parallel (also known as spin up) or anti-parallel (also known as spin down) to B_0. The two spin states have different energy ratings, as shown in Figure 12. Spin-up protons have a lower energy than spin-down protons, which means that more protons are typically in the spin-up orientation rather than the spin-down orientation. The separation between the energy levels (ΔE) is given by Equation 2:

Equation 2 $\Delta E = \hbar \omega_0$

where $\hbar$ is the reduced Planck's constant and ω_0 is the Larmor frequency of the precessing proton spins, which is itself proportional to the strength of B_0 (see Equation 1). The number of protons in each energy level is also dependent on temperature (T), as described by the Boltzmann distribution (Equation 3) (where k is the Boltzmann constant).

Equation 3 $\text{N spin down protons/N spin up protons} = e^{-\Delta E/kT}$

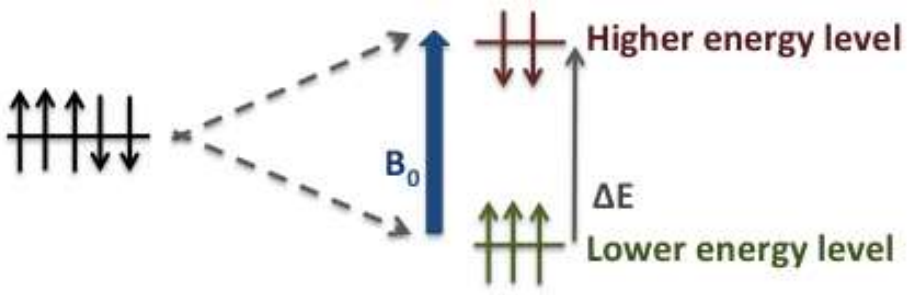

Figure 12 Zeeman diagram.

The difference (ΔE) between the high and low energy levels of proton spins in B_0 are shown.

The greater number of protons in the spin-up orientation as opposed to the spin-down orientation means that there is net magnetisation in the same direction as B_0. This net magnetisation is known as M_o. The magnitude of M_o is proportional to B_0, as shown by Equation 4 where χ is the magnetic susceptibility of the tissue. Magnetic susceptibility arises from weak diamagnetic and paramagnetic responses of paired and un-paired electrons, respectively.

Equation 4 $M_o = \chi B_0$

The M_o induced in the presence of the magnetic field B_0 forms the basis for generation of the NMR signal. Its proportionality to B_0 means that a greater magnetic field strength will result in a greater net magnetisation, and hence a stronger final MR signal. 1.5T MRI scanners have typically been used in the clinic and research. However, higher field strengths, such as 3T and 7T, are increasingly being employed.

2.4.4 Resonance

The next step in evoking proton NMR is the application of an RF energy pulse, often called an excitation pulse, at the Larmor frequency of the protons. When protons from the lower energy spin-up state absorb the RF pulse they are excited to the higher energy spin-down state. Conversely, protons in the spin-down energy state are stimulated to release their energy and revert to the lower energy spin-up state. Since the majority of protons experiencing B_0 are in the lower energy state, there is net energy absorption. This induces a switch in the net magnetisation from spin-up (parallel with B_0) to spin-down (anti-parallel with B_0). Net magnetisation following application of the RF pulse is known as M.

Protons cannot remain at the elevated energy state indefinitely, and will re-emit the absorbed RF energy at the same Larmor frequency it was absorbed; this is called the resonant frequency.

2.4.5 Relaxation

Relaxation is the process by which protons release absorbed RF energy and return to their original energy state within the magnetic field B_0. It is the process by which M returns parallel to B_0 after it has been shifted perpendicular to B_0 by the RF pulse. Protons can release their excess energy in two different ways – characterised by the so-called spin-lattice (or T_1) and spin-spin (or T_2) relaxation times.

2.4.5.1 T_1 relaxation

T_1 relaxation is the dispersion of the absorbed energy from the proton to the surrounding environment, otherwise known as the lattice. It is therefore known as spin-lattice relaxation. It is initiated by energy supplied to the proton from the motion (or tumbling) of neighbouring protons and other nuclei, including vibration

and rotation. Tumbling protons have an associated magnetic moment which interacts with the magnetic moment of other protons; known as dipole-dipole interaction, where a dipole is another term for a magnetic moment. The magnetic moments of protons have an associated frequency, which is dependent on the molecular structure which the proton is residing in. In order to provide a neighbouring proton with sufficient energy to stimulate T_1 relaxation, the magnetic moment of the neighbouring proton must be of the same Larmor frequency.

Since initiation of T_1 relaxation depends on the presence of protons or other nuclei tumbling with magnetic moments at the Larmor frequency, the T_1 relaxation time is heavily dependent on the chemical environment of a tissue. A more efficient T_1 relaxation, and thus a shorter T_1 relaxation time, is found in tissues with a greater number of protons tumbling at or near the Larmor frequency. This can generally be found in tissues with intermediate binding, whilst longer T_1 relaxation times are measured in free fluids. T_1 relaxation time is also shorter at lower resonant frequencies. This is because there is more efficient energy transfer due to the increased likelihood that protons will be tumbling at the lower resonant frequency.

2.4.5.2 T_2 relaxation

T_2 relaxation is the transfer of absorbed energy from one proton to a neighbouring proton. Both of the protons are spinning so it is also referred to as spin-spin relaxation. T_2 relaxation occurs when two protons are in close proximity to one another and they are occupying opposing energy states i.e. one proton is in the high-energy spin down state whilst the other is in the lower-energy spin up state. Their close proximity enables the release of energy at the Larmor frequency from the spin down proton to the spin up proton. No energy is lost from the spin system overall and it can continue to occur for as long as the protons remain in close proximity and at the same resonant frequency. However, rotation and vibration result in fluctuations in the resonant frequency of the protons. This prevents spin-

spin energy transfer from occurring any more, and results in dephasing of the protons, which leads to the decay of the transverse magnetisation and a loss of the NMR signal.

Initiation of T_2 relaxation is dependent on the molecular organisation of the tissue and magnetisation of neighbouring protons at the Larmor frequency. Therefore, different tissues will undergo different rates of T_2 relaxation. Tissues with many tightly bound protons are more readily able to undergo T_2 relaxation due to the close proximity of the protons and greater incidence of tumbling interactions; they therefore have very short T_2 relaxation times compared to free protons. T_2 relaxation times are always shorter than or equal to T_1 relaxation times.

2.4.6 The magnetic resonance signal

The signal measured during MRI is M. However, M is very small compared to B_0, which means that it cannot be measured when it is anti-parallel to B_0. Instead, the RF pulse is applied in the transverse plane, which generates an associated magnetic field, called B_1, perpendicular to B_0. M moves away from B_0 towards B_1 for as long as the RF pulse is on (as shown in Figure 13), and the MR signal is measured by a receiver coil in the transverse plane.

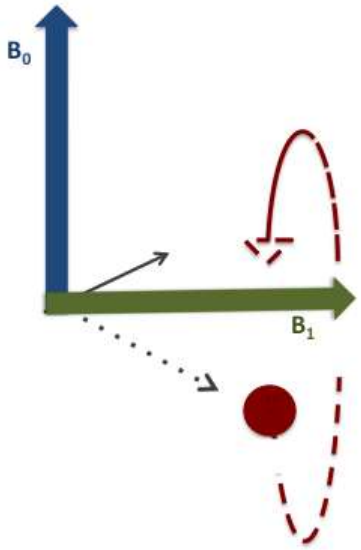

Figure 13 Application of an RF pulse in the transverse plane results in a magnetic field B_1, around which the proton precesses.

The degree that M moves, known as the flip angle (α), is proportional to the length of time the RF pulse is applied and the strength of the magnetic field associated with the RF pulse (B_1), as shown by Equation 5 where γ is the gyromagnetic ratio and t_p is the duration of the RF pulse:

Equation 5 $\alpha = \gamma B_1 t_p$

The flip angle is typically modified by altering the RF pulse strength rather than changing the duration of the pulse. This is because time is crucial during MRI: shorter scans mean that a greater number of scans can be obtained, and patient discomfort is reduced. Once the RF pulse is switched off the protons release the absorbed energy and slowly move back to their original alignment – parallel or anti-parallel with B_0. They are still precessing whilst they do this.

The RF pulse also brings the proton spin vectors into phase coherence, such that that they are all at the same point in the precessing circle at the same time. This strengthens the recorded M signal. The M signal induces a voltage corresponding to the Larmor frequency in the receiver coil in the transverse plane. This induced voltage is the MR signal and is known as a Free Induction Decay (FID). At the start of the recording, the FID signal is strong because the protons are still in phase and M is primarily along the transverse plane. The signal oscillates due to the precessionary motion of the protons. However, the protons do not remain in this elevated energy state for long. They soon begin to relax back to their original energy state via T_1 and T_2 relaxation processes, and the spins dephase. The signal disappears once the protons are fully relaxed back to their original state, as shown in Figure 14.

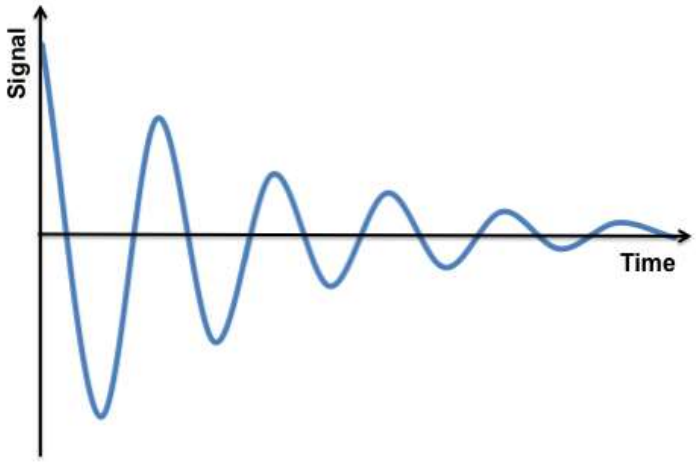

Figure 14 The oscillating FID signal measured by a receiver coil.
The signal is at high magnitude at the start as the protons are in phase. Signal magnitude then decreases over time due to dephasing.

2.5 Magnetic field gradients

As outlined, the MRI signal is generated from the energy emitted by excited nuclei during the process of NMR. However, this signal needs to contain spatially-specific

information in order to produce an anatomically-correct image. This must be location, orientation and scale specific. Spatial encoding is created by superimposing linear gradients on the applied magnetic field B_0 in all three dimensions. As described by Equation 6, these applied gradients change the magnetic field experienced (B_i) at location (r_i) within the magnet, where G_T is the total gradient amplitude:

Equation 6 $$\mathbf{B_i = B_0 + G_T r_i}$$

As highlighted previously, the precessional frequency of protons is proportional to the strength of the magnetic field experienced. This means that, under the linear gradients applied on B_0, the frequency and phase of a proton's spin depend on its location in 3D-space. It is important to note that these gradients operate on a macroscopic scale and over a very short time period. This means that they do not alter the microscopic-scale properties of T_1 and T_2 relaxation times, but merely enable spatially-specific activation and encoding of NMR signals.

Three types of 3D linear gradient are applied during MRI scanning. Each one applies a different spatial encoding on the MRI signal, and they are applied in sequence during MRI scanning.

2.5.1 Slice selective gradient

The slice selective gradient (G_{ss}) is the first gradient applied on B_0. It restricts the MR signal to a 2D segment of the patient in a process called selective excitation. Each 2D segment is called a slice, and slices covering the entire area to be scanned are combined to generate the final 3D scan. During selective excitation, a narrow-bandwidth RF pulse centred on the Larmor frequency is applied. In addition the G_{ss}

is applied which has a linear gradient in the orientation chosen for slice selection. The G_{SS} causes proton resonant frequency to vary with position. In the middle of the magnet (the isocentre) protons resonate at the Larmor frequency, but protons outside of this central region will have a different resonant frequency. As a result, the RF pulse applied at the Lamor frequency will only excite protons at or near the isocentre and an MR signal will only be produced in this region. The G_{SS} is stopped and a gradient with an equal, yet opposite slope is applied for a short time. This rephases the resonant protons within the selected slice, which will have dephased as a result of their chemical environment eliciting slight differences in the magnetic field they experience. This serves to strengthen the MR signal recorded within the activated slice.

The next slice in the sample can then be selectively excited by raising or lowering the frequency of the applied RF pulse so that it is now at the frequency required to excite a different portion of protons in the sample. The size of the slices can be adjusted by changing the bandwidth of the RF pulse or the strength of the G_{SS} gradient. Multiple slices can be activated in order to reduce scan acquisition time (see Figure 15).

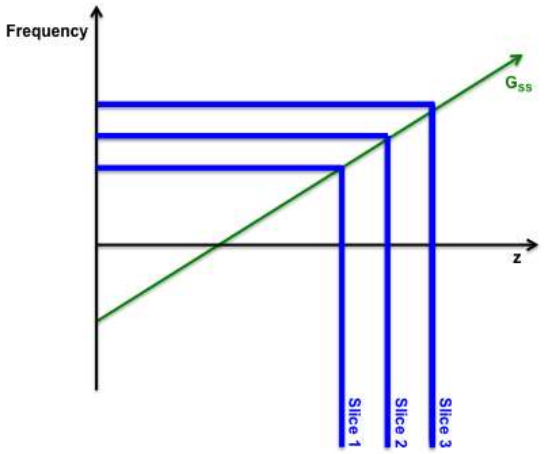

Figure 15 Application of the G_{SS}.

The G_{SS} enables the activation of certain slices within the target being scanned. Multiple slices can be activated simultaneously.

2.5.2 Phase encoding gradient

The second type of gradient applied on B_0 during scanning is the phase encoding gradient (G_{PE}). G_{PE} is a linear gradient applied orthogonally to G_{SS} that spatially encodes the MR signal along its axis by further altering the magnetic field that protons experience. This means that protons at one end of a slice are subject to a stronger field strength than protons at the other end. Since the precessional frequency of protons is proportional to the applied magnetic field, all of the protons in the slice now precess at different frequencies depending on their position along the axis. This causes the protons in the slice to become out of phase with one another to a degree that is dependent upon their position on that axis; phase is spatially determined. The gradient is then switched off. The dephasing induced by G_{PE} is not removed by a rephasing gradient, which means that this dephasing remains through to measurement of the MR signal and is therefore encoded in the slice (see Figure 16).

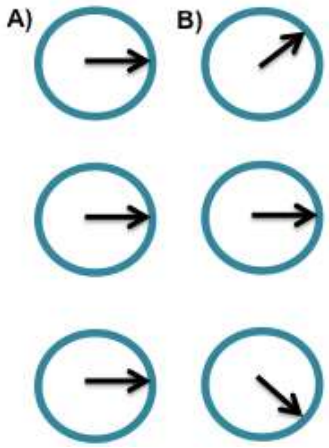

Figure 16 G_{PE}.

The figure shows a) proton spins in phase prior to application of G_{PE}, and b) application of G_{PE} induces position-dependent changes in proton phase. These remain following removal of G_{PE}, and phase-encode the protons according to their position.

Application of a small G_{PE} doesn't result in much alteration in the phases of the spins, thus ensuring a strong MR signal, but collecting little spatial detail about the spins. Small G_{PE} gradients therefore measure low spatial frequency information. Application of stronger G_{PE} causes greater change in the phase of the spins, which reduces the strength of the MR signal measured but means that adjacent spins are now phase-shifted and can be spatially encoded. Stronger gradients therefore provide higher spatial frequency information.

2.5.3 Frequency-encoding gradient

A frequency encoding gradient (G_{FE}), often called the readout gradient (G_{RO}), is the third linear gradient applied on B_0. It is applied at the same time or just following each successive application of G_{PE}. G_{FE} and G_{PE} complement one another to fully spatially encode each proton. G_{FE} consists of two linear gradients: the first is applied orthogonally to both G_{SS} and G_{PE} and causes protons within each slice to precesses at different frequencies depending on their position relative to G_{FE} (see Figure 17). This is again due to the dependence of proton precessional frequencies on the strength of the magnetic field, as described by the Larmor equation. However, this also means that the spins within a slice dephase. Dephasing reduces the strength of the MR signal, which would limit the usefulness of the data. Therefore, an opposite G_{FE} gradient is applied, which begins to rephase the protons along its axis by switching the direction of their precession. The MR signal is measured when the spins are in phase and the signal is strongest.

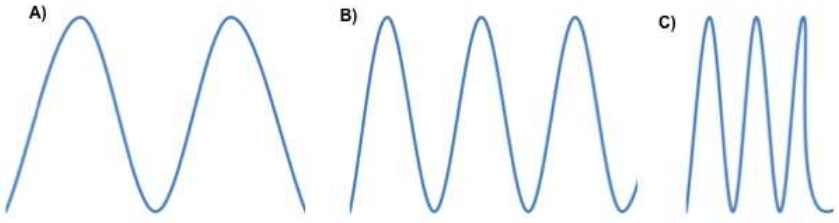

Figure 17 When G_{FE} is applied the frequency of the proton spin depends upon its location along the gradient.
The figure shows a) low frequency proton, b) typical frequency, and c) frequency proton spins that are induced along the G_{FE}.

2.5.4 The three gradients working together

To summarise, the MR signal is restricted to a slice of the area being scanned using the G_{SS}, and protons in this slice are spatially encoded further using G_{PE} and G_{FE}. The three gradients work together, and are applied in very quick succession. An example MRI sequence is shown in Figure 18. The repetition time (TR) is the time between successive excitation RF pulses for each slice.

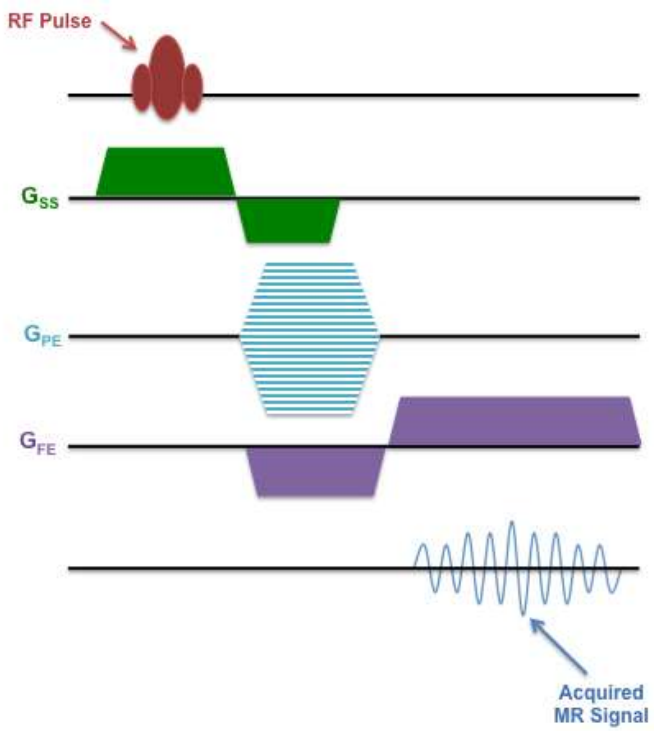

Figure 18 An example of a simple pulse sequence.

The figure shows application of the RF pulse, and the G_{SS}, G_{PE}, and G_{FE} gradients, in addition to measurement of the MR signal.

2.6 Echoes

When the protons are first flipped to the transverse plane using the excitation RF pulse they are in phase. However, this quickly degrades due to dephasing of the spins and the spatial encoding generated by application of the magnetic field gradients. This dephasing is reversed to some extent by the application of additional magnetic field gradients, and sometime refocusing RF pulses, to produce an 'echo', of the original signal. It is this echo that forms the final signal that is usually measured in an MRI acquisition. There are two commonly used methods for generating the echo during MRI scanning: the gradient echo and the spin echo.

The echo time (TE) is the time from the first RF pulse to measurement of the MR signal from the echo. A shorter TE allows for a shorter TR, and thus reduces the overall scan time. Gradient echo sequences are generally shorter than spin echo sequences, but they are susceptible to B_0 inhomogeneity. Inhomogeneities in the magnetic field affect T_2 relaxation, which is then referred to as T_2^* (T_2 + B_0 inhomogeneity).

2.6.1 Gradient echo

In a gradient echo sequence, the echo is created using an applied magnetic field gradient to rephase the spins. The applied gradient is in the opposite direction to previous gradients, thus reversing the protons' direction of precession. This brings them back into phase with one another and the MR signal is strongest at this point. The spins will eventually dephase again due their varying precessional frequencies. The gradient used to generate the echo is the G_{FE} gradient, which rephases the spins in addition to frequency encoding them. A schematic of a basic gradient echo pulse sequence is shown below in Figure 19.

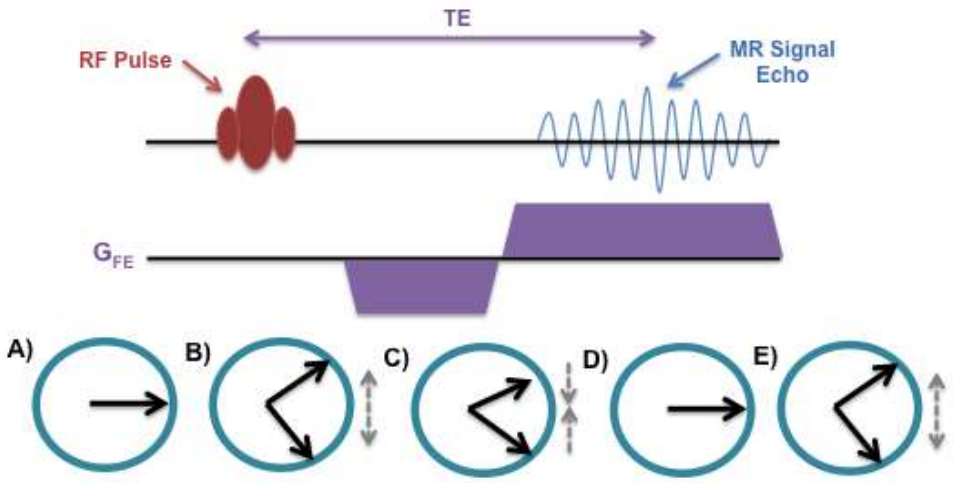

Figure 19 A gradient echo sequence.

The figure shows a) proton spins initially in phase, b) proton spins dephase due to application of the magnetic field gradient, c) proton spins begin to rephase due to application of an opposite gradient, d) the MR signal is measured when the proton spins are rephased and form an echo of the original signal. The time between application of the RF pulse and formation of the echo is TE. e) the proton spins will naturally dephase following measurement of the MR signal and removal of the magnetic field gradients.

2.6.2 Spoiled gradient echo

In spoiled gradient echo sequences, the MR signal is quickly removed, or spoiled, by the application of an additional gradient along the G_{SS} axis which dephases the proton spins, thus removing the coherence of their signal. The next TR then begins with a new RF pulse. Spoiling removes any transverse magnetisation remaining after the MR signal has been measured. This can occur in scans with a short TR. Spoiling ensures that the net magnetisation induced in subsequent TRs only arises from longitudinal magnetisation which is flipped by the RF pulse and not from residual transverse magnetisation, thus improving the quality of the MRI scan. A fast low angle shot (FLASH) sequence is a type of spoiled gradient echo sequence which employs a low flip angle. The small flip angle means that the sequence has a short TR, thus reducing scan time.

2.6.3 Spin echo

Spin echo sequences are the same as gradient echo sequences, aside from the application of a second refocusing RF pulse. Proton spins are flipped into the transverse plane by the first RF pulse, after which the second RF pulse is applied, with a flip angle of 180°. This flips the spins over so that they are still precessing at the same frequency, but their direction of precession is switched. This means that they begin to move back towards their starting position and thus return to phase. This is quickly followed by G_{FE} which frequency encodes the spins and generates the final MR signal. This is shown in Figure 20.

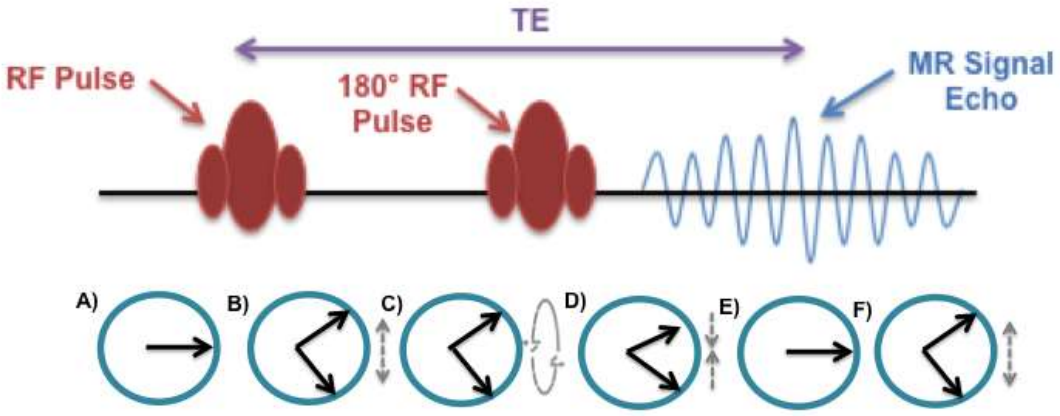

Figure 20 A spin echo sequence.

The figure shows proton spins initially in phase, b) proton spins dephase naturally, c) application of a 180° RF pulse causes the proton spins to flip over, d) however the proton spins continue to dephase in the same direction as before. e) continued dephasing of the flipped protons actually results in rephasing of the protons and the MR signal is measured at this point, which forms an echo of the original signal. The time between application of the RF pulse and formation of the echo is TE. f) the proton spins will naturally dephase following measurement of the MR signal and removal of the magnetic field gradients.

2.7 MRI contrast

Contrast is the way in which specific tissues or structures are represented differently to one another in an MR image. It enables differentiation of tissue types, and can show diseased tissue in contrast to healthy tissue. Contrast differences are mediated by variations in the intensity of the MR signal from between tissue types.

Proton density is one type of contrast that is based on the concentration of protons within a tissue. T_1 and T_2 relaxation times vary depending on proton environment. Different tissues have a unique molecular structure and will therefore have unique chemical environments, leading to characteristic T_1 and T_2 relaxation times. Certain parameters in the pulse sequence can be adjusted in order to harness these different relaxation times to provide proton density, T_1-, T_2-, and T_2*-weighted contrast. T_1-weighted and T_2-weighted scans were generated and analysed during the work described in this thesis, so the basis of their contrast is outlined here.

2.7.1 T_1-weighted scans

The contrast on T_1-weighted scans is provided by variations in T_1 relaxation time. As outlined in section 2.4.5.1, T_1 relaxation is the transfer of absorbed RF energy from proton spins to the lattice, and results in the protons returning to their relaxed energy state. Tissues with densely-packed protons have short T_1 relaxation times due to the increased initiation of energy transfer to the lattice by neighbouring protons spinning at the Larmor frequency. Conversely, areas with more sparsely-packed protons have much longer T_1 relaxation times due to the lack of neighbouring protons to efficiently initiate this energy transfer. In order to enhance the T_1 differences between tissues, the TR and TE are kept short. A short TR means that not all of the protons have relaxed back to the z-axis before the next TR is initiated. Only protons in tissues with short T_1 relaxation times will have been able

to fully relax and will form a strong signal in the following TR. Tissues with long T_1 relaxation times will form a weak signal in the next TR because fewer of the protons would have relaxed back to the z-axis in time. This means that a stronger MR signal is obtained for tissues with a short T_1 relaxation time and have a brighter intensity on a T_1-weighted scan, whilst tissues with long T_1 relaxation times have a weaker MR signal and are dark, low signal intensity on a T_1 scan (see Figure 21).

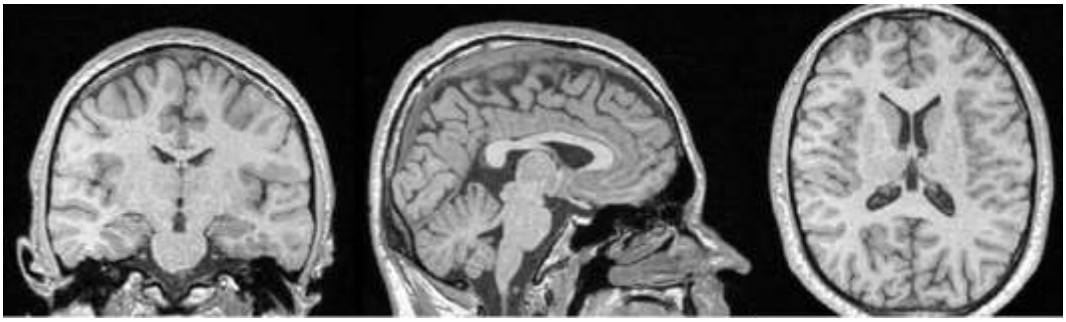

Figure 21 A T_1-weighted scan, with low signal intensity in the grey matter and high signal intensity in the white matter.

T_2 relaxation does not strongly influence contrast in T_1-weighted images because significant T_2 relaxation does not have time to occur in the short TE. In T_1-weighted scans generated using gradient echo sequences, the angle at which the spins are flipped by the initial RF pulse affects the generation of T_1 contrast. A greater angle means that protons are flipped further and T_1 relaxation takes longer, even in short T_1 tissues, whereas a smaller angle means that T_1 relaxation takes less time for all tissues. Therefore, a flip angle is chosen that enables some short-T_1 tissues to relax as much as possible within the TR, but does not enable longer T_1 tissues to do the same. This allows for creation of T_1 contrast within a short TR.

2.7.2 T_2-weighted scans

The contrast on T_2-weighted scans is generated by differences in T_2 relaxation times. As outlined in Section 2.4.5.2, T_2 relaxation is the transfer of absorbed RF energy from one proton spin to neighbouring spins, and it causes dephasing of the proton spins. It occurs more readily in tissues which are densely packed with protons; therefore T_2 relaxation times are shorter in densely-packed tissues and longer in sparsely-packed regions. The measured MR signal is weaker in short T_2 tissues, since the spins in those tissues are more dephased. In contrast, the MR signal is stronger in long T_2 tissues that haven't undergone as much T_2 relaxation and are mainly in phase. Therefore, regions with a long T_2, such as the CSF, have the highest signal intensities on T_2-weighted images, whilst tissues with a short T_2, such as grey matter, have lower signal intensity on T_2-weighted images (see Figure 22).

T_2-weighted scans are generated by SE sequences with long TR and TE. A longer TE is selected to ensure the T_2-weighted contrast; T_2 relaxation will have largely occurred in the short T_2 tissues, but tissues with long T_2 relaxation times will not have relaxed as much. T_1 relaxation does not provide much of the contrast for T_2-weighted scans because the long TR guarantees that that the vast majority of the T_1 relaxation will have taken place by the time the MR signal is measured.

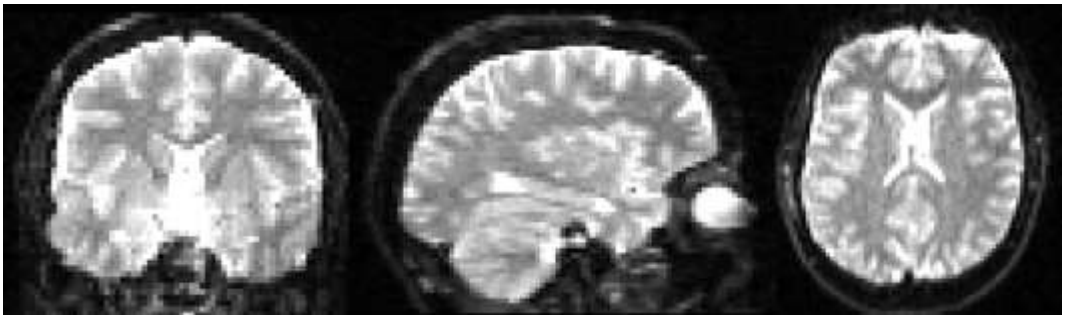

Figure 22 T_2-weighted scan.

2.8 Generating MRI scans from the MR signal

The spatially-encoded MR signals obtained from each readout of an MRI scan are first digitised, then stored in matrix form, known as K-space. The K-space matrix is then subjected to Fourier Transformation, which produces the final image.

2.8.1 K-space

The three magnetic field gradients, G_{SS}, G_{PE} and G_{FE}, spatially encode the protons in an imaging volume. The central row of K-space corresponds to the raw analogue MR signal without phase encoding. Successive rows of K-space are filled as the magnitude of the G_{PE} increases. Therefore, the central portion of K-space contains low spatial frequency information, such as the overall brightness of the image, and high spatial frequency information, for instance the detailed contrast between voxels, is stored towards the edges of K-space.

2.8.2 Conversion of the analogue MR signal to a digital signal

The raw MR signal is a continuous, rapidly oscillating voltage that is measured by the receiver coil. It is an analogue signal, which has to be converted to a digital signal via an analogue-to-digital converter for storage on a computer. Firstly, the base RF frequency is removed from the raw signal, and the conversion is performed on the remaining receive bandwidth of the signal. The conversion of the analogue signal takes a finite amount of time and, as such, the raw signal becomes 'sampled', as it can only be measured at discrete time intervals. If the sampling frequency of the analogue-to-digital converter is too low, the digitised signal will lose certain information stored in the raw analogue signal. This can lead to artefacts in the image, in which high frequency signals are inadequately sampled and appear as lower-frequency digitised signals. In general, the highest-frequency analogue signal that can be accurately digitised is half of the sampling frequency, which is known as the Nyquist frequency. Often, the sampling frequency is increased beyond what is

required for a given image display resolution, thus ensuring that the highest-frequency component of the raw signal is well below the Nyquist frequency. This is known as frequency oversampling.

2.8.3 Fourier transformation

The digitised MR signal in K-space is transformed into the final MR image using Fourier transformation in the frequency and phase encoding directions. Fourier transformation converts the MR signal from a measure of voltage with time into amplitude for each of the constituent frequencies that make up the raw MR signal. The resulting MR image is a matrix of voxels (volume elements). The image matrix has the same dimensions as the K-space matrix, but each point in K-space does not directly correspond to the same voxel in the image matrix.

2.9 MRI scan formats

MRI scans are saved by the scanner in digital imaging and communications in medicine (DICOM) format. In DICOMs the image is stored in conjunction with the details of the scan, such as the date and time, and information about the person who was scanned, such as date of birth. This information is highly confidential which means that DICOMs must be stored in encrypted hard drives and in locked cupboards when physically copied to disc. In order to maintain privacy and facilitate blinded data analysis, DICOM data is often converted to neuroimaging informatics technology initiative (NIfTI) format prior to analysis. Another benefit of NIfTI is that the format is widely supported by imaging software.

MR imaging planes are: axial (head-foot), coronal (anterior-posterior), and sagittal (left-to-right). MRI scans are often visualised according to radiological convention,

whereby the left side of the image corresponds to the right hemisphere of the brain, and *vice versa*.

2.10 MRI scan quality

The quality of each MRI scan governs how much useful structural and functional information can be obtained. Several considerations for scan quality are discussed below.

2.10.1 Magnetic field inhomogeneities

Magnetic fields can never be generated completely uniformly, which results in inhomogeneities. Inhomogeneities in the magnetic field can also be caused by susceptibility effects – local changes in B_0 generated by anatomical variations in magnetic susceptibility within a patient, such as air pockets, and differences in bone density. Inhomogeneities modify the magnetic field that the protons experience from the intended magnetic field, causing protons to precess at slightly different frequencies and dephase. This reduces the amplitude of the final echo MR signal. The RF pulse-induced 180° flip of proton spins enables correction of dephasing caused by magnetic field inhomogeneities, which means that spin echo imaging is less susceptible to inhomogeneities in B_0 than gradient echo imaging (see Section 2.6.3).

2.10.2 Signal-to-noise ratio

The signal-to-noise ratio (SNR) is the strength of the MR signal in each voxel of the MR image, relative to any extraneous noise confounding the signal. Noise can be induced by fluctuations in electrical current, caused by the RF coils which measure the MR signal. Noise can also arise from any electrically conducting tissues within a patient, such as neurons. Motion of electrically-conducting tissues within a magnetic

field generate electrical currents. These electrical currents have an associated, fluctuating magnetic field which is picked up by the RF coils and generates noise in the MR signal. MR images with a low SNR appear grainy due to the confounding noise, which masks subtle contrast changes and fine detail, limiting the usefulness of the scan.

To increase SNR, one can either reduce the level of noise or increase the MR signal measured by the MRI scanner. One way to reduce noise is to use small coils or an array coil that focuses attention on the area of interest without including areas that could contribute additional noise. A commonly used way of increasing signal is to average several measurements of the signal, but this increases the scan time. Increasing the voxel volume will elevate the number of protons within each voxel. However this creates a trade-off with spatial resolution. The magnet strength can also be increased, such as from 1.5T to 3T. This is expensive, but can greatly increase the signal strength (see Section 2.4.3).

2.10.3 Spatial resolution

Spatial resolution is the number of voxels that are utilised in the creation of the MRI image: a greater number of voxels means that the image has a higher resolution, and is better able to discriminate structures. The field of view (FOV) is the total area scanned, and is fixed for a given study. A FOV large enough to encompass a multitude of patients, each with different body masses is selected. Therefore, the spatial resolution in most MRI studies is defined by the size of the voxels in the image: smaller voxel size enables a greater number of voxels to fill the FOV, and thus confers greater spatial resolution. Voxel size is also fixed in a given study, and is determined by the slice thickness, G_{PE} and G_{FE}.

Partial volume is the occurrence of two or more different tissue types within the same voxel. This occurs in boundary areas between tissues where one tissue does not fill the entire voxel, and can lead to voxels containing a mixture of cerebrospinal fluid (CSF), grey matter and white matter. The signal intensity in these voxels is the weighted sum of the contributions from these components. Partial volume can affect MRI scan metrics, such as measurements of the volume of anatomical areas. The simplest way to reduce partial volume is to reduce voxel size. However, smaller voxels have a lower SNR and greatly increase scan acquisition time.

2.10.4 Artefacts

Artefacts are unwanted features on an MRI scan that misrepresent the object being scanned. A wide range of artefacts can occur, but the most common artefacts arise from patient motion, magnetic field inhomogeneity, or image processing anomalies.

Large patient movements can cause widespread blurring, ghosting, or signal drop-out. They arise when the patient's body moves between successive TRs. Movement artefacts are minimised by strapping the patient in and asking them to remain still. However, some vulnerable patient groups are not always able to comply with this. Motion artefacts also arise from normal biological events, such as respiration and cardiac motion. Their degree of influence depends on the region being imaged. Respiratory and cardiac motion artefacts can be reduced by measuring respiratory and cardiac motion, and synchronising this with the scan acquisition protocol. However, these methods are limited by the regularity of the patient's respiration.

Inhomogeneity artefacts are caused by imperfections in the magnet as well as inherent susceptibility effects in the patient. They result in signal intensity alterations and distortions in the MRI scan. The magnetic field gradients can only produce truly linear gradients over a short distance, which means that larger FOVs

are more likely to contain regions of non-linearity, which typically compresses the scan at the edges of the FOV. Susceptibility artefacts occur because different tissues are magnetised to varying degrees within the scanner's magnetic field. Bone and air have low magnetic susceptibility, whilst blood has a high magnetic susceptibility. At the boundaries between these tissues (for example, in the medial temporal lobes) the different magnetic fields generated within the tissues cause microgradients which increase the dephasing of protons at the tissue boundary, thus reducing the MR signal. Large magnetic field inhomogeneities can be caused by metallic objects. Most metallic objects have a much higher magnetic susceptibility than tissues in the body. Metals also absorb RF energy more readily, which poses a safety issue since they can heat up, and can also lead to artefacts caused by the distortion of the B_0 field. Susceptibility and metal artefacts can be reduced or eliminated with the use of spin echo pulse sequences, due to the ability of spin echo to cancel out inhomogeneity effects. Short TEs can also be used, and loose metallic objects should always be removed prior to scanning.

Digital imaging artefacts can be caused by a large number of issues, including limitations with discrete FTs. Phase wrap-around artefacts occur when an area of anatomy continues outside of the FOV and is displayed at the opposite edge of the scan in the phase-encode direction. Wrap-around artefacts can be prevented by saturating MR signals just outside the FOV. Alternatively, phase oversampling is employed, which increases the FOV in the phase-encode direction whilst also increasing the number of phase-encode steps so that the voxel size remains the same. The unwanted edges can be cut off by the computer once the scan is complete. This also elevates SNR, but does increase scan time.

2.10.5 Scanning conflicts

MRI scans are a trade-off between the spatial resolution, SNR, and scanning time. As we have seen, reducing voxel size will reduce partial volume effects. However, it

will decrease the SNR and increase the scanning time. Each scan is a compromise between the voxel size needed for a satisfactory SNR and appropriate visualisation of the relevant anatomy. Ultimately the best protocol depends upon the aim of the MRI scan, and the nature of the area being scanned. For example, it may be important to have a very short scanning time for vulnerable patients. Alternatively, when imaging highly-detailed structures it may be necessary to obtain a scan with a higher spatial resolution, accepting the concomitant SNR reduction and increased scan time.

2.11 EPI

Thus far, the basic principles of MRI have been outlined and the principle behind the generation of T_1- and T_2-weighted MRI scans has been described. This section focuses on the principles of echo planar imaging (EPI) [147]. EPI sequences are very fast and are used to obtain diffusion-weighted scans for the study of structural connectivity and functional MRI (fMRI) scans for the investigation of functional activations.

EPI can be used as the 'read-out' module in either a gradient echo or spin echo sequence. Spin echo-EPI gives T_2-weighted contrast and gradient-echo EPI gives T_2^*-weighted contrast. T_1-weighted contrast can be obtained in EPI via the addition of an inversion pre-pulse prior to the excitation 90° RF pulse. The pre-pulse flips all of the spins by 180°, meaning that, by the time of the 90° excitation pulse, tissues will start with different levels of longitudinal magnetisation, depending on their T_1 relaxation time. The time between the inversion pre-pulse and the excitation pulse is the inversion time (TI), which can be altered in order to control the strength of the T_1 contrast.

EPI sequences are either single-shot or multi-shot. In single-shot EPI the whole of k-space is acquired from one RF excitation, whilst multi-shot EPI covers a portion of k-space at a time, thus requiring multiple excitations. The EPI sequence can also be blipped or non-blipped, depending on how the G_{PE} is applied. In a non-blipped EPI sequence, a constant G_{PE} is applied at the same time as the G_{FE} which oscillates between positive and negative gradients. The MR signal is measured in concert with the G_{FE}. In contrast to this, a blipped EPI sequence uses a small G_{PE} blip near the end of each G_{FE} pulse (at the point of the reversal of G_{FE}). The G_{PE} blips are constant in size, but add further phase encoding to one another. This means that more phase encoding is added as the sequence continues (see Figure 23).

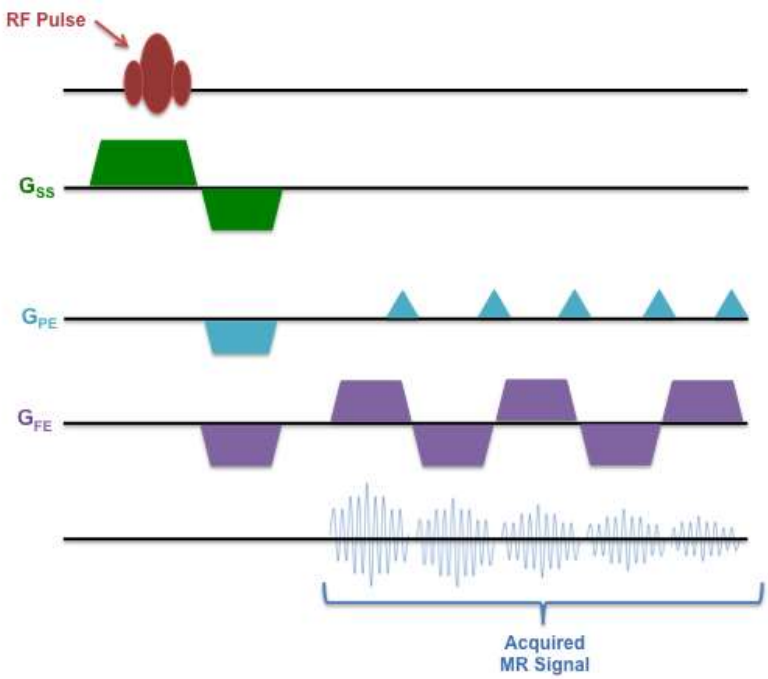

Figure 23 A blipped gradient echo EPI sequence. The acquired MR signal is reduced over time due to T_2* decay.

The speed of EPI sequences is offset by low resolution and enhanced sensitivity to artefacts. The most common type of artefact is the Nyquist ghost, caused by imperfections in the rephasing-dephasing cycle induced by the rapidly switching

G_{FE}. Chemical shifts are also very common in EPI due to the high G_{FE} amplitudes employed. Due to the shielding effect of hydrocarbon chains, fat is a major cause of chemical shift; therefore, fat suppression is essential in EPI. The high amplitude G_{FE} also means that small magnetic field inhomogeneities result in fairly large distortions. Furthermore, eddy currents are induced due to the rapidly changing magnetic fields in EPI. The magnetic fields generated by these eddy currents cause distortions in the resulting image. The use of reference scans and pre-emphasis in the gradient coil hardware are used to reduce eddy current-related artefacts.

Diffusion-weighted EPI is the subject of the work described in this thesis, so a description of diffusion-weighted MRI is given in the following sections. A main reference for this section is [148].

2.12 Diffusion-weighted MRI

Diffusion is the spontaneous, random movement of molecules that causes mixing. It was first observed in pollen grains suspended in water by Brown [149], and is sometimes referred to as Brownian motion. As described by Fick's law (Equation 7), the net movement of molecules (J) in free diffusion is governed by the particle concentration gradient (∇C) and the diffusion coefficient (D). The diffusion coefficient is an intrinsic property, dependent upon the size of the molecules and temperature, since molecules have greater kinetic energy at higher temperatures.

Equation 7 $\mathbf{J = -D\nabla C}$

The diffusion-driven displacement of molecules within a specified timeframe (τ) can be quantified in an equation developed by Einstein [150][151] as the mean-squared displacement of a collection of molecules ($\langle r^2 \rangle$) (see Equation 8).

Equation 8 $\langle r^2 \rangle = 6D\tau$

Water molecules are highly prevalent in the human body, and diffuse, as defined by the principles of diffusion, with random Brownian motion. Water molecules (chemical symbol H_2O) consist of hydrogen atoms bound to one oxygen atom. As outlined in Section 2.4, hydrogen nuclei (protons) undergo NMR which can be harnessed to create an image of body tissues using MRI. This means that the protons in water molecules can be targeted in order to measure water diffusion in the body. This forms the basis of the diffusion-weighted MRI scan. Diffusion-weighted MRI generates images representing the degree of mobility of water in a given direction for each tissue. This provides information regarding the microstructure of tissues, since water will only diffuse where cellular structures permit its transit.

The most common sequence used to generate diffusion-weighted MRI is the pulsed gradient spin echo (PGSE) followed by an EPI readout (see Figure 24). PGSE consists of a 90° RF pulse followed by application of a magnetic field gradient called the diffusion gradient. The diffusion gradient results in a range of proton precessional frequencies along its axis, thus dephasing the spins. A 180° RF pulse is then applied followed by a second diffusion gradient. The second diffusion gradient is equal in magnitude, but opposite in direction to the first diffusion gradient. A typical EPI readout then follows where the MR signal is measured. TE is often comparatively long in diffusion-weighted imaging so that adequate diffusion gradients can be applied, although modern scanners with faster gradients can counteract this to some extent.

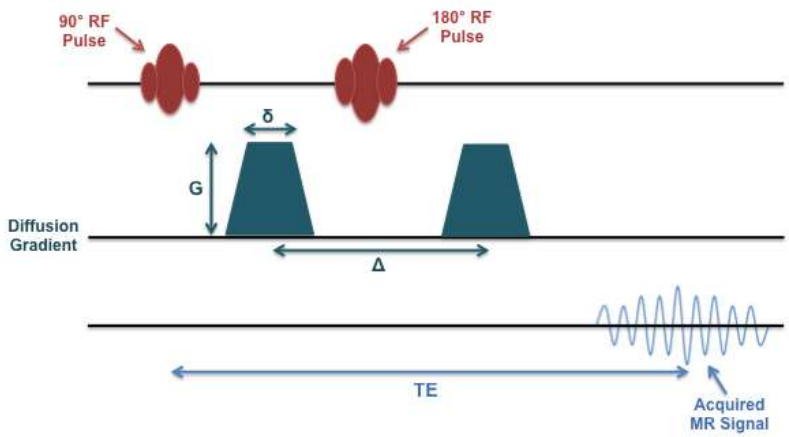

Figure 24 A pulsed gradient spin echo (PGSE) sequence that precedes a spin echo EPI sequence in order to generate a diffusion-weighted image.
The diffusion gradient has a magnitude (G), a duration (δ), and the distance between the centre of each diffusion gradient is denoted by (Δ).

The strength (G) and duration (δ) of the diffusion gradients can be adjusted, in addition to the interval between them (Δ) – often referred to as the leading edge separation. Adjustments in the diffusion gradients enables control of the degree of diffusion-weighting in the scan, otherwise known as the b-value (see Equation 9), where the (Δ-δ/3) parameter is also known as the diffusion time τ.

Equation 9 $b = \gamma^2 G^2 \delta^2 (\Delta - \delta/3)$

Equation 10 describes how the strength of the diffusion-weighted signal (S) relative to the signal intensity without diffusion weighting (S_0) relates to the b value, and to the diffusion coefficient. Typically b-values of 1000 s mm^{-2} are required for diffusion-weighted contrast. Imaging volumes with a b value of 0 are also acquired during diffusion-weighted MRI. These b=0 volumes are inherently T_2-weighted (see Section 2.7.2), and are used in later stages of data analysis.

Equation 10 $S/S_0 = e^{-bD}$

2.12.1 Diffusion-weighted contrast

The contrast on diffusion-weighted scans represents the amount water-bound protons have diffused during the diffusion time (see Figure 25). The initial diffusion gradient dephases the proton spins, based on their position along the diffusion gradient. Water molecules in tissues that restrict diffusion are not able to diffuse much, and thus cannot spread in random directions. This constraint to their diffusion means that the majority of the proton spins have not significantly changed location and are rephased by the second diffusion gradient, which is equal but opposite to the first diffusion gradient. This means that a stronger MR signal is measured, and the area has a high-intensity on the diffusion-weighted scan. Conversely, in tissues in which water molecules can diffuse freely, the proton spins are not rephased by the second diffusion gradient. This dephasing results in attenuation of the measured MR signal; thus regions with freer water diffusion have lower signal intensity on a diffusion-weighted scan.

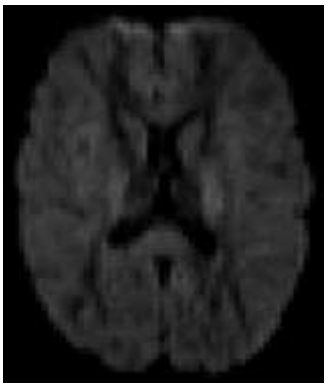

Figure 25 A diffusion-weighted scan.

Low signal intensity is shown in regions of high water diffusion, such as the CSF, and high signal intensity in regions with restricted water diffusion, such as the white matter.

The diffusion coefficient (introduced in Equation 7) applies only to free diffusion. In reality, the diffusion of water molecules is hindered by tissue structures, so the apparent diffusion coefficient (ADC) is measured. The ADC is calculated from the combination of the diffusion-weighted scan and the b=0 scan, and is visualised in an ADC map (see Figure 26). The contrast on an ADC map is the opposite of the diffusion-weighted contrast. Areas with a high ADC, and thus a greater degree of diffusion, have high signal intensity and appear bright, whereas areas with a low ADC have low signal intensity.

Figure 26 An ADC map.

High intensities reflect greater diffusion and low intensity voxels represent less diffusion [image courtesy of Dr Matthew Grech-Sollars].

2.12.2 Anisotropy

The contrast on diffusion-weighted scans and ADC maps depends on the direction in which the diffusion gradient is applied. Only water diffusion along the direction of the applied diffusion gradient will be measured, and thus contribute to the signal on the diffusion-weighted image and the ADC map. This directional dependency means that the full picture of diffusion can only be visualised with the application of several diffusion gradients in multiple directions. This is known as the angular resolution, whereby the amount of diffusion information that can be extracted from a scan increases with the number of directions the diffusion gradients are applied in.

However, there is a trade-off because a greater number of gradient directions increases the length of time a scan takes, and longer scans increase the likelihood of participant discomfort and motion artefacts in the resulting image. It is now typical to scan using high angular resolution diffusion-weighted imaging (HARDI) acquisition protocols [152], which measure the diffusion-weighted signal using a large number of uniformly distributed DW gradient directions that are able to capture the higher angular frequency features of diffusion. When using multiple diffusion gradient directions, the entire scan area is re-scanned with each new gradient direction. This produces a new image for each gradient direction, called a volume. At the end of the scan all the volumes are concatenated together to form the final diffusion-weighted scan. Also included in the final scan are several volumes with no diffusion weighting applied (b=0), which act as reference images during processing (see Figure 27).

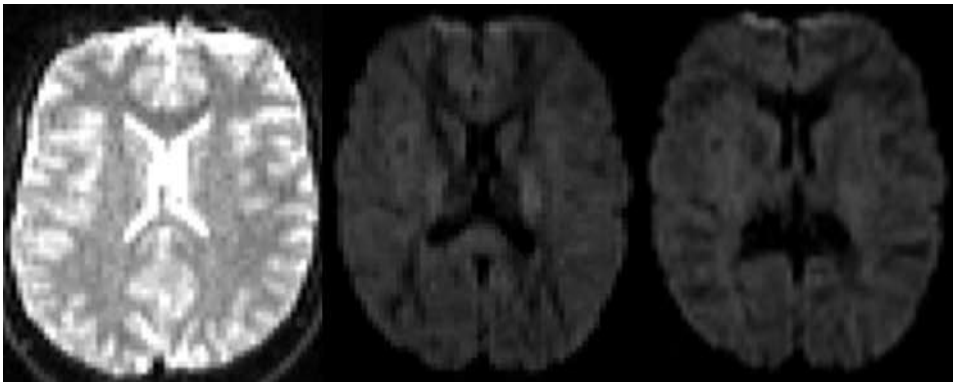

Figure 27 Three volumes from a diffusion-weighted scan, showing the effect of diffusion-weighted gradients on contrast.
A volume with no diffusion weighting (b=0) is shown on the left, and two volumes with different diffusion-weighted gradients (b=1000 s mm^{-2}) are shown in the middle and right panels.

The directionality of water diffusion in a tissue arises from its microstructural organisation. Water in extracellular spaces is free to diffuse equally in all directions.

This is termed isotropic diffusion. Water molecules within cells are more constrained in their diffusion – both in terms of the direction they can diffuse, and the distance that they can travel during the diffusion time. This limitation primarily arises from cell membranes which impede the diffusion of water between cells. Directionally-restricted diffusion is termed anisotropy.

The work presented in this thesis focuses on MRI of the brain. As outlined in Section 1.2.1, neurons in the brain have a near-spherical cell body. Water molecules in this part of the cell are reasonably free to diffuse and so the diffusion is close to isotropic. Neurons also have a long, narrow axon that projects towards other neurons in order to relay electrical signals. Water molecules in the axon are constrained by the narrow, directional nature of the structure. They are also restricted by the myelin sheath which surrounds the axon and increases the efficiency of information relay. Thus, water molecules are relatively free to diffuse parallel with the axon, but are very limited in their diffusion perpendicular to the axon. This means that diffusion within the axon is anisotropic. Extracellular water diffusion in the brain is also guided by the shape and packing density of cells – with relatively more extracellular diffusion occurring in tissues with loosely-packed cells, than tightly-packed regions. Neuron cell bodies are termed the grey matter, and the myelinated axons the white matter (see Section 1.2.1).

2.12.3 The diffusion tensor model

The amount of directional restriction in each voxel of a diffusion-weighted scan can be calculated, and forms the basis of measurements of microstructure using a method called diffusion tensor imaging (DTI) [153]. The diffusion tensor enables rotationally-invariant quantification of anisotropy, and at least 6 diffusion gradients are needed to produce a diffusion tensor that is capable of visualising water diffusion in multiple directions. The diffusion tensor is a 3x3 matrix that characterises diffusion in 3D (see Figure 28). It is mathematically described by its

eigenvectors (ε_1,ε_2 and ε_3), the three main diffusion directions, and eigenvalues (λ_1, λ_2 and λ_3) which measure the magnitude of diffusion along these eigenvectors. The direction with the highest eigenvalue (λ_1), and thus the greatest diffusion, is known as the principal diffusion direction (PDD). Diffusion tensors can also be denoted using ellipsoids, with isotropic diffusion represented using a spherical ellipsoid, and anisotropic diffusion by a cigar-shaped ellipsoid (see Figure 29 and Figure 29).

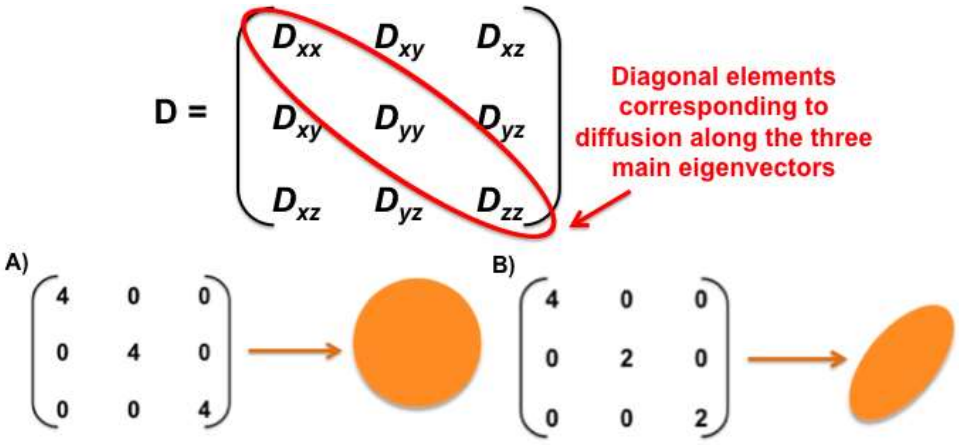

Figure 28 The diffusion tensor matrix.

The diagonal elements of the matrix represent ADC along the three orthogonal axes, and the off-diagonal elements correspond to the correlation between displacements along these three axes. Examples of a) an isotropic diffusion tensor and its associated matrix, and b) an anisotropic diffusion tensor and its associated matrix.

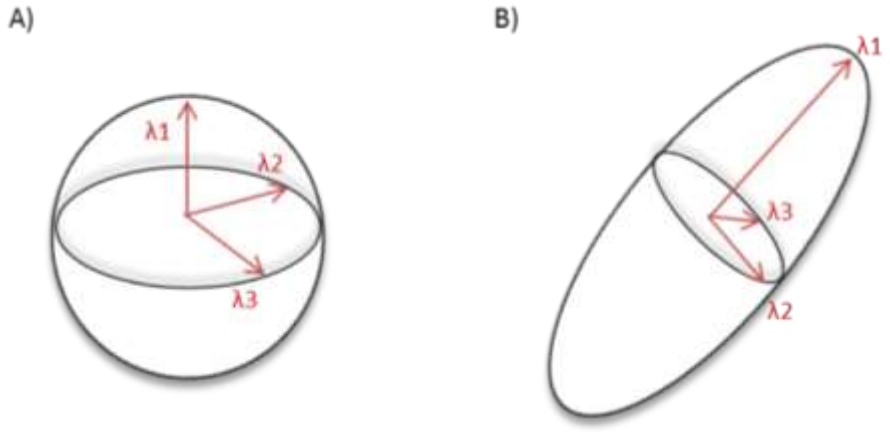

Figure 29 Diffusion tensors.

Principal (λ_1) and minor (λ_2 and λ_3) diffusion directions are shown. a) An isotropic diffusion tensor in which diffusion is uniform in all directions, thus λ_1, λ_2 and λ_3 are equal. b) An anisotropic diffusion tensor with increased diffusion in the principal direction, λ1.

2.12.3.1 Fractional anisotropy

The degree of anisotropy, and thus the extent of the directionality, of the diffusion tensor can be quantified using fractional anisotropy (FA) [154]. FA is a scalar value calculated from the tensor eigenvalues (see Equation 11), where $\hat{\lambda} = (\lambda_1 + \lambda_2 + \lambda_3)/3$.

Equation 11

$$\mathrm{FA} = \sqrt{\frac{3}{2}} \frac{\sqrt{(\lambda_1 - \hat{\lambda})^2 + (\lambda_2 - \hat{\lambda})^2 + (\lambda_3 - \hat{\lambda})^2}}{\sqrt{\lambda_1^2 + \lambda_2^2 + \lambda_3^2}}$$

Values of FA range from 0 for an entirely isotropic tensor to 1 for a fully anisotropic tensor. FA is used as a biomarker of white matter microstructure. The white matter of the brain is anisotropic due to the long thin structures of the axon which align in tract bundles forming a directed, coherent structure. FA values in the white matter range from 0.2 to values approaching 0.8, reflecting the underlying coherence of the structure. Healthy white matter will have numerous axons, each with cell

membranes inhibiting the perpendicular diffusion of water, resulting in a relatively high FA. In contrast, atrophied or damaged white matter is likely to have fewer axons due to processes such as cell death. This reduced number of axons means that diffusion is less directionally-restricted and FA is reduced. Dendritic pruning – a developmental process in which sporadic axonal connections are pruned to leave a more coherent structure – also reduces FA. Additionally, axons with reduced membrane integrity due to malformation or damage will be compromised, and permit greater perpendicular diffusion where it would otherwise be hindered by the membrane. This will also result in a reduction of FA. This means that white matter FA is a useful measure for probing the health, or coherence, of the white matter.

The FA value for the diffusion tensor in each voxel of the diffusion-weighted MRI data can be visualised in an FA map. Voxels with a high intensity on the FA map have a diffusion tensor with a high FA value and are more anisotropic, whilst those voxels with more isotropic diffusion tensors have a reduced FA value and are lower intensity (see Figure 30).

Figure 30 A fractional anisotropy map.
Low signal intensity is shown in regions with a lower FA value (more isotropic diffusion) and higher signal intensity in areas with a higher FA (more anisotropic diffusion).

2.12.3.2 Diffusivity

Mean diffusivity (MD) is an average of the magnitude of water diffusion over all directions in a given voxel (see Figure 31). It is therefore independent of direction, and thus provides a measure of the magnitude of water diffusion occurring locally. Low MD values are a marker of reduced water displacement in a voxel, and signify that diffusion is restricted by microstructures, such as the myelinated cell membranes or tightly-packed cell bodies. Conversely, elevated MD values are a biomarker of increased water diffusion that is reflective of phenomena including reduced cell density, a lack of myelination, increased axon diameter or oedema.

Figure 31 A mean diffusivity map.
Low signal intensity is shown in regions with a lower MD value (less diffusion) and higher signal intensity in areas with a higher MD (more diffusion).

Greater directional specificity can be obtained by measuring radial (RD) and axial diffusivity (AD). RD quantifies the average amount of diffusion along the two minor axes of the tensor perpendicular to the PDD (λ_2 and λ_3). In contrast, AD reflects the magnitude of diffusion along the PDD (or λ_1), which in white matter is parallel with the axon bundle. These values can enable greater interpretation of MD results by assessing whether an increase or decrease in diffusion is predominately associated with microstructural changes in the white matter that are parallel or

perpendicular to the axon bundle. For example, an elevation of MD in white matter may be associated with elevated RD but no change in AD. This would suggest that the increased diffusivity of the tissue is related to an increase in perpendicular diffusion, which may be caused by a rise in membrane permeability and/or deficits in axon myelination.

2.12.4 Ball and sticks model

Alternative models to the diffusion tensor for estimating fibre orientation and reconstructing white matter tracts using tractography are outlined in Chapter 9. One such model is the ball-and-stick model in FSL [155], which estimates diffusion orientation using an isotropic 'ball' and multiple linear 'sticks' and thus allows for the representation of multiple diffusion orientations within a voxel (see Figure 32).

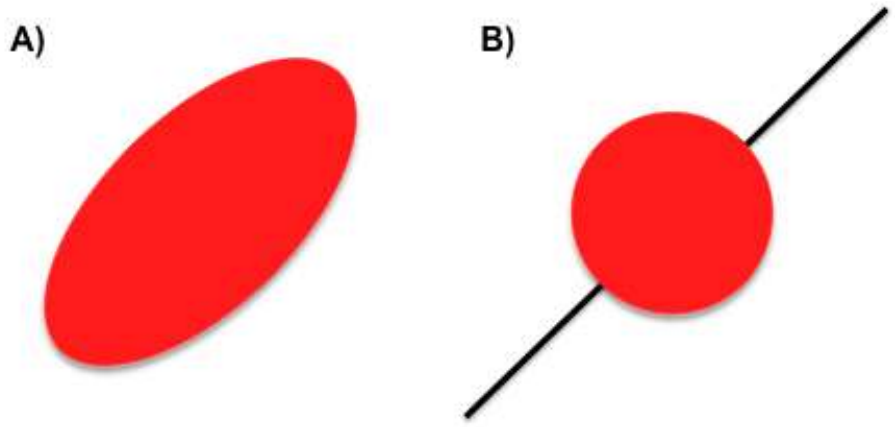

Figure 32 Estimation of diffusion and its uncertainty within a voxel.
The figures shows the use of a) diffusion tensor and b) the ball and sticks model.

2.12.5 Analysis methods

DTI scans can be used to obtain information about the microstructure of tissues with an inherent directionality, such as the white matter of the brain. Two branches of

analysis are employed in DTI analysis: region-of-interest (ROI) or voxel based comparisons, and tractography. These two methods are introduced below.

2.12.5.1 Region-of-interest/voxel-based analysis

FA and MD values within each voxel of a DTI scan can be compared between groups using methods such as voxel-based morphometry (VBM) [156] and tract-based spatial statistics (TBSS) [157]. These voxel-wise methods enable precise localisation and identification of anomalies in the microstructure of the white matter, and can thus provide rich information regarding disease pathologies. Such methods are limited by the requirement for scans from numerous participants to be registered and aligned near-perfectly, and by partial volume artefacts that introduce error to the data.

Alternatively, a collection of voxels can be grouped into a defined ROI across which FA and MD are averaged, and the average value compared between subjects. The ROI can be delineated manually or using automated software. ROI-based methods enable the investigation of several equivalent anatomical regions in multiple subjects, such as those voxels forming the corpus callosum – a large white matter tract joining the two hemispheres of the brain. However, ROI-based approaches are limited by the accuracy of the segmentation, may be operator-dependent, and restrict the analysis to those tracts that are the basis of *a priori* predictions.

2.12.5.2 Tractography

The white matter axons of the brain collect to form bundles, known as tracts, which structurally connect regions of grey matter to one another. As outlined in Section 1.2, information is relayed along white matter tracts via action potentials, thus enabling different portions of the brain to interact and operate coherently. The directionally-restrictive structure of white matter means that one can assume that

the path of greatest diffusion within the brain occurs parallel to the axon fibre bundles, where diffusion is less hindered. Tractography aims to reconstruct the fibre bundles connecting ROIs using the PDD. During DTI data processing, the PDD within each voxel is recorded, representing the path of greatest diffusion. Figure 33 shows a colour-coded representation of PDDs.

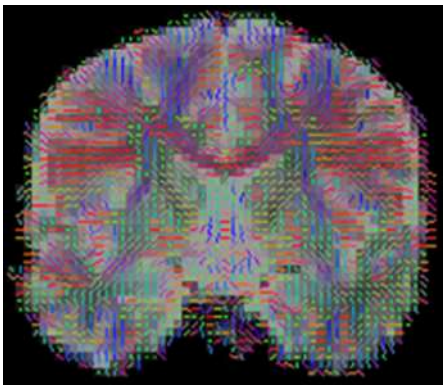

Figure 33 A colour map showing the PDD in each voxel.
Left-right PDD is shown in red, anterior-posterior (front-back) in green, and superior-inferior (top-bottom) in blue.

In deterministic tractography, each voxel's PDD is used to determine lines of connections across voxels to form a pathway of greatest diffusion. The resulting streamlines are representative of the major white matter tracts of the brain.

However, DTI tractography uses the orientation of water diffusion, known as the diffusion orientation density function (dODF), as a proxy for the true white matter fibre orientation, known as the fibre ODF (fODF). The dODF will differ from the fODF due to noise and because, although water is most free to diffuse along the fibre bundle, water is also able to diffuse along other orientations perpendicular to the fibre bundle. This means that there is inherent uncertainty in estimations of the white matter tract orientation. Probabilistic tractography takes the uncertainty of

fibre orientation estimation into account by repeated sampling in order to obtain the probability of different white matter pathways, and weighting each pathway depending on its probability. Thus paths with a greater probability are assigned a greater weight and the most probable tract distribution is generated.

Both deterministic and probabilistic tractography can proceed from a seed ROI to one or more target ROIs. Alternatively, models of expected white matter tract pathways can be used to guide tractography, such as neighbourhood tractography in TractoR [158] or TRACULA in FreeSurfer [159]. False positives can arise in probabilistic tractography due to the inclusion of a range of likely pathways; conversely, deterministic tractography is often associated with false negatives because it doesn't take uncertainty into account. Nevertheless, there is good agreement between anatomy and tractography findings [160][161].

2.12.6 Advantages of diffusion MRI

The main benefit of diffusion MRI is that it enables the non-invasive investigation of connectivity, which would otherwise be restricted to post-mortem dissection or tracer-based investigation. Diffusion MRI has been used clinically for applications such as the early identification of stroke [162], and in order to localise white matter lesions [163]. Diffusion MRI is often used in surgical planning to ensure that important white matter tracts are not resected during the removal of a tumour [164][165]. Research focuses on the utility of diffusion MRI to distinguish pathology, and increase the understanding of both typical and atypical brain structure and development.

2.12.7 Limitations of diffusion MRI

Noise and the presence of artefacts from sources such as eddy currents limit the accuracy of diffusion MRI measurements. However, image processing methods aim

to remove or reduce the effect of these from the data. A major limitation of diffusion MRI is resolution and associated partial volume. Voxel size is limited by the SNR. A small voxel is beneficial because it reduces the amount of partial volume – the presence of more than one tissue type within the same voxel. However small voxels contain less signal, which is a problem confounded by the fact that the signal is purposefully attenuated in order to measure diffusion. This limits voxels to a size much larger in size than that of a single axon and means that the MR signal for each voxel arises from a combination of inter- and intracellular sources. It is not possible to determine the directionality of white matter tracts using tractography, and it is not possible to establish whether a tract is functionally competent. Further, water diffusion is a proxy measure of fibre orientation. Therefore, diffusion MRI scans represent an approximation of microstructure. Nevertheless, comparison of tractography with post-mortem dissection in humans [160] and with tracers in animals [161] has reported good agreement, and diffusion MRI provides a great deal of clinically useful information.

Chapter 3 MRI Studies of Autism Spectrum Disorder

As MRI methods have become more accessible, advances have been made in the study of brain structure and function in ASD. The work reported in this thesis builds on our understanding of brain structure in ASD, and this chapter summarises the substantial body of work that has been published in this field thus far. The overarching aims and hypotheses underpinning the thesis are outlined at the end of the chapter.

3.1 Structural MRI studies of autism

3.1.1 Whole brain volume

Volumetric MRI studies have reported elevated whole brain volume in young children with ASD compared to control [166][167] and developmentally delayed [168] groups. This increase in brain volume in ASD is thought to affect the cerebrum to a greater extent than the cerebellum [169]. Indeed, reduced cerebellar grey matter volume has been reported in children and adolescents with ASD [166].

Longitudinally, the cerebrum is thought to grow at a faster rate in infants with ASD [170]; however similar cerebral growth rates in ASD and control groups have also been reported [171], and whole brain volume appears to be similar between ASD and control groups in older children and adolescents [167]. Recent work has suggested that caution must be maintained in light of recent evidence that estimates of early brain overgrowth in ASD may be exaggerated by inadequate reference ranges [172]. In a large-scale study by Courchesne et al. [173], whole brain volume was elevated in infants and toddlers with ASD and more rapid growth trajectories were observed; however, this was followed by deceleration of growth in the ASD group, leading to similar or smaller whole brain volumes, on average, in ASD by

adolescence and adulthood. Similar findings were reported by another large-scale longitudinal study carried out by Lange et al. [174].

3.1.2 Grey matter, white matter, and CSF volumes

Elevated grey matter and white matter volumes have been reported in volumetric MRI studies in children with ASD compared to control [173] and developmental delay [175] groups. A longitudinal study of toddlers found abnormally rapid cerebral grey and white matter growth trajectories in ASD [176]; however, grey and white matter volumes in older children and adolescents were similar between ASD and control groups [166], and Lange et al. [174] recently reported reduced mean white matter volume in ASD compared to controls. These studies indicate that the patterns of both grey and white matter volume changes in ASD mirror that of overall brain volume, with early rapid growth tailing off to result in similar volumes between groups in adolescence.

In studies of ASD across a wide range of participant ages, mean ventricle volume was elevated [174][177], and a longitudinal study has reported elevated CSF volume in infants with ASD between 6 and 24 months of age [170]. These findings indicate that brain volume is decreased in ASD, but this inference is called into question when coupled with the evidence of early brain volume increases in ASD. These studies controlled for intracranial volume, so a likely explanation is that the ratio of brain volume to CSF volume shifts throughout development in ASD, with reduced brain volume and increased CSF volume, on average, throughout the lifespan.

After controlling for total intracranial volume, disproportionate increases in temporal lobe grey matter and white matter volumes have been reported in comparison to controls [171] and developmentally delayed subjects [175], in addition to reduced corpus callosum volume in ASD [177]. Regional differences in

grey and white matter volume in ASD have also been identified using voxel-based approaches [178][179]. This indicates that certain regions of the brain are particularly affected in ASD.

3.1.3 Sub-cortical grey matter volumes

Volumetric MRI studies report both amygdala enlargement [180][181][168] and reduction [115][182] in ASD. A recent review of amygdala volume in ASD by Bellani et al. [183] identified that, on average, more studies reported enlarged amygdala volume in ASD. Two longitudinal MRI studies have identified early, accelerated amygdala growth in ASD [184][185]. Amygdala volume in ASD is discussed in greater detail in Chapter 6, where a study of amygdala structural connectivity is presented.

In a study of amygdala and hippocampal volumes in adults, left amygdala volume was smaller in ASD compared to controls, while left hippocampal volume was larger [182]. A longitudinal study, also in adults, identified elevated right hippocampal volume in ASD and marginally different hippocampal growth trajectories in ASD compared to controls, while amygdala volume and growth were similar between groups [186]. Conversely, another longitudinal study found group differences in amygdala volume and growth and no significant results for hippocampal volumes and growth trajectories [187]. This indicates that both the amygdala and hippocampus are of interest in ASD, but that there is variability in their relative growth trajectories.

Reduced thalamus volume has been recorded in ASD [188][189], which may be related to an association between thalamus volume and whole brain volume that is different in ASD compared to healthy controls [190]. Relatively few studies have investigated basal ganglia volumes in ASD. Elevated caudate [191] and putamen

volumes have been shown in ASD [192], although another study did not identify any significant group differences [193].

3.1.4 Cortical folding and thickness

In a longitudinal study of children, no significant group differences in cortical thickness were identified [171]. Conversely, Raznahan et al. [194] and Haar et al. [177] identified focal regions of elevated cortical thickness in ASD compared to controls. Auzias et al. [195], reported increased sulcal folding in ASD compared to controls for the right intraparietal sulcus, the left medial frontal sulcus, and the left central sulcus. These findings suggest that the cortical grey matter is, in general, similar between ASD and control groups, but that small regions of the cortex develop with increased thickness and folding in ASD. This finding is concomitant with the observation of localised grey and white matter volume changes in ASD.

3.2 Diffusion-weighted MRI studies of autism

There has been a rapid increase in the number of MRI studies published in recent years, particularly with regards to DTI studies in ASD. It is likely that this rise has been afforded by increased availability of MR technology, greater development of diffusion MRI methods that are applicable to a variety of clinical and research questions, and a rationale for the investigation of structural connectivity in ASD.

As would be anticipated from such a heterogeneous condition, the results of DTI studies in ASD are variable. It is likely that this variability arises from several quarters including, but not limited to: MRI scanner; scan protocol; analysis method applied; subject age and neurodevelopmental stage; biological sex; IQ; race; handedness; medication use; clinical severity and the nature of symptom presentation; diagnostic criteria employed. These influences can be roughly divided

into three main categories – methodology, demography, and clinical features. Depending on the aim of a particular research study, each of these three influencer categories is either of interest or a confound. For example, a study motivated by the effect of development on the brain in ASD will wish to sample different ages or developmental stages though keep all other parameters constant. With this in mind, the following section details published DTI studies in ASD, with reference to each study's aims and category (in terms of participant and methodological features). Table 1 lists the majority of these studies ordered by ascending age of the ASD participants. PubMed searches and several review papers [196][197][198][199] were used to identify studies of interest.

Study	Participants: mean age years (SD); sex	Study Design	Method	Diffusion Indices	Main Findings	Correlation Findings
Ben Bashat et al. (2007) [200]	7 ASD: 1.8-3.3 41 TD (18M:23F): 9.6 (4mts-23yrs)	Cross-section	Whole brain & ROI	FA Probability Displacement	↑FA in ASD: corpus callosum (genu & splenium); left corticospinal tract. ↑ FA and probability and ↓ displacement in ASD: left internal capsule; left external capsule; left forceps minor. ↑ probability and ↓ displacement in ASD: bilateral internal capsule; left corticospinal tract; right forceps minor. ↑ probability in ASD: right corticospinal tract.	Age effects: ↑ restriction in forceps minor diffusion in ASD relative to TD developmental trajectory.
Elison et al. (2013) [201]	16 HR+ASD (11M:5F) 40 HR-ASD (20M:20F) 41LR (24M:17F) 6mths	Cross-section	Streamline tractography: corpus callosum (genu, splenium).	FA AD RD	n/a	Correlation: Splenium RD & visual orienting latencies in LR.
Elison et al. (2013) [202]	16 HR+ASD 40 HR-ASD 41LR 6mths	Cross-section	Streamline tractography: arcuate fasciculus	FA	n/a	FA of right uncinate fasciculus predicts response to joint attention. No relationship with responsive language ability.
Wolff et al. (2012) [203]	28 HR+ASD (21M:7F): 6.8mths (0.8) 17 HR+ASD (13M:4F): 12.7mths (0.7) 17 HR+ASD(13M:4F): 24.5mths (0.6) 64 HR-ASD (38M:26F): 6.7mths (0.8) 49 HR-ASD (38M:26F): 12.7mths (0.6) 33 HR-ASD (19M:14F): 24.7mths (0.8)	Longitudinal	Streamline tractography: anterior thalamic radiation, corpus callosum, uncinate fasciculus, fornix, inferior longitudinal fasciculus, internal capsule.	FA AD RD	↑FA in HR+ 6 months: corpus callosum (body); left fornix; left inferior longitudinal fasciculus; left uncinate fasciculus; bilateral internal capsule. ↓FA in HR+ 24 months: left internal capsule; left anterior thalamic radiation.	Age effects: ↓ rate of change in FA in ASD related to TD developmental trajectory 6-24mths: bilateral fornix; inferior longitudinal fasciculus; uncinate fasciculus; corpus callosum (body); internal capsule; left anterior thalamic radiation.
Xiao et al. (2014) [175]	50 ASD (42M:8F): 29.9mths (5.54) 28 DD (22M:6F): 28.2mths (4.4)	Cross-section	VBM	FA MD	↑FA in ASD: corpus callosum; posterior cingulate; limbic lobe. ↓MD in ASD: corpus callosum; posterior cingulate; left limbic lobe; left insula.	n/a

Study	Participants: mean age years (SD); sex	Study Design	Method	Diffusion Indices	Main Findings	Correlation Findings
Weinstein et al. (2011) [204]	22 ASD: 3.2 (1.1) 32 TD: 3.4 (1.3)	Cross-section	TBSS & Streamline tractography: corpus callosum, arcuate fasciculus, cingulum	FA MD AD RD	TBSS: ↑ FA and ↓ RD in ASD: left arcuate fasciculus; corpus callosum (genu & body); bilateral cingulum. Tractography: ↑ FA.	n/a
Abdel Razek et al. (2014) [205]	19 ASD (16M:3F): 55.2mth (5.3mth) 10TD (8M:2F): 53.2mth (4.1mth)	Cross-section	ROI	ADC	ADC in ASD: corpus callosum (genu, splenium); frontal lobe; temporal lobe.	Positive correlation: ADC & CARS in the genu, splenium, and frontal and temporal lobe white matter. ADC frontal white matter & social skills. Temporal lobe ADC & language
Walker et al. (2012) [206]	39 ASD (28M:11F): 4.6 (1.8) 39 TD (26M:13F): 4.7 (1.8)	Cross-section	TBSS	FA MD AD RD	↓ FA in ASD: whole white matter. ↑ MD, AD and RD in ASD: posterior white matter.	Positive correlation: FA & age. Negative correlation: MD, AD and RD & age.
Sundaram et al. (2008) [207]	50 ASD (43M:7F): 4.8 (2.4) 16 TD (11M:5F): 6.8 (3.5)	Cross-section	Streamline tractography: short and long-range frontal tracts	FA ADC Average fibre length	↓ FA in ASD: short-range frontal tracts. ↑ ADC in ASD: short and long-range frontal tracts.	No significant results after correction.
Kumar et al. (2010) [208]	32 ASD (29M:3F): 5 (1.9) 12 DI-ASD: 4.6(3-9) 16 TD: 5.5 (2)	Cross-section	TBSS & Streamline tractography: inferior fronto-occipital fasciculus, uncinate fasciculus, cingulum, arcuate fasciculus, corpus callosum	FA MD Fibre length, volume and density	TBSS: ↓ FA in ASD: right uncinate fasciculus; corpus callosum; right cingulum; left arcuate fasciculus. Tractography: ↓ FA in ASD: right uncinate fasciculus; left arcuate fasciculus; right cingulum; corpus callosum. ↑ ADC in ASD: right arcuate fasciculus. ↑ Fibre length, volume & density in ASD: right uncinate fasciculus. No significant differences in FA or ADC between ASD and DI.	Positive correlation: left uncinate fasciculus fibre volume & GARS AQ, GARS stereotypic behaviour and GARS social isolation in ASD. Left uncinate fasciculus fibre density & GARS stereotypic behaviour and GARS social isolation in ASD. Right uncinate fasciculus fibre volume and right arcuate fasciculus fibre volume and fibre density & GARS stereotypic behaviour in ASD. Corpus callosum fibre density and length & VABS communication in ASD.

Study	Participants: mean age years (SD); sex	Study Design	Method	Diffusion Indices	Main Findings	Correlation Findings
Sivaswamy et al. (2010) [209]	27 HFA (24M:3F): 5 (2.6-9) 16 TD (12M:4F): 5.9 (2.6-8.9)	Cross-section	ROI: cerebellum	FA MD	↑ MD in ASD: bilateral superior cerebellar peduncle.	n/a
Jeong et al. (2011) [210]	32 ASD (29M:3F): 5 (1.9) 16 TD: 5.5 (2)	Cross-section	Tract-based morphometry: arcuate fasciculus, uncinate fasciculus, corpus callosum (genu)	FA AD RD Curvature	↓ FA in ASD: corpus callosum (genu); bilateral arcuate fasciculus; left uncinate fasciculus. ↑ RD in ASD: corpus callosum (genu); bilateral arcuate fasciculus; bilateral uncinate fasciculus. ↑ curvature in ASD: arcuate fasciculus; uncinate fasciculus; corpus callosum (genu).	n/a
Jeong et al. (2012) [211]	13 HFA (11M:2F): 5.2 (3.4) 11LFA (10M:1F): 4.1 (2.1) 14TD (11M:3F): 6.8 (3.1)	Cross-section	Tractography & Tract-based morphometry: cerebellum	FA AD RD Fibre volume	↓ FA in HFA and LFA: dentatorubrothalamic tract. ↓ FA in LFA: caudal midbrain; dorsal-caudal dentate; ventral-caudal dentate.	Positive correlation: right ventral-rostral and ventral-caudal tract FA & communication in HFA+LFA. Right dorsal-rostral tract and daily living skills.
Billeci et al. (2012) [212]	22 ASD: 5.5 (2) 10 TD: 5.3 (2.5)	Cross-section	TBSS & streamline tractography: cingulum, corpus callosum, arcuate fasciculus	FA MD AD RD Number of streamlines Streamline length	TBSS: ↑ FA in ASD. Tractography: ↑ FA, MD and AD in cingulum and arcuate fasciculus.↑ streamline length in ASD: cingulum; corpus callosum. ↓ number of streamlines in ASD: arcuate fasciculus.	Positive correlation: arcuate fasciculus streamline length and left cingulum AD & non-verbal IQ in TD; bilateral arcuate fasciculus streamline length & language in ASD. Negative correlation: arcuate fasciculus MD and AD & language in ASD; corpus callosum MD, AD and RD & language in ASD. Interactions with age in both groups.
Mengotti et al. (2011) [213]	20 ASD (18M:2F): 7 (2.75) 22TD (20M:2F): 7.68 (2.03)	Cross-section	VBM & ROI	ADC	↓ ADC in ASD: bilateral frontal cortex; left corpus callosum (genu).	Negative correlation: widespread ADC & age in ASD group. No significant correlation in TD.
Hong et al. (2011) [214]	18 HFA (M): 8.7 (2.2) 16 TD (M): 9.8 (1.9)	Cross-section	Streamline tractography: corpus callosum	FA ADC Number of fibres Average fibre length	↓ ADC and number of streamlines in ASD: anterior corpus callosum.	No significant results after correction.

Study	Participants: mean age years (SD); sex	Study Design	Method	Diffusion Indices	Main Findings	Correlation Findings
Ke et al. (2009) [215]	12 HFA (M): 8.8 (2.3) 12 TD (M): 9.4 (2.1)	Cross-section	VBM	FA	↑ FA in ASD: right medial temporal gyrus; right frontal lobe. ↓ FA in ASD: bilateral medial frontal gyrus; left inferior frontal gyrus; left superior temporal gyrus.	Positive correlation: right frontal FA and total CARS score.
Koldewyn et al. (2014) [216]	40 ASD (35M:5F): 8.98 (1.81) 43 TD (35M:8F): 8.90 (1.87)	Cross-section	Probabilistic tractography	FA MD AD RD	No significant differences.	Interaction: age.
Cheung et al. (2009) [217]	13 HFA (12M:1F): 9.3 (2.6) 14 TD (13M:1F): 9.9 (2.5)	Cross-section	VBM	FA	↑ FA in ASD: right arcuate fasciculus; left occipital lobe. ↓ FA in ASD: bilateral prefrontal cortex; temporal lobe; cerebellum.	Positive correlation: left precentral gyrus and ADI-R communication. Negative correlation: FA fronto-striatal-temporal tracts & ADI-R communication and social reciprocity. FA corpus callosum and cerebellum & ADI-R repetitive behaviours. Several white matter tracts and ADI-R-A, repetitive behaviours and communication.
Brito et al. (2009) [218]	8 ASD (M): 9.5 (1.8) 8 TD (M): 9.6 (1.4)	Cross-section	ROI: corpus callosum, cingulum, arcuate fasciculus, internal capsule, frontal lobe, optic radiation, corticospinal tract, cerebellum	FA	↓ FA in ASD: corpus callosum (anterior); right corticospinal tract; bilateral posterior internal capsule; cerebellar peduncle.	n/a
Hanaie et al. (2014) [219]	18 ASD (17M:1F): 9.5 (2.6) 12TD (11M:1F): 10.8 (2.1)	Cross-section	Tractography: corpus callosum	FA AD RD Fibre density Average fibre length	↓ average fibre length in ASD: corpus callosum (body); forceps major. ↓ AD in ASD: tapetum.	Negative correlation: FA forceps major & ADOS-G communication within ASD. Other correlations do not survive correction.
Poustka et al. (2011) [220]	18 ASD (16M:2F): 9.7 (2.1) 18 TD (16M:2F): 9.7 (1.9)	Cross-section	Streamline tractography: fornix, arcuate fasciculus, uncinate fasciculus, corpus callosum	FA	↓ FA in ASD: right arcuate fasciculus; bilateral uncinate fasciculus.	Negative correlation: FA & ADOS and FA & ADI-R.

Study	Participants: mean age years (SD); sex	Study Design	Method	Diffusion Indices	Main Findings	Correlation Findings
Mills et al. (2013) [221]	10 ASD (8M:2F): 9.8 (1.4) 17 TD (8M:9F): 9.2 (1.8)	Cross-section	Streamline tractography: Inferior fronto-occipital fasciculus, inferior longitudinal fasciculus, superior longitudinal fasciculus.	FA ADC RD	↑ ADC and RD in ASD: right inferior longitudinal fasciculus.	Positive correlation: right inferior longitudinal fasciculus FA & language ability in ASD. Negative correlation: right inferior longitudinal fasciculus MD and RD and language ability in ASD.
Hanaie et al. (2013) [222]	13 ASD (12M:1F): 9.8 (2.8) 11 TD (10M:1F): 10.7 (1.9)	Cross-section	Tractography: cerebellum	FA AD RD	↓ FA in ASD: right superior cerebellar peduncle.	Positive correlation: FA right superior cerebellar peduncle & motor score.
Barnea-Goraly et al. (2010) [223]	13 ASD (11M:2F): 10.5 (2) 11 TD: 9.6 (2.1)	Cross-section	TBSS	FA AD RD	↓ FA in ASD: medial prefrontal cortex; frontal corona radiata; corpus callosum (body); right internal capsule; arcuate fasciculus; bilateral external capsule; superior temporal gyrus; temporo-parietal junction. ↑ AD in ASD: bilateral medial prefrontal cortex; right forceps minor; internal capsule; arcuate fasciculus; corona radiata; superior temporal gyrus.	No significant results.
Peterson et al. (2014) [224]	36 HFA (31M:5F): 10.5 (1.4) 37 TD (31M:6F): 10.1 (1.4)	Cross-section	ROI	FA MD	↑ MD average left hemisphere; left parahippocampal gyrus; left sagittal stratum; left superior temporal gyrus.	Negative correlation: MD & age.
Jou et al. (2011) [225]	15 ASD (M): 10.9 (3.7) 8 TD (M): 11.5 (2.6)	Cross-section	TBSS	FA	↓ FA in ASD: bilateral inferior fronto-occipital fasciculus; forceps minor.	No significant results.
Cheon et al. (2011) [226]	17 HFA (M): 11 (2.1) 17 TD (M): 10.2 (2)	Cross-section	TBSS & ROI: anterior thalamic radiation, posterior thalamic radiation, superior thalamic radiation, uncinate fasciculus, inferior longitudinal fasciculus, corpus callosum	FA MD AD RD	TBSS: ↓ FA and ↑ MD in ASD: right anterior thalamic radiation; corpus callosum; left uncinate fasciculus. ROI: ↓ FA and ↑ RD in ASD: bilateral anterior thalamic radiation; corpus callosum; left uncinate fasciculus; left inferior longitudinal fasciculus. ↑ MD in ASD: corpus callosum. ↓ AD in ASD: bilateral inferior longitudinal fasciculus	Negative correlation: anterior thalamic radiation and right uncinate fasciculus FA & SRS.

Study	Participants: mean age years (SD); sex	Study Design	Method	Diffusion Indices	Main Findings	Correlation Findings
Lai et al. (2012) [227]	16 LFA (14M:2F): 11 (3.7) 18 TD (14M:4F): 11.2 (4.4)	Cross-section	Probabilistic tractography: arcuate fasciculus, inferior fronto-occipital fasciculus	FA MD Tensor norms	↓ FA in ASD: left arcuate fasciculus. ↓ Tensor norms in ASD: bilateral inferior fronto-occipital fasciculus	No significant results.
Nagae et al. (2012) [228]	18 ASD-SLI: 11.3 (6.7-17.5) 17 ASD+SLI: 9.6 (6.8-14.8) 25TD: 11.4 (6.5-18)	Cross-section	Streamline tractography: arcuate fasciculus, corticospinal tract.	FA MD λ1 λ2 λ3	↑ MD and λ1 in ASD+SLI: left superior longitudinal fasciculus. ↑ MD in ASD+SLI and ASD-SLI: corticospinal tract.	Negative correlation: left superior longitudinal fasciculus MD & CELF-4 across all participants. No group-specific age effects.
Ameis et al. (2011) [229]	19 ASD (16M:3F): 12.4 (3.1) 16TD (8M:8F): 12.3 (3.6)	Cross-section	TBSS & ROI: corona radiata, corpus callosum, inferior fronto-occipital fasciculus, inferior longitudinal fasciculus, uncinate fasciculus, arcuate fasciculus.	FA MD AD RD	TBSS in children only: ↑ MD and RD in ASD: bilateral corona radiata; uncinate fasciculus; inferior fronto-occipital fasciculus; arcuate fasciculus; right inferior longitudinal fasciculus; forceps minor; forceps major. ROI in children only: ↑ MD and RD in ASD: bilateral corona radiata; right inferior longitudinal fasciculus; uncinate fasciculus.	TBSS: No age by group interaction. ROI in children: age by group interaction in right inferior longitudinal fasciculus; uncinate fasciculus RD; bilateral corona radiata.
Ameis et al. (2013) [230]	19 ASD (16M:3F): 12.4 (3.1) 16TD (8M:8F): 12.3 (3.6)	Cross-section	Streamline tractography: cingulum	FA MD AD RD	↓ FA and ↑ MD in children <11 years with ASD: cingulum.	n/a
Shukla et al. (2010) [231]	26 ASD (25M:1F): 12.7 (6) 24 TD (23M:1F): 13 (0.6)	Cross-section	ROI	FA MD AD RD	↓ FA and ↑ RD in ASD: whole white matter; corpus callosum; internal capsule; middle cerebellar peduncle. ↑ MD in ASD: whole brain white matter; internal capsule. ↓ AD in ASD: corpus callosum.	No significant results.
Shukla et al. (2011) [232]	26 ASD (25M:1F): 12.7 (6) 24 TD (23M:1F): 13 (0.6)	Cross-section	ROI: short vs long-distance tracts	FA MD RD	↓ FA in ASD: long-distance white matter in whole brain. ↓ FA in ASD: short-distance frontal tracts. ↑ MD and RD in ASD: short-distance frontal, temporal, and parietal tracts.	Negative correlation: FA, MD and RD & age in ASD.

Study	Participants: mean age years (SD); sex	Study Design	Method	Diffusion Indices	Main Findings	Correlation Findings
Shukla et al. (2011) [233]	26 ASD (25M:1F): 12.7 (6) 24 TD (23M:1F): 13 (0.6)	Cross-section	TBSS	FA MD AD RD	↓ FA and ↑ MD and RD in ASD: inferior longitudinal fasciculus; inferior fronto-occipital fasciculus; arcuate fasciculus; cingulum; anterior thalamic radiation; corticospinal tract; forceps major.	Correlation: FA and MD & age in TD.
Sahyoun et al. (2010) [234]	9 HFA (7M:2F): 12.8 (1.5) 12 TD (9M:3F): 13.3 (2.5)	Cross-section	TBSS	FA	↓ FA in ASD: forceps minor; left inferior occipital fasciculus; left arcuate fasciculus; right inferior fronto-occipital fasciculus ↑ FA in ASD: bilateral uncinate fasciculus; right arcuate fasciculus.	Negative correlation: FA & reaction time in different brain regions in ASD vs TD, particularly superior temporal sulcus and superior longitudinal fasciculus.
Jou et al. (2011) [235]	10 ASD (M): 13 (3.9) 10 TD (M): 13.9 (4.2)	Cross-section	VBM & Tractography	FA	↓ FA in ASD: corpus callosum (anterior); left arcuate fasciculus; bilateral inferior fronto-occipital fasciculus; bilateral inferior longitudinal fasciculus.	n/a
Sahyoun et al. (2010) [236]	12 HFA (10M:2F): 13.3 (2.1) 12 TD (9M:3F): 13.3 (2.5)	Cross-section	Probabilistic tractography: inferior parietal sulcus, inferior longitudinal fasciculus, medial temporal gyrus, superior temporal sulcus, frontal gyrus.	FA	↓ FA in ASD: inferior frontal sulcus to frontal gyrus and medial temporal gyrus to inferior frontal sulcus.	n/a
Noriuchi et al. (2010) [237]	7 HFA (6M:1F): 13.4 (2.7) 7TD (6M:1F): 13.4 (2.7)	Cross-section	VBM	FA λ1 λ2 λ3	↓ FA in ASD: anterior cingulate cortex; left dorsolateral prefrontal cortex; right temporal sulcus; amygdala; arcuate fasciculus; inferior frontal occipital fasciculus; corpus callosum (mid and left). ↓ λ1 in ASD: superior temporal sulcus and temporo-parietal junction. ↑ λ1 cerebellar vermis.	Negative correlation: Dorsolateral prefrontal cortex FA & total SRS score.

Study	Participants: mean age years (SD); sex	Study Design	Method	Diffusion Indices	Main Findings	Correlation Findings
Cheng et al. (2010) [238]	25 ASD (M): 13.7 (2.5) 25 TD (M): 13.5 (2.2)	Cross-section	TBSS	FA AD RD	↑ FA and ↓ RD in ASD: left insula; right arcuate fasciculus; corona radiata; anterior thalamic radiation; inferior fronto-occipital fasciculus; internal capsule; bilateral middle cerebellar peduncle. ↓ FA and AD and ↑ RD in ASD: right cerebellar peduncle; left internal capsule; arcuate fasciculus.	Positive correlation: bilateral arcuate fasciculus FA & age in TD. Negative correlation: bilateral arcuate fasciculus FA & age in ASD.
Verhoeven et al. (2012) [239]	19 ASD+SLI (16M:3F): 13.8 (1.6) 21 TD (16M:5F): 14.4 (1.5)	Cross-section	Streamline tractography: arcuate fasciculus	FA ADC	No significant differences.	n/a
Verly et al. (2013) [240]	17 ASD (14M:3F): 167.41mths (16.8mths) 25 TD (19M:6F): 173.72mths (15.89mths)	Cross-section	Tractography: superior longitudinal fasciculus and arcuate fasciculus	FA ADC Number of streamlines	No significant differences.	Presence of right hemisphere arcuate fasciculus interacted with group for verbal IQ, picture vocabulary test, and CELF-4 scores.
Nair et al. (2013) [241]	26 ASD (22M:4F): 14.1 (2.5) 27 TD (23M:4F): 14.2 (2.2)	Cross-section	Probabilistic tractography: thalamo-cortical tracts	FA MD RD Tract volume	↑ MD and RD in ASD for connections with motor and sensory cortices. ↓ connection probability in ASD.	Negative correlations: FA & ADOS total and ADOS social. MD & non-verbal IQ.
Fletcher et al. (2010) [242]	10 HFA (M): 14.3 (1.9) 10 TD (M): 13.4 (1.3)	Cross-section	ROI: arcuate fasciculus	FA MD AD RD	↑ MD and RD in ASD: left arcuate fasciculus.	No effect of group on the relationship between DTI measures & CELF-3.
Groen et al. (2011) [243]	17 HFA (14M:3F):14.4 (1.6) 25 TD (22M:3F): 15.5 (1.8)	Cross-section	VBM	FA MD	↑ MD in ASD: whole white matter.	n/a
Barnea-Goraly et al. (2004) [244]	7 HFA (M): 14.6 (3.4) 9 TD (M): (13.4 (2.8)	Cross-section	VBM	FA	↓ FA in ASD: anterior cingulate cortex; corpus callosum (genu); ventromedial prefrontal cortex; prefrontal cortex; temporo-parietal junction; superior temporal sulcus; right medial temporal gyrus.	n/a

Study	Participants: mean age years (SD); sex	Study Design	Method	Diffusion Indices	Main Findings	Correlation Findings
Bode et al. (2011) [245]	27 ASD (20M:7F): 14.7 (1.6) 26 TD (17M:5F): 14.5 (1.5)	Cross-section	TBSS	FA MD λ1 λ2 λ3	↑ FA in ASD: right temporal lobe.	n/a
Lo et al. (2011) [246]	15 HFA (M): 15.2 (1) 15 TD (M): 15 (0.8)	Cross-section	Streamline tractography: cingulum, arcuate fasciculus, uncinate fasciculus, corpus callosum	GFA	↓ GFA in ASD: corpus callosum.	n/a
Travers et al. (2015) [247]	67 ASD (M): 15.1 (6.96) 42 TD (M): 15.99 (6.46)	Cross-section	ROI	FA MD	n/a	Positive correlation: bilateral inferior corticospinal tract FA & grip strength and ASD symptom severity; whole brain mean FA and superior cerebellar peduncle FA & tapping.
Bakhtiari et al. (2012) [248]	16 ASD (15M:1F): 15.5 (2.8) 18 TD(17M:1F): 15.5 (2) 14 ASD (12M:2F): 28.1 (6.5) 19TD (16M:3F): 28.6 (5.6)	Cross-section	TBSS	FA	↓ FA in ASD adolescents: widespread.	Negative correlations: FA in the inferior fronto-occipital fasciculus & ADOS and ADI-R communication scores; FA in the left superior longitudinal fasciculus & ADI-R communication; FA in the inferior longitudinal fasciculus & ADOS and ADI-R social scores in ASD adolescents. Inferior fronto-occipital fasciculus FA & ADOS communication, ADOS social and ADI-R social; inferior longitudinal fasciculus FA & ADOS social; FA corpus callosum (splenium) & ADI-R communication in ASD adults. Right superior longitudinal fasciculus, left cingulum and left corticospinal tract FA & AQ across all participants. Interaction: group by age.

Study	Participants: mean age years (SD); sex	Study Design	Method	Diffusion Indices	Main Findings	Correlation Findings
Lange et al. (2010) [249]	30 HFA (M): 15.8 (5.6) 30 TD (M): 15.8 (5.6)	Cross-section	ROI: superior temporal gyrus & temporal sulcus	FA MD AD RD	↓ FA in ASD: left superior temporal gyrus ↑ MD, AD and RD in ASD: right temporal sulcus.	Negative correlation: right temporal sulcus RD & performance IQ and language. Positive correlation: left superior temporal gyrus FA & Vineland
Alexander et al. (2007) [250]	43 ASD (M): 16.2 (6.7) 34 TD (M): 16.4 (6)	Cross-section	ROI: corpus callosum	FA MD AD RD	↓ FA and ↑ MD and RD in ASD: corpus callosum.	Positive correlation: FA and performance IQ. Negative correlation: RD and performance IQ. No significant correlation between FA and MD & ADOS-G and ADI.
Lee et al. (2007) [251]	43 ASD (M): 16.2 (6.7) 34 TD (M): 16.4 (6)	Cross-section	ROI: superior temporal gyrus & temporal sulcus	FA MD AD RD	↓ FA and ↑ RD in ASD: bilateral superior temporal gyrus and superior temporal sulcus. ↑ MD in ASD: right temporal sulcus and bilateral superior temporal sulcus; ↑ MD and AD in ASD: right superior temporal gyrus.	Group by age interaction: right superior temporal gyrus FA and AD.
Lee et al. (2009) [252]	43 ASD (M): 16.2(6.7) 34 TD (M): 16.4 (6)	Cross-section	VBM	FA MD	↓ FA and ↑ MD in ASD: corpus callosum; bilateral superior temporal gyrus; anterior cingulate	Negative correlation: corpus callosum FA and MD & processing speed.
Knaus et al. (2010) [253]	14 ASD (M): 16.8 (2.4) 20 TD (M): 14.4 (2.5)	Cross-section	Probabilistic tractography: arcuate fasciculus	FA	No significant differences.	n/a
McGrath et al. (2013) [254]	25 ASD (M): 17.28 (2.87) 25 TD (M): 17.37 (2.67)	Cross-section	Tractography	FA	↓ FA in ASD: right inferior fronto-occipital fasciculus	Negative correlation: FA & mean response time in mental rotation task.
McGrath et al. (2013) [255]	22 ASD (M):17.56 (2.91) 22 TD (M): 17.51 (2.76)	Cross-section	Tractography: left occipital lobe (BA19) to subcortical targets	FA	↓ FA in ASD: tracts connecting BA19 to left caudate head and left thalamus.	Negative correlation: FA and mean response time during a mental rotation task.

Study	Participants: mean age years (SD); sex	Study Design	Method	Diffusion Indices	Main Findings	Correlation Findings
Ikuta et al. (2014) [256]	21 ASD (18M:3F): 18.1 (2.7) TD 18M:3F): 18.2 (2.9)	Cross-section	Probabilistic tractography: cingulum, anterior thalamic radiation	FA MD AD RD	↓ FA in ASD: cingulum.	Negative correlation: cingulum FA & BRIEF score in FA.
Travers et al. (2015) [257]	100 ASD (M): 18.3 (8.5) 56 TD (M): 18.9 (7.8)	Longitudinal	ROI: corpus callosum	FA MD AD RD	↓ FA in ASD: corpus callosum (genu, splenium, body). ↑ MD in corpus callosum (splenium).	Interaction: age by group for FA in the corpus callosum (genu, splenium, body) and MD in the corpus callosum (splenium).
Keller et al. (2007) [258]	34 HFA (M): 18.9 (7.3) 31 TD (M): 18.9 (6.2)	Cross-section	VBM	FA	↓ FA in ASD: corpus callosum (posterior); bilateral corona radiata; right internal capsule.	Age by group interaction: right internal capsule. ↑ right internal capsule FA with age in ASD group compared to reduction in TD.
Travers et al. (2014) [259]	67 ASD (M): 20.4 (6.5) 54TD (M): 20.2 (7.1)	Cross-section	ROI	FA MD AD RD	↓ FA in ASD. ↑ MD, AD and RD in ASD.	Positive relationship: FA and processing speed index across all participants.
Kana et al. (2014) [107]	8 ASD: 21.1 (0.99) 13 TD: 22.3 (1.1)	Cross-section	TBSS	FA	↓ FA in ASD: right temporal lobe.	No association: DTI and fMRI theory of mind results.
Kleinhans et al. (2012) [260]	25 ASD (16M:9F): 21.29 (5.66) 28TD (22M:6F): 21.31 (7.27)	Cross-section	TBSS	FA MD AD RD	↓ FA in ASD: widespread. ↑ MD and RD in ASD: widespread.	Interaction: group by age.
Pugliese et al. (2009) [261]	24 Asperger's (M): 23 (12.4) 42 TD (M): 25 (10.3)	Cross-section	Streamline tractography: Inferior fronto-occipital fasciculus, uncinate fasciculus, cingulum, inferior longitudinal fasciculus, fornix	Number of streamlines FA MD	↑ number of streamlines in ASD: right cingulum.	No correlation: Number of streamlines & age.
Peeva et al. (2013) [262]	18 ASD (15M:3F): 25.6 (9.2) 18 TD (12M:6F): 28.5 (8.7)	Cross-section	Probabilistic tractography: speech network	FA Number of streamlines Tract volume	↓ number of streamlines left supplementary motor area-ventral premotor cortex tracts.	n/a

Study	Participants: mean age years (SD); sex	Study Design	Method	Diffusion Indices	Main Findings	Correlation Findings
Langen et al. (2012) [263]	21 HFA (M): 26 (6) 22 TD (M): 28 (6)	Cross-section	Streamline tractography: fronto-striatal tracts	FA MD AD RD	↓ FA in ASD: bilateral fronto-striatal tracts from putamen. ↑ MD in ASD: right fronto-striatal tracts from nucleus accumbens.	Positive correlation: putamen tract FA & No-go task performance across all participants. No significant relationship within separate groups, and no significant relationship between DTI measures & ADI-R or ADOS.
Conturo et al. (2008) [264]	17 HFA (14M:3F): 26.5 (2.7) 17 TD: 26.1 (2.7)	Cross-section	Streamline tractography: Hippocampus and amygdala to frontal gyrus	AD RD	↓ RD in ASD: right hippocampus to frontal gyrus. ↑ AD and RD in ASD: bilateral amygdala to frontal gyrus; left hippocampus to frontal gyrus.	Positive correlation: right hippocampus to frontal gyrus RD & Benton face recognition and performance IQ.
Thomas et al. (2011) [265]	12 HFA (M): 28.5 (9.7) 18 TD (M): 22.4 (4.1)	Cross-section	Streamline tractography: corpus callosum, inferior longitudinal fasciculus, uncinate fasciculus, inferior fronto-occipital fasciculus	Number of voxels and streamlines	↓ number of voxels and streamlines in ASD: forceps minor; corpus callosum (body). ↑ number of voxels and streamlines in ASD: inferior longitudinal fasciculus; uncinate fasciculus; inferior fronto-occipital fasciculus.	Negative correlation: corpus callosum number of streamlines & ADI-R restricted and repetitive behaviours.
Roine et al. (2013) [266]	14 ASD (M): 28.6 (5.7) 19 TD (M):26.4 (4.7)	Cross-section	TBSS & tractography	FA MD	↑ mean FA in ASD.	Positive correlation: mean FA & AQ attention switching.
Roine et al. (2015) [267]	14 Asperger's (M): 28.6 (5.7) 19 TD (M): 26.4 (4.7)	Cross-section	TBSS & Probabilistic tractography	FA MD RD	TBSS: ↑ FA in ASD. Tractography: ↑ FA in ASD: left inferior longitudinal fasciculus.	TBSS: no significant correlations. Tractography: negative correlation left anterior thalamic radiation FA & empathising quotient.
Thakkar et al. (2008) [268]	12 ASD (10M:2F): 30 (11) 14 TD (8M:6F): 27 (8)	Cross-section	ROI: anterior cingulate cortex	FA	↓ FA in ASD: rostral anterior cingulate cortex.	Negative correlation: Anterior cingulate cortex FA & ADI-R restricted repetitive behaviours.
Catani et al. (2008) [269]	15 Asperger's (M): 31 (9) 15 TD (M): 35 (11)	Cross-section	Tractography: cerebellum	FA MD	↓ FA in ASD: right superior cerebellar peduncle; right short intra-cerebellar tracts.	Negative correlation: FA left superior cerebellar peduncle & ADI-social.

Study	Participants: mean age years (SD); sex	Study Design	Method	Diffusion Indices	Main Findings	Correlation Findings
Lewis et al. (2012) [270]	20 ASD (M): 31.7 (9.5) 20 TD (M): 32.3 (10)	Cross-section	Probabilistic tractography: corpus callosum	RD Fibre length	No significant differences.	n/a
Mueller et al. (2013) [271]	12 HFA (9M:3F): 35.5 (11.4) 12TD (8M:4F): 33.3 (9)	Cross-section	TBSS	FA	↓ FA in ASD.	Positive correlation: right temporo-parietal junction FA & Freiburger personality inventory emotionality score.
Pardini et al. (2009) [272]	10 LFA (M): 35.9 (3.9) 10 TD (M): 19.9 (2.6)	Cross-section	Probabilistic tractography: orbitofrontal cortex	FA Tract volume	↓ FA and tract volume in ASD: left orbitofrontal white matter.	Positive correlation: orbitofrontal cortex FA & performance IQ.
Bloemen et al. (2010) [273]	13 Asperger's (M): 39 (9.8) 13 TD(M): 37 (9.6)	Cross-section	VBM	FA MD RD	↑ RD and ↓ FA in ASD: corpus callosum; bilateral inferior fronto-occipital fasciculus; anterior thalamic radiation; inferior longitudinal fasciculus; arcuate fasciculus; corticospinal tract; cingulum.	n/a

Table 1 Research papers investigating white matter microstructure in ASD using diffusion tensor imaging (DTI) that have been published to date.

Papers are ordered by the average age of the ASD study participants, which are in years unless otherwise stated. Prior studies on unaffected siblings, hemispheric asymmetry, sex-based differences, classification of ASD, and network-based analysis are not included on this table. Abbreviations: axial diffusivity (AD); apparent diffusion coefficient (ADC); autism diagnostic inventory-revised (ADI-R); autism diagnostic observation schedule (ADOS); autism spectrum disorder (ASD); autism quotient (AQ); Brodmann area (BA); behaviour rating inventory of executive function (BRIEF); childhood autism rating scale (CARS); clinical evaluation of language fundamentals (CELF); developmentally delayed (DD); developmentally impaired (DI); fractional anisotropy (FA); functional magnetic resonance imaging (fMRI);

Gilliam autism rating scale (GARS); generalised fractional anisotropy (GFA); high functioning autism (HFA); high risk (HR); intelligence quotient (IQ); low functioning autism (LFA), low risk (LR); mean diffusivity (MD); radial diffusivity (RD); region of interest (ROI); specific language impairment (SLI); social responsiveness scale (SRS); tract-based spatial statistics (TBSS); typically developing (TD); Vineland adaptive behaviour scale (VABS); voxel-based morphometry (VBM); diffusion tensor eigenvalues (λ1) (λ2) (λ3).

3.2.1 Cross-sectional approaches

3.2.1.1 Voxel-based methods

Voxel-based morphometry (VBM) is a voxel-based technique [274] that has been used to investigate white matter microstructure in ASD. VBM studies have been carried out in children [175][217][215][213], adolescents [244][251][237][243][235], and adults [258][273] with ASD. Findings of these VBM studies indicate that white matter microstructure is altered in ASD compared to controls. However, the direction of this is not certain, with studies reporting increased FA and reduced MD [175] and reduced ADC [213], but also reduced FA and increased diffusivity [273][252], reduced FA [244][258][237][235] and increased MD [243] in ASD. Both increased and decreased FA have been reported in different regions of the brain in the same study [217][215]. The direction of the group differences in these VBM findings appears to depend upon the age of the participants, with those studies investigating similar age groups reporting similar results.

Tract-based spatial statistics (TBSS) [157] is an automated method that enables voxel-wise comparison of DTI parameters. TBSS has been applied to DTI scans of ASD children [223][208][226][225][204][212][206], adolescents [245][238][234][229][233], combined adolescent and adult groups [248][260], and adults [271][266][107][267]. These studies have shown increased FA [245][212][266][267], increased FA and reduced RD [204], but also reduced FA [225][208][248][271][107], increased diffusivity [229], and reduced FA and increased diffusivity [223][226][233][260][206] in ASD. Both increased and decreased FA have been reported in different regions of the brain [238][234]. The majority of studies reflect a pattern of increased FA and decreased MD in ASD. There is a less clear-cut explanation for the disparity in TBSS results than for the VBM studies, which suggests that more factors than age influence white matter microstructure in ASD.

3.2.1.2 ROI and tractography methods

ROI methods typically involve overlaying a mask or segmentation of the ROI directly on each scan, either by hand or using an automated method. ROI-based studies have been carried out in children [200][218][209][226][213][224], adolescents [250][251][242][249][231][229][232] and adults [268][259] with ASD. Findings show increased FA [200], and reduced diffusivity [213], but also reduced FA [268][218], increased diffusivity [242][209][229][224], and reduced FA and increased diffusivity [250][251][249][231][226][232][259].

As outlined in Section 2.12.5.2, tractography is used to reconstruct the white matter tracts of the brain. Tractography has been applied to studies of children [207][208][214][220][204][212] [227][228][222][221][219][216], adolescents [253][236][235][246][239][230][256][240][241][254][255], and adults [269][264][272][261][265][263][270][262][266][267] with ASD. Results show reduced FA [269][272][236][235][246][220][227][222][256][254][255], increased diffusivity [228][241], and reduced FA and increased diffusivity [207][208][263][230], but also increased FA [204][266][267], increased FA and increased diffusivity [212][221], reduced diffusivity [214][219]. Both reduced and increased diffusivity have been reported in different white matter tracts in the same study [264]. Increased number of streamlines [261], reduced number of streamlines [262], and both increased and reduced numbers of streamlines [265] have also been reported in ASD compared to controls. No significant group differences were found in some studies [253][270][239][240].

It is evident that the results of tractography and ROI studies in ASD are highly variable. Overall, the majority of the results show significantly altered white matter microstructure in ASD compared to neurotypical controls. The nature of these changes is more commonly that FA is reduced and diffusivity is increased in ASD. However, variability is present, which is likely to be due to the white matter tract

being studied, experimental design (for example, scanner type), and participant demographics, such as age and race. A comparison of like-by-like protocols is therefore important when considering the implications of each study. One point to note is that the correlations with behavioural measures (discussed in Section 3.2.9) indicate that reductions in FA are typically associated with increased severity of ASD traits. This gives greater weight to the FA decreases observed in the majority of these group difference analyses.

3.2.2 Longitudinal approaches and investigations of age

Evidence suggests that white matter tract formation and maturation are complete by early adulthood [275], though the typical white matter developmental process is non-linear [276]. Age-related changes in DTI parameters are widely reported in neurotypical development, with FA increasing and MD falling from early childhood through to early adulthood at different trajectories within each white matter tract (see review by Yap et al. [276]). It is therefore likely that age and developmental stage contribute to DTI findings, as individuals' progress through white matter maturation.

There are very few published longitudinal DTI studies in ASD – the reason for this is that they are expensive and, by virtue of their design, take many years to complete and are technically demanding, requiring careful registration of MR images from different time points, depending on the approach taken. In 2012, Wolff et al. [203] published findings from a longitudinal study of very early development, finding abnormal developmental trajectories for many white matter tracts, including the corpus callosum, inferior longitudinal fasciculus, and uncinate fasciculus, in ASD between the ages of 6, 12, and 24 months. This was characterised by initially elevated FA in the ASD group, which plateaued and then fell, relative to the typical values at 24 months. Travers et al. [259] recently published findings of a longitudinal analysis of the corpus callosum in male children and adolescents, with

an average scan interval of 2.6 years. Findings also indicate that early corpus callosum maturation, as measured by FA and MD changes, follows an aberrant trajectory in ASD.

Some cross-sectional DTI studies in ASD have included a wide age range [200][248]. Age has been shown to influence group differences in white matter microstructure in many studies [200][258][251][229][248][260][206][216][224], and to correlate differently with DTI metrics in ASD and control groups [238][213][233][232]. These results provide support for the hypothesis that white matter development is aberrant in ASD, and that participant age must be taken into account when comparing studies.

3.2.3 IQ

The majority of DTI studies in ASD have focussed on high-functioning subjects. This is mainly due to ethical concerns with obtaining informed consent and scanning low-functioning individuals, increased difficulty obtaining high-quality scans free of motion, and the importance of having directly comparable ASD and control groups. However, as outlined in Section 1.1, ASD often presents in combination with learning difficulties and/or developmental delay. To date, only four DTI studies have investigated white matter microstructure in low-functioning individuals with ASD, with microstructural deficits reported in ASD compared to developmentally impaired [208], developmental delay [175] and typically-developing control [227] groups. Jeong et al. [211] investigated both high-functioning and low-functioning ASD groups, and identified some regions of shared microstructural dysfunction, as measured by reduced FA, in both groups, in addition to more widespread regions of white matter disruption in the low-functioning ASD group. This highlights the greater extent of structural deficits that affect a low-functioning individual above and beyond their ASD diagnosis.

However, Kumar et al. [208] did not identify any significant differences in FA or ADC between ASD and developmentally-impaired ASD groups.

Correlation analyses in high-functioning groups have identified associations between reduced performance IQ and reduced FA in the orbitofrontal cortex [272], reduced FA and elevated RD of the corpus callosum [250], elevated RD of the right temporal sulcus [249], and elevated MD of thalamo-cortical tracts [241]. However, reduced performance IQ also correlated with reduced RD of right hippocampo–frontal white matter tracts [264] and reduced AD in the left cingulum [212]. This suggests that the nature of any association between IQ and microstructure is dependent upon the white matter tract of interest. Widespread differences in the localisation of FA–performance IQ correlations have been observed between ASD and neurotypical control groups [277], suggesting that ASD affects the typical pattern of association between brain structure and intellectual function.

3.2.4 Hemispheric asymmetry

As can be seen from many of the studies featured in Table 1, there is evidence that white matter tracts in each hemisphere of the brain are differently affected in ASD – for example, Sivaswamy et al. [209] reported bilateral superior cerebellar peduncle DTI alterations in children with ASD, while the results in Catani et al. [85] were restricted to the right cerebellar peduncle in adults with ASD. However there does not appear to be a consistent and confirmed directionality to hemispheric asymmetry in ASD. Lange et al. [249] and Lo et al. [246] investigated hemispheric asymmetry in more detail, and identified that ASD was not characterised by hemispheric asymmetry *per se*, rather a reversal or loss of the typical pattern of hemispheric asymmetry observed in the white matter microstructure of healthy controls. This seems particularly apparent for the arcuate fasciculus [242][253][278][279], a tract involved in language that is typically lateralised.

3.2.5 White matter microstructure as a biomarker of autism

Several studies have been published in recent years investigating whether an individual can be classified as 'ASD' or 'non-ASD' based on their white matter microstructure, as measured using DTI. Classification needs to be both sensitive to ASD and specific – i.e. the classifier must be able to distinguish someone with ASD from an individual with a similar neurodevelopmental disorder, such as ADHD. Uddin et al. [280] and Ingalhalikar et al. [281] achieved diagnostic accuracies of ~85% when classifying children, whilst Lange et al. [249] reported 94% sensitivity and 90% specificity in a sample of children and adults. A recent study identified DTI metrics as key classifiers in a multi-modal classification system that achieved 92% classification accuracy in adults [282]. These studies indicate that white matter microstructure is a useful tool in the identification of ASD-related brain anomalies, and that it may have potential as a biomarker. However, each of these studies included healthy control and ASD participants, and did not attempt to classify ASD in comparison to other neurodevelopmental disorders. Further work is therefore needed to estimate the utility of DTI as a biomarker of ASD for mixed participant samples.

3.2.6 White matter microstructure as an endophenotype of autism

DTI studies investigating brain structure in the unaffected siblings of autistic probands have been published in recent years, with the aim of examining whether connectivity is an endophenotype of ASD [223][203][283][284]. White matter microstructure in siblings of probands and the results of these studies are discussed in Chapter 8, which includes a TBSS study of white matter microstructure in unaffected siblings.

3.2.7 Studies of sex-based differences

As discussed in Section 1.1, ASD is far more likely to affect males compared to females. Chapter 8 describes an investigation of sex-based differences in white

matter microstructure in ASD, therefore prior studies of the effects of biological sex on brain structure in ASD [285][286][287][288] are discussed in that chapter of this thesis.

3.2.8 Studies of brain networks in ASD

Very recently several studies have taken a holistic approach to exploration of the network of structural connections in ASD [289][283][290][291][292][293]. This has been made possible with the advent of graph theoretical analysis techniques. The network approach and the results of published studies in ASD are discussed in Chapter 7 of the thesis, in which graph theory is applied to the investigation of whole brain and limbic structural networks in young adults with ASD.

3.2.9 Associations between structural and diffusion-weighted MRI measures and ASD traits

As shown in Table 1, there is evidence to suggest that the severity of ASD traits is associated with white matter microstructure in clinically-diagnosed populations. Greater ASD severity, as measured by the ADI-R, has been shown to correlate with reduced white matter coherence, as measured by FA, in white matter tracts of adults and children with ASD [238][265][220]. Bakhtiari et al. [248] found several more specific associations between reduced FA of several white matter tracts and ADOS social, ADI-R social and ADI-R communication scores, a finding that was similarly observed by Catani et al. [85] for left superior cerebellar peduncle FA and ADI social score. Likewise, increased severity of ADI-R restricted and repetitive behaviours have been shown to correlate with reduced anterior cingulate cortex FA [268]. Poustka et al. [220], Hanaie et al. [219], and Nair et al. [241] provided evidence for similarly negative correlations between white matter tract FA and ADOS scores. Correspondingly, Abdel Razek et al. [205] recently reported a correlation between increased diffusion in temporal lobe white matter and elevated score on the childhood autism rating scale (CARS). Worse outcomes on the social responsiveness

scale (SRS) were associated with reduced coherence of dorsolateral prefrontal cortex tracts [237], and the anterior thalamic radiation and uncinate fasciculus (as measured by FA) [226]. All these studies indicate that reductions in the microstructural coherence of the white matter, as measured by DTI metrics, are associated with greater ASD severity.

Associations between reduced coherence of white matter microstructure and ASD traits have also been reported in less frequently-used metrics of autistic behaviours, including joint attention [202], executive function deficits, as measured by the BRIEF [256], adaptive functioning deficits, as measured by the Vineland, [249], emotion regulation, as assessed by the Freiburger personality inventory emotionality score [271], daily living skills [211], motor score [222], more specific motor functions – grip strength and tapping performance [247], functional processing anomalies [294], processing speed [252], longer reaction time [234][254][255], and language function [212][221]. These findings indicate that correlations exist between brain structure and a greater array of traits associated with ASD than merely social communication ability, and that the microstructure of many specific certain WM tracts are implicated in these functions. This indicates that there is specificity and selectivity to associations between ASD traits and white matter microstructure.

Significant correlations between DTI measures of white matter microstructure and ASD severity have not been detected by all studies [207][223][231][214][225] [260][227][263][107]. There is evidence that the outcome of a correlation analysis depends upon the behavioural/psychological metric employed. For example, Alexander et al. [250] found correlations between DTI metrics and performance IQ, but not with ADI and ADOS-G. This may reflect subtleties in the association between the microstructure of a white matter tract and specific ASD traits, or it may be indicative of statistical inadequacies in certain metrics that make them less suitable for correlation analyses (e.g. the ADOS is a categorical variable with a small

range of scores, and is therefore less appropriate for a correlation study than measures such as the IQ which are semi-continuous and have a greater range). Sample size, and the method used to identify and assess white matter microstructural deficits may also influence the outcome of association studies. For example, Roine et al. [267] identified significant DTI–symptom associations using tractography but not TBSS. This indicates that methodology influences findings, and that association results may be affected by the use of tract of interest vs voxel-based or whole white matter averaged measures of white matter microstructure.

Additionally, some studies have found that the association between white matter microstructure and ASD traits is opposite to the direction typically reported: For example, Cheung et al. [217], identified several associations between worse ADI-R scores and reduced white matter coherence (as measured by reduced FA) in children with ASD, but conversely the study also identified an association between increased FA and worse ADI-R communication scores. Ke et al. [215] reported that increased right frontal FA was correlated with worse ASD symptoms, as measured by the CARS. Additionally, Roine et al. [267] showed that reduced left anterior thalamic radiation FA was associated with greater empathy, as measured by the empathising quotient. A further study demonstrated that diffusivity of right hippocampo-frontal tracts (as measured by RD) was correlated with Benton face recognition score, such that greater diffusivity associated with better performance [264]. These studies are suggestive of a greater complexity to the relationship between white matter microstructure and ASD behaviours. There does not appear to be a common thread between each of these studies – two are VBM methods in children [217][215] and the other two are tractography-based studies in adults [264][267]. Therefore, the specifics of white matter–ASD associations require further investigation.

3.2.10 Studies in neurotypical populations

Autism is known to comprise a spectrum of symptoms and severities [26][295][296]. This spectrum exists both within the realm of clinically-diagnosed cases and, to a less debilitating extent, within the population at large. It is therefore of interest to examine the incidence of ASD-like traits within the general population, and whether these traits are correlated with features of the brain. Two DTI studies specifically investigating structural correlates of ASD traits in healthy individuals have been published to date. Iidaka et al. [297] identified a positive correlation between imagination, as measured by the AQ, and the volume of white matter tracts connecting the superior temporal sulcus and the amygdala in healthy individuals. This means that reduced volume of these white matter tracts was associated with weaker imagination, which is characteristic of ASD. Hirose et al. [298] used TBSS to demonstrate that reduced FA was correlated with higher AQ scores, and thus greater incidence of ASD traits in widespread regions of the white matter. Tractography of the superior temporal sulcus localised the correlation between FA and AQ to the inferior fronto-occipital fasciculus in this region. This study is suggestive of more widespread associations between white matter microstructure and ASD traits in healthy individuals than would have otherwise been anticipated.

Some studies have investigated correlations in typical subjects as an adjunct to their investigation of such a relationship in subjects with ASD. Alexander et al. [250] report a negative correlation between corpus callosum FA and SRS scores in a heterogeneous sample of neurotypical and ASD children and adults. Bakhtiari et al. [248] identified a negative correlation between AQ score and FA of the right superior longitudinal fasciculus, left cingulum, and left corticospinal tract across all study participants (both ASD and neurotypical). Similarly, Nagae et al. [228] reported an association between increased bilateral superior longitudinal fasciculus MD and worse CELF-4 scores (a measure of language function) across all study participants; a finding that was not altered by inclusion of a group by CELF-4 interaction term, thus indicating that group did not alter the association. Both of

these studies indicate that deficits in white matter microstructure, as measured by FA and MD, particularly those affecting the superior longitudinal fasciculus, are associated with ASD traits. Travers et al. [259] reported a positive correlation between average whole white matter FA and processing speed across all participants in their study, again with no FA by group interaction, which suggests that a lower processing speed, which is associated with ASD, is related to reduced FA of the white matter, on average. Langen et al. [263] showed a positive correlation between putamen tract FA and performance in a No-Go task across all participants, meaning that reduced FA was associated with poorer task performance, and thus relatively impaired ability for cognitive inhibition. Each of these studies provides evidence that ASD traits are present in the neurotypical population, and that these are related to white matter microstructure. This is supportive of the concept of a spectrum of ASD.

3.3 Summary

In summary, MRI techniques can be used to investigate brain structure in ASD, both in terms of brain volume and the microstructural integrity of the white matter. The number of MRI studies in ASD has increased in recent years. Results indicate that overall and regional brain volumes differ in ASD, and that the microstructural features of structural connections within the brain are significantly different in ASD compared to the neurotypical profile. The most consistent findings are of elevated brain volume in ASD, and reduced white matter coherence – as evidenced by reduced FA and elevated MD – in ASD. However, there is a great deal of variability in findings. This is likely to depend on research methodology, participant demographics, and the brain region under investigation. Correlational analyses indicate that features of structural connectivity are related to symptom severity. Further work is needed to fully elucidate the picture of brain structure in ASD.

3.4 The aims of this thesis

The principal aim of this thesis is to assess the microstructure of the white matter in ASD, and to investigate possible associations between white matter microstructure and ASD traits. High-functioning individuals have been selected for this analysis. This does prevent investigation of the whole clinical population of ASD sufferers, but it enables mitigation of the effect of IQ on brain structure, and ensures a homogenous research cohort. Ancillary to this overarching aim are several questions that this thesis aims to explore: what are the nature of any microstructural differences in ASD? Are connections within the social brain disproportionately affected? Do these microstructural alterations occur in all cases of ASD, or are they more common or severe in males vs females or children vs adults? Does white matter microstructure act as a biomarker of ASD? Do white matter measures reflect an endophenotype of ASD or enhanced vulnerability in families of ASD sufferers? Is there evidence in support of the various neural theories of ASD outlined in Section 1.3? Do one or more of these theories appear to best fit the evidence?

Several approaches have been employed in order to resolve these aims in this thesis: In Chapter 5, TBSS is used to study white matter microstructure in young adults with ASD. The white matter tracts that are most different in the ASD group are identified, and associations with ASD traits investigated with reference to the spectrum of presentations. This study is supplemented by the work outlined in Chapter 8, in which TBSS is applied to the investigation of sex-based differences in white matter microstructure in children with ASD, and a study of white matter microstructure in the unaffected siblings of probands. This work enables investigation of the 'extreme male brain' theory of ASD and whether an endophenotype or familial vulnerability to ASD or ASD-related structural brain alterations exists (see Section 1.1 for more detail on these concepts). In Chapter 6, a more particular focus is placed on the microstructure of connections within the social brain in ASD, and whether the connectivity of amygdala sub-regions relate differently to particular ASD traits, including an investigation of putative links with

the theory of mind and emotion recognition theories of ASD. Chapter 7 reflects a more universal view, and reports on an investigation of the network of structural connections in ASD, thus facilitating an examination of the disconnection and weak central coherence theories of ASD (see Section 1.3 for an outline of these theories). The chapters of work that comprise this thesis combine to form an investigation of white matter microstructure in ASD, and the association between brain structure and behaviour.

3.5 Hypotheses

In light of the previous studies highlighted within this chapter, my hypotheses are:

a) That white matter microstructure will be adversely affected in ASD, and that this will differ between children and adults due to neurodevelopmental processes, and between the sexes due to disparity in the susceptibility to ASD between males and females.
b) That these microstructural deficits will be more pronounced in those connections that join social regions of the brain.
c) That white matter microstructure will be associated with ASD behaviours and that more severe symptoms will be associated with greater changes to the brain structure, but that the nature of the relationship will depend upon the functions of each given white matter tract.
d) That siblings will show increased vulnerability to ASD traits and increased white matter microstructural deficits compared to controls without a family history of ASD.
e) That the work described in this thesis will corroborate the concepts described in several of the neural theories of ASD, but that the complex nature of ASD and its causes will preclude any one theory from dominating.

Chapter 4 Methods

This chapter outlines the methods involved in data collection, cognitive testing, and MRI scan processing at the UCL Institute of Child Health for the experimental work described in Chapter 5, Chapter 6, and Chapter 7 of this thesis. Additional information regarding specific analysis techniques are provided in the respective chapters.

The experimental work outlined in Chapter 8 of this thesis was carried out during a 3-month exchange visit to Yale University during the PhD. Specific methods related to that analysis, including participant recruitment and MRI scan sequences, are outlined within Chapter 8.

4.1 Study approval

The study was approved by the local Ethics committee (REC reference 11/LO/0044) and accepted by UCL/GOSH R&D. All participants gave written informed consent, and were told of their right to withdraw from the study at any time. Participant confidentiality was maintained at all times, and identifiable participant data stored in locked cupboards and encrypted hard drives.

4.2 Participants

Participant recruitment was carried out in 2011-2012, led by Juejing Ren, a PhD student in the Behavioural and Brain Sciences Unit (BBSU) at the UCL Institute of Child Health, with assistance from myself. Twenty-six young adults previously diagnosed with an autism spectrum disorder (ASD) were recruited to the study, in addition to 25 neurotypical control participants. Recruitment was carried out via advertisements in local autism support groups and local Universities. None of the

participants had a history of neuropsychiatric disorders, including anxiety, attention deficit hyperactivity disorder, depression, or epilepsy. Age and handedness were obtained upon recruitment via a questionnaire, and are shown with other participant demographics in Table 2.

	Control (n = 26)	ASD (n = 25)
Gender	21M:5F	21M:4F
Handedness	26R:0L	23R:2L
Age (yrs)[1]	24.73 (4.10) [18.83 – 33.30]	23.22 (4.05) [18.31 – 31.90]
Full-scale IQ[1]	122.00 (7.98) [105 – 138]	119.4 (11.59) [94 -136]
Verbal IQ[1]	119.73 (9.01) [102 – 136]	116.84 (12.56) [84 – 135]
Performance IQ[1]	118.73 (7.07) [103 – 129]	117.36 (11.04) [88 - 135]
AQ[1]	13.35 (7.81) [4 - 37]	36.56 (6.53) [22 - 49]
ADOS[2]	-	9.22 (4.11) [3 – 20]

Table 2 Participant demographics and cognitive test scores.

[1] Data are expressed as mean (standard deviation) [range]. [2] Combined social and communication sub-scores.

4.3 Cognitive testing

4.3.1 IQ

Full-scale, performance, and verbal intelligence quotient (IQ) scores were obtained for all participants using the Wechsler abbreviated scale of intelligence (WASI)

[299], which consists of four sections: vocabulary, block design, similarities, and matrix reasoning. IQ scores for participants are summarised in Table 2. All participants had an IQ >80.

4.3.2 AQ

All participants completed the autism quotient (AQ) [26], a self-reported questionnaire with 50 questions probing social skills, communication ability, and capacity for attention switching, attention to detail, and imagination. The AQ is a semi-continuous measure, covering the dimensionality of autistic traits across the entire population from healthy through to severely autistic. Higher scores are associated with greater autistic traits; typically, scores greater than 32/50 are associated with clinical diagnosis of ASD, however there is no fixed cut-off value. Scores for each of the five domains of the AQ can also be investigated separately in order to assess the pattern of autistic traits in an individual. The overall AQ scores for participants are outlined in Table 2. The relationship between scores in the AQ and specific measures of brain structure were investigated in Chapter 5, Chapter 6, and Chapter 7 of this thesis.

A limitation of the AQ is its self-report nature, which is reliant on candid answers from participants who may lack insight, want to minimise symptoms or feel compelled to respond in a way that they believe is expected from them. The chances of this were reduced by giving the participants time and privacy to complete the form, and assuring them that their answers would remain confidential.

4.3.3 ADOS

Charlotte Sanderson, a PhD student in the BBSU at the UCL Institute of Child Health conducted the autism diagnostic observation schedule (ADOS) [11] module 4 with all of the participants recruited to the ASD group in order to confirm

eligibility for participation in the study. The ADOS module 4 is a semi-structured interview designed to test for the presence of deficits in communication, reciprocal social interaction, and imagination/creativity, in addition to the presence of stereotyped behaviours and restricted interests. Scores are given for a variety of behaviours and abilities, typically ranging from 0 – no clinical concerns – through to 2 – severe impairments. These scores are entered into an algorithm in order to provide a total score in each category. As discussed in Section 1.1.3, a score indicative of autism or an autism spectrum disorder on the ADOS is informative, and facilitated confirmation of eligibility to this study, but does not form the sole basis for a clinical diagnosis, which is the outcome of interviews and assessments with a variety of specialists.

Following administration of the ADOS, one participant recruited to the ASD group was excluded from all analyses because their diagnosis could not be ratified. This left a total of 25 participants in the ASD group. The sum of scores in the social and communication sections of the ADOS give an overall indication of the outcome of the ADOS, and are summarised in Table 2.

4.4 MRI scanning

MRI scanning was performed by research radiographer Tina Banks at Great Ormond Street hospital (GOSH). An MRI safety questionnaire was completed by all participants prior to scanning in order to screen for MRI-incompatible conditions, such as pregnancy or the presence of non-MR-safe medical implants, and to ensure the removal of any loose metallic objects. All participants received whole-brain MRI on a 1.5T Siemens Magnetom Avanto Scanner (Siemens, Erlangen, Germany) with 40mT/m gradients. A 12-channel receive head coil was used. The scanning protocol lasted a total of 30-40 minutes, consisting of a localiser (~30 seconds), T_1-weighted scan (5 minutes), resting-state fMRI (8 minutes), task-based fMRI (12 minutes), and a diffusion-weighted scan (8 minutes).

Analysis of the T_1-weighted and diffusion-weighted data is the foundation of this thesis. All T_1-weighted and diffusion-weighted data were visually inspected for abnormalities, motion and other artefacts. No anomalies were discovered. All scans were converted from DICOM to NIfTI format using TractoR version 2.1 [300].

The fMRI data were analysed by PhD student Juejing Ren and will not be discussed in this thesis. A description of the fMRI task is included here because the quantitative outcome of the task was investigated in relation to structural measures of the brain, as outlined in Chapter 6.

4.4.1 T_1-weighted scans

The T_1-weighted scan was acquired using a three-dimensional FLASH sequence (see Section 2.6.2 for more sequence information) using the following parameters: flip angle=15°; TR=11 ms; TE=4.94 ms; voxel size=1mm isotropic; slices=176. The T_1-weighted scans were processed using the following techniques:

4.4.1.1 SIENAX

Whole brain, total grey matter and total white matter were segmented on the T_1-weighted scans using the FMRIB software library (FSL) tool SIENAX [301] [302] (see Figure 34). SIENAX begins by extracting the brain from the skull and neck image. The brain-extracted image is then affine-registered to Montreal Neurological Institute and Hospital (MNI)152 space. Affine registration is a linear registration step that aligns two images via rotation, scaling, and transformation of the voxels from the input scan to those of the reference scan. The skull image is used to determine the scaling of the registration step, thus calculating the scaling factor required for normalisation of brain volume with respect to head size. A person with

a larger head typically has a concomitantly large brain, and *vice versa*, which can mask any differences in relative brain volume; normalisation of brain volumes with respect to head size ensures that regional volumes can be accurately compared between individuals. SIENAX then uses partial volume estimation to segment tissue types. Raw whole brain, grey matter, and white matter volumes, and those normalised for head size, are generated. Group comparisons of whole brain volume, calculated using linear regression with age, gender and full-scale IQ as covariates due to their relationship with brain size, are described in Chapter 5 and Chapter 7. Whole brain volumes are used as a covariate in analyses described within Chapter 5-Chapter 8.

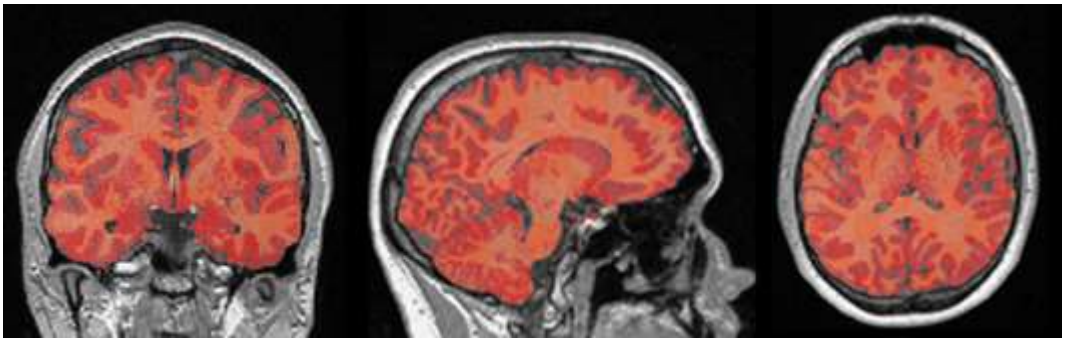

Figure 34 An example SIENAX rendering of the brain overlaid on a T_1-weighted scan.

Coronal (left), sagittal (middle), and axial (right) views are shown. The SIENAX rendering is displayed in red, with darker red for grey matter and lighter red showing white matter.

4.4.1.2 FIRST

Subcortical grey matter structures, including the amygdala, caudate, globus pallidus, hippocampus, nucleus accumbens, putamen, and thalamus, were segmented on the T_1-weighted scans using the FSL tool FIRST [303] (see Figure 35). FIRST begins by affine-registering all scans to the MNI152 standard-space template in two steps: initially, registration to the entire template, and then registration to a subcortical mask of the template in order to optimally align the subcortical

structures. FIRST then uses shape and appearance models that have been generated from manually-traced masks in combination with signal intensity information in order to guide segmentation of each subcortical grey matter structure. The intensity of the voxels is used in this process because the subcortical grey matter structures have a much lower intensity compared to surrounding white matter (see Section 2.7.1 for more information), and are thus partly distinguishable using the contrast in T_1-weighted scans. Boundary correction is the final stage in the FIRST process, and operates to correct any overlapping voxels. Volumes for each ROI were obtained using FSL utilities [304].

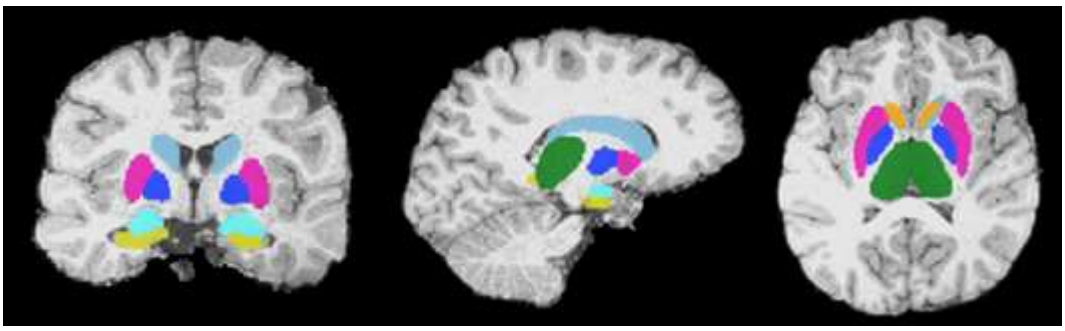

Figure 35 An example FIRST output overlaid on a T_1-weighted scan. Coronal (left), sagittal (middle), and axial (right) views are shown. Subcortical structures in both brain hemispheres are segmented as follows: caudate (mid blue), nucleus accumbens (orange), putamen (magenta), globus pallidus (dark blue), thalamus (green), amygdala (bright light blue), hippocampus (yellow).

All registrations and segmentations were visually inspected for accuracy. In the study participants, several registration failures occurred using the standard procedure. This was most likely due to the presence of large neck regions in some scans confounding the FIRST algorithm. In order to prevent these registration failures, the FIRST process was modified (cf. [305]), such that the T_1-weighted scans were firstly brain-extracted in order to isolate the brain image from the neck and skull. The transformation required to align the T_1-weighted scan with the MNI152

template was estimated using the brain image. FIRST was then carried out on the original whole-head scan using the transformation calculated with the brain image in place of the original transformation matrix. This modification successfully prevented any registration errors, so was applied to the entire cohort in order to maintain a standardised protocol across participants. After testing the various options, a boundary correction method of 'none' was selected in order to prevent gaps and overly-exclusive crops to the outlines of the ROIs. The FIRST ROIs are included in the analysis described in Chapter 7. The amygdala ROIs obtained using FIRST are discussed in Chapter 6.

4.4.1.3 FreeSurfer

Cortical grey matter structures were segmented using FreeSurfer [306] (see Figure 36). FreeSurfer firstly removes non-brain tissue, including the skull and neck, from the T_1-weighted scans. The brain images are then registered to Talairach standard space, and subcortical grey and white matter structures segmented. The intensity of the T_1-weighted scans is normalised in order to remove any inconsistencies in signal intensity across the image, which can occur as a result of magnetic field inhomogeneities or noise. The boundaries between grey matter/white matter and grey matter/CSF are then estimated via identification of large shifts in voxel intensity. This process delineates the cerebral cortex, which is then parcellated into 68 ROIs based on gyral and sulcal structure [307].

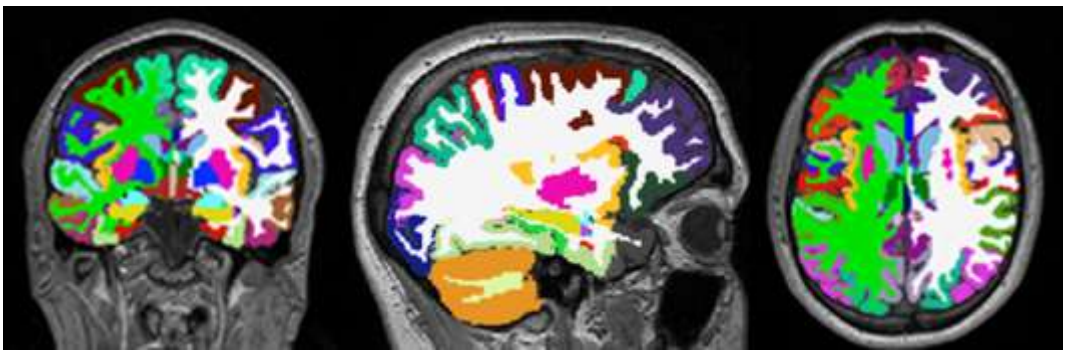

Figure 36 An example FreeSurfer output overlaid on a T_1-weighted scan. Coronal (left), sagittal (middle), and axial (right) views are shown. Cortical grey matter is seen segmented in a rainbow of colours, with each colour representing one of the 68 cortical regions. White matter is shown in bright green (right hemisphere) and white (left hemisphere), and subcortical grey matter structures are also visible.

All registrations and segmentations were visually checked. Poor segmentation of anterior temporal lobe structures was observed, which appeared to result from misclassification of white matter voxels in this region. FreeSurfer uses 'control points' to indicate white matter voxels during its processing stages. In order to combat the segmentation error, the normalisation step of the typical FreeSurfer pipeline was modified to increase the signal intensities included when estimating control points, thus including more of the misclassified white matter. The number of iterations used in the normalisation step was also increased. This revised protocol greatly improved the cortical segmentation by FreeSurfer, therefore all participants' data were analysed using the adjusted pipeline in order to maintain consistency. The FreeSurfer cortical ROIs were used in the analyses detailed in Chapter 6 and Chapter 7.

4.4.2 Diffusion-weighted scans

The diffusion-weighted scan protocol consisted of a twice-refocused spin echo diffusion-weighted EPI sequence with 60 unique gradient directions (b=1000 s/mm^2)

(see Section 2.11 for background on the sequence). Three images without diffusion weighting (b=0) were interleaved. The sequence parameters were: TR=7300 ms; TE=81 ms; voxel size=2.5mm isotropic; 60 axial slices. The diffusion-weighted data were pre-processed using TractoR which formed a wrapper around FSL version 4.1 [308]. The first step in pre-processing is the selection and brain-extraction of the first reference b=0 scan volume from each participant [309]. Following that, the diffusion-weighted scan volumes were registered to the brain-extracted reference volume in order to correct for eddy current distortions. A diffusion tensor was derived at each voxel using a standard least-squares process. This resulted in generation of voxel-wise calculations of FA, MD, RD and AD.

FSL's BEDPOSTX [310] was applied to each of the diffusion-weighted scans in order to estimate the orientation and magnitude of diffusion, and thus infer white matter fibre orientations, within each voxel. BEDPOSTX uses a ball-and-sticks model, which allows for estimation of up to two white matter fibre directions per voxel (the 'sticks') in addition to the amount of free water diffusion within the voxel (the 'ball'). A limitation of the ball-and-two-sticks model is that it cannot accurately distinguish crossing white matter tracts from those that 'kiss' i.e. tracts that touch, but do not cross over. Recent advances aimed at resolving 'kissing' fibres from crossing fibres, and future directions for diffusion-weighted imaging are outlined in Chapter 9. Head motion has been reported to affect the results of diffusion-weighted studies in ASD [311]. Therefore, plots of estimated head motion during the diffusion-weighted scan were visually inspected. This is discussed in Chapter 5.

4.4.3 Task-based fMRI scans

The fMRI task was a version of 'reading the mind in the eyes' [312][313], in which participants viewed images of eyes and were asked to identify the person's emotional state from a choice of four descriptions (see Figure 37). All participants were familiarised with the emotion descriptions prior to scanning. A control task

was included in which participants were required to assess the age of the person from the picture of their eyes, thus capturing brain activations as a result of viewing the image which could be subtracted from the brain activations arising from the emotion recognition task. Participants viewed alternate blocks of 10 emotion estimations and 10 age assessments, with three blocks of each in total. The order in which each task block was presented was randomised. Participants correctly identifying more emotions received a higher score. The relationship between emotion recognition scores and structural brain measures is explored in Chapter 6 and Chapter 7 of this thesis.

Figure 37 An example emotion recognition question in the 'reading the mind in the eyes' fMRI task.

4.5 Correlation of brain structure with clinical severity

Associations between ASD traits and measures of brain structure and microstructure are investigated throughout the thesis. All correlations were partial, with age, gender, and full-scale IQ included as covariates. Where appropriate, the volumes of ROI, such as un-normalised whole brain volume and amygdala volume were also included as covariates. These parameters were selected as covariates because they have previously been shown to influence DTI parameters [250][314][315][316] and could thus confound findings.

Scores in the AQ and the 'reading the mind in the eyes' fMRI task were used as estimates of ASD traits in the correlation analyses. As outlined in section 4.3.2, the AQ measures the extent of autistic traits displayed by both neurotypical controls and individuals with ASD in social, communication, attention switching, attention to detail, and imagination domains. The AQ and 'reading the mind in the eyes' were chosen due to their applicability to both healthy and ASD populations, the inclusion of several ASD-related behaviours, and their semi-continuous structures; all of which make them an ideal tool for assessing ASD traits in the whole study population, and for subsequent correlation with structural measures.

Chapter 5 White Matter Microstructure and Autistic Traits

The work reported in this chapter has been published in *NeuroImage:Clinical*, 2014 [317]. Please see Appendix C: Publication Attributed to Thesis for a copy of the paper.

5.1 Introduction

As outlined in Chapter 3, autistic symptoms are thought to arise from aberrant neurodevelopment in childhood. Early excessive brain growth [166] is thought to be followed by a decline in growth rate during later childhood, such that adolescents and adults with ASD have a similar whole brain volume to neurotypical controls, as measured by MRI [167]. This abnormal neurodevelopmental profile is likely to result in aberrant brain connectivity in ASD. Social and communication functions, which are impaired in ASD, are mediated by specialized brain regions that are connected into co-operative networks, including the limbic system [318] and mirror neuron systems [319]. The limbic network is supported structurally by white matter tracts, including the cingulum, inferior longitudinal fasciculus (ILF) and arcuate fasciculus [320][85]. The white matter connections underlying the mirror neuron system, which is made up of frontal motor areas, posterior parietal cortex and the superior temporal sulcus [321], are less-well defined, but are likely to include the cingulum and superior longitudinal fasciculus (SLF) [320][85]. These structural underpinnings to brain networks involved in socially-motivated behaviours suggests that autistic symptoms are caused or maintained by abnormal white matter microstructure.

DTI provides information about white matter microstructure using measures of water diffusion in tissue [154] (see Section 2.12 for background information). Most previous DTI studies of ASD have been carried out in children and adolescents. The

majority have reported decreases in FA and increases in MD compared to neurotypical controls [244][261][243][233]. Such changes are indicative of aberrant white matter and may represent irregular organization of white matter tracts, relatively low axon density and/or deficient axon myelination [322]. Age-related changes in DTI parameters are widely reported in neurotypical development, with FA increasing and MD falling from early childhood into adolescence and early adulthood (reviewed in [276]). It is likely that age and developmental stage contribute to DTI findings in ASD studies of children and adolescents as they progress through the developmental process [260]. Thus, heterogeneity in age may explain contradictory reports that children with ASD have increased FA [200][204]. Evidence suggests that brain maturation, in terms of white matter tract formation, is virtually complete by early adulthood [275]; studies of white matter maturation, in terms of FA and MD, show that the majority of FA and MD changes occur prior to 30 years of age, though maturation trajectories differ in each white matter tract and some tracts do not peak until approximately 40 years [323][324]. Some DTI studies have been conducted with adults included in the cohort, but samples have often been heterogeneous in terms of age, which may confound their findings [250][258][260]. The typical white matter developmental process is non-linear [276] and is therefore difficult to control for. Thus, in order to reduce age-related heterogeneity this study focussed on a relatively homogeneous adult population.

Previous DTI investigations of ASD adults have tended to employ voxel-based techniques, including statistical parametric mapping (SPM), or ROI-based techniques, such as deterministic tractography which follows pathways of maximal diffusion in order to trace white matter tracts. Findings in adults with ASD using these techniques include reduced FA in the corpus callosum, which mediates cross-talk between the two cerebral hemispheres [268]. Reduced corpus callosum FA was also reported in a combined sample of children and adults with ASD [250]. Reduced FA in adults with ASD has been further reported in the inferior fronto-occipital fasciculus (IFOF), uncinate fasciculus [261] and cerebellar white matter tracts [269].

Increased MD, another marker of altered white matter microstructure, has been measured in the ILF and cingulum [261]. Co-localised reductions in FA and increases in RD have been reported in frontal, medial, temporal and parietal brain regions [273]. Alterations in the number of streamlines obtained using tractography have been reported in the ILF, IFOF, uncinate fasciculus and corpus callosum [265].

A limitation of techniques such as deterministic tractography and other ROI methodologies is that their interpretation requires a prior hypothesis. Only those white matter tracts pre-selected as ROIs can be subject to analysis; thus white matter alterations that occur in other tracts will not be observed. Voxel-based methodologies are limited by partial volume which can arise from registration error and smoothing techniques [325][157]. In contrast, there are advantages to employing tract-based spatial statistics (TBSS) [157], an automated method that enables voxel-wise comparison of white matter parameters, including FA and MD. Like other voxel-based techniques, TBSS removes the requirement for prior determination of tracts of interest, but TBSS additionally moderates registration errors and reduces partial volume effects. It achieves this by aligning the FA data from each subject to a common space before extracting a white matter skeleton comprising the core of the white matter voxels, thus excluding the more variable voxels at the extremities of the white matter [157] [326]. TBSS has been applied to DTI scans of children and adolescents with ASD, and white matter tract alterations have been reported compared to controls [229][245][225][233][232][204][208][223][238][237][234]. Recently, Kleinhans et al [260] applied TBSS to a combined adolescent-adult cohort, with findings showing widespread reductions in FA and increases in MD and RD. This study is the first time that TBSS has been used to study brain structure in a purely adult cohort of ASD.

Clinical characteristics of ASD are often considered to occur at the extreme of a continuum of social and communication skills found in the general population

[26][295][296]. Some evidence indicates that the severity of ASD traits is related to white matter microstructure in clinical populations: for example, a negative correlation has been shown between FA and Autism Diagnostic Interview-Revised (ADI-R) restricted and repetitive behaviour score in the cingulum of adults with ASD [268]. Catani et al. [269] reported a negative correlation between ADI-R social score and FA of the left cerebellar peduncle in adults diagnosed with Asperger's syndrome. However, correlations between white matter characteristics and measures of ASD severity have not been supported by all studies [223] [231] [260]. Some groups have investigated whether the presence of sub-clinical ASD traits in neurotypical populations is correlated with white matter microstructure characteristics. Alexander et al. [250] reported a negative correlation between abnormalities in corpus callosum FA and social responsiveness scale (SRS) scores in a heterogeneous sample of neurotypical and autistic children and adults. Kumar et al. [208] reported a positive correlation between ASD traits and tract volume of the left uncinate fasciculus, and Iidaka et al. [297] identified a positive correlation between ASD traits and the volume of white matter tracts connecting the superior temporal sulcus and the amygdala in healthy individuals. Both studies suggest that larger white matter tract volume is associated with more severe ASD-like symptoms in neurotypical subjects. Further work is needed to confirm a) whether the relationship between white matter microstructure and ASD traits is a continuous spectrum between clinical ASD and neurotypical populations, b) if any association between white matter microstructure and autistic symptoms holds true for all ASD characteristics, and c) which regions and characteristics of white matter microstructure are most associated with particular autistic traits. These questions form the aim of the work reported in this chapter.

IQ has been shown to correlate with white matter microstructure [250] and is therefore likely to influence, or be influenced by, DTI parameters. In light of this high-functioning individuals were recruited to the study in order to minimise any confounds from IQ, thus enabling the investigation of ASD-specific effects.

5.2 Methods

The methods used for MRI acquisition and whole brain volume estimation are outlined in Chapter 4. Two-tailed t-tests were used to compare demographic measures between groups. Group comparison of normalised whole brain volumes were calculated using linear regression with age, gender and full-scale IQ as covariates.

5.2.1 Tract-based spatial statistics

TBSS was carried out using FSL version 4.1 [308]. All participants' FA data were projected onto a mean FA image using the non-linear registration tool FNIRT. The registered data was thinned to create a mean FA skeleton that was restricted to voxels with the highest FA; these voxels typically occur at the centre of the major white matter tracts. Following visual assessment of the optimal threshold, the skeleton was thresholded at FA=0.2 in order to remove any voxels that had a low FA, and were therefore unlikely to represent white matter. Each participant's aligned FA data were projected onto the skeleton and voxel-wise cross-participant statistics were applied using non-parametric permutation testing within TBSS. Age, gender, full-scale IQ and un-normalised whole brain volume were entered as covariates. The vast number of statistical tests made in each voxel of the white matter skeleton during TBSS increases the probability of a significant p-value occurring by chance. Therefore, results were corrected for multiple comparisons using family wise error (FWE) correction, in which each p-value is adjusted in light of the number of statistical tests performed, thus reducing the likelihood of false positives. Threshold-free cluster enhancement (TFCE) was applied, as per the TBSS protocol. TFCE compares neighbouring voxels in order to identify clusters of similar voxels; this increases confidence that each voxel's results are genuine and not an isolated chance occurrence. Only clusters surviving FWE $p<0.05$ are reported. The locations of significant clusters were determined using the FSL atlas tools [327]. This

process was repeated for MD, RD and AD. TBSS fill was used for visualization purposes in figures.

FSL tools were used to ascertain those white matter tracts that were most significantly different between the ASD and neurotypical groups. A skeletonised version of the John's Hopkins University (JHU) ICBM-DTI-81 atlas was overlaid on top of the TBSS results in order to localise each voxel to its white matter tract. In each tract, the number of voxels with significant group differences in FA and/or MD was recorded. To control for tract size, the number of significant voxels was normalized as a percentage of the total number of voxels within that tract. Any significant white matter voxels that lay outside the JHU ICBM-DTI-81 atlas were recorded as 'unclassified white matter'.

5.2.2 Averaging DTI measures within the TBSS skeleton

In order to investigate the average properties of the white matter in each participant's brain, mean values for each DTI metric were calculated across the whole white matter skeleton. Group comparisons of mean FA, MD, RD and AD were made using linear regression with age, gender, full-scale IQ and un-normalised whole brain volume as covariates.

5.2.3 Correlations between DTI metrics and clinical scores

The Lillie test was used to estimate the normality of the data. Due to non-normality of the AQ data, Spearman correlation was used to correlate DTI parameters averaged across the whole white matter skeleton with overall AQ score. Since AQ measures the extent of autistic traits in both neurotypical controls and individuals diagnosed with ASD, it is an ideal tool for assessing symptoms in the whole study population. The overall AQ score comprises results in social, communication, attention switching, attention to detail, and imagination domains. In order to obtain

a more detailed analysis of the relationship between white matter microstructure and autistics traits, Spearman correlation was subsequently used to investigate the relationship between the average white matter skeleton diffusion parameters and each domain of the AQ score. The high number of statistical tests involved in this domain-based correlation analysis increases the likelihood of incurring false positives by chance. In order to reduce the chance of this, false discovery rate (FDR) multiple comparisons correction was applied, in which each p value is divided by the total number of significant p values; only p values <0.05 after correction were considered significant. Correlations were carried out in a combined sample of all subjects in order to investigate whether any relationship between ASD traits and white matter microstructure applied across the entire study population in a continuous manner, as would be anticipated in a spectrum.

In order to assess whether this continuous model appropriately explained any relationship between white matter microstructure and autistic behaviours, the similarity of the relationship between DTI parameters and AQ across all subjects was compared to the relationship observed within each group. ANCOVA was used to model both the intra- and inter-group relationships between AQ and white matter microstructure, with age, gender, full-scale IQ and un-normalised whole brain volume as covariates. A group term was included in the ANCOVA in order to model the AQ-white matter relationships once group effects were taken into account. Following this, regression slopes from each fit were plotted and pairwise t-tests were used to statistically compare the slopes. These analyses enabled the investigation of whether correlations between AQ and white matter microstructure were driven by the within-group and/or between-group differences, and to test for presence of the Simpson-Yule paradox, which states that aggregated data can reveal a trend that is not representative of relationships within sub-groups.

In order to locate the white matter regions that were contributing to the correlations, voxel-wise DTI measures were correlated with AQ across all subjects using TBSS. Only clusters surviving TFCE $p<0.05$ are reported.

All correlations were partial, with age, gender, full-scale IQ and un-normalised whole brain volume included as covariates.

5.3 Results

5.3.1 Demographics

Due to outlying scores on all DTI metrics averaged from the TBSS white matter skeleton one control participant was excluded from the analyses that follow in this chapter. Their diffusion-weighted scan was examined for quality purposes, and no errors or anomalies were observed. Attempts were made to re-run the TBSS protocol to see if this would result in a more sensible estimation of the white matter skeleton and resulting DTI metrics, but outlying results were still obtained. Thus, it was concluded that the participant's data could not be adequately processed using TBSS and should be excluded from the TBSS analyses. The demographics for the remaining participants are shown in Table 3. Two-tailed t-tests showed no significant group differences in age, verbal IQ, performance IQ or full-scale IQ. AQ was significantly higher in the ASD group, with an overlap in scores between the groups.

	Control (n = 25)	ASD (n = 25)	t-statistic	p value
Gender	20M:5F	21M:4F	-	-
Handedness	25R:0L	23R:2L	-	-
Age (yrs)[1]	24.50 (4.02) [18.83 – 33.30]	23.22 (4.05) [18.31 – 31.90]	1.12	0.27
Full-scale IQ[1]	122.08 (8.02) [94 – 138]	119.4 (11.59) [94 -136]	0.95	0.35
Verbal IQ[1]	120.44 (8.43) [106 – 136]	116.84 (12.56) [84 – 135]	1.19	0.24
Performance IQ[1]	118.40 (7.01) [103 – 129]	117.36 (11.04) [88 - 135]	0.40	0.69
AQ[1]	13.60 (7.86) [4 - 37]	36.56 (6.53) [22 - 49]	-11.23	<0.0001
ADOS[2]	-	9.22 (4.11) [3 – 20]	-	-

Table 3 Participant demographics and cognitive test scores.

The results of group comparisons using paired t-tests are shown. [1] Data are expressed as mean (standard deviation) [range]. [2] Combined social and communication sub-scores.

5.3.2 Brain volume

Linear regression analysis controlling for age, gender and full-scale IQ showed no significant group differences in whole brain volume (t=-0.69; p=0.49), total grey matter volume (t=-0.80; p=0.43) or total white matter volume (t=-0.36; p=0.72).

5.3.3 Average DTI measures from the white matter skeleton

FA values averaged across the whole white matter skeleton in each subject were significantly lower in the ASD group compared to controls (t=-3.54; p=0.001), whilst MD (t=2.78; p=0.008) and RD (t=3.32; p=0.002) were significantly elevated in the ASD group. There were no significant group differences in AD (t=0.98; p=0.33).

5.3.4 Voxel-wise DTI measures from the white matter skeleton

The voxel-wise group comparison between ASD and controls showed widespread clusters of significantly reduced FA in the ASD group ($p<0.05$; TFCE-corrected) (see Figure 38A). This included white matter tracts bilaterally in the frontal, temporal, parietal and occipital lobes, in addition to the corpus callosum. The same group-wise comparison for MD showed similarly widespread increases of MD in the ASD group compared to controls (Figure 38B). This was comparable to those seen in the FA comparison, though the fornix did not contain any significant clusters and affected voxels were more widespread in the temporal lobe and the right cingulum. Widespread significant increases in RD in the ASD group compared to controls were observed in a very similar pattern (Figure 38C). No significant group differences in AD were detected.

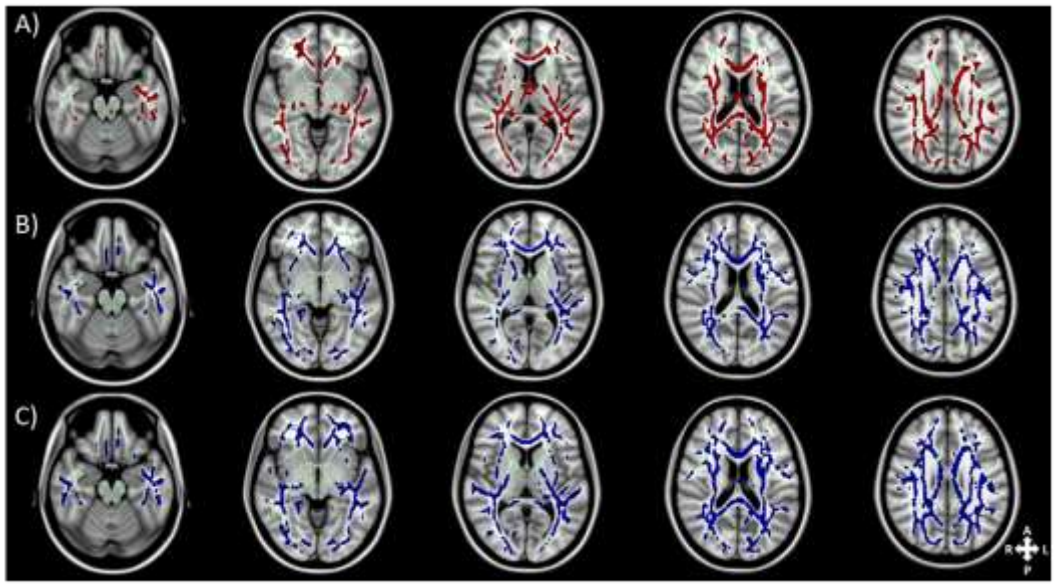

Figure 38 Axial slices of the cohort's mean white matter skeleton (green) overlaid with the TBSS results.

The figure shows (A) red clusters depicting white matter voxels with significantly lower fractional anisotropy (FA) in subjects with autism spectrum disorder (ASD) compared to healthy controls ($p <0.05$; FWE-corrected). (B & C) Blue clusters showing regions with significantly higher mean diffusivity (MD) (B) and radial diffusivity (RD) (C) in ASD compared to controls ($p <0.05$; FWE-

corrected). There were no significant differences in axial diffusivity (AD) between the two groups. TBSS fill was used for visualization.

Table 4 shows the 20 white matter tracts, as outlined by the JHU-ICBM-DTI-81 atlas, which had the highest percentage of voxels showing significantly reduced FA and elevated MD in the ASD group in comparison to neurotypical controls. White matter tracts key for long-range pathways in the brain, such as the corona radiata, superior longitudinal fasciculus (SLF), and the corpus callosum contained large areas with significant group differences in white matter microstructure. Tracts involved in social processing, such as the fornix, ILF and IFOF also presented with large proportions of affected white matter microstructure in ASD. In white matter not encompassed by the atlas, 29.69% had significantly reduced FA in ASD compared to neurotypical controls, whilst 30.27% showed significantly elevated MD.

White Matter Tract	Proportion of Voxels with Significantly (p<0.05) Reduced FA in ASD (%)	White Matter Tract	Proportion of Voxels with Significantly (p<0.05) Reduced MD in ASD (%)
Left tapetum	100	CC – genu	80.25
Right tapetum	100	Left SFOF	79.49
Left SFOF[a]	89.74	Left sagittal stratum[b]	77.55
Right retrolenticular IC[a]	80.84	Right sagittal stratum	75.17
Right superior Cr[a]	79.97	Left SLF	71.20
Right PTR[a]	79.59	Right posterior CR	64.64
CC[a]- genu	76.99	Left PTR	63.59
Fornix – column and body	76.61	Left retrolenticular IC	62.26
Left fornix – stria terminalis	72.78	Right anterior CR	60.86
Left PTR[a]	72.39	Left anterior CR	60.04
Left UF[a]	68.85	Right PTR	58.20
CC – splenium	68.40	Right retrolenticular IC	56.47
Right posterior CR	67.86	Right SLF	55.59
Right SLF[a]	67.02	Left superior CR	54.12
Left superior CR	62.21	Right superior CR	53.89
CC – body	58.62	Left posterior CR	51.20
Right SFOF	58.57	Left external capsule	47.19
Left posterior CR	57.28	Left fornix – stria terminalis	46.84
Left SLF	56.90	CC – body	42.64
Left retrolenticular IC	56.29	Right external capsule	40.58

Table 4 The 20 white matter tracts in the skeletonized JHU-ICBM-DTI-81 atlas which had the greatest proportion of voxels showing significantly reduced FA and significantly elevated MD in ASD compared to neurotypical controls.

[a] Abbreviations: CC (corpus callosum); CR (corona radiata); IC (internal capsule); L (left); PTR (posterior thalamic radiation); R (right); SFOF (superior fronto-occipital fasciculus); SLF (superior longitudinal fasciculus); UF

(uncinate fasciculus). [b] Sagittal stratum includes the inferior longitudinal fasciculus (ILF) and inferior fronto-occipital fasciculus (IFOF).

5.3.5 Relationship between DTI measures and clinical scores

In the entire study population, whilst controlling for age, gender, full-scale IQ and whole brain volume, FA averaged over the whole white matter skeleton was negatively correlated with AQ (rho=-0.42; p=0.003). Highly significant positive correlations were observed between MD and AQ (rho=0.44; p=0.001) and RD and AQ (rho=0.46; p=0.0008). A weaker positive correlation was seen between AD and AQ (rho=0.22; p=0.12). Figure 39 contains plots of the correlations. One control participant had a high AQ score (an indication of autistic traits that approach clinical significance). Despite a small reduction in the significance of the correlations, regression slopes excluding that participant were very similar to regression slopes found whilst including them, thus the participant was left in the analyses.

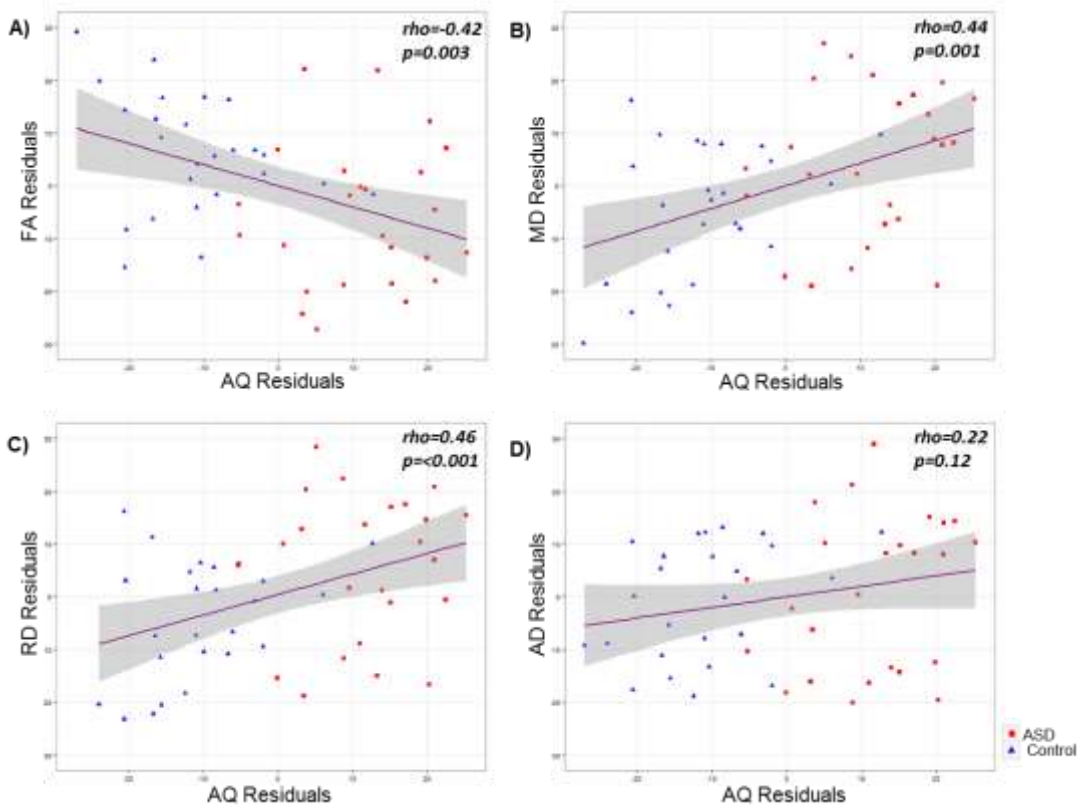

Figure 39 Scatter plots showing results of partial Spearman correlations controlling for age, gender, full-scale IQ and whole brain volume.

Red squares denote participants diagnosed with an autism spectrum disorder (ASD); blue triangles represent neurotypical controls. Grey shading shows the standard error of the fit. (A) A significant negative correlation between autism quotient (AQ) and fractional anisotropy (FA) (rho = -0.42; p = 0.003) in addition to significant positive correlations for AQ with (B) mean diffusivity (MD) (rho = 0.44; p = 0.001) and (C) radial diffusivity (RD) (rho = 0.46; p = 0.0008). (D) There was a weak positive correlation between AQ and axial diffusivity (AD) (rho = 0.22; p = 0.12).

ANCOVA was used to model whether correlations between white matter microstructure and autistic traits, as measured by the AQ, were driven by within-group and/or between-group differences, and to test for presence of the Simpson-Yule paradox. Results identified a significant positive relationship between MD and AQ across the entire study population (F=4.38; p=0.04). There was a non-significant

positive correlation between AD and AQ across all subjects (F=3.85; p=0.06). This relationship applied within groups even after the between-group differences in AQ, MD and AD measures were taken into account. There was no significant relationship between the AQ and FA (F=0.29; p=0.59) or RD (F=2.65; p=0.11) after taking into account the significant group differences in these measures. This means that the relationships between ASD traits and FA and RD are mainly driven by the between-group differences in these measures, as opposed to within-group differences. No interaction between slope and AQ was found for any of the DTI measures, meaning that the Simpson-Yule paradox does not apply. In Figure 40, plots of regression slopes from correlations across all study participants are shown alongside regression slopes from within-group correlations. The slopes of the regressions look similar, if slightly more consistent in the neurotypical controls. Two-tailed t-tests showed that the slopes in the ASD and neurotypical control groups were not significantly different from one another (FA: t=0.88; p=0.38; MD: t=-1.10; p=0.28; RD: t=-1.34; p=0.19; AD: t=-1.34; p=0.19). This indicates that the AQ-white matter relationships are consistent across the spectrum from neurotypical controls through to autism. However, the regression slopes for the AQ-FA and AQ-RD relationships within the ASD group do appear more different from the same slopes within the control and combined groups. Variance was higher in the individual groups, particularly the ASD group, as would be expected.

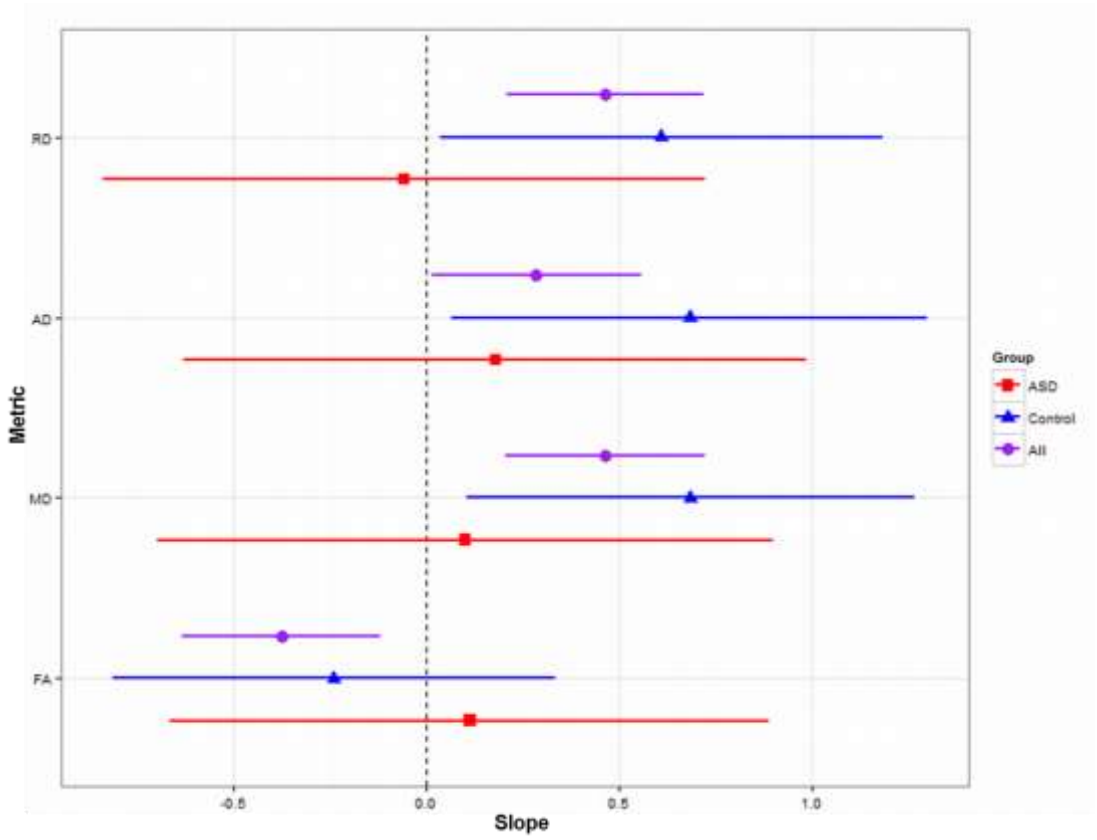

Figure 40 Plots of regression slopes arising from partial Spearman correlations between DTI metrics and AQ.

Results are shown across all participants (purple circle), and within ASD (red square) and neurotypical control (blue triangle) groups separately. All correlations controlled for age, gender, full-scale IQ and whole brain volume. Points represent the value of the regression slope; lines show the 95% confidence interval of the fit. The plots show greater variance in the separate groups, particularly the ASD group. Slopes were similar for correlations in the combined sample in comparison with correlations in the separate groups: two-tailed t-tests showed no significant differences between the slopes of the correlation fits in any of the DTI metrics (all $p > 0.05$).

Voxel-wise analysis in TBSS of correlations between the diffusion measures and AQ, controlling for age, gender, full-scale IQ and whole brain volume, indicated widespread clusters throughout the white matter of the left hemisphere and

bilaterally in the occipital lobe with a significant ($p<0.05$; FWE-corrected) positive correlation between AQ and MD (Figure 41A). There was a significant positive correlation between AQ and RD in a limited number of voxels from the SLF in the left hemisphere only (Figure 41B). There were no significant voxel-wise correlations between AQ and either FA or AD.

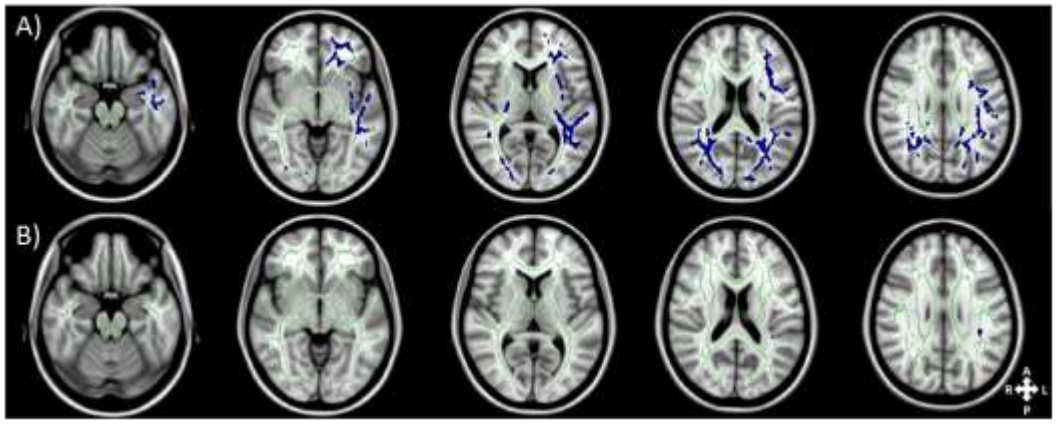

Figure 41 Axial slices of the group white matter skeleton (green) overlaid with blue clusters showing white matter voxels in which autism quotient (AQ) is positively correlated ($p <0.05$; FWE-corrected).
Results show (A) mean diffusivity (MD) widespread through the left hemisphere and bilaterally in the occipital lobe and (B) with radial diffusivity (RD) in voxels of the left hemisphere forming part of the left superior longitudinal fasciculus (SLF). There were no significant correlations between AQ and fractional anisotropy (FA) or axial diffusivity (AD).

Partial correlations between sub-domains of AQ and diffusion measures averaged across the whole white matter skeleton, controlling for age, gender, full-scale IQ and whole brain volume, are summarized in Table 5. There were significant negative correlations between FA and the AQ social, communication and attention switching domains. MD and RD showed highly significant positive correlations with the AQ social, communication, attention switching and imagination domains. The only significant correlation for AD was with the imagination domain.

AQ Domain	DTI Metric	rho	p value[a]
Social	FA	-0.39	**0.006**
	MD	0.38	**0.007**
	RD	0.42	**0.003**
	AD	0.15	0.32
Communication	FA	-0.46	**<0.001**
	MD	0.40	**0.004**
	RD	0.44	**0.002**
	AD	0.14	0.32
Attention Switching	FA	-0.52	**<0.001**
	MD	0.40	**0.004**
	RD	0.47	**<0.001**
	AD	0.07	0.64
Imagination	FA	-0.28	**0.05**
	MD	0.40	**0.004**
	RD	0.39	**0.006**
	AD	0.31	**0.03**
Attention to Detail	FA	-0.24	0.10
	MD	0.31	**0.03**
	RD	0.28	**0.05**
	AD	0.24	0.10

Table 5 Correlations across both groups between AQ sub-scores and DTI parameters averaged throughout the white matter skeleton.

[a]p values were adjusted for multiple comparisons using false discovery rate correction. Those p values remaining significant ($p < 0.05$) after FDR correction are displayed in bold text.

5.4 Discussion

The work presented in this chapter reports on an investigation of white matter microstructure in adults with ASD, and the relationship between white matter microstructure and the spectrum of autistic traits across clinical and non-clinical populations.

The first major finding of the study was of very widespread white matter disruption, as measured by FA, MD, and RD, in the group diagnosed with ASD in comparison to neurotypical controls. No significant group differences in AD were identified. These results are compatible with Kleinhans et al.'s [260] recent report of widespread white matter anomalies in a heterogeneous cohort of adolescents and adults with ASD using TBSS. The finding of widespread white matter aberrations in ASD adults is also consistent with the results of previous voxel-based and tractography studies in adults showing ASD-related white matter anomalies in temporal lobe and cortico-thalamic tracts [251]; limbic tracts, such as the cingulum, fornix and uncinate fasciculus [261]; the arcuate fasciculus [228]; tracts of the mirror neuron system, such as the arcuate fasciculus and IFOF [261]; and in the corpus callosum which connects the two cerebral hemispheres [250][268][265]. The analysis was not limited to prior regions of interest and so is able to demonstrate the widespread nature of white matter anomalies in ASD. The relative contribution of particular white matter tracts to the group difference in white matter microstructure was assessed, and results showed that large proportions of tracts that link widespread regions of the brain were affected in ASD. These included the superior fronto-occipital fasciculus, corpus callosum, internal capsule and corona radiata. Tracts associated with social processing were also majorly affected, including the fornix and uncinate fasciculus for FA, and the ILF, IFOF, and to a lesser extent, the fornix for MD. However, limbic tracts were not singularly affected to extent which would have been expected based on previous ROI-based studies. This suggests that the structural deficits associated with ASD are more wide-reaching than previously hypothesised. This is intuitive, since many deficits associated with ASD, such as

imagination difficulties, repetitive behaviours and a lack of flexibility, are likely to require the recruitment of several brain regions, and the interpretation of complex and rapid social situations involves many interconnected neural regions.

Reductions in FA and increases in MD are thought to reflect reduced organization of the white matter, reduced axonal density, and/or reduced myelination, [154][322] although the precise biology underpinning particular FA and MD values cannot be determined due to restrictions in the resolution of DTI. Elevated RD represents increased water diffusion perpendicular to axon bundles, which may reflect reduced axon density, increased axon diameter, increased membrane permeability [328] and/or reduced myelination [329]. Maintenance of AD coupled with an increase in RD could signify reduced axon myelination [329] or increased membrane permeability [328]. These observations are suggestive of involvement of processes responsible for the myelination and preservation of axons in development of ASD, though this is outside the remit of DTI.

Another major finding was that white matter microstructure, as measured by reduced FA and increased MD and RD, correlated with ASD symptom severity in the entire study sample. Correlations within each group were very similar in strength to corresponding correlations within all subjects. This finding indicates that there is a relationship between white matter microstructure and autistic symptoms, and that it is consistent across the spectrum of symptoms, from clinically-severe autism through to controls with no social difficultly. ASD, particularly in highly-functioning individuals, is often considered to be at the extreme of a continuum of social and communication skills [26][295][296]. Our findings provide support for the hypothesis that dimensionality of ASD traits is closely related to white matter microstructure. This finding is compatible with Alexander et al. [250] who indicated that there was a dimensional relationship between corpus callosum microstructure and ASD traits in a combined clinical and non-clinical sample of adolescents and

adults. It is also consistent with previous studies that have reported correlations between ASD traits and white matter tract volume in neurotypical young adults [208][297]. Further, the results ally with prior reports of correlations between ASD severity and greater white matter disruption within adult ASD groups [268][269][265]. The results of the ANCOVA indicated that the white matter measures had different associations with ASD traits across the study population, with FA more associated with the large inter-group differences in AQ, and MD more related to the gradual continuum of autistic traits. Taken together, these results support the concept of a dimensional relationship between white matter microstructure and ASD symptomatology in young adults; however a threshold or watershed of white matter changes, as measured by FA and RD, appears to be associated with clinically-severe symptoms. This finding also suggests that different white matter changes affect white matter function, and thus autistic behaviours, in different ways. This could be studied using high-resolution techniques and histological analyses.

In order to identify any specificity in the relationship between autistic behaviours and white matter microstructure, sub-domains of the AQ were correlated with each white matter metric. The correlation between FA and ASD traits was strongest for social, communication and attention switching domains and weakest for imagination and attention to detail. This supports the concept of distributed white matter connectivity influencing flexibility, social and communication ASD behaviours. MD and RD also showed strong associations with the core social and communication features of ASD and with attention switching and imagination. Interestingly, MD had a stronger relationship with imagination than with social ability. This is in contrast to FA and RD which were more strongly related to social skills. These results indicate that MD is more strongly associated with a wider complement of ASD traits, including imagination, than FA which is more linked to attention switching and the core social-communication ASD behaviours. A

disconnect between FA and MD correlation results was also observed by Catani et al. [269]. This work provides further evidence for the nature of this disconnect.

The widespread nature of the white matter anomalies found in this study is perhaps surprising given that the participants are all high-functioning. Further, the group comparisons and correlations between ASD traits and white matter microstructure were independent of IQ which was well matched between groups and controlled for in all statistical tests. The relationships identified in this study between white matter microstructure and the severities of ASD impairments are thus independent of general cognitive ability. The finding of a disconnect concerning the relationship between white matter microstructure and social cognition from general cognition is consistent with evidence that corpus callosum agenesis is associated with increased incidence of ASD traits, but no significant difference in IQ scores [330]. This disconnect may occur as a result of differences in the way in which social cues and behaviours are processed in comparison to the logical processing required for the IQ test. Evidence suggests that social and communication processing involve co-ordinated activation of a network of brain areas in both hemispheres [318][319]. This need for recruitment of dispersed brain regions during social processing means that white matter abnormalities are likely to have a negative impact on effective communication between these regions of the 'social brain', and hence may explain the strong relationship between white matter microstructure and ASD traits which is independent of IQ. Kanwisher [331] reviews evidence suggesting that several social functions, including face recognition and thinking about another person's thoughts, are localized to functionally specialised brain regions, each of which will need to communicate via white matter tracts. Additional recent evidence indicates that intelligent cognition may occur via multiple networks [332], suggesting that some element of duplication may provide a 'back-up' for functions required for the IQ test. This finding supports the hypothesis that ASD is associated with a deficit in understanding social situations, which are often complex, rapid, and context-dependent, alongside relative sparing of the capacity for logic and attention to detail

– skills that are probed by cognitive tests. Further work investigating the separation between IQ and social cognition would shed light on this.

No significant differences in whole brain, total grey matter or total white matter volume were found between the groups. This is consistent with previous reports that brain volumes of adults with ASD are similar to those of neurotypical controls [166][167], implying that alterations in the structural wiring of the brain underpin ASD symptomatology to a greater extent than brain volume itself.

At present only post-mortem studies could confirm the exact nature of the white matter changes reported here, since DTI cannot resolve single axons. The values of white matter indices in our participants are variable. This variability may be reduced by larger sample sizes, but does limit the usefulness of DTI measures as biomarkers of change at an individual level. Findings indicate that there could be a threshold of white matter change required for clinically-significant ASD symptoms, and studies with larger sample sizes would be useful when testing this hypothesis. A larger sample size would also provide greater power to investigate hypotheses. The AQ is a self-report measure, which may affect its validity, and a correlation does not mean that a causal relationship has been identified. Further study could include a combination of DTI and fMRI, which would enable analysis of the relationship between white matter microstructure and brain activity in ASD, and relationships between ASD traits and both brain structure and function. This would enable elucidation of the holistic relationship between structural and functional brain characteristics and ASD behaviours.

5.5 Conclusion

In conclusion, the findings of this study indicate that the spectrum of ASD traits in the study population is related to a spectrum of white matter characteristics, and

that white matter anomalies are more severe in those diagnosed with ASD. Tracts involved in functions such as social and communication processing and attention switching ability are implicated. There may be a threshold of effect. IQ was maintained in the individuals included in this study, thus the findings imply that there is a dissociation between white matter features linked to IQ-related abilities and the white matter characteristics associated with ASD traits.

Chapter 6 Structural Connectivity of the Amygdala in Autism

The work reported in this chapter utilises tractography to analyse the structural connectivity of the amygdala in ASD. The amygdala is sub-divided based on connectivity to the cortex, and the association between these white matter connections and autistic traits was investigated.

6.1 Introduction

Impairments in the recognition of emotional facial expressions and in 'theory of mind' — which includes the ability to ascribe emotional states to others — are typical in ASD. Lesion studies have shown that the amygdala is involved in the recognition of emotionally-charged facial expressions, in particular fear [333], and in the acquisition of 'theory of mind' abilities during development [334]. This association between the amygdala and emotional intelligence suggests that changes in the amygdala play a pivotal role in the development and maintenance of autistic behaviours [335]. Current evidence is somewhat ambiguous: structural MRI studies report both amygdala enlargement [180][181] and reduction [115][182] in ASD, and fMRI studies have identified both hypoactivation [108] and hyperactivation [336] of the ASD amygdala in response to social cues. Nonetheless, amygdala volume has been related to the severity of autistic symptoms across a variety of measures [337][186], and longitudinal MRI studies have consistently identified early accelerated amygdala growth in ASD [184][185].

The amygdala is structurally connected to other brain regions via a network of white matter tracts that enable it to fulfil its functions; linking the amygdala, and its ability to process emotional stimuli, to sensory regions that receive inputs and regions that mediate physiological responses. As outlined in previous chapters, DTI provides biomarkers of white matter microstructure [154]. Despite evidence highlighting the importance of the amygdala in ASD, and functional connectivity

studies suggesting that the autistic amygdala is 'wired' differently (e.g. [338][339]), surprisingly few DTI studies have investigated the structural connectivity of the amygdala in ASD. Noriuchi et al. [237] reported significantly reduced FA in white matter surrounding the amygdala in children with ASD, and Jou et al. [235] observed reduced FA in the inferior longitudinal fasciculus and the inferior fronto-occipital fasciculus (IFOF) (both of which connect temporal lobe structures, including the amygdala). Radua et al. [340] conducted a meta-analysis of voxel-based morphometry studies in ASD and reported elevated volume in the IFOF and the uncinate fasciculus, which links the temporal and frontal lobes; this is in contrast to Ecker et al. [341] who showed reduced volume of the IFOF and the uncinate fasciculus in ASD. This study uses DTI tractography to addresses the lack of research into the structural connectivity of the amygdala in ASD, and directly investigates the relationship between these structural connections and autistic behaviours.

Studies of animal and human pathology have shown that the amygdala comprises several nuclei (e.g. [342][343][344]), each associated with a unique cytoarchitecture and specialised function: for instance, pyramidal cells within the lateral nucleus mediate stimulus-effect memory [345], and behavioural responses to stimuli are thought to arise in the central nucleus [346]. Some amygdala–cortical projections are nucleus-specific: for example, the lateral nucleus connects to medial orbitofrontal, parainsula, and temporal cortices [347], whilst the central nucleus is connected to the brainstem [348]. Recent tractography studies in healthy adults have reported that it is possible to segment the amygdala into sub-regions *in vivo* using white matter connectivity-based parcellation schemes: Bach et al. [349] used a k-means algorithm to parcellate the amygdala into two clusters based on connectivity to the ventromedial pre-frontal cortex and the temporal pole; Saygin et al. [344] used expressions describing expected connections between amygdala nuclei and cortical targets in order to sub-divide the amygdala into four clusters, which were in good agreement with manual tracing on a high-resolution T_1-weighted image. Sub-

division of the amygdala enables identification of voxels that share similar connectivity, and determines whether similarly-connected voxels lie adjacent to one another in defined clusters. It is likely that the type and strength of cortical projections from each amygdala sub-region are related to different amygdala functions.

Evidence suggests that sub-regions of the amygdala are cytoarchitectonically altered in ASD [350][351]. In this study, sub-division of the amygdala enables exploration of whether the structural connectivity of amygdala sub-regions is different in ASD, and if this is associated with particular autistic traits. A 'winner takes all' method was selected [352] which identifies the target a voxel maximally connects to, and uses this information to divide structures into clusters of voxels with the same 'winning' target. This removes the need to decide on the number of clusters in advance, as is necessary with k-means clustering, and allows the data to drive the results, as opposed to imposing prior expectations on the underlying anatomy. The aim was not to validate or replicate amygdala nuclei as identified using post-mortem dissection and cytoarchitecture, which is beyond the limits of current diffusion MRI on standard clinical MRI systems applied to humans *in vivo*; the intention was to apply a robust data-driven parcellation scheme to investigate pathways of amygdala–cortical connectivity, whether they can be distinguished in sufferers of ASD compared to neurotypical controls; and in order to dissect out those amygdala–cortical connections most strongly associated with autistic traits. Parcellation of the amygdala on the basis of cortical connectivity enables one to look beyond amygdala–cortical connectivity as a whole, and permits the identification those areas of the amygdala that are most similar in their gross-level cortical connectivity. This approach facilitates identification of whether amygdala voxels that share the same 'winning' cortical target lie adjacent to one another in defined clusters, which would support evidence that different portions of the amygdala are predisposed towards particular patterns of connectivity and different functions. To

the best of my knowledge this is the first time that amygdala sub-structure and structural connectivity has been investigated in ASD.

To summarise, the amygdala is highly important for the recognition, interpretation, and response to emotional stimuli; abilities which are impaired in ASD. ASD-related amygdala abnormalities have been reported in MRI studies, however amygdala connectivity has been relatively understudied in this population. Histopathological investigations have indicated that the amygdala is sub-divided into regions, each with specific connectivity profiles and functions. The aim was to investigate amygdala–cortical connectivity, and to explore the relationship between particular amygdala–cortical connections and autistic traits using *in vivo* white matter tractography. Studying amygdala connectivity enhances understanding of the biological basis of ASD symptomatology.

6.2 Methods

6.2.1 Participants

Twenty-five high-functioning young adults with autism and 26 age-matched neurotypical controls were recruited locally, as outlined in Section 4.2. Scores for the AQ [26] sub-domains: social skills, communication ability, capacity for attention switching, attention to detail, and imagination were correlated with brain measures in this study. Emotion recognition scores from the 'Reading the Mind in the Eyes' fMRI task [312][313], in which participants viewed images of eyes and were asked to identify the person's emotional state from a choice of four emotional descriptors, were also correlated with structural brain measures in this study. Participant scores for the emotional component of the task were higher in subjects who accurately identified the emotion being portrayed in the picture. Two-tailed t-tests were used to compare demographic measures between groups.

6.2.2 Data acquisition and pre-processing

Data acquisition and pre-processing proceeded as described in Chapter 4. FSL's BEDPOSTX [308]. was applied in order to estimate diffusion parameters within each voxel using a ball and two sticks model, thus allowing for estimation of up to two white matter fibre directions per voxel [310].

6.2.3 Region of interest segmentation and volume estimation

Whole brain volume was calculated on the T_1-weighted scans using the FSL tool SIENAX [301][302], as outlined in Section 4.4.1.1.

Left and right amygdala volumes were calculated on the T_1-weighted scans using the FSL tool FIRST [303], as described in Section 4.4.1.2. The amygdala regions of interest were separated from the other FIRST subcortical segmentations and amygdala volume estimated using FSL utilities. Amygdala volume was compared between groups using linear regression with age, gender, full-scale IQ and whole brain volume as covariates.

Cortical grey matter was segmented into 68 regions of interest using FreeSurfer [306], which is described in Section 4.4.1.3. These cortical grey matter regions of interest were grouped into frontal, parietal, occipital, temporal, and insula lobes using FSL utilities.

6.2.4 'Winner takes all' amygdala parcellation

All regions of interest were registered from T1 space into diffusion space using a combination of FSL's linear registration tool FLIRT [353] and non-linear method FNIRT. All registrations were visually assessed.

TractoR was used to seed probabilistic tractography from each amygdala voxel using the five ipsilateral cortical regions of interest as targets, and the contralateral target as an exclusion mask in order to prevent streamlines from crossing the midline. 5000 streamlines were seeded from each amygdala seed voxel. Since tracking was propagated in both directions from the seed voxel, only portions of the streamlines that proceeded from the seed in the direction of the target and terminated at the target were retained. The numbers of streamlines connecting every amygdala voxel to each ipsilateral cortical target were recorded in a connectivity matrix.

An iterative 'winner takes all' process based on the method outlined by Behrens et al. 2003 [352] was used to interrogate the connectivity matrix and parcellate the amygdala based on its structural connections. Each amygdala voxel was assigned to a cluster based on the cortical target it was maximally connected to, as defined by the highest number of connecting streamlines. If fewer than 50% of participants had a particular cluster it was excluded. New 'winners' were then found in those voxels. This process was repeated until each participant's amygdala voxels were assigned to a cluster found in at least 50% of participants. Cluster volumes were measured using FSL utilities and included as a covariate in group comparison and correlation analyses performed using each clusters' white matter tract characteristics.

6.2.5 Estimation of DTI parameters in white matter tracts

In each participant, FA and MD values in every voxel of white matter tracts connecting amygdala clusters to their 'winning' target were weighted by the number of streamlines in that voxel. The weighted FA and MD values were then averaged across the whole of the white matter tract. The use of weighted FA and MD values prevented rarely-visited voxels from dramatically affecting the average thus ensuring that the microstructure of the tract was accurately represented in the

average measure, and that the potential for noise in the FA and MD measurements was mitigated. These metrics, representative of white matter microstructure, were compared between groups using linear regression with age, gender, and full-scale IQ as covariates. Ipsilateral amygdala volume was additionally included as a covariate when comparing FA and MD for the whole amygdala; amygdala cluster volume was used when comparing FA and MD for tracts arising from each of the amygdala clusters. False discovery rate (FDR) multiple comparisons correction was applied to the group comparison of DTI parameters; results remaining significant ($p<0.05$) following FDR correction are highlighted in the results section using the symbol **.

6.2.6 Relationship between structural measures and clinical scores

In order to investigate the specificity of relationships between particular autistic traits and the amygdala, the AQ sub-scores were correlated with amygdala volume and amygdala–cortex white matter tract microstructural properties. Correlations were also carried out between amygdala measures and score in the emotion recognition portion of the adjusted 'Reading the Mind in the Eyes' task, which was completed during the task-based fMRI scan.

Due to non-normality of the data, partial Spearman correlation was applied with age, gender and full-scale IQ included as covariates for all correlations. Additionally, whole brain volume was included as a covariate for correlations with amygdala volume; respective amygdala cluster volume was included as a covariate for correlations of cluster tract DTI measures. FDR multiple comparisons correction was applied to the correlation tests; correlation results remaining significant ($p<0.05$) following FDR correction are highlighted in the results section using the symbol **, whilst results becoming a non-significant trend ($p<0.09$) following FDR correction are denoted using the symbol *.

6.3 Results

6.3.1 Participant demographics

Table 6 summarises participant demographics. Analysis using two-tailed t-tests showed no significant group differences in age, verbal IQ, performance IQ or full-scale IQ. Somewhat surprisingly, no significant group differences in emotion recognition score were detected. AQ was significantly higher in the ASD group, as would be expected.

	Control (n = 26)	ASD (n = 25)	t-statistic	p value
Gender	21M:5F	21M:4F	-	-
Handedness	26R:0L	23R:2L	-	-
Age (yrs)[1]	24.73 (4.10) [18.83 – 33.30]	23.22 (4.05) [18.31 – 31.90]	1.32	0.20
Full-scale IQ[1]	122.00 (7.98) [105 – 138]	119.4 (11.59) [94 – 136]	0.86	0.39
Verbal IQ[1]	119.73 (9.01) [102 – 136]	116.84 (12.56) [84 – 135]	0.94	0.35
Performance IQ[1]	118.73 (7.07) [103 – 129]	117.36 (11.04) [88 – 135]	0.53	0.60
AQ[1]	13.35 (7.81) [4 - 37]	36.56 (6.53) [22 – 49]	-11.53	**<0.0001**
Emotion Recognition Score[1]	18.75 (4.07) [10 – 25]	17.09 (4.36) [6 – 22]	1.35	0.18
ADOS[2]	-	9.22 (4.11) [3 – 20]	-	-

Table 6 Participant demographics and cognitive test scores.

The results of group comparisons using paired t-tests are shown. [1] Data are expressed as mean (standard deviation) [range]. [2] Combined social and communication sub-scores.

6.3.2 Whole brain and amygdala volume

As shown in Table 7, linear regression analysis controlling for age, gender and full-scale IQ showed no significant group differences in whole brain volume normalised for skull size (t=0.49; p=0.63). Right amygdala volume, covarying for age, gender, IQ, and whole brain volume, was elevated in the ASD group compared to neurotypical controls (t=1.98; p=0.05). There was no significant group difference in left amygdala volume (t=0.78; p=0.44).

	Control (n = 26)	ASD (n = 25)	t-statistic	p value
Whole brain[1]	1304.76 (121.68) [1100.18 – 1628.93]	1320.30 (104.95) [1040.45 – 1579.89]	0.49	0.63
Left Amygdala[1]	1.79 (0.26) [1.36 – 2.44]	1.87 (0.30) [1.16 – 2.44]	0.78	0.44[a]
Right Amygdala[1]	1.60 (0.29) [0.93 – 2.16]	1.81 (0.32) [1.04 – 2.54]	1.98	**0.05**[a]

Table 7 Whole brain and amygdala volumes (cm^3) by group.

[1] Data expressed as mean (SD) [range]. [a] Covaried for whole brain volume.

6.3.3 Microstructure of amygdala white matter tracts

Average MD in white matter tracts connecting the right amygdala with right hemisphere cortical grey matter was significantly elevated in the ASD group in comparison with controls (t=2.35; p=0.02**) (see Figure 42). No other significant group differences in amygdala white matter microstructure were detected.

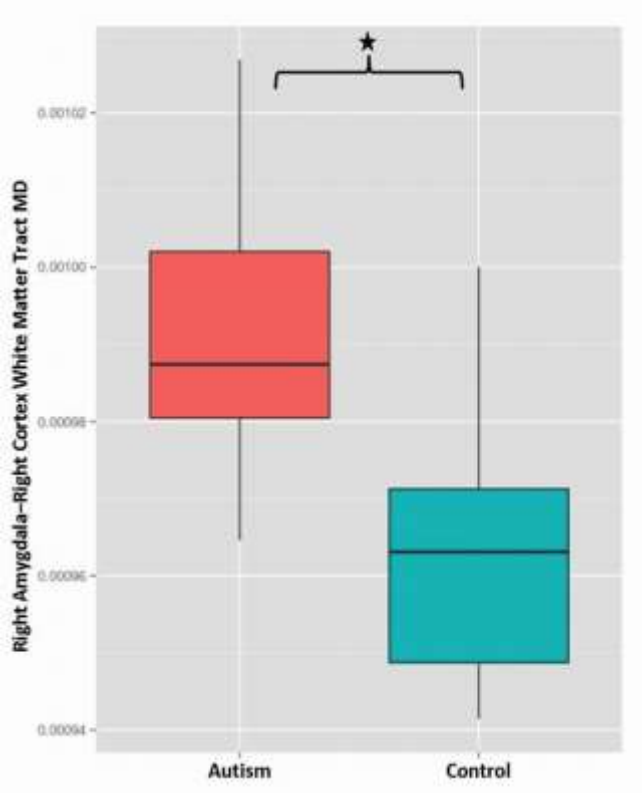

Figure 42 Box and whisker plot showing significantly elevated mean diffusivity (MD) in white matter tracts connecting the right amygdala with the right cortex.

Results are shown for the ASD group (left) compared to the controls (right) following correction for the influence of age, gender, full-scale IQ and right amygdala volume (t=2.35; p=0.02 [p<0.05 after FDR correction]).

6.3.4 Relationship between amygdala–cortex white matter tract microstructure and measures of autism severity

In the ASD group, FA in white matter tracts connecting the right amygdala with the whole right cortex was negatively correlated with AQ (rho=-0.44; p=0.03*). MD in these same white matter tracts joining the right amygdala with the right cortex was negatively correlated with performance in the 'Reading the mind in the eyes' task (rho=-0.53; p=0.006**). See Figure 43 for plots of the correlations.

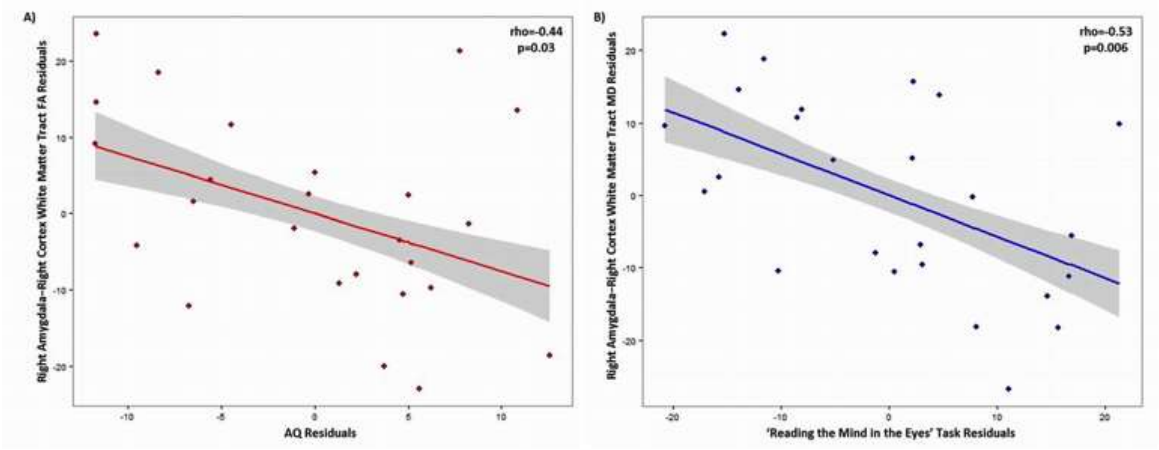

Figure 43 Plots showing results of partial Spearman correlations in the ASD group.

Correlations are shown between (panel A) autism quotient (AQ) score and fractional anisotropy (FA) of white matter tracts connecting the right amygdala with the right-hemisphere cortical grey matter (rho=-0.44; p=0.03 [p<0.09 following FDR correction]), and (panel B) mean diffusivity (MD) of the same right-hemisphere tracts with score in a 'Reading the Mind in the Eyes' task (rho=-0.53; p=0.006 [p<0.05 after FDR correction]). Higher AQ and lower 'Reading the Mind in the Eyes' scores reflect greater autism severity, whilst lower FA and higher MD scores are associated with reduced microstructural integrity of the white matter. Age, gender, full-scale IQ, and right amygdala temporal cluster volume were covariates. The shaded panel represents standard error.

Across the entire study sample, FA in white matter tracts linking the amygdala to the cortex was negatively correlated with AQ in both the left (rho=-0.30; p=0.03**) and the right hemisphere (rho=-0.34; p=0.01**). MD in the same white matter tracts was positively correlated with AQ (left hemisphere: rho=0.31; p=0.03** and right hemisphere: rho=0.44; p=0.001**). There were no significant correlations between DTI metrics and emotion recognition score across the entire study sample.

6.3.5 Amygdala parcellation

Parcellation of control and autism amygdalae using the 'winner takes all' algorithm identified clusters of amygdala voxels demonstrating maximal white matter connectivity to the same cortical grey matter target, thus segmenting the amygdala in vivo based upon its structural connectivity, as shown in Figure 44.

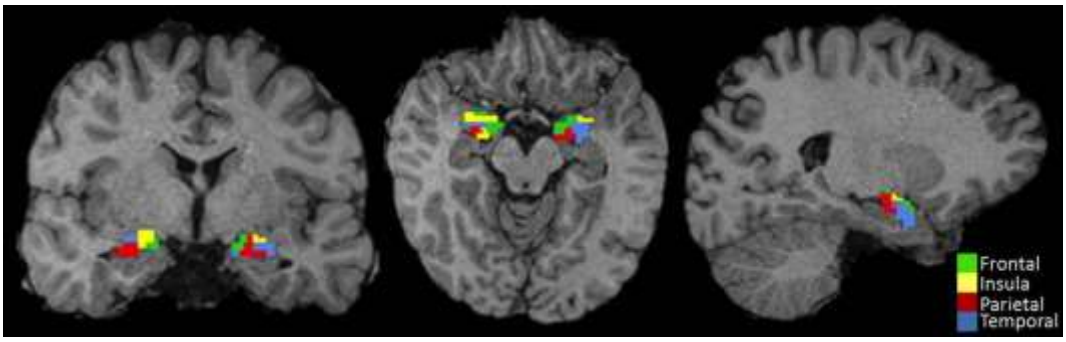

Figure 44 A representative subject showing the results of 'winner takes all' parcellation of the amygdala in vivo overlaid on the participant's T_1-weighted image.

Parcellation was based on the amygdala's structural connectivity profile: probabilistic tractography was seeded from each amygdala voxel to ipsilateral frontal, parietal, temporal, occipital, and insula cortices; each voxel was assigned a 'winning' target which it maximally connected to: frontal cortex (green), parietal cortex (red), temporal cortex (blue), and insula cortex (yellow). The occipital lobe was not a winning target for any voxel.

In both the left and right amygdalae, this resulted in four possible clusters connecting to the frontal lobe, parietal lobe, temporal lobe, and insula cortices. There was no cluster connecting to the occipital lobe in any subject, which indicates that it was not a 'winning' target for the number of subjects required to denote a cluster. Figure 45 shows an example of the probabilistic tractography results, showing connectivity between the amygdala clusters and the four 'winning' cortical targets.

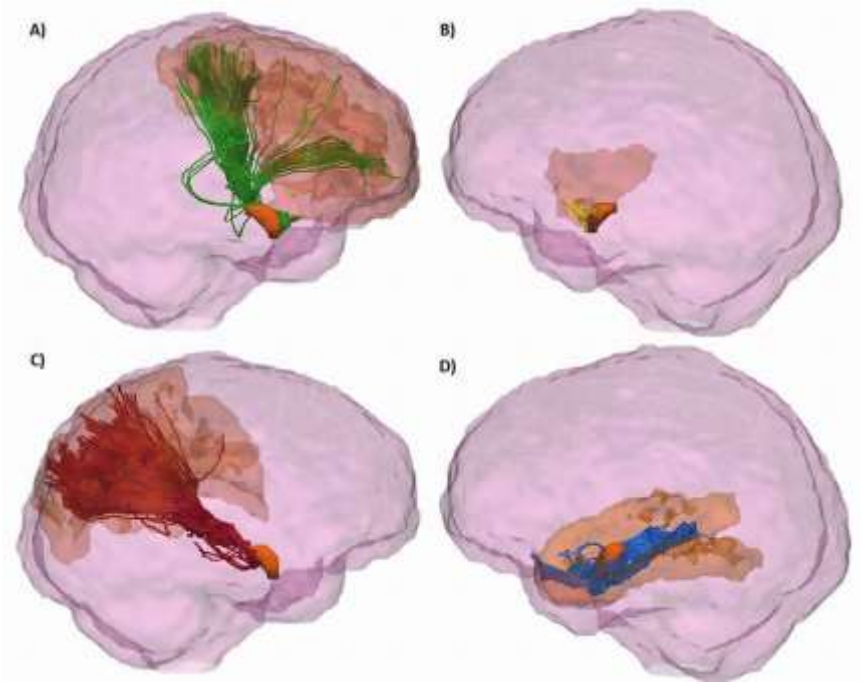

Figure 45 An example of the results of probabilistic tractography seeded from clusters of amygdala voxels and terminating at each cluster's 'winning' cortical target.

Tracts connecting the amygdala frontal cluster with the frontal cortex are shown in green (panel A), yellow for connections between the amygdala and the insula cortex (panel B), red for the parietal cortex (panel C), and blue for the temporal cortex (panel D). The amygdala and cortical targets are shown in orange within each panel. The images were obtained by visualising the tracts and regions of interest in TrackVis [354]**, and overlaying these on a glass representation of the brain. A cut-off in the X-plane was applied in order to allow for better visualisation of the tract pathways.**

6.3.6 Microstructure of amygdala cluster white matter tracts

Average FA in white matter tracts connecting the right amygdala insula cluster with the right insula cortex was reduced in autism (t=-2.32; p=0.03). There were no other

significant group differences in FA or MD of white matter tracts from amygdala clusters.

6.3.7 Relationship between amygdala cluster white matter tract microstructure and measures of autism severity

Within the ASD group, FA in tracts joining the left amygdala temporal cluster with the left temporal cortex were negatively correlated with AQ communication (rho=-0.44; p=0.03 (Figure 46A)) and AQ attention switching (rho=-0.61; p=0.001** (Figure 46C)). Average MD in tracts linking the left amygdala temporal cluster to the left temporal cortex were positively correlated with scores for AQ communication (rho=0.46; p=0.02 (Figure 46B)) and AQ imagination (rho=0.41; p=0.04 (Figure 46D)). AQ attention switching score was negatively correlated with average FA (rho=-0.50; p=0.01 (Figure 46E)) and positively correlated with MD (rho=0.43; p=0.03 (Figure 46F) in tracts joining the right amygdala temporal cluster and the right temporal cortex.

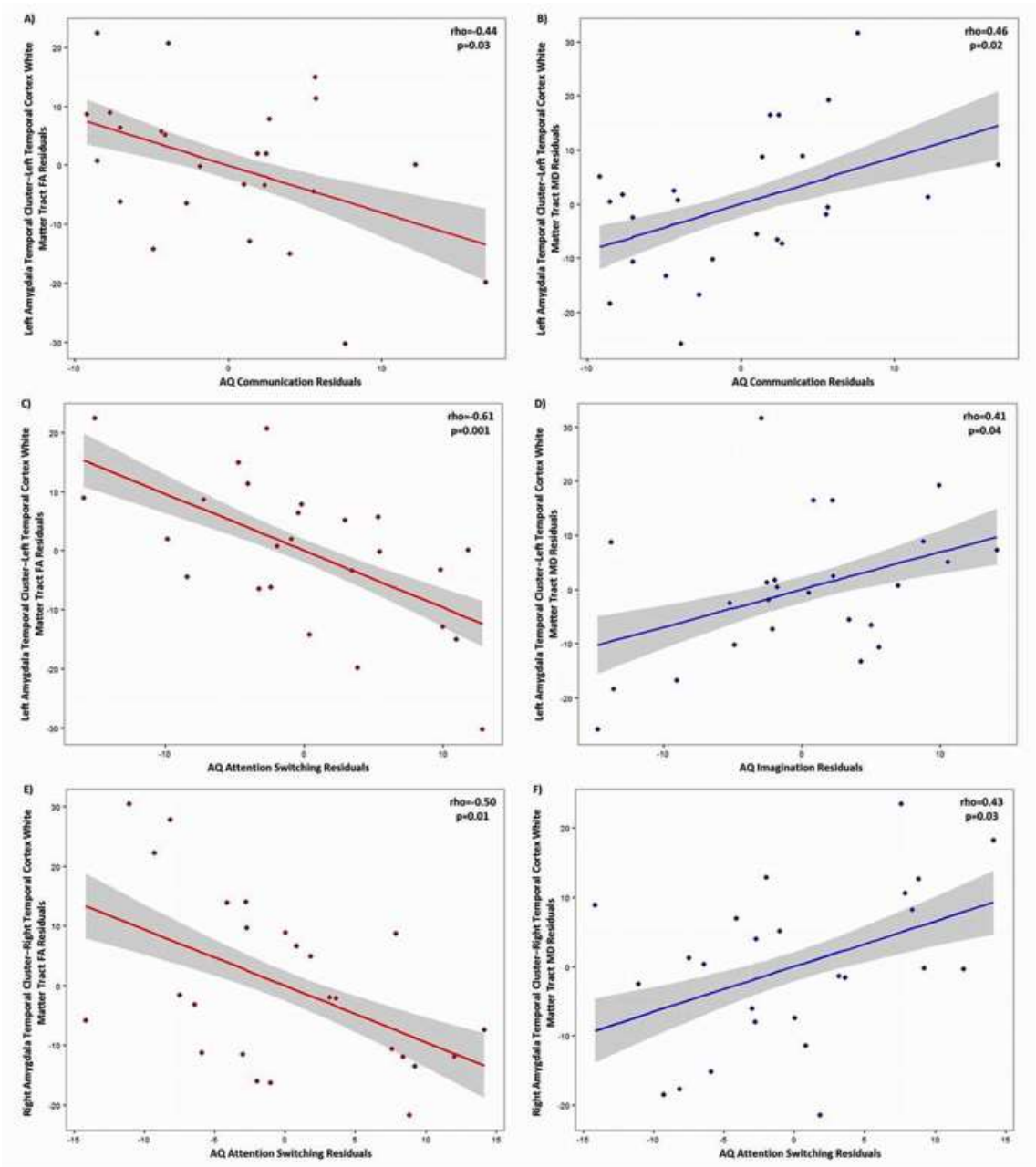

Figure 46 Plots showing results of partial Spearman correlations in the ASD group.

Fractional anisotropy (FA) of white matter connecting the left amygdala temporal cluster to the temporal cortex correlated with autism quotient (AQ) communication score (rho=-0.44; p=0.03) (panel A), and the same measure of FA with AQ attention switching score (rho=-0.61; p=0.001 [p<0.05 after FDR correction]) (panel C). Mean diffusivity (MD) in the same left hemisphere tracts correlated with AQ communication (rho=0.46; p=0.02) (panel B) and AQ imagination scores (rho=0.41; p=0.04) (panel D). AQ attention switching score

was correlated with both FA (rho=-0.50; p=0.01) (panel E) and MD (rho=0.43; p=0.03) (panel F) of white matter tracts linking the right amygdala temporal cluster with the right temporal cortex. Elevated AQ scores are associated with greater symptom severity; lower FA and higher MD scores are reflective of reduced white matter microstructural integrity. Age, gender, full-scale IQ, and respective amygdala temporal cluster volume were covariates. The shaded panel represents standard error.

Positive correlations were observed between average MD of white matter tracts connecting the left amygdala parietal cluster with the left parietal cortex and AQ communication (rho=0.39; p=0.05 (Figure 47A)) and AQ attention switching (rho=0.47; p=0.02 (Figure 47B)) scores. FA in white matter connecting the right amygdala parietal cluster with the right parietal cortex was negatively correlated with AQ communication (rho=-0.46; p=0.02 (Figure 47C)).

Within the ASD group, there was a positive correlation between score on the 'Reading the Mind in the Eyes' task and FA of white matter connecting the left parietal lobe with the left amygdala parietal cluster (rho=0.45; p=0.02* (Figure 47D)).

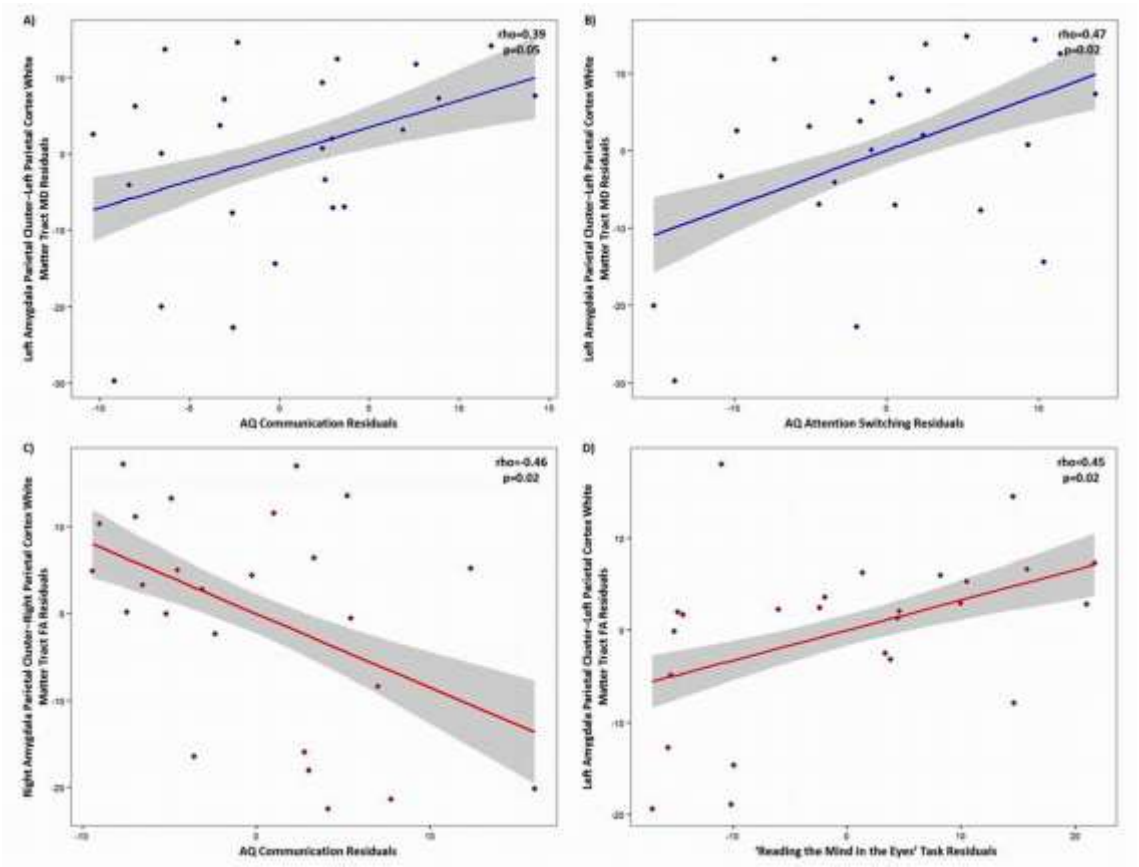

Figure 47 Plots showing results of partial Spearman correlations in the ASD group.

Mean diffusivity (MD) of white matter tracts linking the left amygdala parietal cluster with left parietal cortex and autism quotient (AQ) communication score (rho=0.39; p=0.05) (panel A), and the same tract measure of MD with AQ attention switching score (rho=0.47; p=0.02) (panel B). Panel C shows a plot of the relationship between AQ communication score and fractional anisotropy (FA) of tracts joining the right amygdala parietal cluster with right parietal cortex (rho=-0.46; p=0.02), whilst panel D shows the relationship between FA of the same parietal tracts in the left hemisphere with score in a 'Reading the Mind in the Eyes' task (rho=0.45; p=0.02 [p<0.09 following FDR correction]). Higher AQ scores and lower 'Reading the Mind in the Eyes' task scores reflect greater autism severity, whilst lower FA and higher MD values are associated with reduced microstructural integrity of the white matter. Age, gender, full-scale IQ, and respective amygdala parietal cluster volume were covariates. The shaded panel represents standard error.

When looking at the combined study sample, a positive correlation was observed between FA in white matter tracts connecting the left amygdala temporal cluster and the left temporal cortex with AQ attention switching score (rho=-0.35; p=0.01*). There was a positive correlation for MD in the same white matter tracts with AQ attention to detail (rho=0.37; p=0.007**) and AQ imagination (rho=0.28; p=0.05 [not significant after FDR correction]) scores. A positive correlation was measured for MD in the same tract in the right hemisphere with AQ attention to detail (rho=0.28; p=0.04 [not significant following FDR correction]).

Also in the combined study sample, negative correlations were identified between average FA of white matter tracts connecting the right amygdala insula cluster and the right insula cortex and AQ social (rho=-0.30; p=0.03** (Figure 48A)), AQ communication (rho=-0.31; p=0.03** (Figure 48C)), AQ attention to detail (rho=-0.27; p=0.05* (Figure 48E)), and AQ imagination (rho=-0.31; p=0.03** (Figure 48G)) scores. Positive correlations were identified for MD in the same white matter tracts and AQ social (rho=0.36; p=0.009** (Figure 48B)), AQ communication (rho=0.31; p=0.03** (Figure 48D)), AQ attention switching (rho=0.37; p=0.007** (Figure 48H)), and AQ attention to detail (rho=0.36; p=0.009** (Figure 48F)) scores.

Further, a positive correlation was observed between average MD for tracts connecting the left amygdala frontal cluster to the left frontal cortex and AQ attention to detail score (rho=0.29; p=0.04 [not significant following FDR correction]). There were no significant correlations between cluster tract DTI measures and emotion recognition score in the combined study sample.

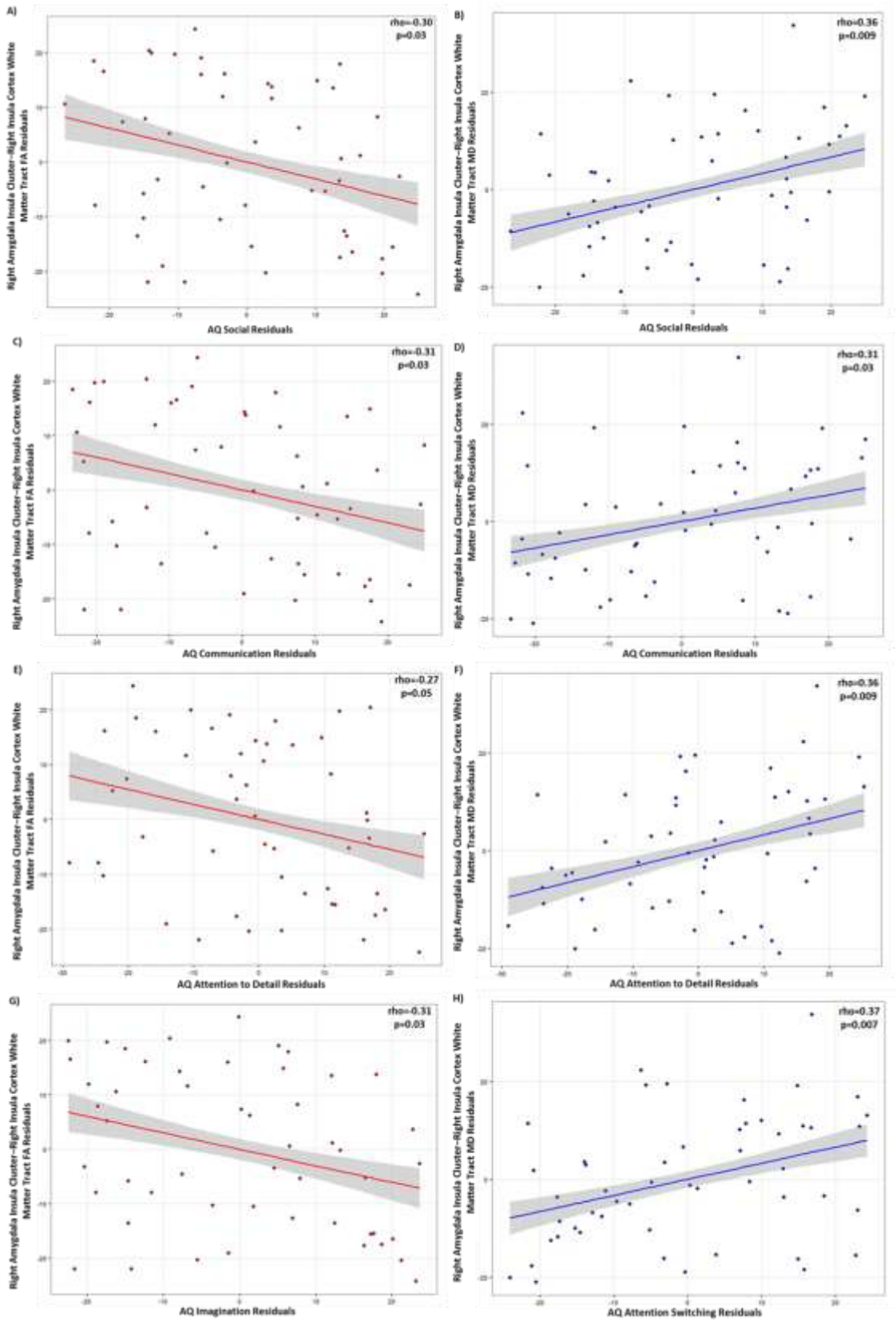

Figure 48 Plots showing results of partial Spearman correlations across the entire cohort.

Fractional anisotropy (FA) of white matter tracts linking the right amygdala insula cluster with right insula cortex were correlated with autism quotient (AQ) social score (rho=-0.30; p=0.03) (panel A), AQ communication score (rho=-0.31; p=0.03) (panel C), AQ attention to detail score (rho=-0.27; p=0.05) (panel E), and AQ imagination score (rho=-0.31; p=0.03) (panel (G). Mean diffusivity (MD) in the same white matter tracts were correlated with AQ social score (rho=0.36; p=0.009) (panel B), AQ communication score (rho=0.31; p=0.03) (panel D), AQ attention to detail score (rho=0.36; p=0.009) (panel F), and AQ attention switching score (rho=0.37; p=0.007) (panel H). Higher AQ scores reflect greater autism severity, whilst lower FA and higher MD values are associated with reduced microstructural integrity of the white matter. Age, gender, full-scale IQ, and respective amygdala parietal cluster volume were covariates. The shaded panel represents standard error.

6.4 Discussion

Using a 'winner takes all' approach the amygdalae of both neurotypical and autistic subjects were parcellated using measures of structural connectivity. Clusters of amygdala voxels that were maximally connected to either frontal, parietal, temporal, or insula cortices were identified. White matter microstructure was investigated for each of these amygdala–cortex connections, in addition to the ipsilateral cortex as a whole. The main finding of this study is that, in this sample of young adults with ASD, the right amygdala is larger compared to neurotypical controls and its connections with ipsilateral cortical grey matter are less microstructurally coherent; a finding that is associated with the severity of the autistic phenotype, as measured by higher AQ and lower emotion recognition scores. A second finding of importance is that parcellation of the amygdala into sub-regions that share similar cortical connectivity enabled identification of those amygdala–cortical connections most associated with autistic behaviours: connections between the amygdala and the insula cortex were altered in ASD

compared to controls, and reduced microstructural integrity of amygdala–parietal and amygdala–temporal connections was related to greater ASD-related difficulties. Further, results indicated that there is both regional and hemispheric specialisation of amygdala–cortical connectivity and its association with ASD symptoms.

Findings using the whole amygdala suggest that right amygdala volume and anomalies in its structural connections with the cortex are more associated with the autistic phenotype than the left amygdala. This is in agreement with Murphy et al.'s [187] study in which right, but not left, amygdala volume group differences survived correction for brain volume, and report of an association between right amygdala volume and anxiety in children with ASD that was not significant for the left amygdala [355]. Additionally, anomalously elevated functional activation of the right, but not left, amygdala when autistic participants were shown socially-valent stimuli has been reported [336]. The exaggerated right amygdala response correlated with participants' amplified behavioural responses to sensory stimuli [336]. However, volumetric differences in both left and right amygdalae have been reported in ASD [115][356], correlating with clinical characteristics of autism [337], and functional deficits in response to social stimuli have been reported bilaterally in the amygdalae of autistic subjects [108][115]. Additionally, significant correlations between white matter microstructure and ASD severity, as measured by the AQ, were identified for amygdala–cortical tracts in both the left and right hemispheres when looking across the entire study sample. This implies that greater statistical power, as afforded by the combined study sample, enables the identification of further associations between white matter microstructure and ASD trait severity than investigations within the ASD group alone. An alternative explanation is that the right amygdala is more associated with clinically-significant ASD traits than the left amygdala, though this hypothesis requires further explanation.

Parcellation analysis enabled further investigation of amygdala–cortical connectivity, and identified hemispheric specificity with regards to amygdala–cortical connectivity dysfunction in ASD: bilateral anomalies in white matter microstructure associated with poorer communication and attention switching abilities in ASD, while aberrations in left amygdala–cortical tracts were associated with poor imagination skills and reduced ability to recognise and label emotional facial expressions. Hemispheric specificity has been reported for the volume [180][182][186], and functional activation [108][336] of the amygdala in ASD, and for the microstructure of adjacent white matter in ASD [237][235][340][341]. The results of this study showed that the microstructure of both left- and right-hemisphere amygdala–cortical connections is associated with wider aspects of the autistic phenotype, but that deficits in left amygdala connections are associated with some more specific ASD-related cognitive processes. This is consistent with evidence that the left amygdala interprets physiological arousal arising from specific stimuli, while the right amygdala mediates non-specific, automatic activations in response to stimuli [357]. Distinct, yet corresponding roles for the left and right amygdalae have been reported in women with Turner syndrome [358], a condition associated with increased incidence of ASD [359] and elevated amygdala volume [360]. Our results, along with previous evidence, show that the amygdalae and their cortical connections are lateralized with regards to their structural connections and impact on ASD symptoms, and that amygdala sub-regions have different cortical connectivity profiles and associations with ASD traits. This supports the rationale for independent investigation of amygdala sub-regions in autism

Following parcellation of the amygdala, it could be observed that white matter microstructure, as measured by FA, was altered in the ASD group for connections between the amygdala and insula cortex, and that this was associated with ASD trait severity across the entire study sample. The insula is highly connected to structures of the social brain, including the amygdala [361]. It is also claimed to be

the locus of self-awareness [362], an ability that is impaired in ASD. Microstructural white matter deficits in the insula lobe have been reported in ASD compared to controls [225][238]. However, in this study, the microstructure of white matter tracts connecting the amygdala and the insula cortex was only significantly correlated with ASD trait severity in the combined study sample, and not in the ASD group alone. This indicates that amygdala–insula connectivity is more associated with the wider spectrum of ASD traits than the microstructure of other amygdala cluster tracts, which were also significant in the ASD group alone, or that the greater statistical power afforded by the combined study sample enable the elucidation of smaller effects. The finding of reduced structural connectivity between the amygdala and the insula cortex aligns with the findings of functional studies in ASD: von dem Hagen et al. [339] report reduced resting functional connectivity between the amygdala and the insula, and Baron-Cohen et al. [108] showed reduced insula and amygdala activation in response to social stimuli.

This study identified that microstructural impairments, as measured by FA and MD, in white matter linking the amygdala and temporal cortex are associated with communication, attention switching, and imagination difficulties in ASD. Associations between impairments in local amygdala-temporal cortex tracts and particular autistic behaviours are supported by previous research: Cheung et al. [217], found an association between temporal lobe FA and autism diagnostic interview (ADI)-social score, but not with any other sub-score of the ADI; Abdel Razek et al. [205] recently reported a correlation between increased diffusion in temporal lobe white matter and scores on the childhood autism rating scale. In healthy subjects, Iidaka et al. [297] identified an association between impaired imagination, as measured by the AQ, and elevated volume of white matter tracts connecting the amygdala and the superior temporal sulcus. In a review of animal and clinical studies, Bachevalier [363] emphasised the importance of temporal lobe structures in the clinical features of ASD. Taken together our results suggest that larger, but less microstructurally ‘coherent’ white matter tracts connecting the

amygdala with local structures are associated with particular autistic characteristics, across the spectrum from healthy individuals through to those clinically diagnosed with ASD — a finding that is supported by my previous work using tract-based spatial statistics [317] (described in Chapter 5). This indicates that temporal lobe structures, and their discourse with one another via white matter tracts, are of principal importance in the generation and/or maintenance of the autism phenotype In contrast, Noriuchi et al. [237] did not observe a significant relationship between amygdala-related white matter tract characteristics and the social responsiveness scale observed; however that study sample was smaller than reported here, indicating that there was a lack of power to identify the effect.

Deficits in communication, attention switching, and the perception of emotional stimuli in ASD were associated with compromise of white matter tracts, as measured by FA and MD, linking the amygdala to the parietal cortex, an area that integrates sensory information and mediates motor responses [364]. Microstructural anomalies in parietal lobe white matter tracts have been reported in prior studies of ASD [294][232][215]. Kana et al. [294] identified a correspondence between ASD-related processing deficits and aberrations in parietal lobe white matter. In functional studies of ASD, Green et al. [336] reported hyperactivation of primary sensory cortex and the amygdala in response to social stimuli; in addition, Baron-Cohen et al. [108] identified reduced functional activation of the inferior parietal lobule and temporal lobe structures, including the amygdala, in response to emotions. Collectively our work indicates that amygdala–parietal connections are aberrant in ASD, and that the extent of these anomalies is associated with symptom severity. No significant correlations between amygdala–parietal white matter tract microstructure and ASD symptom severity, as measured by the AQ, were identified in the combined study sample, which indicates that amgydala–parietal connectivity is more associated with clinically-significant ASD symptoms than the wider spectrum of sub-clinical ASD traits.

This study has some limitations. The occipital cortex was not represented in the amygdala parcellation results. This does not mean that these connections are not present, rather that each amygdala voxel maximally connected to another cortical target or that the number of subjects with 'winning' occipital connections was below threshold. Connection probability decreases with distance; to limit the effects of this a high number of streamlines were seeded and DTI values were averaged over the tracts. The low resolution of MRI scans relative to actual white matter tract dimensions may cause partial volume effects, and the directionality of white matter connections cannot be determined using tractography; post-mortem or tracer studies would be necessary. Errors may be introduced during registration and segmentation, although this was mitigated by visual assessment. It is not possible to infer causality using correlation analyses. Some correlation results did not survive multiple comparisons correction. This may be ameliorated by a larger sample size; however, some correlation results did survive correction in this study sample.

Future studies could reduce the number of statistical tests by restricting hypotheses to those connections that this study has identified as pertinent. Investigation of the functional connectivity of each of the amygdala sub-regions identified in this study would further understanding of the complex interface between brain structure and function. This study indicates that amygdala connectivity has potential as a biomarker of severity in different domains of ASD, which could be used to inform patient assessment and response to intervention; larger, longitudinal cohorts would be needed to support this. The parcellation method could also be applied to investigate the connectivity of other brain regions known to be important in autism, such as the orbitofrontal cortex.

6.5 Conclusion

In conclusion, the findings of this study indicate that amygdala connections are structurally compromised in ASD, and that microstructural aberration in different amygdala–cortical white matter tracts, notably those with insula, parietal, and temporal cortices, are associated with particular ASD-related impairments. Associations were trait-, hemisphere-, and region-specific. Results suggest that the amygdala is 'wired' differently in autism, and that the microstructure of particular amygdala–cortical connections is associated with different aspects of the autistic phenotype. This study advances understanding of the neurological underpinnings of autistic behaviours, and has implications for further studies of amygdala connectivity; suggesting that richer information can be gleaned by investigating amygdala sub-regions independently. The results provide evidence that amygdala sub-region connectivity could be used to measure the brain's response to therapies aimed at ameliorating particular autistic behaviours.

Chapter 7 Structural Networks in Autism Spectrum Disorder

The analysis described in this chapter considers the network of structural connections present in the brain in ASD, and analyses them using graph theory. Jonathan Clayden and Fani Deligianni (both from the Developmental Imaging and Biophysics Section, UCL Institute of Child Health) developed the code used in this analysis, and provided valuable advice on its usage.

7.1 Introduction

ASD is a neurodevelopmental condition, and it has been proposed that atypical brain development in ASD is characterised by disconnection (for more details see Section 1.3). Brain disconnection, in the structural sense, can take many forms: including reduced speed of information transfer (perhaps as a result of synaptic dysfunction), a reduction in the number of connections, surplus unnecessary connections (that may result from deficient synaptic pruning), connections that do not co-operate with one another, or a lack of efficiency as a result of nerve impulses taking a tortuous path to their destination. There is evidence for synaptic dysfunction [88] and a lack of dendritic pruning in ASD [87], in addition to the studies that have reported reduced 'coherence' in the microstructure of white matter in ASD, as measured using diffusion-weighted imaging – a body of work that the studies presented in this thesis expand upon.

Relatively few studies have investigated the efficiency of information transfer within the brain network in ASD. Graph theory is a branch of mathematics used to delineate and analyse graphs (see reviews [365][366]). In mathematical terms, a graph is a representation of a series of nodes (or vertices) and their interconnecting edges, as shown in Figure 49.

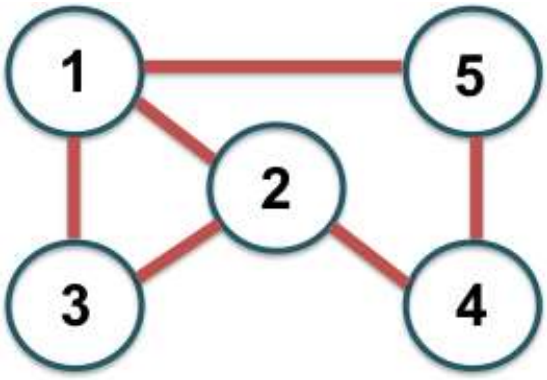

Figure 49 A basic graph with five nodes and six edges.

The complex network of structural connections in the brain can be considered as a graph, with grey matter regions forming the nodes of the graph, and the white matter tracts the edges that connect the nodes. These graphs can be binary (two nodes are either connected by an edge or not) or weighted (an edge that represents a 'stronger' connection, typically measured as a greater number of streamlines or a higher FA, receives greater weight, or importance, in the graph). Graphs can theoretically be directed (i.e. an edge travels *to* or *from* a node), although diffusion-weighted tractography cannot provide directional information so structural graphs obtained using diffusion-weighted imaging are always undirected.

Once the graph has been generated, graph theoretical analysis techniques can be applied in order to measure the properties of the graph. Common graph properties include [367][365]: clustering coefficient – a measure of connection density between neighbouring nodes (i.e. how connected the immediate neighbours of a node are to one another); characteristic path length – the average number of steps connecting one node to another in the network; small worldness – the ratio between normalised clustering coefficient and normalised characteristic path length (a small-world network has high levels of clustering and short characteristic path lengths); local efficiency – the efficiency, as measured by the inverse of the path length, of

connectivity for a given node (this is repeated for all of the nodes' subnetworks to obtain the local efficiency of the network); and global efficiency – efficiency across the entire network. Healthy brains typically have communities of nodes that are highly connected.

Graph analysis methods can therefore provide a wealth of information regarding network arrangement, or topology, connectedness, and efficiency. Very recently graph analysis techniques have been used to investigate the properties of structural networks in ASD. Some results indicate that structural networks are less connected and less efficient in ASD, as measured by reductions in global efficiency and global clustering coefficient in children with ASD [289]. Reduced network efficiency in ASD is supported by a study in young children; those at high risk and diagnosed with ASD showed reduced local and global efficiency in temporal, parietal, and occipital lobes in comparison with high-risk children who had not received a diagnosis of ASD and low-risk infants. Symptom severity in the high-risk infants was associated with reduced network efficiency [283]. Further graph theoretical analyses have indicated that brains are more connected in ASD, particularly for local networks, as shown by elevated clustering coefficient and reduced path lengths in children with ASD [290] and increased connectivity in rich clubs – interconnected hub regions – as measured by a connectedness coefficient [291]. Taken together these studies indicate that ASD brains are less efficient, but more connected at a local level. This is indicative of disconnection as a result of surplus, maladapted white matter tracts or synapses as opposed to a lack of connectivity *per se*. In contrast, an investigation of children and adolescents did not identify any significant differences in graph metrics between ASD and control groups; although alterations in white matter integrity, as measured by elevated FA and reduced MD, were observed in the ASD group [292]. This is suggestive of variability, the effect of age on results, and/or that white matter can be microstructurally compromised in ASD, with relative sparing of its topology at the network level.

Some graph theoretical analyses have been performed on particular networks in ASD. Support for the hypothesis that macrocephaly is associated with disorganised brain connectivity in ASD was published by Lewis et al., who reported reduced local and global efficiency in adults with ASD, and associations between increased intracranial volume and reductions in local and global efficiency [293]. In examinations of language networks in ASD, significantly reduced local clustering coefficient and betweenness centrality – a proxy for the importance of a node, as measured by the number of shortest paths that pass through it – were observed in Wernicke's area, in addition to reduced local clustering coefficient in Broca's area [289]. This suggests that brain regions important for language are less connected in ASD. Surprisingly, Li et al. [290] demonstrated an association between greater oral language ability and stronger local connectivity in ASD, which was contrary to the opposite relationship (i.e. stronger local connectivity was associated with poorer oral language skills) in neurotypical controls.

The aim of this study was to further investigate the properties of the structural brain network in ASD using graph theory in order to clarify prior findings of reduced efficiency and hyperconnectivity in ASD. Graph theoretical methods enable the estimation of both local and global graph properties, and provide a more detailed description of the structural connections (or connectome) of the brain than voxel-wise methods such as TBSS. The relationship between network properties and ASD traits has been relatively under-explored by previous studies, and is therefore a key aim of this work; associations between graph metrics and ASD symptoms, as measured by the AQ and performance on an emotion recognition task, the 'reading the mind in the eyes', will be carried out.

As outlined in Section 1.2.3.1, the limbic system consists of interconnected brain regions that are associated with emotional responses and behaviours [368]; such as the insula, which is involved in the processing of emotions and sensory-motor

actions [369][370] and the hippocampus, which is responsible for long-term memory and spatial navigation [371][372]. Certain white matter tracts, including the cingulum, the inferior longitudinal fasciculus, the arcuate fasciculus, and the fornix, form the network of limbic connections [320][85]. Studies of the limbic system have identified both structural [261][265][197] and functional [373][197] variation in ASD. However, relatively little is understood regarding the properties of the limbic network as a whole, and its role in ASD; consequently, a further aim of this study was to isolate the limbic sub-network and compare its features in neurotypical controls and individuals with ASD. Further analysis of the limbic system in ASD will provide a greater understanding of the role that this sub-network plays in ASD traits, and the use of graph theory techniques will advance identification of the properties of this network in ASD.

To summarise, the brain's white matter tracts form a network of physical connections between functional brain regions. This structural network can be analysed using graph theory, which assesses both network topology and efficiency. It is thought that ASD arises as a result of disconnection in the brain, and graph theoretical approaches provide a means of investigating the nature of this disconnection. Recent graph theory-based analyses in ASD have reported reduced efficiency, but over-connectivity in ASD. Additional work is needed to further catalogue structural disconnection in the ASD brain, and to ascertain the relationship between the brain's network of white matter connections and autistic traits.

7.2 Methods

7.2.1 Participants

Twenty-five high-functioning young adults with autism and 26 age-matched neurotypical controls were recruited locally, as outlined in Chapter 4. Two-tailed t-

tests were used to compare demographic measures between groups, and the results are shown in Chapter 5.

7.2.2 Data acquisition and pre-processing

Data acquisition and pre-processing proceeded as described in Chapter 4, and FSL's BEDPOSTX was applied as per Chapter 6.

7.2.3 Region of interest segmentation

Within each participant's T_1-weighted scan, subcortical structures – including the nucleus accumbens, caudate, putamen, pallidum, thalamus, hippocampus and amygdala – were segmented using FIRST, and cortical grey matter was segmented into 68 regions of interest using FreeSurfer; both methods are described in Chapter 4. The regions of interest generated from FIRST and FreeSurfer were imported into TractoR and merged together to create a single mask.

7.2.4 Generating structural networks

TractoR version 2.5.2's graph analysis package (http://www.tractor-mri.org.uk/connectivity-graphs) was used to generate structural graphs from each participants' diffusion-weighted data. Briefly, probabilistic tractography was carried out across the whole brain, with one streamline seeded for every voxel with an FA value ≥0.2 in order to confine tracking to voxels that were more likely to contain white matter than grey matter or cerebrospinal fluid. Seeds were jittered to ensure that they appeared at random locations within each voxel, thus ensuring that the sampling strategy was unbiased. The regions of interest on the mask of combined FIRST and FreeSurfer outputs were non-linearly registered to diffusion space and were used as the tractography targets. Each streamline terminated once it reached a target, and the resulting set of streamlines was used to build an undirected graph for each participant.

7.2.5 Generating limbic sub-networks

Thirty limbic nodes were identified from the FIRST and FreeSurfer parcellations, and consisted of the bilateral amygdala, hippocampus, insula, caudal anterior cingulate cortex, entorhinal cortex, fusiform gyrus, inferior temporal gyrus, cingulate gyrus (isthmus), lateral orbitofrontal cortex, medial orbitofrontal gyrus, parahippocampal gyrus, inferior frontal gyrus (pars orbitalis), posterior cingulate gyrus, rostral anterior cingulate cortex, and temporal pole. Limbic sub-networks comprising of these nodes were generated from the whole brain network in each participant by selecting the nodes of interest, and isolating out the edges that connected them.

7.2.6 Measuring graph properties

Whole brain and limbic graphs were visually checked for processing errors in TractoR. The edges in each graph were weighted by the visitation count (i.e. the number of streamlines in the edge divided by the average volume of the two nodes that the edge connects), in order to provide a representation of the 'strength' of each connection in the visualisation of the graph.

Both whole brain and limbic graph properties were calculated using the graph-props command in TractoR, which calls on the igraph package (http://igraph.org/r/). A threshold of ≥1 streamline was applied before binarising the graph so that edges above the threshold were included on the graph as 'connected' and those edges below the threshold were removed as 'not connected'. Binarising at this stage means that the measured graph metrics were obtained from an unweighted graph and thus the graph properties are easier to estimate and compare between subjects; thresholding prior to binarisation removes spurious connections from the graph. The graph metrics edge density (i.e. the number of edges in the graph), mean

shortest path (Figure 50), mean local efficiency, global efficiency (Figure 50), mean clustering coefficient (Figure 51) and small worldness (Figure 51) were then calculated. Group differences in each metric were calculated using linear regression, with age, sex, and full-scale IQ as covariates. FDR multiple comparisons correction was applied to the results.

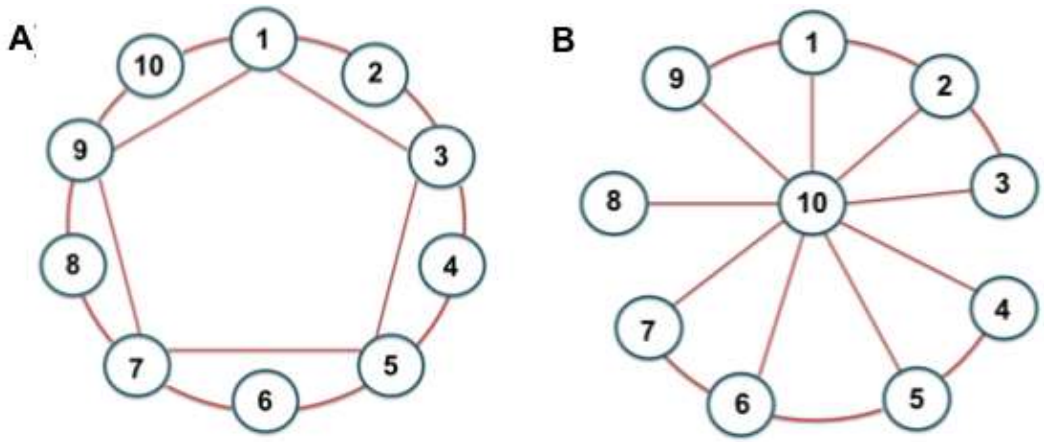

Figure 50 Shortest path, efficiency, and clustering coefficient, as represented by two networks with 10 nodes and 15 edges.

a) has high path lengths, and thus has low network efficiency. b) has shorter path lengths and higher efficiency.

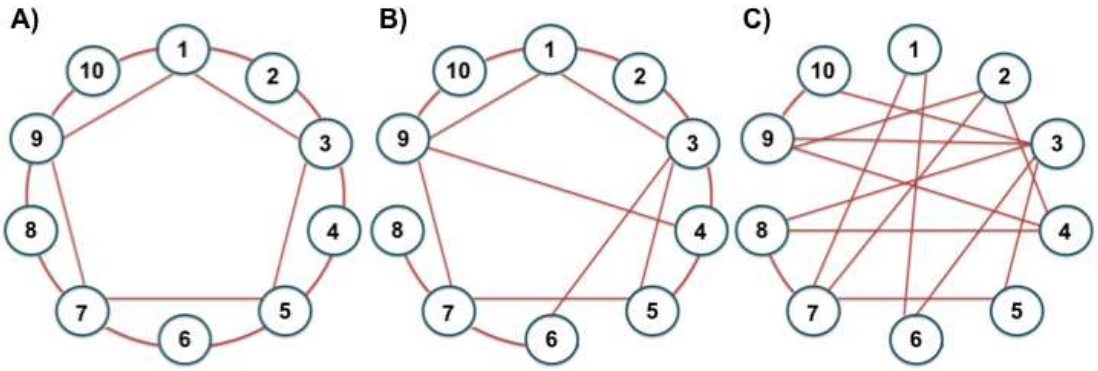

Figure 51 Small worldness, as demonstrated by three networks with 10 nodes and 15 edges.

a) An ordered network, with high characteristic path lengths and high clustering coefficients b) a small world network, with low characteristic path lengths and high clustering coefficients c) a random network, with low characteristic path lengths and low clustering coefficients.

7.2.7 Measuring average FA and MD in each graph

Separately, the tractography results were used to generate whole brain and limbic graphs weighted using FA and MD instead of number of streamlines. Average FA and MD values were calculated for each graph by taking a weighted average of the FA and MD for each set of streamlines that passed through a node and reached another node. This average value for each node was then averaged across all nodes. Using weighted values meant that those voxels with a greater number of streamlines were afforded greater weight in the final estimation. Average whole brain and limbic network FA and MD values were compared between groups using linear regression, with age, sex, and full-scale IQ as covariates.

7.2.8 Associations with ASD symptoms

In the ASD group, associations between ASD symptom severity, as measured by the AQ and 'reading the mind in the eyes' emotion recognition task, and graph metrics, average FA and average MD were investigated. Scores in the AQ sub-categories – social, communication, attention to detail, attention switching, and imagination – were considered separately. Partial correlation was used, with age, sex, and full-scale IQ as covariates. FDR multiple comparisons correction was applied to analyses of associations with AQ subsets, since these involved a high number of tests.

7.2.9 Identifying connections of interest

In an exploratory analysis, the edges that were most significantly and most often different between the ASD and control groups in terms of number of streamlines, FA, and MD were identified from the whole brain networks using the flip package for permutation analysis in R (https://cran.r-project.org/web/packages/flip/index.html). Methods such as principal component analysis (PCA) and principal networks [374] are often used in the identification of important connections; however a trial analysis using principal networks identified

strong self-connections in some nodes that occupied the majority of the principal networks. These intra-nodal connections are interesting to note, but it was felt that these methods masked inter-nodal connections of interest within sub-networks. Permutation testing using 1000 permutations was therefore selected because it does not assume independent tests and iterates the question 'are there significant differences between the groups for each edge, and what is the likelihood that this has occurred by chance?' over many repeats – thus strengthening the validity of the results. Age, sex, full-scale IQ, and whole brain volume were included as covariates in the permutation model. Family-wise error (FWE) multiple comparisons correction was applied.

7.3 Results

7.3.1 Graphs of the whole brain structural network

Graphs of whole brain structural connections were generated in each participant using cortical and sub-cortical grey matter regions of interest as the nodes and white matter connections, as generated using tractography, as the edges. Figure 52 shows an example of one participant's whole brain connectivity matrix, which indexes each of the edges in the graph, whilst Figure 53 shows the graph overlaid on the participant's brain in three-dimensional space.

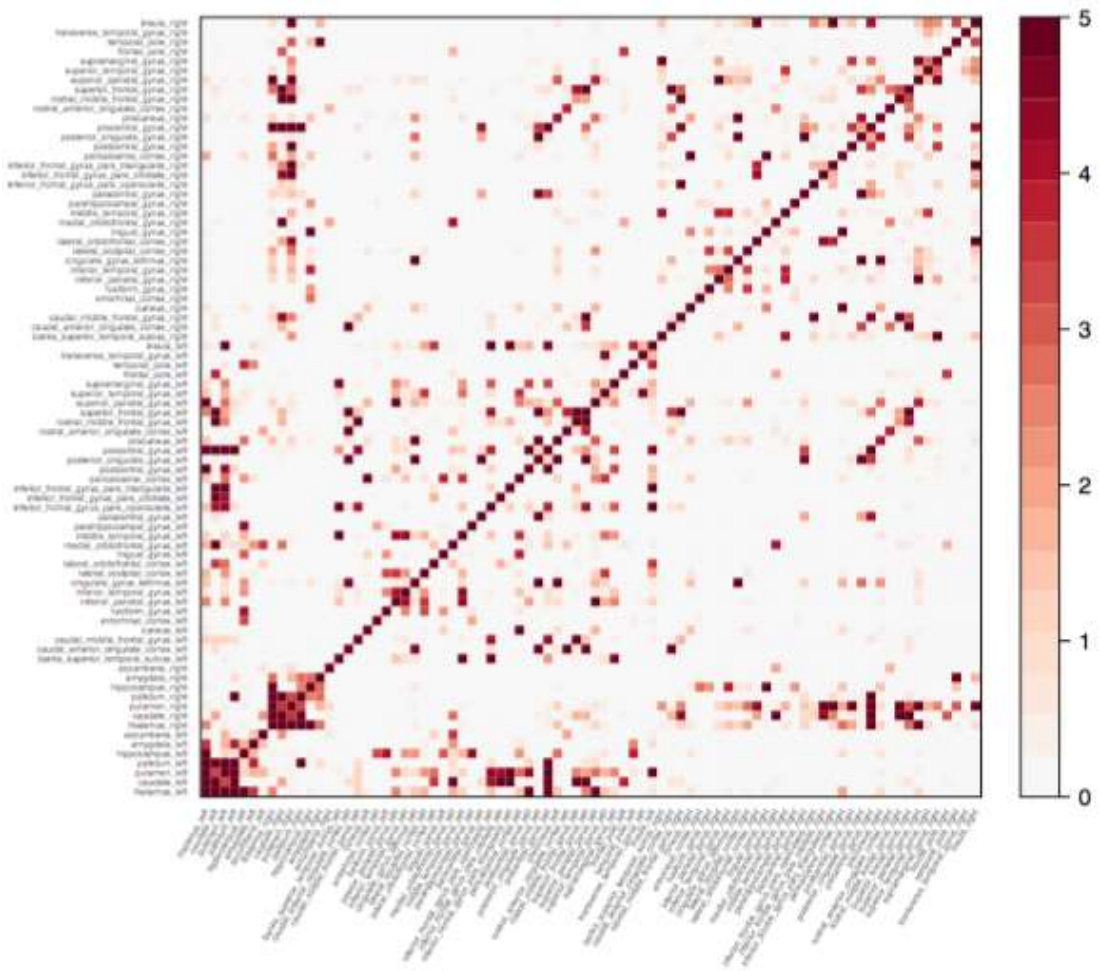

Figure 52 Symmetrical connectivity matrix showing the structural connections within the whole brain of a representative subject.

Each brain region, or node, is listed along the x and y axes, and thus occupies both a row and a column. The edges connecting each node are represented in the central squares of the matrix, with the connection strength of each edge ranging from 0 to 5 – higher values indicate a greater number of streamlines connecting each region (as a ratio of region volume). Self-connections are at the maximum, and can be seen along the diagonal.

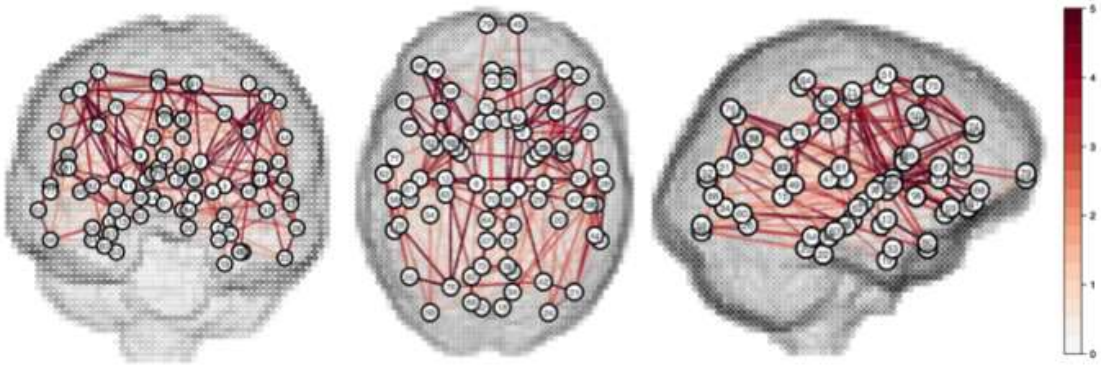

Figure 53 Graphical depiction of a representative participant's whole brain structural network overlaid on a surface image of their brain.

The nodes of the graph are shown as numbers within a circle, and represent brain regions. The red lines connecting pairs of nodes are the edges of the graph. As in Figure 51, the shade of each edge represents the number of streamlines contributing to the connection, with darker shades indicative of greater connectivity and thus greater weight in the final graph, and paler hues showing edges with fewer streamlines, and thus less weight in the final graph.

There were no significant differences between ASD and control groups in the graph metrics edge density, mean shortest path, mean clustering coefficient, mean local efficiency, global efficiency, and small worldness. In the ASD group, there were no significant correlations with the AQ or the 'reading the mind in the eyes' emotion recognition task.

Average FA across the whole brain network was significantly lower in the ASD group compared to the controls (t=-2.14; p=0.04 [no need to correct for multiple comparisons]). In the ASD group average FA across the whole network was positively associated with emotion recognition score, as measured by the 'reading the mind in the eyes' task (rho=0.51; p=0.009 [no need to correct for multiple comparisons]). There were no significant associations between average network FA

and the AQ. There were also no significant results when looking at average MD over the whole brain network.

7.3.2 Graphs of the limbic network

Limbic sub-networks were generated in each participant, and an example can be seen in Figure 54.

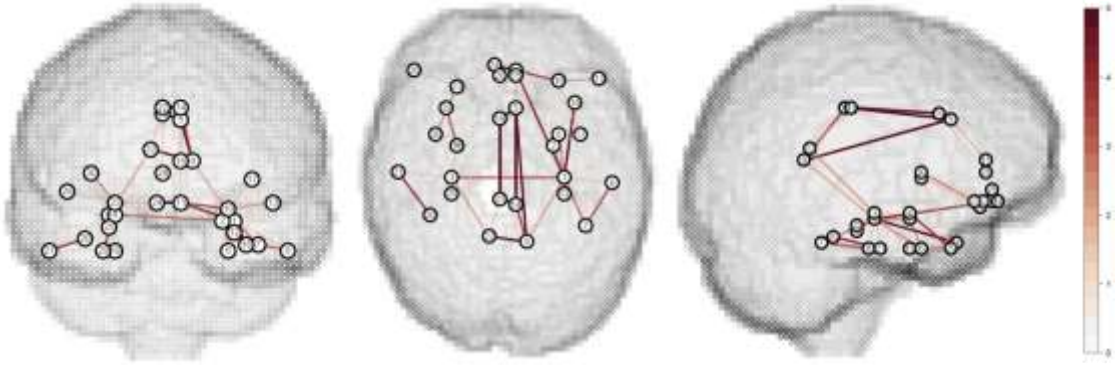

Figure 54 Graphical depiction of a representative participant's limbic structural network overlaid on a surface image of their brain.
The nodes of the graph (the circled numbers), represent limbic brain regions and the edges (red lines) show the connections between pairs of nodes. As before, the shade of each edge represents the number of streamlines contributing to the connection, with darker shades indicating greater connectivity and thus greater weight in the graph, and paler edges representing connections with fewer streamlines, and thus less weight in the graph.

Mean shortest path in the limbic network was reduced in the ASD group compared to neurotypical controls (t=-2.08; p=0.04; does not survive FDR correction). No other significant group differences were detected. Within the ASD group, there were no significant correlations between limbic graph metrics and emotion recognition score, as measured by the 'reading the mind in the eyes' task. Mean clustering

coefficient (rho=0.43; p=0.03; does not survive FDR correction) and mean local efficiency (rho=0.40; p=0.05; does not survive FDR correction) were positively correlated with AQ imagination score.

In the ASD group, average FA in the limbic network was positively correlated with emotion recognition score (rho=0.47; p=0.02 [no need for multiple comparisons correction]). There were no significant results for the association between limbic network FA and the AQ, and no significant results for any tests involving average MD across the limbic network.

7.3.3 Connections of interest

In an exploratory analysis, permutation testing was applied to the whole brain networks in order to identify those edges that were most significantly different between the groups. No results survived FWE multiple comparisons correction. However, less conservative correction using a cut-off of $p \leq 0.005$ (uncorrected) in place of the typical $p \leq 0.05$ (corrected) identified several connections that were most significantly different between the ASD and control groups. These are listed in for number of streamlines (Table 8), average FA (Table 9), and average MD (Table 10).

Region 1	Region 2	Connection Type	p value
Left cingulate gyrus (isthmus)	Left superior frontal gyrus	Parietal – Frontal	0.002
Left cingulate gyrus (isthmus)	Right frontal pole	Interhemispheric: Parietal – Frontal	0.002
Left superior parietal gyrus	Right frontal pole	Interhemispheric: Parietal – Frontal	0.003
Left caudal anterior cingulate cortex	Right rostral middle frontal gyrus	Interhemispheric: Frontal – Frontal	0.003
Left accumbens	Right inferior temporal gyrus	Interhemispheric: Sub-cortex – Temporal	0.004
Left inferior temporal gyrus	Right inferior frontal gyrus (pars orbitalis)	Interhemispheric: Temporal – Frontal	0.004
Right pericalcarine cortex	Right temporal pole	Occipital – Temporal	0.004

Table 8 Edges that were significantly different between the ASD and control groups at $p \leq 0.005$, following permutation analysis of whole brain networks generated using number of streamlines.

Region 1	Region 2	Connection Type	p value
Left caudal middle frontal gyrus	Left middle temporal gyrus	Frontal – Temporal	0.001
Left middle temporal gyrus	Left supramarginal gyrus	Temporal – Parietal	0.001
Right fusiform gyrus	Right superior frontal gyrus	Temporal – Frontal	0.001
Left paracentral gyrus	Right transverse temporal gyrus	Interhemispheric: Frontal – Temporal	0.001
Right superior frontal gyrus	Right transverse temporal gyrus	Frontal – Temporal	0.001
Right inferior parietal gyrus	Right insula	Parietal – Insula	0.001
Left middle temporal gyrus	Left postcentral gyrus	Temporal – Parietal	0.002
Left middle temporal gyrus	Left rostral middle frontal gyrus	Temporal – Frontal	0.002
Left paracentral gyrus	Left superior frontal gyrus	Frontal – Frontal	0.002
Left inferior temporal gyrus	Left supramarginal gyrus	Temporal – Parietal	0.002
Left cingulate gyrus (isthmus)	Right frontal pole	Interhemispheric: Parietal – Frontal	0.002
Left middle temporal gyrus	Left superior frontal gyrus	Temporal – Frontal	0.003
Left inferior frontal gyrus (pars triangularis)	Right caudal middle frontal gyrus	Interhemispheric: Frontal – Frontal	0.003
Left accumbens	Right cingulate gyrus (isthmus)	Interhemispheric: Subcortex – Parietal	0.003
Left precentral gyrus	Right lateral orbitofrontal cortex	Interhemispheric: Frontal – Frontal	0.003
Left accumbens	Right precuneus	Interhemispheric: Subcortex – Parietal	0.003
Left medial orbitofrontal gyrus	Right insula	Interhemispheric: Frontal – Insula	0.003
Left inferior parietal gyrus	Left superior parietal gyrus	Parietal – Parietal	0.004
Left superior frontal gyrus	Right fusiform gyrus	Interhemispheric: Frontal – Temporal	0.004
Left inferior temporal gyrus	Right lateral orbitofrontal cortex	Interhemispheric: Temporal – Frontal	0.004
Right amygdala	Right paracentral gyrus	Subcortex/Temporal – Frontal	0.004
Left cingulate gyrus (isthmus)	Right superior parietal gyrus	Interhemispheric: Parietal – Parietal	0.004
Right lingual gyrus	Right transverse temporal gyrus	Occipital – Temporal	0.004
Left inferior parietal gyrus	Left middle temporal gyrus	Parietal – Temporal	0.005
Left thalamus	Left middle temporal gyrus	Subcortex – Temporal	0.005
Left lateral occipital cortex	Left precentral gyrus	Occipital – Frontal	0.005
Left inferior parietal gyrus	Left superior temporal gyrus	Parietal – Temporal	0.005
Right inferior parietal gyrus	Right superior parietal gyrus	Parietal – Parietal	0.005
Left paracentral gyrus	Right supramarginal gyrus	Frontal - Parietal	0.005

Table 9 Significant connections at p≤0.005 following permutation analysis of whole brain networks generated using FA.

Region 1	Region 2	Conenction Type	p value
Left paracentral gyrus	Right transverse temporal gyrus	Interhemispheric: Frontal – Temporal	0.001
Left rostral middle frontal gyrus	Left superior parietal gyrus	Frontal – Parietal	0.003
Left precuneus	Right cuneus	Interhemispheric: Parietal – Occipital	0.003
Left inferior temporal gyrus	Right lateral orbitofrontal cortex	Interhemispheric: Temporal – Frontal	0.003
Left accumbens	Right precuneus	Interhemispheric: Subcortex – Parietal	0.003
Left cingulate gyrus (isthmus)	Right frontal pole	Interhemispheric: Parietal – Frontal	0.003
Left precentral gyrus	Right inferior parietal gyrus	Interhemispheric: Frontal – Parietal	0.004
Right superior frontal gyrus	Right transverse temporal gyrus	Frontal – Temporal	0.004
Right amygdala	Left precentral gyrus	Interhemispheric: Subcortex/Temporal – Frontal	0.005
Left precentral gyrus	Right lateral orbitofrontal cortex	Interhemispheric: Frontal – Frontal	0.005
Right fusiform gyrus	Right superior frontal gyrus	Temporal – Frontal	0.005
Right pericalcarine cortex	Right transverse temporal gyrus	Occipital – Temporal	0.005

Table 10 Significant connections at p≤0.005 following permutation analysis of whole brain networks generated using MD.

7.4 Discussion

The structural network of the brain was identified and analysed using graph theory. No significant differences in whole brain networks were identified between ASD and control groups for the graph metrics investigated – edge density, mean shortest path, mean clustering coefficient, mean local efficiency, global efficiency, and small worldness – and there were no significant correlations with behavioural measures within the ASD group. There were some significant group difference and correlation results when looking at graph metrics from limbic networks, but these did not survive correction for multiple comparisons. Average FA across the whole brain and limbic networks was reduced in ASD compared to neurotypical controls, and lower FA was correlated with poorer emotion recognition ability within the ASD group. An exploratory permutation analysis identified those edges in which alterations in the number of streamlines, FA, and MD from the whole brain network were most associated with ASD.

The lack of significant findings for the graph analysis was unexpected in the light of significant findings from previous studies, which identified reduced local and global efficiency [289][293][283], and reduced clustering coefficient and betweenness centrality [289] of structural networks in ASD. Conversely, elevated clustering coefficient and reduced path length [290], and increased connectivity within rich clubs [291] have also been identified in ASD structural networks. These findings indicate that the structural brain network is less efficient in ASD, but that there is some heterogeneity regarding local connectivity, with some studies indicating elevated and others reduced clustering of nodes in ASD. However, the lack of significant findings in the study reported in this Chapter is in agreement with those of Rudie et al. [292] who reported no significant group differences in graph measures in spite of microstructural differences in the ASD network.

The discrepancies in the results of graph theory-based network analyses of ASD could arise from differences in the methods used to generate the structural graph. For example, two studies use the AAL mask in order to generate graphs consisting of 90 nodes [293][283], The FreeSurfer Destrieux atlas was used to generate 192 nodes in one study [289] whilst other studies generated graphs with 46 nodes [290], and 200 [291] and 264 equally-sized nodes [292], respectively. In contrast, this study included 82 nodes, some of which were subcortical. Further, weighted graph measures were obtained by some studies [293][283][290][291] in contrast to the binary metrics employed by this study and others [292][289]. In addition, one study used group-averaged graphs in place of individual graphs [291]. Another source of heterogeneity could occur as a result of differences in the demographics of each study cohort. For instance, this study investigated network properties in young adults, whilst the majority of prior structural graph theory analyses have investigated children. The only prior study of structural networks in adults [293] included a greater range of ages (19 – 51 years) than was investigated in the current study (18 – 33 years), and consisted of an entirely male cohort (this study included both males and females).

Reduced FA was identified across the whole brain network in the ASD group compared to controls, and reduced FA was associated with worse emotion recognition ability in the ASD group. This finding is in agreement with those of the TBSS study reported in Chapter 5 that identified widespread reductions in FA across the white matter tracts. This finding, combined with the null results when looking at graph theory metrics across the whole brain, signifies that the topology of the structural network is relatively unchanged in ASD, but that its microstructural quality is compromised; a similar finding to that reported by Rudie et al. [292]. This is suggestive that the ASD brain suffers from disconnection as a result of reduced information transfer, as opposed to the tortuous pathways and inefficient synaptic pruning that have been hypothesised; however, it is important to note that the graph theoretical findings from several other prior studies have indicated the presence of reduced network efficiency in ASD. Therefore, the picture is more complicated – perhaps an over-abundance of synapses confer reduced network efficiency in children with ASD compared to controls, followed by greater topological similarity between ASD and controls in adults. This hypothetical pattern would mirror the trajectory observed for whole brain volumes in ASD [173][174] (see Section 3.1 for more detail), and warrants further investigation.

The work presented in this Chapter extends that of previous studies by the inclusion of subcortical structures and investigation of the limbic network, which is known to be involved in the processing of emotion [368][84]. The results of the limbic analysis did not survive correction for multiple comparisons, but suggested that path length is reduced in ASD compared to controls, and that greater imagination deficits, as measured by the AQ, are associated with increases in mean clustering coefficient and local efficiency. These findings suggest that the limbic network in ASD is characterised by greater local interconnectedness, and that more severe ASD-related imagination deficits are associated with increased density of connections with neighbouring limbic nodes and, contrary to expectations,

increased efficiency of these limbic connections. Local efficiency is the inverse of the path length, so by graph theoretical standards a shorter neural pathway equates to greater efficiency. However, when coupled with the finding of microstructural deficits in the edges of the network, as measured by reduced FA, the results suggest that the limbic network has greater structural connections, but that these connections are themselves less structurally intact. One could hypothesise from this finding that increased local limbic connectivity may develop in the autistic subjects during development as a result of difficulties in information transfer arising from microstructural deficits in the white matter. However this is merely conjecture; the limbic network results did not survive correction for multiple comparisons and thus any interpretation must proceed with caution, but they do suggest interesting lines of enquiry for future studies.

No significant group differences in MD were identified for whole brain or limbic networks. This is in contrast to the results of the TBSS analysis in the same cohort (see Chapter 5), which showed widespread regions of elevated MD in ASD. The discrepancy in this result is likely to arise from the differences in the methodology applied: TBSS restricts the analysis to the centre of the white matter tracts, as identified by high FA values, whilst the probabilistic tractography that forms the basis of network generation incorporates a greater proportion of the white matter tracts, and can therefore result in different readings for microstructural properties. It may be that FA is more robust to these methodological changes than MD within this cohort, perhaps due to the use of FA as the selector for the TBSS skeleton, or that FA is significantly altered over a greater proportion of the ASD white matter than MD, which would suggest that the directionality of water diffusion is more altered in ASD than the total amount of diffusion.

The results of the exploratory permutation testing in the whole brain network did not survive multiple comparisons correction. However, findings using a less

stringent correction scheme indicated that a greater number of edges are associated with ASD-related differences in FA than for MD and number of streamlines. Alterations in the microstructure of interhemispheric connections, and intrahemispheric connections linking the frontal, parietal, and temporal lobes were most associated with ASD. This suggests that white matter tracts involved in the processing of emotional stimuli (associated with the temporal lobe), sensory stimuli (parietal lobe), and overall decision-making and control functions (frontal lobe) are most structurally affected in ASD. These findings are consistent with prior studies of the microstructure of interhemispheric white matter tracts, such as the corpus callosum [250][257], and tracts that connect temporal, parietal, and frontal lobe structures, such as the cingulum, uncinate fasciculus, and inferior fronto-occipital fasciculus [230][273][208]. Many of the connections highlighted by the permutation analysis can be traced to the limbic network, which further supports its association with ASD.

A limitation of this study is that tractography can only estimate the true path of white matter tracts within the brain because it is predicated on the diffusion of water rather than direct measurement of the white matter itself. Another limitation is the relatively poor resolution of imaging in comparison to tract size. A further limitation is distance – longer connections are less likely to be represented in the network than shorter ones due to their reduced probability and dense tract systems that must be traversed [375][376]. Some of the results did not survive correction for multiple comparisons; further studies in larger sample sizes may enable clearer elucidation of small effects. Future work could more closely examine the limbic network in ASD, and study how the properties of structural brain networks relate to those of functional networks, which have been shown to differ in ASD [291][292][377].

7.5 Conclusion

In summary, the network of structural connections in the brain can be considered as a whole and analysed using graph theory, which assesses the topological characteristics of the edges (white matter tracts) and nodes (brain regions) of the network. Results indicate that the overall topology of the whole brain network in young adults with ASD is similar to that of neurotypical controls, but that the connectome is microstructurally compromised and this microstructural deficit is associated with poorer emotion recognition. There is a suggestion of enhanced local connectivity of the limbic network in ASD, which is associated with imagination impairments. Post-hoc analysis indicates that reduced microstructural coherence in a wide array of interhemispheric, frontal, parietal, and temporal connections are associated with ASD. Further work investigating the properties of the limbic network in ASD, the impact of methodology and participant demographics, such as age, on results, and associations between structural networks and functional connectivity within the brain would be beneficial.

Chapter 8 White Matter Microstructure Comparison in Males and Females with Autism, and in Unaffected Siblings

The work reported in this chapter was carried out during a three-month placement in the Yale Child Neuroscience Lab at the Child Study Center, Yale University, USA, under the supervision of Dr Roger Jou and Professor Kevin Pelphrey. The placement was awarded and funded by the Yale-UCL Collaborative.

8.1 Introduction

The studies reported in prior chapters of this thesis are based on investigation of a cohort of young adults with ASD. Since ASD is a neurodevelopmental condition, the majority of research has focused on investigation of the biology and behaviour of children and adolescents as they develop. The exchange visit to Yale afforded me a valuable opportunity to investigate white matter microstructure in a cohort of children and young adolescents, and thus to compare and contrast the findings of this study with those reported in adults in Chapter 5. Prior DTI findings in children with ASD are heterogeneous (see Section 3.2 for more details) but, in general, voxel-based methods have reported reduced FA and elevated MD in children and adolescents with ASD in comparison with controls [223][236][229][226][235][233]. An aim of this study was to see whether the prior findings of reduced FA and elevated MD in children and adolescents with ASD could be replicated in this cohort.

ASD is more common in males than females, with a male:female ratio of 4:1 typically reported [28], though ratios of up to 8:1 have been identified by the WHO [7]. There are several theories regarding the higher incidence of ASD in males (see Section 1.3 for more details), and it is likely that the discrepancy in ASD incidence between the sexes may be due to a combination of factors, including: a) differences

in the ASD phenotype i.e. the number and/or type of behavioural features [378]; b) inherent sex differences in regions of the genome that are associated with genetic vulnerability to ASD, such as XX in females vs XY in males; c) different exposure to hormones – for example increased testosterone in males [379]; d) a conceptualisation of autism that is skewed towards the typical male phenotype, leading to inadequate expertise in ASD diagnosis in females and reduced ability of diagnostic tools to capture cases; e) social support structures making it easier to 'mask' cases in females; f) inherent differences in brain structure and function in the sexes, which reduce vulnerability to ASD in females.

The last putative factor listed above – that of sex-based differences in brain structure and function that make males more susceptible to ASD – has been expressed in the 'extreme male brain' theory by Baron-Cohen [29]. As outlined in Section 1.3.9, the 'extreme male brain' theory proposes that ASD occurs as a result of overly 'male' brain features that are associated with extreme 'male' behaviours, which are characterised as an heightened propensity for systematising and a reduced predisposition for empathy [380][126]. This hypothesis implies that females with ASD have brains and behavioural characteristics that are more similar to males than to typical females, which suggests that females with a diagnosis of ASD have experienced more severe neurodevelopmental aberrations than males diagnosed with ASD. In 2005 Baron-Cohen et al. reviewed evidence for the neurological basis of the extreme male brain in ASD [380], identifying larger whole brain and amygdala volumes and contrastingly reduced corpus callosum and internal capsule volumes in typical males compared to females that were more pronounced in ASD. A more recent, relatively large-scale, VBM study reported evidence for an 'extreme male brain' in ASD, as shown by sex-based grey and white matter differences in ASD compared to controls that overlapped with typically sexually dimorphic brain regions in the females, but not the males [285]. This suggests that in females with ASD, greater aberrations occur in brain regions that are typically associated with sex-based differences. Bloss and Courchesne [381] published evidence for sex-

specific brain volume differences in ASD that were associated with age in females, but not in males; thus hypothesising that the trajectory of aberrant brain development in ASD differs between the sexes. A longitudinal study reported anomalies in the trajectory of brain growth in more regions in females with ASD than autistic males [176]. Conversely, no significant sex differences in corpus callosum volume were identified in a study of adults with ASD [382], thus indicating that sex-specific brain volume effects may not always be observed in ASD, or that they depend upon factors such as the white matter tract of interest or participant age.

In terms of white matter microstructure, Beacher et al. [286] reported sex effects on FA in certain white matter tracts, including the corpus callosum, which indicated that the typical pattern of sexual dimorphism in these brain structures was lacking in ASD. Nordahl et al. [287] also reported sex-based differences in corpus callosum connectivity in ASD. In a study of children with ASD in comparison to healthy controls [245], a group difference in FA was observed; when grouped by sex, the result remained the same in the boys, but was not present for the girls which, conversely to the majority of the volumetric evidence, suggests that girls with ASD have more similar microstructure to controls of their own sex than is the case for boys. In a study of healthy adults [383], in females FA in the white matter underlying the inferior parietal lobule and the superior temporal gyrus positively associated with empathy, as measured by the empathising quotient (EQ), and FA of the occipital and postcentral gyrae negatively correlated with systematising, as measured by the systematising quotient (SQ); the associations were reversed in males. This signifies that the microstructure of the white matter in certain brain regions has sexually dimorphic associations with traits that are associated, at the extreme, with the presence of ASD. These studies provide evidence that biological sex has an effect on white matter microstructure in ASD, though there is heterogeneity with regards to the nature of this effect. Contrary to this, a TBSS study in adults with ASD did not identify any effect of biological sex [288]. There is,

therefore, a rationale for further clarification of the effect of biological sex on white matter microstructure in ASD, and also to investigate possible sex-based differences in the severity of ASD traits.

Interestingly, biological sex also appears to affect the likelihood of siblings being diagnosed with ASD: a recent study reported increased risk of ASD symptoms in the siblings of females severely affected by ASD compared to siblings of similarly-afflicted male probands [384]. This suggests that females with ASD have a greater etiological load than males, which in turn confers greater vulnerability to siblings, though genetic analysis would be needed to clarify this. The presence of an endophenotype of ASD-related cognitive and/or social difficulties has been described in both twin [37][38] and family studies [39]. An endophenotype of reduced social responsiveness has also been reported in families with at least one individual diagnosed with ASD [385]. Further, relatively large head sizes have been measured in un-affected family members of autistic probands [65][66][67], suggesting that familial brain structures are conserved, and may be related to ASD.

In 2010, Barnea-Goraly et al. [223] published the first investigation of microstructural endophenotypes in the brains of unaffected siblings of ASD probands. Results showed significant microstructural aberrations, as measured by FA, in the white matter of the unaffected siblings in comparison to neurotypical controls, in addition to even more widespread aberrations in the ASD group compared to controls. This suggests that there is a step-wise increase in abnormal white matter structure from controls, to unaffected siblings, and finally to ASD. A step-wise pattern of structural aberrations has also been reported in a study of network properties from low-risk infants, to high-risk infants (i.e. those with a sibling previously diagnosed with ASD) without ASD, through to high-risk infants with a diagnosis of ASD themselves [283]. Some of these microstructural changes are likely to be endophenotypic of ASD, and others form biomarkers of ASD. There

is evidence that endophenotypic changes in microstructure are related to the developmental trajectory: for example, Lisiecka et al. [284] reported a reduced association between age and λ_2 in the right superior longitudinal fasciculus in ASD probands and their siblings compared to neurotyptical controls. A step-wise relationship has also been identified in a functional study of brain activation in response to biological motion: some unique – perhaps compensatory – brain activations were recorded in unaffected siblings in addition to some shared activations – potentially endophenotypic – that occurred in both the unaffected and affected siblings, and some ASD-specific responses [386]. Therefore, a second aim of this project was to examine white matter microstructure in unaffected siblings in order to identify endophenotypic or unique (perhaps compensatory) structural differences, in addition to investigating how these vulnerabilities relate to the presence or absence of ASD traits themselves.

In summary, ASD is a neurodevelopmental condition so it is useful to assess white matter microstructure at each stage of the developmental process. Further, ASD disproportionately affects males and the reasons for this are unclear, though are likely to include a combination of genetic, biological, and societal factors. It has been proposed that male brains are more vulnerable to ASD, which suggests that females with ASD undergo greater neurodevelopmental assault than males in order to present with the same condition. One aim of this study was to investigate this hypothesis by assessing white matter microstructure in a cohort of males and females with ASD and measuring its association with different ASD symptoms. Furthermore, ASD is highly heritable and siblings of probands are at a greater risk of diagnosis than the general population. Vulnerabilities and/or endophenotypes of ASD are likely to occur in these families, so another aim of this study was to investigate white matter microstructure in unaffected siblings in order to further elucidate the nature of this association.

8.2 Methods

8.2.1 Participant recruitment

127 children and adolescents aged between 4 and 17 years of age were recruited to this study, consisting of 75 children diagnosed with ASD, 21 unaffected siblings of probands, and 31 neurotypical controls. Participants included both related proband and sibling pairs in addition to un-related siblings and probands. ASD diagnoses were confirmed based on clinical history, parent interview, and expert evaluation using the ADI or ADOS. Semi-structured interviews were conducted with control participants and/or their primary caregiver in order to rule out a family history of ASD or the presence of siblings with ASD. No participant had a history of neurological disease or neurological injury. The study was approved by the Yale University Human Investigations Committee, and informed consent was obtained from each participant's parent or guardian, as well as the child's verbal consent.

8.2.2 Cognitive testing

Full-scale IQ was measured using the DAS II [387]. Three participants were excluded due to missing IQ data, and 9 for IQ scores ≤70, which resulted in 115 participants from the original 127 recruited to the study. The parent/guardian-assessed social responsiveness scale (SRSp) [388] was administered in order to measure autistic traits across five sub-scales – awareness, cognition, communication, mannerisms, and motivation. Higher scores in the SRSp indicate a greater amount and severity of ASD behaviours in these categories. A benefit of the SRSp is that it is designed to assess autistic traits across the spectrum from individuals in the general population through to those individuals with a clinical diagnosis of ASD.

8.2.3 MRI data acquisition and pre-processing

Participants were given a practise session on a mock MRI scanner, and then completed the imaging protocol in one session. Whole-head MRI was conducted

using a 3T Siemens Magnetom Tim Trio (Siemens, Erlangen, Germany) scanner. T_1-weighted MRI was carried out using a sagitally-acquired MP-RAGE sequence with the following parameters: flip angle = 7°; TR = 2530ms; TE = 3.66ms; voxel size: 1mm isotropic; slices = 176. The scan lasted for 8 minutes. Additionally, three diffusion-weighted images were acquired, each lasting 11 minutes, with 30 unique gradient directions (b=1000s/mm^2) and five reference b=0 images. The diffusion imaging parameters were: TR = 6200ms; TE = 85ms; voxel size = 2.5mm isotropic; slices = 55.

The diffusion-weighted scans were pre-processed with TractoR and FSL using the procedure described in Section 4.4.2. The scans were eddy-corrected as per the typical procedure, with the highest quality b=0 volume selected as the control for eddy correction. The process was then modified in order to average the three diffusion-weighted scans, thus ameliorating the effects of any motion artefacts, which are more apparent in MRI scans from children, and providing more representative, high-quality images. The modified procedure involved visually assessing each volume of the three eddy-corrected diffusion-weighted scans and noting down those volumes with significant motion artefacts – defined as blurring or signal drop out affecting the white matter. For an example, see Figure 55.

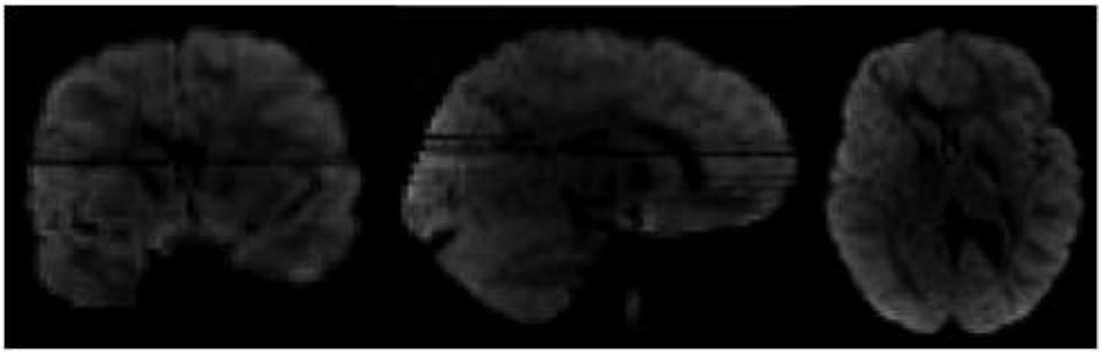

Figure 55 An example of signal dropout in the diffusion-weighted scan following motion during the scan sequence.

The signal dropout results in characteristic horizontal black lines across the resulting scan.

Each diffusion-weighted scan was then divided into its constituent volumes using FSL utilities, and those volumes deemed to have significant motion artefacts were removed prior to averaging the remaining scan volumes using FSL utilities. This process resulted in one average diffusion-weighted scan for each participant. On occasions in which all three versions of a scan volume was satisfactory, the average volume was generated from all three of the original volumes; where one scan volume was excluded due to motion artefact, the average volume was generated from the two remaining original scan volumes; in cases where two of the original scan volumes were excluded, the one remaining volume was passed straight to the final scan. In some cases all three versions of a volume were excluded, and thus could not be incorporated into the final scan. Since the scans were acquired using 30 unique gradient directions, it was still possible to estimate the diffusion tensor with one direction missing (six unique gradient directions are the minimum required to estimate the most basic diffusion tensor [389]), though the greater the number of gradient directions, the more accurately the diffusion tensor can be estimated. In order to preserve accuracy, a threshold was applied, such that a participant was excluded from the study in the event that they had greater than seven volumes (and thus over seven gradient directions) excluded. This meant that 12 participants were excluded from the study due to inadequate DTI data, leaving a total of 103 participants from the original 127 recruited (as mentioned above, a further 12 participants were excluded due to missing or low IQ scores).

Each of the final averaged diffusion-weighted images was visually assessed prior to pre-processing in the typical fashion using TractoR and FSL, as outlined in Section 4.4.2.

8.2.4 Whole brain volume measurements

The T_1-weighted scans were visually assessed for motion artefacts and noise, and 8 participants' (2 ASD, 3 controls, and 3 unaffected siblings) T_1-weighted data was excluded from the study. Some participants had more than one T_1-weighted scan; in these cases the highest quality scan was used for the following analysis. SIENAX was used to estimate whole brain volume, as outlined in Section 4.4.1.1.

8.2.5 Tract-based spatial statistics

TBSS was run using a slightly amended version of the protocol reported in Chapter 5 of this thesis. The mask used in the typical TBSS protocol was developed using adult reference scans and so was not applicable to the young participants in this study. In order to take this into account, the TBSS analysis stream was adjusted to select the most 'typical' scan as the registration target image, instead of the adult-generated reference mask. Further, a typical threshold for the TBSS skeleton is FA=0.2 (as was used in the analysis in Chapter 5), but following visual assessment a higher threshold of FA=0.4 was selected for the TBSS skeleton in this study in order to ensure that each participant's major tracts aligned well with the skeleton. This may be due to greater variation in the young cohort's brains, which are still undergoing development. The remainder of the TBSS protocol continued as per the process described in Chapter 5 for FA, MD, AD, and RD.

Group-wise comparisons of FA, MD, AD, and RD were carried out using the FSL tool randomise, which carries out permutation tests using a general linear model, for the following comparisons – a) ASD vs neurotypical controls; b) ASD vs unaffected siblings; c) unaffected siblings vs controls – all with age, sex, full-scale IQ, and whole brain volume as covariates. These four tests were then repeated separately in males and females (without biological sex as a covariate), in order to identify whether group comparisons differ between the sexes. All tests were

corrected for multiple comparisons using FWE and employed TFCE, as per the TBSS protocol.

Significant voxels were identified using a skeletonised version of the John's Hopkins University (JHU) ICBM-DTI-81 atlas, as described in Chapter 5.

8.2.6 Averaging DTI measures within the TBSS skeleton

FA, MD, AD, and RD values were averaged across the white matter skeleton in each of the participants, as per the protocol described in Section 5.2.2. These average values were used for the correlation analysis, described below.

8.2.7 Correlations between DTI metrics and clinical scores

Associations between white matter microstructure, as measured by FA, MD, AD, and RD, and ASD symptom severity, as measured by the SRSp subsets – awareness, cognition, communication, motivation, and mannerisms – were assessed via partial correlation using the DTI metrics averaged across the white matter skeleton, covarying for age, sex, full-scale IQ, and whole brain volume. Multiple comparisons correction was applied using FDR. The same correlations were also carried out within the TBSS protocol in order to establish which voxels were contributing to any association.

SRSp scores were missing in 7 participants (7 ASD, 4 control, and 1 unaffected sibling), so these subjects were excluded from the correlation analyses.

8.3 Results

8.3.1 Demographics

Participant demographics following the exclusion of 12 participants for motion in the DTI data, 3 participants for low IQ scores, and 9 for missing IQ data are shown in Table 11. The unaffected sibling group was significantly older than the ASD group (p=0.009). This is not wholly unexpected since a sibling group is likely to contain participants that are either older or younger than their related probands. Race was significantly different between the ASD and control groups (p=0.003), which can be attributed to greater numbers of participants identifying as White or Multiple races and fewer identifying as Black or Asian in the ASD group compared to the controls. SRSp total scores were significantly higher in the ASD group compared to both controls and unaffected siblings (both p<0.0001), as expected. There were no significant differences in SRSp scores between the control and unaffected sibling groups (p=0.33), which indicates that the unaffected siblings do not experience a greater incidence of ASD traits than the typical population, and thus questions the concept of a wider autistic phenotype in the families of ASD probands [39][385]. All other metrics were not significantly different between the three groups.

	Control (n = 25)	ASD (n = 58)	Sibling (n = 20)	p value: Control vs Sibling	p value: ASD vs Control	p value: ASD vs Sibling
Sex[1]	13M:12F	45M:13F	12M:8F	0.81	0.12	0.32
Handedness[1]	22R:1L:2U	44R:8L:4A:2U	14R:6L	0.17	0.17	0.17
Age (yrs)[2]	10.17 (3.80) [5.04 – 16.23]	8.72 (3.67) [4.16 – 17.15]	10.85 (2.74) [5.33 – 16.74]	0.49	0.11	**0.009**
Race[1]	14W:8B:2A:1M	49W:2B:1A:5M:1U	18W:1B:1A	0.49	**0.003**	0.12
Full-scale IQ[2]	100.24 (17.16) [73 - 141]	101.81 (17.64) [72 - 136]	107.10 (11.55) [91 - 135]	0.12	0.71	0.13
SRSp total[2]	27.64 (23.69) [3 – 93]	83.35 (29.78) [22 - 147]	21.58 (15.27) [4 - 52]	0.33	**<0.0001**	**<0.0001**

Table 11 Participant demographics and cognitive test scores.

[1]p-values are obtained from Chi-squared tests.[2]Data are expressed as mean (standard deviation) [range], and p-values are obtained from t-tests. For sex: M = male; and F = female; for handedness: R = right, L = left, A = ambidextrous, and U = unknown; for race: W = white, B = black, A = Asian, M = multiple, and U = unknown.

Motion during the diffusion-weighted scan, as measured by average rotation was not significantly different between the groups (all $p \geq 0.10$). Furthermore, there were no significant group differences in the number of diffusion-weighted scans contributing to the final average diffusion-weighted scan used in the subsequent analyses (all $p \geq 0.26$), which indicates that SNR was consistent across the groups.

8.3.2 Whole brain volume

Whole brain volume was significantly higher in the ASD group compared to controls ($t=3.09$; $p=0.003$), and in unaffected siblings compared to controls ($t=2.62$; $p=0.01$). There was no significant difference in whole brain volume between the ASD and unaffected sibling groups ($t=0.20$; $p=0.84$).

8.3.3 Group differences in white matter microstructure

Average FA, MD, AD, and RD across the TBSS white matter skeleton were assessed using box-and-whisker plots. Four vastly outlying participants were removed from the analyses because it was deemed that their DTI metrics could not be relied upon, and that they would skew results.

FA was significantly reduced in the ASD group compared to controls in the left anterior corona radiata and the genu and body of the corpus callosum (see Figure

56). There were no other significant group differences in FA, and no significant differences for MD, AD, or RD.

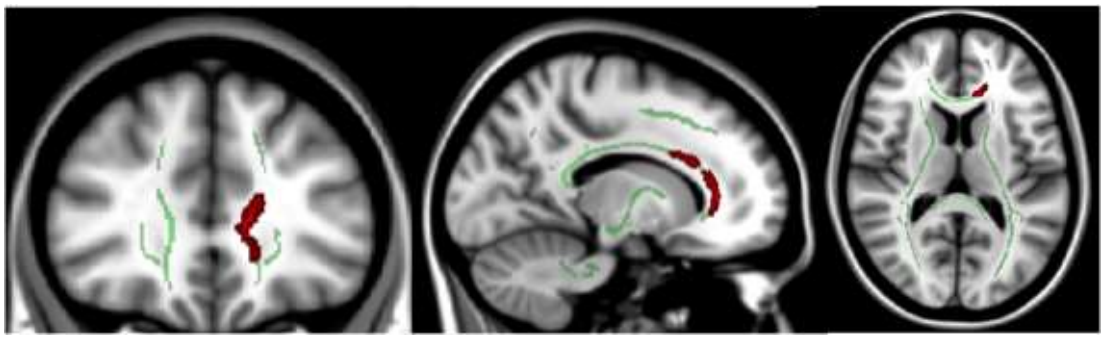

Figure 56 Voxels with reduced FA in the ASD group compared to neurotypical controls are shown in red.
Significant regions include regions of the left anterior corona radiata and the body and genu of the corpus callosum. Results are shown overlaid on the TBSS white matter skeleton, which is shown in green. TBSS fill was used to aid visualisation.

8.3.4 Association between white matter microstructure and ASD traits

The association between DTI metrics averaged over the entire white matter skeleton with ASD traits, as measured by subsets of the SRSp, were investigated. See Figure 57 for the resulting correlation plots; though please note that to save space only those correlations that were also significant in the TBSS analysis (see below) are shown in the figure. For DTI metrics averaged across the white matter skeleton, FA was positively correlated with each of the SRSp subsets in the control group (awareness: rho=0.53, p=0.01; cognition: rho=0.69, p=0.0003; communication: rho=0.58, p=0.005; mannerisms: rho=0.64, p=0.001; motivation: rho=0.72, p=0.0001 (see Figure 57A) (all $p \leq 0.05$ following FDR)). In contrast, FA was negatively correlated with SRSp mannerisms in the ASD group (rho=-0.31, p=0.02; does not survive FDR), however this finding did not survive FDR correction for multiple comparisons. A similar pattern of associations was found for MD and RD. MD was

negatively correlated with each of the SRSp subsets in the control group (awareness: rho=-0.46, p=0.03; cognition: rho=-0.63, p=0.002 (see Figure 57B); communication: rho=-0.46, p=0.03 (see Figure 57C); mannerisms: rho=-0.57, p=0.005 (see Figure 57D); motivation: rho=-0.65, p=0.001 (see Figure 57E) (all p≤0.05 following FDR)) and positively correlated with SRSp mannerisms in the ASD group (rho=0.30, p=0.03; does not survive FDR), although this did not survive correction. Likewise, RD was negatively correlated with each of the SRSp subsets in the control group (awareness: rho=-0.55, p=0.008; cognition: rho=-0.73, p=0.0001 (see Figure 57F); communication: rho=-0.57, p=0.005; mannerisms: rho=-0.66, p=0.0008; motivation: rho=-0.74, p<0.0001 (see Figure 57G) (all p≤0.05 following FDR)) and positively correlated with SRSp mannerisms in the ASD group (rho=0.33, p=0.02; does not survive FDR), although this did not survive correction. There were no significant associations for AD, and none within the unaffected siblings.

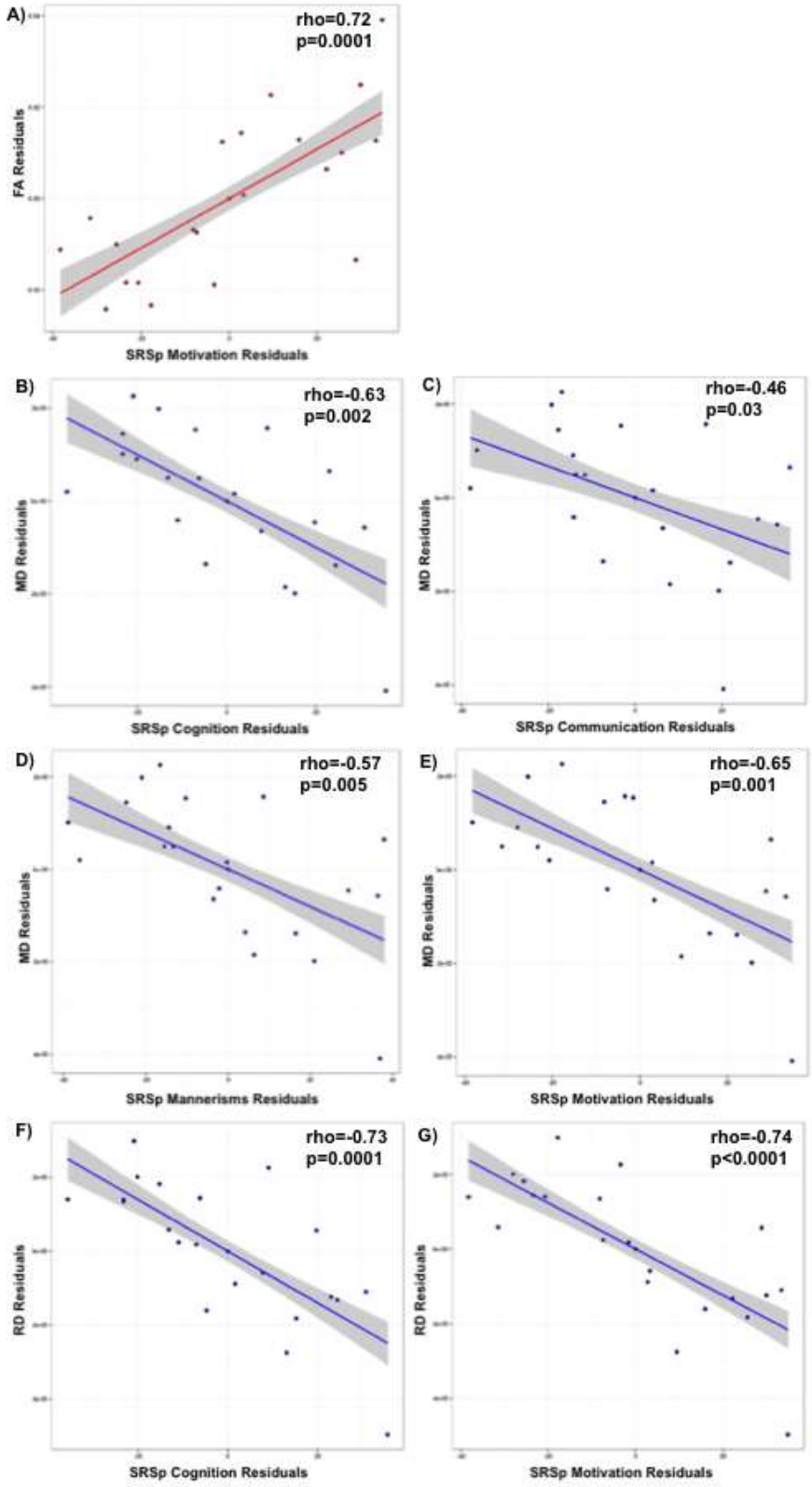

Figure 57 Plots showing DTI–SRSp associations in control participants. Results are shown for a) FA and SRSp motivation (rho=0.72; p=0.0001), b) MD and SRSp cognition (rho=-0.63; p=0.002), c) MD and SRSp communication (rho=-

0.46; p=0.03), d) MD and SRSp mannerisms (rho=-0.57; p=0.005), e) MD and SRSp motivation (rho=-0.65, p=0.001), f) RD and SRSp cognition (rho=-0.73, p=0.0001), g) RD and SRSp motivation (rho=-0.74, p<0.0001). The grey shaded area represents standard error. All analyses controlled for age, full-scale IQ, whole brain volume, and race, and all remained significant (p≤0.05) following FDR multiple comparisons correction.

TBSS was used in order to identify whether particular white matter tracts contributed to the significant correlations between average DTI measures and SRSp subset scores within the control group. As with the correlation analysis for average DTI measures described above, in the TBSS correlation analysis SRSp communication and mannerism scores were negatively correlated with MD, SRSp cognition was negatively correlated with MD and RD, and SRSp motivation was negatively correlated with MD and RD, and positively correlated with FA. All p-values were ≤0.05 following FWE multiple comparisons correction and TFCE. Contrary to the correlation analysis using DTI metrics averaged over the whole white matter skeleton, significant correlations following correction were not found in TBSS for FA and SRSp awareness, cognition, communication, and mannerisms, for MD and SRSp awareness, and for RD and SRSp awareness, communication, and mannerisms. The white matter tracts with the greatest contribution to those correlations that remained significant in the TBSS analysis, as measured by the proportion of the tract with significant voxels are shown in Table 12. Results show that the correlations between FA and SRSp motivation and MD and SRSp mannerisms are restricted to the corona radiata, while the correlations between MD and SRSp cognition, communication, and motivation and RD and SRSp cognition and motivation are widespread across the white matter. As shown in Table 12, the corona radiata is most commonly involved in the correlations, followed by the inferior longitudinal fasciculus, inferior fronto-occipital fasciculus, internal capsule, posterior thalamic radiation, corpus callosum, and tapetum.

Correlation	% of White Matter Tract Affected	White Matter Tract
Positive Correlation: FA & SRSp Motivation	23.91	Right posterior corona radiata
	21.97	Left superior corona radiata
	15.13	Left posterior corona radiata
	13.03	Right superior corona radiata
Negative Correlation: MD & SRSp Cognition	95.01	Right anterior corona radiata
	87.19	Right sagittal stratum (ILF & IFOF)
	84.82	Left anterior corona radiata
	82.97	Right posterior corona radiata
	67.25	Right superior corona radiata
	67.16	Right posterior thalamic radiation
	64.65	Left sagittal stratum (ILF & IFOF)
	62.9	Left superior longitudinal fasciculus
	62.3	Right retrolenticular internal capsule
	62.12	Left superior corona radiata
Negative Correlation: MD & SRSp Communication	81.67	Right anterior corona radiata
	62.81	Right sagittal stratum (ILF & IFOF)
	61.59	Right posterior corona radiata
	54.55	Left sagittal stratum (ILF & IFOF)
	52.84	Right posterior thalamic radiation
	46.73	Right retrolenticular internal capsule
	44.96	Left posterior corona radiata
	44.79	Right superior corona radiata
	37.79	Corpus callosum-splenium
	37.5	Left retrolenticular internal capsule
Negative Correlation: MD & SRSp Mannerisms	48.61	Right anterior corona radiata
	15.51	Right superior corona radiata
Negative Correlation: MD & SRSp Motivation	80.98	Left anterior corona radiata
	80.51	Right anterior corona radiata
	76.36	Left superior corona radiata
	76.09	Right posterior corona radiata
	72.31	Right sagittal stratum (ILF & IFOF)
	71.49	Right posterior thalamic radiation
	63.74	Right retrolenticular internal capsule
	58.55	Right posterior limb internal capsule
	57.22	Right tapetum
	57.14	Left posterior corona radiata
Negative Correlation: RD & SRSp Cognition	83.64	Right anterior corona radiata
	82.26	Right superior corona radiata
	76.92	Right superior fronto-occipital fasciculus
	73.79	Left superior corona radiata
	71.59	Right posterior limb internal capsule
	70.4	Left anterior corona radiata
	60.96	Right tapetum
	51.24	Right sagittal stratum (ILF & IFOF)
	50.33	Corpus callosum-genu
	50	Left posterior corona radiata
Negative Correlation: RD & SRSp Motivation	100	Left superior fronto-occipital fasciculus
	77.05	Right superior corona radiata
	76.21	Left superior corona radiata
	75.15	Left anterior corona radiata
	73.44	Right posterior limb internal capsule
	54.2	Left posterior corona radiata
	53.48	Right tapetum
	51.57	Right retrolenticular internal capsule
	49.49	Left posterior limb internal capsule
	47.83	Left posterior limb internal capsule

Table 12 The top 10 white matter tracts with a significant correlation between DTI metric and SRSp subscore, as measured by the proportion of the tract contributing to the correlation.

Only those white matter tracts with ≥10% of the tract significant were included, hence some correlations have fewer than 10 white matter tracts included in the table.

8.3.5 Sex-based differences in ASD traits and white matter microstructure

Table 13 shows the results of comparison of SRSp total score in females and males with ASD. As shown in the Table, in males SRSp total scores were significantly higher in the ASD group compared to both controls (t=7.90; p<0.0001) and unaffected siblings (t=9.13; p<0.0001). The same remained true for females, with significantly higher SRSp total scores in ASD compared to controls (t=4.95; p=0.0002) and unaffected siblings (t=8.80; p<0.0001). There were no significant differences in SRSp total scores in females with ASD in comparison with males diagnosed with ASD (t=-1.40; p=0.17, or between male and female unaffected siblings (t=-0.95; p=0.36) and controls (t=0.93; p=0.36).

	Control	ASD	Sibling	p value: Control vs Sibling	p value: ASD vs Control	p value: ASD vs Sibling
SRSp total[1] All Subjects	27.64 (23.69) [3 – 93]	83.35 (29.78) [22 – 147]	21.58 (15.27) [4 – 52]	0.33	**<0.0001**	**<0.0001**
SRSp total[1] Females	32.36 (26.58) [3 – 93]	76.36 (12.72) [56 – 95]	17.29 (14.57) [4 – 42]	0.14	**0.0002**	**<0.0001**
SRSp total[1] Males	22.91 (20.57) [6 – 77]	85.09 (32.57) [22 – 147]	24.08 (15.71) [4 – 52]	0.88	**<0.0001**	**<0.0001**
				p value: Control vs Control	p value: ASD vs ASD	p value: Sibling vs Sibling
SRSp total[1] Males vs Females	-	-	-	0.36	0.17	0.36

Table 13 Participant social responsiveness scale (SRS) scores, with score comparison by biological sex.

[1] Data are expressed as mean (standard deviation) [range], and p-values are obtained from t-tests.

Within females there were no significant differences in white matter microstructure, as measured by FA, MD, AD, and RD between the ASD, unaffected sibling and control groups. Within males, AD was significantly reduced in ASD compared to neurotypical controls in the bilateral corona radiata, the left internal capsule, and the genu and body of the corpus callosum (see Figure 58). There were no other significant group differences in FA, MD, AD, or RD for males.

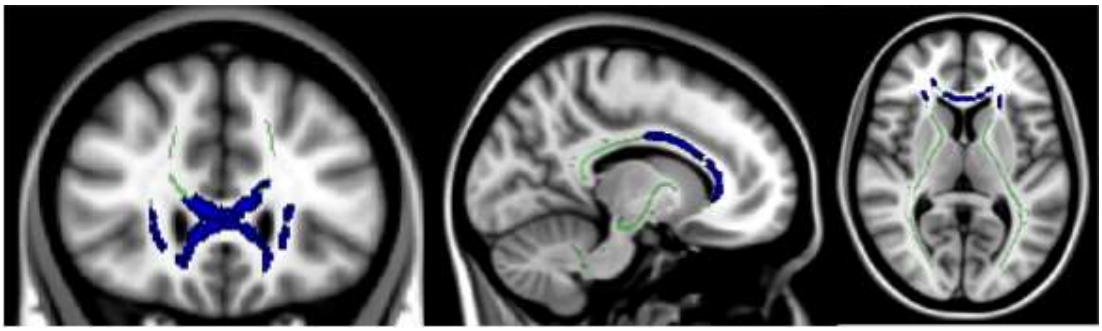

Figure 58 Voxels with reduced AD in males with ASD compared to neurotypical controls are shown in blue.
Significant results are seen in the bilateral corona radiata, the left internal capsule, and the genu and body of the corpus callosum. Results are overlaid on the TBSS white matter skeleton in green. TBSS fill was used for visualisation.

Correlations between white matter microstructure and SRSp subsets were investigated in males and females separately. Similarly to the results for the entire cohort, the only significant results following FDR correction were those in the controls. Significant results are shown in Table 14 for male controls and Table 15 for female controls.

DTI Metric	SRSp Subset	rho	p value
FA	Awareness	0.81	**0.002**
	Cognition	0.70	**0.02**
	Communication	0.76	**0.007**
	Mannerisms	0.73	**0.01**
	Motivation	0.68	**0.02**
RD	Awareness	-0.89	**0.0002**
	Cognition	-0.73	**0.01**
	Communication	-0.77	**0.005**
	Mannerisms	-0.74	**0.01**
	Motivation	-0.78	**0.005**

Table 14 Significant correlations between DTI metrics and SRSp subsets in male controls.

Those in bold remain significant ($p \leq 0.05$) following FDR multiple comparisons correction.

DTI Metric	SRSp Subset	rho	p value
FA	Awareness	0.60	**0.05**
	Cognition	0.79	**0.004**
	Communication	0.61	**0.05**
	Mannerisms	0.82	**0.002**
	Motivation	0.86	**0.0007**
MD	Awareness	-0.82	**0.002**
	Cognition	-0.84	**0.001**
	Communication	-0.73	**0.01**
	Mannerisms	-0.91	**0.0001**
	Motivation	-0.86	**0.0006**
AD	Awareness	-0.80	**0.003**
	Cognition	-0.68	**0.02**
	Communication	-0.66	**0.03**
	Mannerisms	-0.78	**0.005**
	Motivation	-0.69	**0.02**
RD	Awareness	-0.75	**0.008**
	Cognition	-0.84	**0.001**
	Communication	-0.69	**0.02**
	Mannerisms	-0.90	**0.0002**
	Motivation	-0.89	**0.0003**

Table 15 Significant correlations between DTI metrics and SRSp subsets in female controls.

Those in bold remain significant (p≤0.05) following FDR multiple comparisons correction.

8.4 Discussion

This study investigated whole brain volume and white matter microstructure in children and adolescents with ASD, with an additional focus on white matter microstructure in the unaffected siblings of autistic probands and the effect of biological sex on ASD-related white matter changes. Results showed that whole brain volume was similarly elevated in the ASD and unaffected sibling groups in

comparison with controls. White matter microstructure was less coherent, as measured by reduced FA, in ASD compared to controls, but there were no significant group differences in white matter microstructure between unaffected siblings and controls. Correlations between white matter microstructure and SRSp subsets were in the opposite directions in control and ASD participants, though only the correlations in the control group remained significant following multiple comparisons correction. There were no sex-based differences in ASD trait severity, as measured by the SRSp. Males with ASD had significantly reduced AD in comparison with male controls; no significant group differences in white matter microstructure were identified in females.

The finding of elevated whole brain volume in this sample of children and adolescents with ASD is consistent with previous reports [166][167]. Similarly elevated whole brain volume was measured in unaffected siblings of ASD probands, which suggests that whole brain volume may be an endophenotype of ASD – i.e. characteristic of the autistic individual and their close relations, as opposed to a biomarker that is specific to the ASD proband. This is consistent with findings of elevated head circumference in the unaffected siblings of ASD probands [65][66][67] and findings of regional grey matter volume increases in both unaffected and affected siblings [390], but is in contrast to a finding of no significant volumetric differences between high-risk infants and control [391]. Evidence in adults with ASD, including that reported in Chapter 5, has found that whole brain volumes are similar to those of controls, which suggests that there is a trajectory of increased brain growth in the early years of ASD, which levels out in adulthood, such that whole brain volume becomes similar to that of neurotypical controls, a hypothesis supported by longitudinal studies [167][173][174]. In future longitudinal studies, it would be interesting to investigate the trajectory of whole brain growth in unaffected siblings as they develop, in order to observe whether they follow the same pattern of increased whole brain volume followed by levelling off in adulthood as their affected sibling.

FA was significantly reduced in the ASD group in comparison to controls in the left anterior corona radiata and the genu and body of the corpus callosum, indicating that these structures are less coherent in children and adolescents with ASD. This finding is consistent with prior evidence of reduced FA of the corpus callosum [244][237][235] and corona radiata [223], though it is in contrast to the widespread reductions in FA reported in prior DTI studies of the entire white matter in ASD [206], and with disparate evidence of FA increases in children with ASD [238][212]. There were no significant differences in MD, AD or RD between ASD and control groups, which is consistent with several studies of children with ASD in which a significant FA effect was reported in the absence of measurable group differences in diffusivity [245][227][222]. This finding could reflect reduced coherence to the organisation of axons (identified by the FA reduction), but relatively similar axonal density (indicated by no significant difference in diffusivity). The restriction of group differences to FA and their less widespread nature in this study is in contrast to my findings in adults with ASD (Chapter 5). This may be due to the age of the participants, which has a strong effect on white matter microstructure in both healthy and autistic subjects [206][216] (see Section 3.2.2 for more). A further consideration is that a smaller white matter skeleton was employed in this study compared to that in Chapter 5, which means that significant differences in outlying white matter could not be investigated in this study.

There were no significant differences in white matter microstructure between unaffected siblings and controls, which indicates that alterations in white matter microstructure do not form part of a wider endophenotype of ASD and are more likely to be a biomarker of the condition. However, in the present study, no significant group differences in white matter microstructure were identified between unaffected siblings and ASD either. Both of these results are in contrast to evidence from Barnea-Goraly et al. [223] and Lewis et al. [283], who reported step-wise alterations in FA and white matter network arrangement, respectively, in

unaffected siblings and ASD compared to controls; evidence which suggests that some aspects of structural connectivity are endophenotypic, and thus are present in both unaffected siblings and those with ASD, whilst others are restricted to ASD sufferers, and thus may reflect biomarkers of ASD itself. Additional evidence from a longitudinal study of high-risk infants (i.e. infants with a sibling already diagnosed with ASD) has indicated that developmental trajectories of FA are significantly different between those children later diagnosed with ASD compared to those who did not receive a later ASD diagnosis [203]. The lack of significant results in this study does not necessarily mean that there are no ASD-related endophenotypes or step-wise changes in white matter microstructure, rather it may be that they were not detectable in this instance. This may be because they are weak effects, or that they only occur in particular white matter tracts or scenarios, depending upon characteristics of the study group such as age. Further investigation, such as large-scale longitudinal studies in well-defined sibling–proband pairs would be needed to clarify the nature of ASD risks and their effect on brain structure.

To investigate the relationship between white matter microstructure and ASD symptom severity across the groups, correlations between DTI metrics and SRSp score were carried out. Resulting associations in control and ASD groups were in the opposing directions; however, the correlations in the ASD group did not survive correction for multiple comparisons. Furthermore, there were no significant correlations within the unaffected siblings. The correlations in the control group that survived correction for multiple comparisons correction indicated that more severe autistic traits, as evidenced by higher SRSp scores, are associated with elevated FA and reduced MD and RD – findings that one would normally associate with increased coherence of white matter tracts. These correlation results are at odds with the finding of reduced FA in the ASD group compared to controls. However, it is important to remember that the correlation finding is within the control group only, and therefore suggests that the association between white matter microstructure and ASD traits, as measured by the SRSp, is not consistent across the spectrum from

neurotypical to clinically-diagnosed individuals. This finding is at odds with those described in adults in Chapter 5 of this thesis, which supported the concept of a spectrum of white matter microstructural deficits that was reflective of a spectrum of ASD traits across the study population. This discrepancy may reflect the methodological differences between the study – such as the use of the parent-reported SRSp versus the self-reported AQ – and/or differences in the demographics of the cohorts, most obviously that of age. It may be that younger neurotypical children and adolescents are more likely to have ASD traits in the presence of more ordered white matter, and that this association changes as the white matter matures and develops over time. Indeed, some evidence suggests that elevated FA is associated with more severe ASD traits, as measured by the CARS [215], AQ [266], and the empathising quotient [267]. Other studies in children with ASD have provided evidence that the association between age and FA of the internal capsule [258] and the arcuate fasciculus [238] is opposite to that in neurotypical controls. Longitudinal studies would be invaluable to the investigation of white matter–ASD symptom associations over time.

The correlation analyses between DTI metrics and SRSp subsets in the control group were also carried out within TBSS in order to identify the location of voxels that significantly contributed to each association. White matter microstructure in the corona radiata, which is associated with motor and higher functions [392][393], was consistently identified in correlations with ASD-related mannerisms, and deficits in social cognition, communication, and motivation. Microstructure of the inferior longitudinal fasciculus, inferior fronto-occipital fasciculus, internal capsule, and posterior thalamic radiation were associated with ASD-related social cognition, communication, and motivation impairments. Microstructure of the corpus callosum was associated with social cognition and communication difficulties, and the tapetum (a part of the corpus callosum) with ASD-related motivation and cognition deficits. These findings indicate that some ASD-related traits, such as impaired social cognition, are associated with a wider array of white matter tract

characteristics than other ASD traits, such as reduced awareness. This suggests that, within the neurotypical population, social cognition is more generally associated with white matter microstructure than other ASD traits, and that some white matter tracts, such as the corona radiata and inferior longitudinal fasciculus, are associated with a wider range of ASD-related behaviours than other tracts, such as the corpus callosum. It is important to note that some of the correlation results that were significant when looking at DTI metrics averaged across the white matter skeleton were not significant in the voxel-based TBSS analysis stream. This may have occurred because the multiple comparisons correction within the TBSS analysis is more stringent or due to the increased power afforded by averaging measures across the whole of the white matter skeleton compared to within each voxel.

Prior studies in children, adolescents, and adults with ASD have identified significantly altered white matter microstructure of the corona radiata in ASD [258][238][223][229], though no significant correlations have been reported. Several studies that have shown altered white matter microstructure in the inferior longitudinal fasciculus [226][235][229][233][221][266], inferior fronto-occipital fasciculus [237][236][235][229][233][248] [255], and internal capsule [200][258][238][223] in ASD. Correlation analyses in ASD subjects have identified associations between inferior longitudinal fasciculus FA and ASD-related social and communication deficits [248]. Numerous studies have identified white matter deficits in the corpus callosum in ASD (for example, [250][208][214][204][203][219]). Altered white matter microstructure of the tapetum, which forms a part of the corpus callosum, has not been subject to much investigation, though there is some evidence that it is microstructurally affected in ASD [219]. Correlation analyses in ASD subjects have identified associations between corpus callosum FA and ADI restricted and repetitive behaviours [217], corpus callosum FA and CARS [205], and corpus callosum fibre density and length and VABS communication score [208]. In adults, correlations between corpus callosum FA and ADI communication score

[248] and corpus callosum number of streamlines and ADI restricted and repetitive behaviours [265] have been reported.

Following sub-division of the groups by biological sex, results showed that males with ASD had significantly reduced AD compared to male controls. There were no other significant group differences in white matter microstructure in the males, and no significant group differences in the females. Reductions in AD are representative of reduced water diffusion parallel with the axon bundle, and thus may reflect reduced coherence in the white matter tracts along the principal diffusion direction. Reduced AD has been reported by prior studies in children and adolescents with ASD [237][231][226][219]. The lack of significant group differences in DTI metrics in females does not corroborate the evidence suggesting that the typical pattern of sexual dimorphism in white matter microstructure is deficient in females with ASD [286], rather it supports recent evidence of no significant sex differences in a TBSS study of adults with ASD [288], and evidence that girls with ASD have a more similar white matter microstructure to female controls than males with ASD relative to male controls [245]. These findings question the 'extreme male brain' hypothesis [29], and the concept that females with ASD have experienced greater departure from the typical 'female' brain, than males with ASD from the typical 'male' brain, when looking in terms of structural connectivity. Further, there were no sex-based differences in the incidence or severity of ASD traits, as measured by the SRSp. This suggests that males and females are equally affected if they have a clinical diagnosis of ASD, and that this is captured by this particular parent-reported measure. It also indicates that females in the general population have a similar level of ASD-like traits to males from the neurotypical population, which further calls into question the concept that ASD is an extreme expression of typically 'male' behaviours [127][126]. Correlations of white matter microstructural markers with SRSp subset scores within the male and female groups separately showed a greater association in female controls than male controls – with females having significant correlations between all SRSp subsets for FA, MD, AD, and RD and males only showing

significant correlations for all SRSp subsets for FA and RD. This evidence indicates that both neurotypical males and females have an association between white matter microstructure and ASD traits, but that this association occurs with a wider range of microstructural alterations in females. This finding suggests that typical females have a stronger association between white matter microstructure and ASD traits than typical males, which is the opposite of the finding that would be anticipated from theories regarding autism an 'extreme male' condition.

This study has several limitations: The sample sizes are relatively small when the study cohort is sub-divided into groups of males and females. This means that the analyses in the male and female groups have more limited statistical power, and thus may be unable to detect group differences or correlations with a small effect size. This is particularly apparent for the female groups, since females with ASD are relatively rare and thus more difficult to recruit to studies in high numbers. Future work in a larger cohort would enable elucidation of small effects. Another limitation of the study is that the developmental stage of the participants was not measured. Age is a fairly good indicator of development, but there are both individual and sex-based differences in developmental trajectories which means that children of the same age can be at different developmental stages. One means of accounting for different slopes in white matter development in the sexes would be to include an age*sex interaction term as a covariate. A relatively high FA threshold of 0.4 was used in the generation of the TBSS skeleton in this study, compared to the typical selection of FA=0.2 (as used in the TBSS analysis in Chapter 5). The higher FA threshold was selected following visual assessment that revealed inaccuracies in the TBSS white matter skeleton when using a lower FA threshold. These inaccuracies are likely to have occurred because the cohort consisted of children and adolescents, rather than adults as per the typical TBSS protocol. An effect of the higher FA threshold is that the resulting white matter skeleton is more compact and statistical tests are constrained to the very central white matter tracts, resulting in a smaller test area that does not include the more peripheral white matter tracts; however, no

major white matter tracts were lost as a result of the high FA threshold. The averaging of diffusion-weighted scan acquisitions may have introduced heteroscedasticity, since participants with three diffusion-weighted scans would have had greater variability in the final averaged volumes than those participants with only two or one diffusion-weighted scan contributing to the final averaged scan. However, there were no significant group differences in the number of diffusion-weighted scans contributing to the final average diffusion-weighted scan. This indicates that SNR and variability were consistent across the groups. A limitation of using the SRSp to assess ASD traits is that it is a parent-reported measure, and therefore may suffer from bias and/or inadequate reporting. Parents or guardians of a child diagnosed with ASD may have increased ability to identify ASD traits in their other children; however it is conceivable that such parents may be hypersensitive to any signs of similar behaviour in their other children, and they may be eager to either down-play or overstate ASD traits in these siblings, depending on their preference. Nevertheless, the SRSp is a useful approximate of ASD behaviours across the spectrum.

Future work in a larger sample size over a wider range of participant ages or in a longitudinal design would be useful in confirming the findings of this study. A targeted investigation of those white matter tracts that were identified in this study – for example the corona radiata, which was singled out by the correlation analysis – would also be of interest in order to fully characterise the association between white matter microstructure and ASD traits. Further study could compare familial and un-related ASD proband and unaffected sibling pairs, and the effect of a the degree of autism risk – that of having two or more affected siblings and/or a parent with an ASD diagnosis vs one affected sibling – on brain structure in unaffected siblings. This could be combined with genetic analyses in order to identify possible genetic determinants or risk factors. Further study in larger cohorts of females with ASD could also tease out any effect of biological sex on putative endophenotypes.

8.5 Conclusion

In summary, there is evidence that the microstructural characteristics of white matter alter with age, and that this developmental trajectory is altered in ASD. There is much discussion regarding the extent to which ASD-related white matter anomalies are specific to the condition or represent an endophenotype that is shared by closely related family members. Furthermore, ASD is far more common in males than females, so investigation of the effect of biological sex on the brain structure in ASD is of interest. The aims of this study were therefore to investigate white matter microstructure in a cohort of children and adolescents with ASD, in order to add to the young adult study reported in Chapter 5, and to take this further by investigating white matter microstructure in unaffected siblings of ASD probands and carrying out independent investigations of males and females with ASD. The results of this study suggest that white matter microstructure is altered in ASD, but that there is less difference between males and females with ASD and their neurotypical counterparts than would be anticipated from theories that aim to explain the higher diagnosis rates of ASD in males. This study provides evidence that overall brain volume is endophenotypically elevated in ASD probands and their siblings, but that white matter microstructure may be less affected in these unaffected siblings. Overall this work adds to the growing evidence that altered brain structure is associated with ASD, but that there is a great deal complexity and heterogeneity to this association that warrants further investigation.

8.6 Acknowledgements

Thank you to Recruitment Coordinators Heidi Seib and Erin MacDonnell; thanks also to Research Fellows Devon Oosting and Hannah Friedman, and Research Assistant Cara Keifer for participant testing.

Chapter 9 Conclusions

This section brings together the work reported in this thesis, summarising the advances made in our understanding of brain structure in autism, and outlining future studies that could build upon these findings.

9.1 Summary

The aims of this thesis (see Section 3.4) were to investigate white matter microstructure in ASD and its association with symptom severity, and to address a number of specific questions: what are the nature of any microstructural differences in ASD relative to controls? Are connections within the social brain disproportionately affected? Do these microstructural alterations occur in all cases of ASD, or are they more common or severe in males compared to females, or in children compared to adults? Does white matter microstructure act as a biomarker of ASD? Do white matter measures reflect an endophenotype of ASD or enhanced vulnerability in families of ASD sufferers? Is there evidence in support of the various neural theories of ASD outlined in Section 1.3?

Four studies were carried out in order to resolve these questions. The first study investigated white matter microstructure in young adults with ASD using TBSS (Chapter 5). A comparison with neurotypical controls identified reduced white matter coherence in the ASD group, as measured by significant alterations in FA, MD, and RD. A correlation analysis showed that the spectrum of ASD traits in the entire study population, as measured by the autism quotient, is associated with a spectrum of white matter microstructure characteristics. IQ was maintained in the individuals included in this study, thus the findings imply that there is a dissociation between white matter features linked to IQ-related abilities and white matter characteristics associated with ASD traits. The findings of this study showed

that increasing microstructural deficits in the white matter are associated with greater ASD trait severity, which indicates that there may be a threshold at which aberrations in the white matter microstructure propel one towards the extreme of this spectrum and a clinical diagnosis of ASD. This warrants further investigation in a large cohort of participants that fully encompass the two spectra.

The second study investigated the social brain in greater detail, by analysing amygdala connectivity in the same cohort of young adults with ASD (Chapter 6). The findings showed that amygdalo-cortical connections are microstructurally compromised in ASD, and that these aberrations are associated with ASD symptom severity. Interestingly, the microstructure of particular amygdala-cortical connections was associated with different aspects of the ASD phenotype. This work provides evidence for specificity regarding the neural underpinnings of certain autistic behaviours. It also implies that tracts of the social network of the brain are impaired in ASD, although the pattern of brain–behaviour associations is more complex than previously supposed. The findings provide evidence that amygdala sub-regions should be investigated independently from one another, and future work could investigate the functional behaviour of amygdala sub-regions. Future work could also investigate whether particular amygdalo-cortical connections are biomarkers of ASD, and whether these connections can be modulated by therapies aimed at ameliorating particular autistic behaviours.

The third study analysed the network of structural connections in the autistic brain using graph theory within the same cohort of young adults (Chapter 7). The network analysis did not detect a difference in the organisation of the whole brain network in ASD, which was similar to that of healthy controls. FA of the white matter tracts in the network was reduced in the ASD group, and this microstructural deficit was associated with greater ASD symptom severity. These findings suggest that the overall topology of the whole brain network in young

adults with ASD is similar to that of neurotypical controls, but that this network is microstructurally compromised in ASD. There was a suggestion of enhanced local connectivity of the limbic network in ASD, though this did not survive correction for multiple comparisons. Further work investigating the properties of the limbic network in ASD in a larger sample are warranted to further explore these findings, which suggest that the social and emotional networks of the brain are not disproportionately affected in ASD. An investigation of associations between structural and functional networks within the brain would also be beneficial for further understanding of brain topology in ASD.

The fourth study was carried out during a three-month placement at Yale University, and investigated white matter microstructure in a cohort of children and adolescents using TBSS (Chapter 8). Results showed that whole brain volume is endophenotypically elevated in ASD probands and their unaffected siblings. White matter microstructure was altered in the ASD group compared to controls, as measured by reduced FA, but that this was to a lesser extent than observed in the adult cohort described in Chapter 5. Further, white matter microstructure was not significantly altered in unaffected siblings, and as such it is more likely to be a biomarker of ASD than an endophenotype. When groups were stratified by biological sex, fewer differences between males and females with ASD and their neurotypical counterparts were observed than anticipated. This study provides preliminary evidence for a lack of support of the hypotheses of greater neurological assault in females with ASD and ASD as a disorder marked by an 'extreme male brain'.

9.2 Future studies

The fourth study in this thesis (Chapter 8) provokes interesting questions regarding heterogeneity in ASD research, and the impact of methodology and participant

demographics on research findings. ASD is complex, and heterogeneity may reflect a real lack of consensus regarding what autism actually is, and how it should be defined. These questions encourage further research, particularly large study samples and longitudinal study designs, in order to fully resolve the condition, and its characteristics across the lifespan. The findings in this thesis suggest that brain structure is relatively consistently affected in males and females with ASD, and therefore that further elucidation of the causes of the relatively high diagnosis rates in males is warranted. This may involve the analysis of genetic influences on both brain structure and ASD symptom severity, particularly regarding X-chromosome genes, as well as biochemical influences, such as testosterone levels.

High-functioning individuals without comorbidities or significant medication usage, and within tight age ranges were selected for the analyses presented in this thesis. These selection criteria were followed in order to ensure that the research cohort was homogenous, thus increasing the probability that any findings could be attributed to ASD, rather than the effects of extraneous factors. However, the use of a homogenous research cohort means that the study sample and, consequently, the study findings do not reflect the biology of the wider ASD clinical population. There is no such thing as a 'typical' ASD case, but comorbidities and associated medication use (such as SSRIs for comorbid depression and anxiety) are incredibly common, and ASD affects individuals of all ages. Additionally, developmental delays and impairments are often co-associated with ASD. The findings presented in this thesis are only true of the cohorts they were derived from, using the methods selected – a consideration that is true of any clinical research study. However, there is evidence for consanguinity between different studies of brain structure in ASD, and patterns are emerging. Ethical and practical considerations would have to be taken into account prior to conducting research in a truly heterogeneous ASD cohort, and it is likely that incredibly large sample sizes would be required to tease out ASD-specific effects from the noise. Future multi-site studies will prove essential to unravelling the complexities of ASD, and data-sharing initiatives, such as the

NIH's national database for autism research (NDAR) (https://ndar.nih.gov/index.html), will be invaluable in facilitating these efforts.

Recent methodological advances have been made in MR acquisition and analysis methods, and future studies could make use of these to improve the accuracy and reliability of structural analyses – particularly with regards to the elucidation of multiple white matter fibre directions, and to investigate new aspects of white matter structure. One such development is in alternative approaches to the estimation of white matter fibre orientation, such as constrained spherical deconvolution (CSD) [394], which deconvolves the fibre orientation distribution (the fODF) from the diffusion-weighted signal and an estimated fibre response function. Another recent development in MR techniques is neurite orientation dispersion and density imaging (NODDI) [395], which enables quantification of neurite density and the degree of bending and spreading of axons. The g-ratio – the ratio of axon diameter to the diameter of the myelin sheath [396] – can be estimated using a combination of diffusion MRI, using methods such as NODDI, and magnetisation transfer imaging [397][398], and would enable the investigation of axon diameter and the degree of axon myelination in ASD. This would be useful in discovering more about brain structure in ASD, and the subtle effects of microstructure on behaviour. Alternative diffusion-weighted MRI acquisition methods, such as diffusion spectrum imaging (DSI) [399] and Q-ball imaging [400] enable estimation of multiple fibre orientations using fewer assumptions about signal structure than DTI. Studies using higher MR field strengths than those employed in this thesis would enable greater image resolution to be used, which would increase the spatial localisation of results and decrease partial volume effects. A great deal of research is currently focused on the development and application of *in vivo* imaging techniques at very high field strengths, such as 7T [401], and studies of brain structure in ASD could benefit from this in the future.

Future work to investigate the links between brain structure, function, and behaviour is merited. Future studies could focus on areas of the autistic phenotype that have been relatively under-studied, such as hyper-sensitivity to sensory stimuli. Another approach to ASD research could be the investigation of the biological basis for the special skills and abilities that can be afforded by ASD, such as heightened attention to detail, and how to harness these abilities to aid an individual with ASD. One major limitation of research assessing biology and behaviour is that of cause vs effect – it is not yet possible to determine whether structural changes within the brain precede autistic behaviours, co-occur with them, and/or develop and strengthen as a result of learned patterns of behaviour. Large-scale longitudinal studies, initiated early in infancy, may go some way towards revealing the process by which ASD develops and is maintained. Cross-disciplinary work – for example, studies combining brain imaging, genetics, biochemistry, and psychology – will also prove invaluable in identifying the intricacies of autism. The search for a unique autism biomarker will be key to the development and evaluation of both diagnostic tools and behavioural interventions; currently such efforts are relatively qualitative and subjective. The work described in this thesis has identified several avenues for future research in this area, and studies comparing white matter structures in ASD and other neurodevelopmental conditions would be invaluable in order to identify and develop new biomarkers.

9.3 Conclusion

The work presented in this thesis provides evidence for reduced microstructural coherence of the white matter in ASD. Evidence is provided for a) a biological basis for the spectrum of autistic traits, b) relative specificity of the behavioural correlates to microstructural characteristics of particular amygdalo-cortical connections, c) relatively preserved brain topology in ASD, as identified using network analysis, d) brain volume as an endophenotype of ASD, and microstructure as a putative biomarker, and e) no evidence for extreme white matter damage in young females

with ASD. These findings increase understanding of the neurological underpinnings of autism, and provide a fertile basis for future research in this field. Many questions regarding brain structure in ASD require further investigation – in particular the relatively high diagnosis rates in males, heterogeneity within the ASD population, and developmental trajectories. Large-scale longitudinal studies employing recent technological advances will help to realise these ambitions.

References

[1] Kuhn R. Eugen Bleuler's concepts of psychopathology. Hist Psychiatry 2004;15:361–6. doi:10.1177/0957154X04044603.

[2] Kanner L. Autistic disturbances of affective contact. Nerv Child 1943;2:217–50.

[3] Asperger H. Die "Autistischen Psychopathen" im Kindesalter. Arch Psychiatr Nervenkr 1944;117:76–136.

[4] World Health Organization. International classification of diseases: ICD-9. 9th ed. Geneva, Switzerland: 1978.

[5] American Psychiatric Association. Diagnostic and statistical manual of mental disorders: DSM-III. 3rd ed. Washington, DC: 1980.

[6] Wing L, Gould J. Severe impairments of social interaction and associated abnormalities in children: epidemiology and classification. J Autism Dev Disord 1979;9:11–29. doi:10.1007/BF01531288.

[7] World Health Organization. International classification of diseases: ICD-10. vol. 2. 10th ed. Geneva, Switzerland: World Health Organization; 1994.

[8] American Psychiatric Association. Diagnostic and statistical manual of mental disorders: DSM-V. 5th ed. Washington, DC: 2013.

[9] World Health Organization. The international classification of diseases 11th revision n.d. http://www.who.int/classifications/icd/revision/en/ (accessed February 24, 2015).

[10] Lord C, Rutter M, Le Couteur A. Autism diagnostic interview-revised: A revised version of a diagnostic interview for caregivers of individuals with possible pervasive developmental disorders. J Autism Dev Disord 1994;24:659–85.

[11] Lord C, Rutter M, Goode S, Heemsbergen J, Jordan H, Mawhood L, et al. Autism diagnostic observation schedule: a standardized observation of communicative and social behavior. J Autism Dev Disord 1989;19:185–212.

[12] Skuse D, Warrington R, Bishop D, Chowdhury U, Lau J, Mandy W, et al. The developmental, dimensional and diagnostic interview (3di): a novel computerized assessment for autism spectrum disorders. J Am Acad Child Adolesc Psychiatry 2004;43:548–58. doi:10.1097/00004583-200405000-00008.

[13] Tuchman R, Rapin I. Epilepsy in autism. Lancet Neurol 2002;1:352–8. doi:10.1016/S1474-4422(02)00160-6.

[14] Simonoff E, Pickles A, Charman T, Chandler S, Loucas T, Baird G. Psychiatric disorders in children with autism spectrum disorders: prevalence, comorbidity, and associated factors in a population-derived sample. J Am Acad Child Adolesc Psychiatry 2008;47:921–9. doi:10.1097/CHI.0b013e318179964f.

[15] Baron-Cohen S, Scahill VL, Izaguirre J, Hornsey H, Robertson MM. The

prevalence of Gilles de la Tourette syndrome in children and adolescents with autism: a large scale study. Psychol Med 1999;29:1151–9. doi:10.1017/S003329179900896X.

[16] Creswell CS, Skuse DH. Autism in association with Turner syndrome : Genetic implications for male vulnerability to pervasive developmental disorders. Neurocase 1999:511–8.

[17] Rimland B. Savant capabilities of autistic children and their cognitive implications. In: Serban G, editor. Cogn. defects Dev. Ment. Illn., New York, USA: Brunner/Mazel; 1978, p. 43–65.

[18] Hermelin B. Bright splinters of the mind: A personal story of research with autistic savants. London, UK: Jessica Kingsley Publishers; 2001.

[19] Baron-Cohen S, Scott FJ, Allison C, Williams J, Bolton P, Matthews FE, et al. Prevalence of autism-spectrum conditions: UK school-based population study. Br J Psychiatry 2009;194:500–9. doi:10.1192/bjp.bp.108.059345.

[20] Brugha TS, McManus S, Bankart J, Scott F, Purdon S, Smith J, et al. Epidemiology of autism spectrum disorders in adults in the community in England. Arch Gen Psychiatry 2011;68:459–65. doi:10.1001/archgenpsychiatry.2011.38.

[21] Center for Disease Control and Prevention (CDC). Community report on autism. Autism Dev Disabil Monit Netw 2014.

[22] Lotter V. Epidemiology of autistic conditions in young children. Soc Psychiatry 1966:124–37.

[23] Gillberg C, Wing L. Autism: not an extremely rare disorder. Acta Psychiatr Scand 1999;99:399–406. doi:10.1111/j.1600-0447.1999.tb00984.x.

[24] Hansen SN, Schendel DE, Parner ET. Explaining the increase in the prevalence of autism spectrum disorders. JAMA Pediatr 2015;169:56. doi:10.1001/jamapediatrics.2014.1893.

[25] Lee BK, McGrath JJ. Advancing parental age and autism: multifactorial pathways. Trends Mol Med 2015;21:118–25. doi:10.1016/j.molmed.2014.11.005.

[26] Baron-Cohen S, Wheelwright S, Skinner R, Martin J, and Clubley E. The autism-spectrum quotient (AQ): evidence from Asperger syndrome/high-functioning autism, males and females, scientists and mathematicians. J Autism Dev Disord 2001;31:5–17.

[27] Baron-Cohen S. The hyper-systemizing, assortative mating theory of autism. Prog Neuro-Psychopharmacology Biol Psychiatry 2006;30:865–72. doi:10.1016/j.pnpbp.2006.01.010.

[28] Ehlers S, Gillberg C. The epidemiology of Asperger syndrome. A total population study. J Child Psychol Psychiatry 1993;34:1327–50.

[29] Baron-Cohen. The extreme male brain theory of autism. Trends Cogn Sci 2002;6:248–54.

[30] Tsai L, Stewart MA, August G. Implication of sex differences in the familial

transmission of infantile autism. J Autism Dev Disord 1981;11:165–73. doi:10.1007/BF01531682.

[31] Dworzynski K, Ronald A, Bolton P, Happé F. How different are girls and boys above and below the diagnostic threshold for autism spectrum disorders? J Am Acad Child Adolesc Psychiatry 2012;51:788–97. doi:10.1016/j.jaac.2012.05.018.

[32] Frazier TW, Georgiades S, Bishop SL, Hardan AY. Behavioral and cognitive characteristics of females and males with autism in the simons simplex collection. J Am Acad Child Adolesc Psychiatry 2014;53:329–40.e3. doi:10.1016/j.jaac.2013.12.004.

[33] Mandy W, Chilvers R, Chowdhury U, Salter G, Seigal A, Skuse D. Sex differences in autism spectrum disorder: Evidence from a large sample of children and adolescents. J Autism Dev Disord 2012;42:1304–13. doi:10.1007/s10803-011-1356-0.

[34] Head AM, McGillivray JA, Stokes MA. Gender differences in emotionality and sociability in children with autism spectrum disorders. Mol Autism 2014;5:19. doi:10.1186/2040-2392-5-19.

[35] Sandin S, Lichtenstein P, Kuja-Halkola R, Larsson H, Hultman CM, Reichenberg A. The familial risk of autism. JAMA 2014;311:1770–7. doi:10.1001/jama.2014.4144.

[36] Colvert E, Tick B, McEwen F, Stewart C, Curran SR, Woodhouse E, et al. Heritability of autism spectrum disorder in a UK population-based twin sample. JAMA Psychiatry 2015:1–9. doi:10.1001/jamapsychiatry.2014.3028.

[37] Bailey A, Le Couteur A, Gottesman I, Bolton P, Simonoff E, Yuzda E, et al. Autism as a strongly genetic disorder: evidence from a British twin study. Psychol Med 1995;25:63–77. doi:10.1017/S0033291700028099.

[38] Le Couteur A, Bailey A, Goode S, Pickles A, Gottesman I, Robertson S, et al. A broader phenotype of autism: The clinical spectrum in twins. J Child Psychol Psychiatry Allied Discip 1996;37:785–801. doi:10.1111/j.1469-7610.1996.tb01475.x.

[39] Spiker D, Lotspeich LJ, Dimiceli S, Myers RM, Risch N. Behavioral phenotypic variation in autism multiplex families: Evidence for a continuous severity gradient. Am J Med Genet - Neuropsychiatr Genet 2002;114:129–36. doi:10.1002/ajmg.10188.

[40] Ozonoff S, Young GS, Carter A, Messinger D, Yirmiya N, Zwaigenbaum L, et al. Recurrence risk for autism spectrum disorders: A baby siblings research consortium study. Pediatrics 2011;128. doi:10.1542/peds.2010-2825.

[41] Jiao Y, Chen R, Ke X, Cheng L, Chu K, Lu Z, et al. Single nucleotide polymorphisms predict symptom severity of autism spectrum disorder. J Autism Dev Disord 2012;42:971–83. doi:10.1007/s10803-011-1327-5.

[42] Chakrabarti B, Dudbridge F, Kent L, Wheelwright S, Hill-Cawthorne G, Allison C, et al. Genes related to sex steroids, neural growth, and social-

emotional behavior are associated with autistic traits, empathy, and asperger syndrome. Autism Res 2009;2:157–77. doi:10.1002/aur.80.

[43] Gilman SR, Iossifov I, Levy D, Ronemus M, Wigler M, Vitkup D. Rare de novo variants associated with autism implicate a large functional network of genes involved in formation and function of synapses. Neuron 2011;70:898–907. doi:10.1016/j.neuron.2011.05.021.

[44] Gai X, Xie HM, Perin JC, Takahashi N, Murphy K, Wenocur AS, et al. Rare structural variation of synapse and neurotransmission genes in autism. Mol Psychiatry 2012;17:402–11. doi:10.1038/mp.2011.10.

[45] De Rubeis S, He X, Goldberg AP, Poultney CS, Samocha K, Ercument Cicek A, et al. Synaptic, transcriptional and chromatin genes disrupted in autism. Nature 2014;3. doi:10.1038/nature13772.

[46] Skuse DH. Imprinting, the X-chromosome, and the male brain: explaining sex differences in the liability to autism. Pediatr Res 2000;47:9–16.

[47] Marco EJ, Skuse DH. Autism-lessons from the X chromosome. Soc Cogn Affect Neurosci 2006;1:183–93. doi:10.1093/scan/nsl028.

[48] Jamain S, Quach H, Betancur C, Råstam M, Colineaux C, Gillberg IC, et al. Mutations of the X-linked genes encoding neuroligins NLGN3 and NLGN4 are associated with autism. Nat Genet 2003;34:27–9. doi:10.1038/ng1136.

[49] Chung R-H, Ma D, Wang K, Hedges DJ, Jaworski JM, Gilbert JR, et al. An X chromosome-wide association study in autism families identifies TBL1X as a novel autism spectrum disorder candidate gene in males. Mol Autism 2011;2:18. doi:10.1186/2040-2392-2-18.

[50] Thomas NS, Sharp AJ, Browne CE, Skuse D, Hardie C, Dennis NR. Xp deletions associated with autism in three females. Hum Genet 1999;104:43–8. doi:10.1007/s004390050908.

[51] Kanner L. Problems of nosology and psychodynamics of early infantile autism. Am J Orthopsychiatry 1949;19:416–26.

[52] Auyeung B, Taylor K, Hackett G, Baron-Cohen S. Foetal testosterone and autistic traits in 18 to 24-month-old children. Mol Autism 2010;1:11. doi:10.1186/2040-2392-1-11.

[53] Kinney DK, Munir KM, Crowley DJ, Miller AM. Prenatal stress and risk for autism. Neurosci Biobehav Rev 2008;32:1519–32. doi:10.1016/j.neubiorev.2008.06.004.

[54] Volk HE, Hertz-Picciotto I, Delwiche L, Lurmann F, McConnell R. Residential proximity to freeways and autism in the CHARGE study. Environ Health Perspect 2011;119:873–7. doi:10.1289/ehp.1002835.

[55] Schanen NC. Epigenetics of autism spectrum disorders. Hum Mol Genet 2006;15:138–50. doi:10.1093/hmg/ddl213.

[56] Ruggeri B, Sarkans U, Schumann G, Persico AM. Biomarkers in autism spectrum disorder: The old and the new. Psychopharmacology (Berl) 2014;231:1201–16. doi:10.1007/s00213-013-3290-7.

[57] Chauhan A, Chauhan V. Oxidative stress in autism. Pathophysiology 2006;13:171–81. doi:10.1016/j.pathophys.2006.05.007.

[58] Deth R, Muratore C, Benzecry J, Power-Charnitsky VA, Waly M. How environmental and genetic factors combine to cause autism: A redox/methylation hypothesis. Neurotoxicology 2008;29:190–201. doi:10.1016/j.neuro.2007.09.010.

[59] Gabriele S, Sacco R, Persico AM. Blood serotonin levels in autism spectrum disorder: A systematic review and meta-analysis. Eur Neuropsychopharmacol 2014;24:919–29. doi:10.1016/j.euroneuro.2014.02.004.

[60] Tordjman S, Anderson GM, Pichard N, Charbuy H, Touitou Y. Nocturnal excretion of 6-sulphatoxymelatonin in children and adolescents with autistic disorder. Biol Psychiatry 2005;57:134–8. doi:10.1016/j.biopsych.2004.11.003.

[61] Modahl C, Green L, Fein D, Morris M, Waterhouse L, Feinstein C, et al. Plasma oxytocin levels in autistic children. Biol Psychiatry 1998;43:270–7. doi:10.1016/S0006-3223(97)00439-3.

[62] Jeste SS, Nelson CA. Event related potentials in the understanding of autism spectrum disorders: An analytical review. J Autism Dev Disord 2009;39:495–510. doi:10.1007/s10803-008-0652-9.

[63] Bolton P, Macdonald H, Pickles A, Rios P, Goode S, Crowson M, et al. A case-control family history study of autism. J Child Psychol Psychiatry Allied Discip 1994;35:877–900. doi:10.1111/j.1469-7610.1994.tb02300.x.

[64] Lainhart JE, Piven J, Wzorek M, Landa R, Santangelo SL, Coon H, et al. Macrocephaly in children and adults with autism. J Am Acad Child Adolesc Psychiatry 1997;36:282–90. doi:10.1097/00004583-199702000-00019.

[65] Miles JH, Hadden LL, Takahashi TN, Hillman RE. Head circumference is an independent clinical finding associated with autism. Am J Med Genet 2000;95:339–50. doi:10.1002/1096-8628(20001211)95:4<339::AID-AJMG9>3.0.CO;2-B.

[66] Lainhart JE, Bigler ED, Bocian M, Coon H, Dinh E, Dawson G, et al. Head circumference and height in autism: A study by the collaborative programme of excellence in autism. Am J Med Genet Part A 2006;140A:2257–74. doi:10.1002/ajmg.a.

[67] Elder LM, Dawson G, Toth K, Fein D, Munson J. Head circumference as an early predictor of autism symptoms in younger siblings of children with autism spectrum disorder. J Autism Dev Disord 2008;38:1104–11. doi:10.1007/s10803-007-0495-9.

[68] Daymont C, Hwang W-T, Feudtner C, Rubin D. Head-circumference distribution in a large primary care network differs from CDC and WHO curves. Pediatrics 2010;126:e836–42. doi:10.1542/peds.2010-0410.

[69] Raznahan A, Wallace GL, Antezana L, Greenstein D, Lenroot R, Thurm A, et al. Compared to What? Early Brain Overgrowth in Autism and the Perils of Population Norms. Biol Psychiatry 2013:1–13.

doi:10.1016/j.biopsych.2013.03.022.

[70] Mraz KD, Green J, Dumont-Mathieu T, Makin S, Fein D. Correlates of head circumference growth 2007:7–9. doi:10.1177/0883073807304005.

[71] Chaste P, Klei L, Sanders SJ, Murtha MT, Hus V, Lowe JK, et al. Adjusting head circumference for covariates in autism: Clinical correlates of a highly heritable continuous trait. Biol Psychiatry 2013;74:576–84. doi:10.1016/j.biopsych.2013.04.018.

[72] Howlin P, Goode S, Hutton J, Rutter M. Adult outcome for children with autism. J Child Psychol Psychiatry Allied Discip 2004;45:212–29. doi:10.1111/j.1469-7610.2004.00215.x.

[73] Turner LM, Stone WL. Variability in outcome for children with an ASD diagnosis at age 2. J Child Psychol Psychiatry Allied Discip 2007;48:793–802. doi:10.1111/j.1469-7610.2007.01744.x.

[74] Helt M, Kelley E, Kinsbourne M, Pandey J, Boorstein H, Herbert M, et al. Can children with autism recover? If so, how? Neuropsychol Rev 2008;18:339–66. doi:10.1007/s11065-008-9075-9.

[75] Weiss MJ. Differential rates of skill acquisition and outcomes of early intensive behavioral intervention for autism. Behav Interv 1999;14:3–36. doi:10.1002/(SICI)1099-078X(199901/03)14:1<3::AID-BIN25>3.0.CO;2-F.

[76] Danielsson S, Gillberg IC, Billstedt E, Gillberg C, Olsson I. Epilepsy in young adults with autism: A prospective population-based follow-up study of 120 individuals diagnosed in childhood. Epilepsia 2005;46:918–23. doi:10.1111/j.1528-1167.2005.57504.x.

[77] King BH, Bostic JQ. An update on pharmacologic treatments for autism spectrum disorders. Child Adolesc Psychiatr Clin N Am 2006;15:161–75. doi:10.1016/j.chc.2005.08.005.

[78] Ji NY, Findling RL. An update on posttraumatic stress disorder in children and adolescents. Curr Opin Psychiatry 2015;28. doi:10.1177/0009922814540793.

[79] Bartz JA, Hollander E. Oxytocin and experimental therapeutics in autism spectrum disorders. Prog Brain Res 2008;170:451–62. doi:10.1016/S0079-6123(08)00435-4.

[80] Hollander E, Novotny S, Hanratty M, Yaffe R, DeCaria CM, Aronowitz BR, et al. Oxytocin infusion reduces repetitive behaviors in adults with autistic and Asperger's disorders. Neuropsychopharmacology 2003;28:193–8. doi:10.1038/sj.npp.1300021.

[81] Dadds MR, MacDonald E, Cauchi A, Williams K, Levy F, Brennan J. Nasal oxytocin for social deficits in childhood autism: A randomized controlled trial. J Autism Dev Disord 2014;44:521–31. doi:10.1007/s10803-013-1899-3.

[82] Seltzer MM, Shattuck P, Abbeduto L, Greenberg JS. Trajectory of development in adolescents and adults with autism. Ment Retard Dev Disabil Res Rev 2004;10:234–47. doi:10.1002/mrdd.20038.

[83] Brodmann K. Vergleichende Lokalisationslehre der Großhirnrinde : in ihren Prinzipien dargestellt auf Grund des Zellenbaues. Leipzig, Germany: Johann Ambrosius Barth; 1909.

[84] Rolls ET. Limbic systems for emotion and for memory, but no single limbic system. Cortex 2014;62:119–57. doi:10.1016/j.cortex.2013.12.005.

[85] Catani M, and Thiebaut de Schotten M. A diffusion tensor imaging tractography atlas for virtual in vivo dissections. Cortex 2008;44:1105–32. doi:10.1016/j.cortex.2008.05.004.

[86] Deoni SCL, Mercure E, Blasi A, Gasston D, Thomson A, Johnson M, et al. Mapping infant brain myelination with magnetic resonance imaging. J Neurosci 2011;31:784–91. doi:10.1523/JNEUROSCI.2106-10.2011.

[87] Tang G, Gudsnuk K, Kuo SH, Cotrina ML, Rosoklija G, Sosunov A, et al. Loss of mTOR-dependent macroautophagy causes autistic-like synaptic pruning deficits. Neuron 2014;83:1131–43. doi:10.1016/j.neuron.2014.07.040.

[88] Zoghbi HY. Postnatal neurodevelopmental disorders: Meeting at the synapse? Science (80-) 2003;302:826–30.

[89] Giovedi- S, Corradi A, Fassio A, Benfenati F. Involvement of synaptic genes in the pathogenesis of autism spectrum disorders: The case of synapsins. Front Pediatr 2014;2:1–8. doi:10.3389/fped.2014.00094.

[90] Minshew NJ, Goldstein G, Siegel DJ. Neuropsychologic functioning in autism: profile of a complex information processing disorder. J Int Neuropsychol Soc 1997;3:303–16.

[91] Williams DL, Goldstein G, Minshew NJ. Neuropsychologic functioning in children with autism: Further evidence for disordered complex information-processing. Child Neuropsychol 2006;12:279–98. doi:10.1016/j.biotechadv.2011.08.021.Secreted.

[92] Brosnan M, Gavin J. Are “friends” electric? Why those with an autism spectrum disorder (ASD) thrive in online cultures but suffer in offline cultures. In: Rosen LD, Cheever N, Carrier LM, editors. Wiley Blackwell Handb. Psychol. Technol. Soc., Chichester, UK: John Wiley & Sons; 2015, p. 250–70.

[93] Courchesne E, and Pierce K. Why the frontal cortex in autism might be talking only to itself: local over-connectivity but long-distance disconnection. Curr Opin Neurobiol 2005;15:225–30. doi:10.1016/j.conb.2005.03.001.

[94] Peters JM, Taquet M, Vega C, Jeste SS, Fernández IS, Tan J, et al. Brain functional networks in syndromic and non-syndromic autism: a graph theoretical study of EEG connectivity. BMC Med 2013;11:54. doi:10.1186/1741-7015-11-54.

[95] Belmonte MK, Allen G, Beckel-Mitchener A, Boulanger LM, Carper RA, Webb SJ. Autism and abnormal development of brain connectivity. J Neurosci 2004;24:9228–31. doi:10.1523/JNEUROSCI.3340-04.2004.

[96] Lewis JD, Elman JL. Growth-related neural reorganization and the autism

phenotype: A test of the hypothesis that altered brain growth leads to altered connectivity. Dev Sci 2008;11:135–55. doi:10.1111/j.1467-7687.2007.00634.x.

[97] Geschwind DH, Levitt P. Autism spectrum disorders: developmental disconnection syndromes. Curr Opin Neurobiol 2007;17:103–11. doi:10.1016/j.conb.2007.01.009.

[98] Frith U. Autism: Explaining the enigma. Oxford, UK: Blackwell; 1989.

[99] Happé F, Frith U. The weak coherence account: detail-focused cognitive style in autism spectrum disorders. J Autism Dev Disord 2006;36:5–25. doi:10.1007/s10803-005-0039-0.

[100] Koldewyn K, Jiang Y, Weigelt S, Kanwisher N. Global/local processing in autism: Not a disability, but a disinclination. J Autism Dev Disord 2013;43:2329–40. doi:10.1016/j.biotechadv.2011.08.021.Secreted.

[101] Just MA, Cherkassky VL, Keller TA, Minshew NJ. Cortical activation and synchronization during sentence comprehension in high-functioning autism: Evidence of underconnectivity. Brain 2004;127:1811–21. doi:10.1093/brain/awh199.

[102] Vermeulen P. Context blindness in autism spectrum disorder: Not using the forest to see the trees as trees. Focus Autism Other Dev Disabl 2014. doi:10.1177/1088357614528799.

[103] Morsanyi K, Handley SJ, Evans JSBT. Decontextualised minds: Adolescents with autism are less susceptible to the conjunction fallacy than typically developing adolescents. J Autism Dev Disord 2010;40:1378–88. doi:10.1007/s10803-010-0993-z.

[104] Skoyles JR. Autism, context/noncontext information processing, and atypical development. Autism Res Treat 2011;2011:1–14. doi:10.1155/2011/681627.

[105] Baron-Cohen S, Leslie AM, Frith U. Does the autistic child have a "theory of mind"? Cognition 1985;21:37–46. doi:10.1016/0010-0277(85)90022-8.

[106] Baron-Cohen S. Theory of mind and autism: A fifteen year review. In: Baron-Cohen S, Tager-Flusberg H, Cohen DJ, editors. Underst. other minds Perspect. from Dev. Cogn. Neurosci. 2nd Editio, New York, USA: Oxford University Press; 2000, p. 3–20.

[107] Kana RK, Libero LE, Hu CP, Deshpande HD, Colburn JS. Functional brain networks and white matter underlying theory-of-mind in autism. Soc Cogn Affect Neurosci 2014;9:98–105. doi:10.1093/scan/nss106.

[108] Baron-Cohen S, Ring HA, Wheelwright S, Bullmore ET, Brammer MJ, Simmons A, et al. Social intelligence in the normal and autistic brain: an fMRI study. Eur J Neurosci 1999;11:1891–8.

[109] Williams JHG, Whiten A, Suddendorf T, Perrett DI. Imitation, mirror neurons and autism. Neurosci Biobehav Rev 2001;25:287–95. doi:10.1016/S0149-7634(01)00014-8.

[110] Rizzolatti G, Fabbri-Destro M. Mirror neurons: From discovery to autism. Exp Brain Res 2010;200:223–37. doi:10.1007/s00221-009-2002-3.

[111] Williams JHG, Waiter GD, Gilchrist A, Perrett DI, Murray AD, Whiten A. Neural mechanisms of imitation and "mirror neuron" functioning in autistic spectrum disorder. Neuropsychologia 2006;44:610–21. doi:10.1016/j.neuropsychologia.2005.06.010.

[112] Fishman I, Keown CL, Lincoln AJ, Pineda JA, Müller R-A. Atypical cross talk between mentalizing and mirror neuron networks in autism spectrum disorder. JAMA Psychiatry 2014;71:751–60. doi:10.1001/jamapsychiatry.2014.83.

[113] Golarai G, Grill-Spector K, Reiss AL. Autism and the development of face processing. Clin Neurosci Res 2006;6:145–60. doi:10.1016/j.cnr.2006.08.001.

[114] Uljarevic M, Hamilton A. Recognition of emotions in autism: A formal meta-analysis. J Autism Dev Disord 2013;43:1517–26. doi:10.1007/s10803-012-1695-5.

[115] Pierce K, Müller RA, Ambrose J, Allen G, Courchesne E. Face processing occurs outside the fusiform "face area" in autism: evidence from functional MRI. Brain 2001;124:2059–73.

[116] Falck-Ytter T, Bölte S, Gredebäck G. Eye tracking in early autism research. J Neurodev Disord 2013;5:28. doi:10.1186/1866-1955-5-28.

[117] Joseph RM, Ehrman K, McNally R, Keehn B. Affective response to eye contact and face recognition ability in children with ASD. J Int Neuropsychol Soc 2008;14:947–55. doi:10.1017/S1355617708081344.

[118] Falck-Ytter T, Carlström C, Johansson M. Eye contact modulates cognitive processing differently in children with autism. Child Dev 2014;86:37–47. doi:10.1111/cdev.12273.

[119] Hammock EAD, Young LJ. Oxytocin, vasopressin and pair bonding: implications for autism. Philos Trans R Soc Lond B Biol Sci 2006;361:2187–98. doi:10.1098/rstb.2006.1939.

[120] Young LJ, Wang Z. The neurobiology of pair bonding. Nat Neurosci 2004;7:1048–54. doi:10.1038/nn1327.

[121] Meyer-Lindenberg A, Domes G, Kirsch P, Heinrichs M. Oxytocin and vasopressin in the human brain: social neuropeptides for translational medicine. Nat Rev Neurosci 2011;12:524–38. doi:10.1038/nrn3044.

[122] Skuse DH, Lori A, Cubells JF, Lee I, Conneely KN, Puura K, et al. Common polymorphism in the oxytocin receptor gene (OXTR) is associated with human social recognition skills. Proc Natl Acad Sci U S A 2014;111:1987–92. doi:10.1073/pnas.1302985111.

[123] Gordon I, Vander Wyk BC, Bennett RH, Cordeaux C, Lucas M V, Eilbott JA, et al. Oxytocin enhances brain function in children with autism. Proc Natl Acad Sci U S A 2013;110:20953–8. doi:10.1073/pnas.1312857110.

[124] Kanat M, Heinrichs M, Domes G. Oxytocin and the social brain: Neural mechanisms and perspectives in human research. Brain Res 2013;1580:160–71. doi:10.1016/j.brainres.2013.11.003.

[125] Baron-Cohen S. Two new theories of autism: hyper-systemising and assortative mating. Arch Dis Child 2006;91:2–5. doi:10.1136/adc.2005.075846.

[126] Baron-Cohen S. Autism: The empathizing-systemizing (E-S) theory. Ann N Y Acad Sci 2009;1156:68–80. doi:10.1111/j.1749-6632.2009.04467.x.

[127] Baron-Cohen S, Knickmeyer RC, Belmonte MK. Sex differences in the brain: implications for explaining autism. Science (80-) 2005;310:819–23. doi:10.1126/science.1115455.

[128] Auyeung B, Baron-Cohen S, Ashwin E, Knickmeyer R, Taylor K, Hackett G. Fetal testosterone and autistic traits. Br J Psychol 2009;100:1–22. doi:10.1348/000712608x311731.

[129] James WH. An update on the hypothesis that one cause of autism is high intrauterine levels of testosterone of maternal origin. J Theor Biol 2014;355:33–9. doi:10.1016/j.jtbi.2014.03.036.

[130] Bachevalier J, Loveland KA. The orbitofrontal-amygdala circuit and self-regulation of social-emotional behavior in autism. Neurosci Biobehav Rev 2006;30:97–117. doi:10.1016/j.neubiorev.2005.07.002.

[131] Samson AC, Huber O, Gross JJ. Emotion regulation in Asperger's syndrome and high-functioning autism. Emotion 2012;12:659–65. doi:10.1037/a0027975.

[132] Chan RCK, Shum D, Toulopoulou T, Chen EYH. Assessment of executive functions: Review of instruments and identification of critical issues. Arch Clin Neuropsychol 2008;23:201–16. doi:10.1016/j.acn.2007.08.010.

[133] Russell J, editor. Autism as an executive disorder. New York, USA: Oxford University Press; 1997.

[134] Blijd-Hoogewys EMA, Bezemer ML, van Geert PLC. Executive functioning in children with ASD: An analysis of the BRIEF. J Autism Dev Disord 2014;44:3089–100. doi:10.1007/s10803-014-2176-9.

[135] Elliott R. Executive functions and their disorders. Br Med Bull 2003;65:49–59. doi:10.1093/bmb/ldg65.049.

[136] Bloch, F; Hansen, W.W; Packard M. Nuclear Induction. Phys Rev 1946;69:127.

[137] Purcell, E.M; Torrey, H.C; Pound R V. Resonance absorption by nuclear magnetic moments in a solid. Phys Rev 1946;69:37–8.

[138] Hahn EL. Spin Echoes. Phys Rev 1950;3:21. doi:10.1063/1.3066708.

[139] Proctor, W.G; Yu F. The dependence of a nuclear magnetic resonance frequency upon chemical compound. Phys Rev 1950;77:717.

[140] Dickinson W. Dependence of the F"nuclear resonance position on chemical compound. Phys Rev 1950;77:736–7.

[141] Damadian R. Tumor detection by nuclear magnetic resonance. Science (80-) 1971;171:1151–3.

[142] Lauterbur P. Image formation by induced local interactions: Examples employing nuclear magnetic resonance. Nature 1973;242:190–1.

[143] Lauterbur PC. Magnetic resonance zeugmatography. Pure Appl Chem 1974;40:149–57. doi:10.1351/pac197440010149.

[144] Damadian, R; Goldsmith, M; Minkoff L. NMR in cancer: XVI. FONAR image of the live human body. Physiol Chem Phys 1977;9:97–100.

[145] Brown M., Semelka R. MRI: Basic principles and applications. 4th Editio. Hoboken, New Jersey, USA: Wiley-Blackwell; 2010.

[146] McRobbie D, Moore E, Graves M, Prince M. MRI: From picture to proton. 2nd Editio. Cambridge, UK: Cambridge University Press; 2010.

[147] Mansfield P. Multi-planar image formation using NMR spin echoes. J Phys C Solid State Phys 2001;10:L55–8. doi:10.1088/0022-3719/10/3/004.

[148] Johansen-Berg H, Behrens TEJ. Diffusion MRI: From quantitative measurement to in vivo neuroanatomy. London, UK: Academic Press, Elsevier; 2009.

[149] Brown R. A brief account of microscopical observations made in the months of June, July, and August, 1827, on the particles contained in the pollen of plants; and on the general existence of active molecules in organic and inorganic bodies. Philos Mag 1828;4:161–73.

[150] Einstein A. Über die von der molekularkinetischen Theorie der Wärme geforderte Bewegung von in ruhenden Flüssigkeiten suspendierten Teilchen. Ann Phys 1905;4:549–60.

[151] Einstein A. Investigations on the theory of the Brownian movement. New York: Dover Publications Inc.; 1926.

[152] Tuch DS, Reese TG, Wiegell MR, Makris N, Belliveau JW, Van Wedeen J. High angular resolution diffusion imaging reveals intravoxel white matter fiber heterogeneity. Magn Reson Med 2002;48:577–82. doi:10.1002/mrm.10268.

[153] Basser PJ, Mattiello J, LeBihan D. MR diffusion tensor spectroscopy and imaging. Biophys J 1994;66:259–67. doi:10.1016/S0006-3495(94)80775-1.

[154] Basser PJ, and Pierpaoli C. Microstructural and physiological features of tissues elucidated by quantitative-diffusion-tensor MRI. J Magn Reson 1996;213:560–70.

[155] Behrens TEJ, Woolrich MW, Jenkinson M, Johansen-Berg H, Nunes RG, Clare S, et al. Characterization and propagation of uncertainty in diffusion-weighted MR imaging. Magn Reson Med 2003;50:1077–88. doi:10.1002/mrm.10609.

[156] Wright IC, McGuire PK, Poline JB, Travere JM, Murray RM, Frith CD, et al. A voxel-based method for the statistical analysis of gray and white matter density applied to schizophrenia. Neuroimage 1995;2:244–52. doi:10.1006/nimg.1995.1032.

[157] Smith S, Jenkinson M, Johansen-Berg H, Rueckert D, Nichols T, Mackay C, et al. Tract-based spatial statistics: voxelwise analysis of multi-subject diffusion data. Neuroimage 2006;31:1487–505. doi:10.1016/j.neuroimage.2006.02.024.

[158] Clayden JD, Storkey AJ, Bastin ME. A probabilistic model-based approach to consistent white matter tract segmentation. IEEE Trans Med Imaging 2007;26:1555–61. doi:10.1109/TMI.2007.905826.

[159] Yendiki A. Automated probabilistic reconstruction of white-matter pathways in health and disease using an atlas of the underlying anatomy. Front Neuroinform 2011;5:1–12. doi:10.3389/fninf.2011.00023.

[160] Lawes INC, Barrick TR, Murugam V, Spierings N, Evans DR, Song M, et al. Atlas-based segmentation of white matter tracts of the human brain using diffusion tensor tractography and comparison with classical dissection. Neuroimage 2008;39:62–79. doi:10.1016/j.neuroimage.2007.06.041.

[161] Dyrby TB, Søgaard L V, Parker GJ, Alexander DC, Lind NM, Baaré WFC, et al. Validation of in vitro probabilistic tractography. Neuroimage 2007;37:1267–77. doi:10.1016/j.neuroimage.2007.06.022.

[162] Mukherjee P. Diffusion tensor imaging and fiber tractography in acute stroke. Neuroimaging Clin N Am 2005;15:655–65. doi:10.1016/j.nic.2005.08.010.

[163] De Groot M, Verhaaren BFJ, De Boer R, Klein S, Hofman A, Van Der Lugt A, et al. Changes in normal-appearing white matter precede development of white matter lesions. Stroke 2013;44:1037–42. doi:10.1161/STROKEAHA.112.680223.

[164] Clark CA, Barrick TR, Murphy MM, Bell BA. White matter fiber tracking in patients with space-occupying lesions of the brain: A new technique for neurosurgical planning? Neuroimage 2003;20:1601–8. doi:10.1016/j.neuroimage.2003.07.022.

[165] Potgieser ARE, Wagemakers M, Van Hulzen ALJ, De Jong BM, Hoving EW, Groen RJM. The role of diffusion tensor imaging in brain tumor surgery: A review of the literature. Clin Neurol Neurosurg 2014;124:51–8. doi:10.1016/j.clineuro.2014.06.009.

[166] Courchesne E, Karns CM, Davis HR, Ziccardi R, Carper RA, Tigue ZD, et al. Unusual brain growth patterns in early life in patients with autistic disorder: an MRI study. Neurology 2001;57:245–54.

[167] Aylward EH, Minshew NJ, Field K, Sparks BF, and Singh N. Effects of age on brain volume and head circumference in autism. Neurology 2002;59:175–83.

[168] Sparks BF, Friedman SD, Shaw DW, Aylward EH, Echelard D, Artru AA, et al. Brain structural abnormalities in young children with autism spectrum disorder. Neurology 2002;59:184–92.

[169] Hazlett H, Poe M, Gerig G, Gimpel-Smith R, Provenzale J, Ross A, et al. Magnetic resonance imaging and head circumference study of brain size in autism: Birth through age 2 years. Arch Gen Psychiatry 2005;62:1366–76. doi:10.1016/S0098-1672(08)70087-0.

[170] Shen MD, Nordahl CW, Young GS, Wootton-Gorges SL, Lee A, Liston SE, et al. Early brain enlargement and elevated extra-axial fluid in infants who

develop autism spectrum disorder. Brain 2013;136:2825–35. doi:10.1093/brain/awt166.

[171] Hazlett HC, Poe M, Gerig G, Styner M, Chappell C, Smith RG, et al. Early brain overgrowth in autism associated with an increase in cortical surface area before age 2 years. Arch Gen Psychiatry 2011;68:467–76. doi:10.1001/archgenpsychiatry.2011.39.Early.

[172] Raznahan A, Wallace GL, Antezana L, Greenstein D, Lenroot R, Thurm A, et al. Compared to what? Early brain overgrowth in autism and the perils of population norms. Biol Psychiatry 2013;74:563–75. doi:10.1016/j.biopsych.2013.03.022.

[173] Courchesne E, Campbell K, Solso S. Brain growth across the life span in autism: Age-specific changes in anatomical pathology. Brain Res 2011;1380:138–45. doi:10.1016/j.brainres.2010.09.101.

[174] Lange N, Travers BG, Bigler ED, Prigge MBD, Froehlich AL, Nielsen J a., et al. Longitudinal volumetric brain changes in autism spectrum disorder ages 6-35 years. Autism Res 2014:n/a – n/a. doi:10.1002/aur.1427.

[175] Xiao Z, Qiu T, Ke X, Xiao X, Xiao T, Liang F, et al. Autism spectrum disorder as early neurodevelopmental disorder: Evidence from the brain imaging abnormalities in 2-3 years old toddlers. J Autism Dev Disord 2014;44:1633–40. doi:10.1007/s10803-014-2033-x.

[176] Schumann CM, Bloss CS, Barnes CC, Wideman GM, Carper RA, Pierce K, et al. Longitudinal MRI study of cortical development through early childhood in autism. J Neurosci 2010;30:4419–27. doi:10.1523/JNEUROSCI.5714-09.2010.Longitudinal.

[177] Haar S, Berman S, Behrmann M, Dinstein I. Anatomical abnormalities in autism? Cereb Cortex 2014:1–13. doi:10.1093/cercor/bhu242.

[178] Calderoni S, Retico A, Biagi L, Tancredi R, Muratori F, Tosetti M. Female children with autism spectrum disorder: An insight from mass-univariate and pattern classification analyses. Neuroimage 2012;59:1013–22. doi:10.1016/j.neuroimage.2011.08.070.

[179] Ecker C, Suckling J, Deoni SC, Lombardo M V, Bullmore ET, Baron-Cohen S, et al. Brain anatomy and its relationship to behavior in adults with autism spectrum disorder: A multicenter magnetic resonance imaging study. Arch Gen Psychiatry 2012;69:195–209.

[180] Abell F, Krams M, Ashburner J, Passingham R, Friston K, Frackowiak R, et al. The neuroanatomy of autism: a voxel-based whole brain analysis of structural scans. Neuroreport 1999;10:1647–51.

[181] Howard MA, Cowell PE, Boucher J, Broks P, Mayes A, Farrant A, et al. Convergent neuroanatomical and behavioural evidence of an amygdala hypothesis of autism. Neuroreport 2000;11:2931–5.

[182] Rojas DC, Smith JA, Benkers TL, Camou SL, Reite ML, Rogers SJ. Hippocampus and amygdala volumes in parents of children with autistic

disorder. Am J Psychiatry 2004;161:2038–44. doi:10.1176/appi.ajp.161.11.2038.

[183] Bellani M, Baiano M, Brambilla P. Brain anatomy of major depression II. Focus on amygdala. Epidemiol Psychiatr Sci 2011;20:33–6. doi:10.1017/S2045796011000096.

[184] Mosconi MW, Cody-Hazlett H, Poe MD, Gerig G, Gimpel-Smith R, Piven J. Longitudinal study of amygdala volume and joint attention in 2- to 4-year-old children with autism. Arch Gen Psychiatry 2009;66:509–16.

[185] Nordahl CW, Scholz R, Yang X, Buonocore MH, Simon T, Rogers S, et al. Increased rate of amygdala growth in children aged 2 to 4 years with autism spectrum disorders. Arch Gen Psychiatry 2012;69:53–61. doi:10.1001/archgenpsychiatry.2011.145.Increased.

[186] Barnea-Goraly N, Frazier TW, Piacenza L, Minshew NJ, Keshavan MS, Reiss AL, et al. A preliminary longitudinal volumetric MRI study of amygdala and hippocampal volumes in autism. Prog Neuropsychopharmacol Biol Psychiatry 2014;48:124–8. doi:10.1016/j.pnpbp.2013.09.010.

[187] Murphy CM, Deeley Q, Daly EM, Ecker C, O'Brien FM, Hallahan B, et al. Anatomy and aging of the amygdala and hippocampus in autism spectrum disorder: an in vivo magnetic resonance imaging study of Asperger syndrome. Autism Res 2012;5:3–12. doi:10.1002/aur.227.

[188] Tsatsanis KD, Rourke BP, Klin A, Volkmar FR, Cicchetti D, Schultz RT. Reduced thalamic volume in high-functioning individuals with autism. Biol Psychiatry 2003;53:121–9. doi:10.1016/S0006-3223(02)01530-5.

[189] Tamura R, Kitamura H, Endo T, Hasegawa N, Someya T. Reduced thalamic volume observed across different subgroups of autism spectrum disorders. Psychiatry Res - Neuroimaging 2010;184:186–8. doi:10.1016/j.pscychresns.2010.07.001.

[190] Hardan AY, Girgis RR, Adams J, Gilbert AR, Keshavan MS, Minshew NJ. Abnormal brain size effect on the thalamus in autism. Psychiatry Res - Neuroimaging 2006;147:145–51. doi:10.1016/j.pscychresns.2005.12.009.

[191] Langen M, Durston S, Staal WG, Palmen SJMC, van Engeland H. Caudate nucleus is enlarged in high-functioning medication-naive subjects with autism. Biol Psychiatry 2007;62:262–6. doi:10.1016/j.biopsych.2006.09.040.

[192] Sato W, Kubota Y, Kochiyama T, Uono S, Yoshimura S, Sawada R, et al. Increased putamen volume in adults with autism spectrum disorder. Front Hum Neurosci 2014;8:1–6. doi:10.3389/fnhum.2014.00957.

[193] Hardan AY, Kilpatrick M, Keshavan MS, Minshew NJ. Motor performance and anatomic magnetic resonance imaging (MRI) of the basal ganglia in autism. J Child Neurol 2003;18:317–24.

[194] Raznahan A, Lenroot R, Thurm A, Gozzi M, Hanley A, Spence SJ, et al. Mapping cortical anatomy in preschool aged children with autism using surface-based morphometry. NeuroImage Clin 2013;2:111–9. doi:10.1016/j.nicl.2012.10.005.

[195] Auzias G, Viellard M, Takerkart S, Villeneuve N, Poinso F, Fonséca D DA, et al. Atypical sulcal anatomy in young children with autism spectrum disorder. NeuroImage Clin 2014;4:593–603. doi:10.1016/j.nicl.2014.03.008.

[196] Travers B, Adluru N, Ennis C, Tromp D, Destiche D, Doran S, et al. Diffusion tensor imaging in autism spectrum disorder: A review. Autism Res 2012;5:289–313. doi:10.1002/aur.1243.Diffusion.

[197] Ameis SH, Catani M. Altered white matter connectivity as a neural substrate for social impairment in Autism Spectrum Disorder. Cortex 2015;62:158–81. doi:10.1016/j.cortex.2014.10.014.

[198] Conti E, Calderoni S, Marchi V, Muratori F, Cioni G, Guzzetta A. The first 1000 days of the autistic brain: a systematic review of diffusion imaging studies. Front Hum Neurosci 2015;9. doi:10.3389/fnhum.2015.00159.

[199] Rane P, Cochran D, Hodge SM, Haselgrove C, Kennedy DN, Frazier JA. Connectivity in autism. Harv Rev Psychiatry 2015;23:223–44. doi:10.1097/HRP.0000000000000072.

[200] Ben Bashat D, Kronfeld-Duenias V, Zachor DA, Ekstein PM, Hendler T, Tarrasch R, et al. Accelerated maturation of white matter in young children with autism: a high b value DWI study. Neuroimage 2007;37:40–7. doi:10.1016/j.neuroimage.2007.04.060.

[201] Elison J, Paterson S. White matter microstructure and atypical visual orienting in 7- month-olds at risk for autism. Am J … 2013;170:1–18. doi:10.1176/appi.ajp.2012.12091150.White.

[202] Elison JT, Wolff JJ, Heimer DC, Paterson SJ, Gu H, Hazlett HC, et al. Frontolimbic neural circuitry at 6 months predicts individual differences in joint attention at 9 months. Dev Sci 2013;16:186–97. doi:10.1111/desc.12015.

[203] Wolff JJ, Gu H, Gerig G, Elison JT, Styner M, Gouttard S, et al. Differences in white matter fiber tract development present from 6 to 24 months in infants with autism. Am J Psychiatry 2012;169:589–600.

[204] Weinstein M, Ben-Sira L, Levy Y, Zachor DA, Ben Itzhak E, Artzi M, et al. Abnormal white matter integrity in young children with autism. Hum Brain Mapp 2011;32:534–43. doi:10.1002/hbm.21042.

[205] Abdel Razek A, Mazroa J, Baz H. Assessment of white matter integrity of autistic preschool children with diffusion weighted MR imaging. Brain Dev 2014;36:28–34. doi:10.1016/j.braindev.2013.01.003.

[206] Walker L, Gozzi M, Lenroot R, Thurm A, Behseta B, Swedo S, et al. Diffusion tensor imaging in young children with autism: Biological effects and potential confounds. Biol Psychiatry 2012;72:1043–51. doi:10.1016/j.biopsych.2012.08.001.

[207] Sundaram SK, Kumar A, Makki MI, Behen ME, Chugani HT, Chugani DC. Diffusion tensor imaging of frontal lobe in autism spectrum disorder. Cereb Cortex 2008;18:2659–65. doi:10.1093/cercor/bhn031.

[208] Kumar A, Sundaram SK, Sivaswamy L, Behen ME, Makki MI, Ager J, et al.

Alterations in frontal lobe tracts and corpus callosum in young children with autism spectrum disorder. Cereb Cortex 2010;20:2103–13. doi:10.1093/cercor/bhp278.

[209] Sivaswamy L, Kumar A, Rajan D, Behen M, Muzik O, Chugani D, et al. A diffusion tensor imaging study of the cerebellar pathways in children with autism spectrum disorder. J Child Neurol 2010;25:1223–31. doi:10.1177/0883073809358765.

[210] Jeong JW, Kumar AK, Sundaram SK, Chugani HT, Chugani DC. Sharp curvature of frontal lobe white matter pathways in children with autism spectrum disorders: Tract-based morphometry analysis. Am J Neuroradiol 2011;32:1600–6. doi:10.3174/ajnr.A2557.

[211] Jeong JW, Chugani DC, Behen ME, Tiwari VN, Chugani HT. Altered white matter structure of the dentatorubrothalamic pathway in children with autistic spectrum disorders. Cerebellum 2012;11:957–71. doi:10.1007/s12311-012-0369-3.

[212] Billeci L, Calderoni S, Tosetti M, Catani M, Muratori F. White matter connectivity in children with autism spectrum disorders: a tract-based spatial statistics study. BMC Neurol 2012;12:148. doi:10.1186/1471-2377-12-148.

[213] Mengotti P, D'Agostini S, Terlevic R, De Colle C, Biasizzo E, Londero D, et al. Altered white matter integrity and development in children with autism: A combined voxel-based morphometry and diffusion imaging study. Brain Res Bull 2011;84:189–95. doi:10.1016/j.brainresbull.2010.12.002.

[214] Hong S, Ke X, Tang T, Hang Y, Chu K, Huang H, et al. Detecting abnormalities of corpus callosum connectivity in autism using magnetic resonance imaging and diffusion tensor tractography. Psychiatry Res - Neuroimaging 2011;194:333–9. doi:10.1016/j.pscychresns.2011.03.009.

[215] Ke X, Tang T, Hong S, Hang Y, Zou B, Li H, et al. White matter impairments in autism, evidence from voxel-based morphometry and diffusion tensor imaging. Brain Res 2009;1265:171–7. doi:10.1016/j.brainres.2009.02.013.

[216] Koldewyn K, Yendiki A, Weigelt S, Gweon H, Julian J, Richardson H, et al. Differences in the right inferior longitudinal fasciculus but no general disruption of white matter tracts in children with autism spectrum disorder. Proc Natl Acad Sci U S A 2014;111:1981–6. doi:10.1073/pnas.1324037111.

[217] Cheung C, Chua SE, Cheung V, Khong PL, Tai KS, Wong TKW, et al. White matter fractional anisotrophy differences and correlates of diagnostic symptoms in autism. J Child Psychol Psychiatry 2009;50:1102–12. doi:10.1111/j.1469-7610.2009.02086.x.

[218] Brito AR, Vasconcelos MM, Domingues RC, Hygino Da Cruz LC, Rodrigues LDS, Gasparetto EL, et al. Diffusion tensor imaging findings in school-aged autistic children. J Neuroimaging 2009;19:337–43. doi:10.1111/j.1552-6569.2009.00366.x.

[219] Hanaie R, Mohri I, Kagitani-Shimono K, Tachibana M, Matsuzaki J, Watanabe Y, et al. Abnormal corpus callosum connectivity, socio-

communicative deficits, and motor deficits in children with autism spectrum disorder: A diffusion tensor imaging study. J Autism Dev Disord 2014:2209–20. doi:10.1007/s10803-014-2096-8.

[220] Poustka L, Jennen-Steinmetz C, Henze R, Vomstein K, Haffner J, Sieltjes B. Fronto-temporal disconnectivity and symptom severity in children with autism spectrum disorder. World J Biol Psychiatry 2012;13:269–80. doi:10.3109/15622975.2011.591824.

[221] Mills BD, Lai J, Brown TT, Erhart M, Halgren E, Reilly J, et al. White matter microstructure correlates of narrative production in typically developing children and children with high functioning autism. Neuropsychologia 2013;51:1933–41. doi:10.1016/j.neuropsychologia.2013.06.012.

[222] Hanaie R, Mohri I, Kagitani-Shimono K, Tachibana M, Azuma J, Matsuzaki J, et al. Altered microstructural connectivity of the superior cerebellar peduncle is related to motor dysfunction in children with autistic spectrum disorders. Cerebellum 2013;12:645–56. doi:10.1007/s12311-013-0475-x.

[223] Barnea-Goraly N, Lotspeich L, and Reiss A. Similar white matter aberrations in children with autism and their unaffected siblings: a diffusion tensor imaging study using tract-based spatial statistics. Arch Gen Psychiatry 2010;67:1052–60.

[224] Peterson D, Mahajan R, Crocetti D, Mejia A, Mostofsky S. Left-hemispheric microstructural abnormalities in children with high-functioning autism spectrum disorder. Autism Res 2015;8:61–72. doi:10.1002/aur.1413.

[225] Jou RJ, Mateljevic N, Kaiser MD, Sugrue DR, Volkmar FR, and Pelphrey KA. Structural neural phenotype of autism: preliminary evidence from a diffusion tensor imaging study using tract-based spatial statistics. Am J Neuroradiol 2011;32:1607–13. doi:10.3174/ajnr.A2558.

[226] Cheon K-A, Kim Y-S, Oh S-H, Park S-Y, Yoon H-W, Herrington J, et al. Involvement of the anterior thalamic radiation in boys with high functioning autism spectrum disorders: A diffusion tensor imaging study. Brain Res 2011. doi:10.1016/j.brainres.2011.08.020.

[227] Lai G, Pantazatos SP, Schneider H, Hirsch J. Neural systems for speech and song in autism. Brain 2012;135:961–75. doi:10.1093/brain/awr335.

[228] Nagae LM, Zarnow DM, Blaskey L, Dell J, Khan SY, Qasmieh S, et al. Elevated mean diffusivity in the left hemisphere superior longitudinal fasciculus in autism spectrum disorders increases with more profound language impairment. Am J Neuroradiol 2012:1–6.

[229] Ameis SH, Fan J, Rockel C, Voineskos AN, Lobaugh NJ, Soorya L, et al. Impaired structural connectivity of socio-emotional circuits in autism spectrum disorders: a diffusion tensor imaging study. PLoS One 2011;6:e28044. doi:10.1371/journal.pone.0028044.

[230] Ameis SH, Fan J, Rockel C, Soorya L, Wang AT, Anagnostou E. Altered cingulum bundle microstructure in autism spectrum disorder. Acta Neuropsychiatr 2013:1–8. doi:10.1017/neu.2013.2.

[231] Shukla DK, Keehn B, Lincoln AJ, and Müller R-A. White matter compromise of callosal and subcortical fiber tracts in children with autism spectrum disorder: a diffusion tensor imaging study. J Am Acad Child Adolesc Psychiatry 2010;49:1269–78, 1278.e1–2. doi:10.1016/j.jaac.2010.08.018.

[232] Shukla DK, Keehn B, Smylie DM, and Müller R-A. Microstructural abnormalities of short-distance white matter tracts in autism spectrum disorder. Neuropsychologia 2011;49:1378–82. doi:10.1016/j.neuropsychologia.2011.02.022.

[233] Shukla DK, Keehn B, and Müller R-A. Tract-specific analyses of diffusion tensor imaging show widespread white matter compromise in autism spectrum disorder. J Child Psychol Psychiatry 2011;52:286–95. doi:10.1111/j.1469-7610.2010.02342.x.

[234] Sahyoun CP, Belliveau JW, and Mody M. White matter integrity and pictorial reasoning in high-functioning children with autism. Brain Cogn 2010;73:180–8. doi:10.1016/j.bandc.2010.05.002.

[235] Jou RJ, Jackowski AP, Papademetris X, Rajeevan N, Staib LH, Volkmar FR. Diffusion tensor imaging in autism spectrum disorders: Preliminary evidence of abnormal neural connectivity. Aust N Z J Psychiatry 2011;45:153–62. doi:10.3109/00048674.2010.534069.Diffusion.

[236] Sahyoun CP, Belliveau JW, Soulieres I, Schwartz S, Mody M. Neuroimaging of the functional and structural networks underlying visuospatial versus linguistic reasoning in high-functioning autism. Neuropsychologia 2010;48:86–95. doi:10.1016/j.neuropsychologia.2009.08.013.Neuroimaging.

[237] Noriuchi M, Kikuchi Y, Yoshiura T, Kira R, Shigeto H, Hara T, et al. Altered white matter fractional anisotropy and social impairment in children with autism spectrum disorder. Brain Res 2010;1362:141–9. doi:10.1016/j.brainres.2010.09.051.

[238] Cheng Y, Chou K, Chen I, Fan Y, Decety J, Lin C. Atypical development of white matter microstructure in adolescents with autism spectrum disorders. Neuroimage 2010;50:873–82. doi:10.1016/j.neuroimage.2010.01.011.

[239] Verhoeven JS, Rommel N, Prodi E, Leemans A, Zink I, Vandewalle E, et al. Is there a common neuroanatomical substrate of language deficit between autism spectrum disorder and specific language impairment? Cereb Cortex 2012;22:2263–71. doi:10.1093/cercor/bhr292.

[240] Verly M, Verhoeven J, Zink I, Mantini D, Oudenhove L Van, Lagae L, et al. Structural and functional underconnectivity as a negative predictor for language in autism. Hum Brain Mapp 2014;35:3602–15. doi:10.1002/hbm.22424.

[241] Nair A, Treiber JM, Shukla DK, Shih P, Müller RA. Impaired thalamocortical connectivity in autism spectrum disorder: A study of functional and anatomical connectivity. Brain 2013;136:1942–55. doi:10.1093/brain/awt079.

[242] Fletcher PT, Whitaker RT, Tao R, DuBray MB, Froehlich A, Ravichandran C, et al. Microstructural connectivity of the arcuate fasciculus in adolescents

with high-functioning autism. Neuroimage 2010;51:1117–25. doi:10.1016/j.biotechadv.2011.08.021.Secreted.

[243] Groen WB, Buitelaar JK, van der Gaag RJ, Zwiers MP. Pervasive microstructural abnormalities in autism: a DTI study. J Psychiatry Neurosci 2011;36:32–40. doi:10.1503/jpn.090100.

[244] Barnea-Goraly N, Kwon H, Menon V, Eliez S, Lotspeich L, Reiss A. White matter structure in autism: preliminary evidence from diffusion tensor imaging. Biol Psychiatry 2004;55:323–6. doi:10.1016/j.biopsych.2003.10.022.

[245] Bode MK, Mattila M, Kiviniemi V, Rahko J, Moilanen I, Ebeling H, et al. White matter in autism spectrum disorders – evidence of impaired fiber formation. Acta Radiol 2011;52:1169–74. doi:10.1258/ar.2011.110197.

[246] Lo YC, Soong WT, Gau SSF, Wu YY, Lai MC, Yeh FC, et al. The loss of asymmetry and reduced interhemispheric connectivity in adolescents with autism: A study using diffusion spectrum imaging tractography. Psychiatry Res - Neuroimaging 2011;192:60–6. doi:10.1016/j.pscychresns.2010.09.008.

[247] Travers BG, Bigler ED, Tromp DPM, Adluru N, Destiche D, Samsin D, et al. Brainstem white matter predicts individual differences in manual motor difficulties and symptom severity in autism. J Autism Dev Disord 2015. doi:10.1007/s10803-015-2467-9.

[248] Bakhtiari R, Zürcher NR, Rogier O, Russo B, Hippolyte L, Granziera C, et al. Differences in white matter reflect atypical developmental trajectory in autism: A Tract-based Spatial Statistics study. NeuroImage Clin 2012;1:48–56. doi:10.1016/j.nicl.2012.09.001.

[249] Lange N, Dubray MB, Lee JE, Froimowitz MP, Froehlich A, Adluru N, et al. Atypical diffusion tensor hemispheric asymmetry in autism. Autism Res 2010;3:350–8. doi:10.1002/aur.162.

[250] Alexander AL, Lee JE, Lazar M, Boudos R, DuBray MB, Oakes TR, et al. Diffusion tensor imaging of the corpus callosum in autism. Neuroimage 2007;34:61–73. doi:10.1016/j.neuroimage.2006.08.032.

[251] Lee JE, Bigler ED, Alexander AL, Lazar M, DuBray MB, Chung MK, et al. Diffusion tensor imaging of white matter in the superior temporal gyrus and temporal stem in autism. Neurosci Lett 2007;424:127–32. doi:10.1016/j.neulet.2007.07.042.

[252] Lee JE, Chung MK, Lazar M, DuBray MB, Kim J, Bigler ED, et al. A study of diffusion tensor imaging by tissue-specific, smoothing-compensated voxel-based analysis. Neuroimage 2009;44:870–83. doi:10.1016/j.neuroimage.2008.09.041.A.

[253] Knaus TA, Silver AM, Kennedy M, Lindgren KA, Kelli C, Siegel J, et al. Language laterality in autism spectrum disorder and typical controls: A functional, volumetric, and diffusion tensor MRI study. Brain Lang 2010;112:1–21. doi:10.1016/j.bandl.2009.11.005.Language.

[254] Mcgrath J, Johnson K, O'Hanlon E, Garavan H, Gallagher L, Leemans A.

White matter and visuospatial processing in autism: A constrained spherical deconvolution tractography study. Autism Res 2013;6:307–19. doi:10.1002/aur.1290.

[255] McGrath J, Johnson K, O'Hanlon E, Garavan H, Leemans A, Gallagher L. Abnormal functional connectivity during visuospatial processing is associated with disrupted organisation of white matter in autism. Front Hum Neurosci 2013;7:434. doi:10.3389/fnhum.2013.00434.

[256] Ikuta T, Shafritz KM, Bregman J, Peters B, Gruner P, Malhotra AK, et al. Abnormal cingulum bundle development in autism: A probabilistic tractography study. Psychiatry Res 2014;221:63–8. doi:10.1016/j.biotechadv.2011.08.021.Secreted.

[257] Travers BG, Tromp DPM, Adluru N, Lange N, Destiche D, Ennis C, et al. Atypical development of white matter microstructure of the corpus callosum in males with autism: a longitudinal investigation. Mol Autism 2015;6. doi:10.1186/s13229-015-0001-8.

[258] Keller TA, Kana RK, Just MA. A developmental study of the structural integrity of white matter in autism. Neuroreport 2007;18:23–7.

[259] Travers BG, Bigler ED, Tromp DPM, Adluru N, Froehlich AL, Ennis C, et al. Longitudinal processing speed impairments in males with autism and the effects of white matter microstructure. Neuropsychologia 2014;53:137–45. doi:10.1016/j.biotechadv.2011.08.021.Secreted.

[260] Kleinhans NM, Pauley G, Richards T, Neuhaus E, Martin N, Corrigan NM, et al. Age-related abnormalities in white matter microstructure in autism spectrum disorders. Brain Res 2012;1479:1–16. doi:10.1016/j.brainres.2012.07.056.

[261] Pugliese L, Catani M, Ameis S, Dell'Acqua F, Thiebaut de Schotten M, Murphy C, et al. The anatomy of extended limbic pathways in Asperger syndrome: a preliminary diffusion tensor imaging tractography study. Neuroimage 2009;47:427–34. doi:10.1016/j.neuroimage.2009.05.014.

[262] Peeva MG, Tourville JA, Agam Y, Holland B, Manoach DS, Guenther FH. White matter impairment in the speech network of individuals with autism spectrum disorder. NeuroImage Clin 2013;3:234–41. doi:10.1016/j.nicl.2013.08.011.

[263] Langen M, Leemans A, Johnston P, Ecker C, Daly E, Murphy CM, et al. Fronto-striatal circuitry and inhibitory control in autism: Findings from diffusion tensor imaging tractography. Cortex 2012;48:183–93. doi:10.1016/j.cortex.2011.05.018.

[264] Conturo TE, Williams DE, Smith CD, Gultepe E, Akbudak E, Minshew NJ. Neuronal fiber pathway abnormalities in autism: An initial MRI diffusion tensor tracking study of hippocampo-fusiform and amygdalo-fusiform pathways. J Int Neuropsychol Soc 2008;14:933–46. doi:10.1017/S1355617708081381.Neuronal.

[265] Thomas C, Humphreys K, Jung K-J, Minshew N, Behrmann M. The anatomy

of the callosal and visual-association pathways in high-functioning autism: a DTI tractography study. Cortex 2010;47:863–73. doi:10.1016/j.cortex.2010.07.006.

[266] Roine U, Roine T, Salmi J, Nieminen-Von Wendt T, Leppämäki S, Rintahaka P, et al. Increased coherence of white matter fiber tract organization in adults with asperger syndrome: A diffusion tensor imaging study. Autism Res 2013;6:642–50. doi:10.1002/aur.1332.

[267] Roine U, Salmi J, Roine T, Wendt TN, Leppämäki S, Rintahaka P. Constrained spherical deconvolution-based tractography and tract-based spatial statistics show abnormal microstructural organization in Asperger syndrome. Mol Autism 2015;6.

[268] Thakkar KN, Polli FE, Joseph RM, Tuch DS, Hadjikhani N, Barton JJS, et al. Response monitoring, repetitive behaviour and anterior cingulate abnormalities in autism spectrum disorders (ASD). Brain 2008;131:2464–78. doi:10.1093/brain/awn099.

[269] Catani M, Jones DK, Daly E, Embiricos N, Deeley Q, Pugliese L, et al. Altered cerebellar feedback projections in Asperger syndrome. Neuroimage 2008;41:1184–91. doi:10.1016/j.neuroimage.2008.03.041.

[270] Lewis JD, Theilmann RJ, Fonov V, Bellec P, Lincoln A, Evans AC, et al. Callosal fiber length and interhemispheric connectivity in adults with autism: Brain overgrowth and underconnectivity. Hum Brain Mapp 2013;34:1685–95. doi:10.1002/hbm.22018.

[271] Mueller S, Keeser D, Samson AC, Kirsch V, Blautzik J, Grothe M, et al. Convergent findings of altered functional and structural brain connectivity in individuals with high functioning autism: A multimodal MRI study. PLoS One 2013;8. doi:10.1371/journal.pone.0067329.

[272] Pardini M, Garaci FG, Bonzano L, Roccatagliata L, Palmieri MG, Pompili E, et al. White matter reduced streamline coherence in young men with autism and mental retardation. Eur J Neurol 2009;16:1185–90. doi:10.1111/j.1468-1331.2009.02699.x.

[273] Bloemen OJN, Deeley Q, Sundram F, Daly EM, Barker GJ, Jones DK, et al. White matter integrity in Asperger syndrome: a preliminary diffusion tensor magnetic resonance imaging study in adults. Autism Res 2010;3:203–13. doi:10.1002/aur.146.

[274] Ashburner J, Friston KJ. Voxel-based morphometry--the methods. Neuroimage 2000;11:805–21. doi:10.1006/nimg.2000.0582.

[275] Ge Y, Grossman RI, Babb JS, Rabin ML, Mannon LJ, Kolson DL. Age-related total gray matter and white matter changes in normal adult brain. Part I: volumetric MR imaging analysis. AJNR Am J Neuroradiol 2002;23:1327–33.

[276] Yap QJ, Teh I, Fusar-Poli P, Sum MY, Kuswanto C, Sim K. Tracking cerebral white matter changes across the lifespan: insights from diffusion tensor imaging studies. J Neural Transm 2013. doi:10.1007/s00702-013-0971-7.

[277] Ellmore TM, Li H, Xue Z, Wong STC, Frye RE. Tract-based spatial statistics reveal altered relationship between non-verbal reasoning abilities and white matter integrity in autism spectrum disorder. J Int Neuropsychol Soc 2013;19:723–8. doi:10.1017/S1355617713000325.

[278] Wan CY, Marchina S, Norton A, Schlaug G. Atypical hemispheric asymmetry in the arcuate fasciculus of completely nonverbal children with autism. Ann N Y Acad Sci 2012;1252:332–7. doi:10.1111/j.1749-6632.2012.06446.x.Atypical.

[279] Joseph RM, Fricker Z, Fenoglio A, Lindgren KA, Knaus TA, Tager-Flusberg H. Structural asymmetries of language-related gray and white matter and their relationship to language function in young children with ASD. Brain Imaging Behav 2014;8:60–72. doi:10.1007/s11682-013-9245-0.

[280] Uddin LQ, Menon V, Young CB, Ryali S, Chen T, Khouzam A, et al. Multivariate searchlight classification of structural magnetic resonance imaging in children and adolescents with autism. Biol Psychiatry 2011;70:833–41. doi:10.1016/j.biopsych.2011.07.014.

[281] Ingalhalikar M, Parker D, Bloy L, Roberts TPL, Verma R. Diffusion based abnormality markers of pathology: Towards learned diagnostic prediction of ASD. Neuroimage 2011;57:918–27. doi:10.1016/j.biotechadv.2011.08.021.Secreted.

[282] Libero LE, Deramus TP, Lahti AC, Deshpande G, Kana RK. Multimodal neuroimaging based classification of autism spectrum disorder using anatomical, neurochemical, and white matter correlates. Cortex 2015;66:46–59. doi:10.1016/j.cortex.2015.02.008.

[283] Lewis JD, Evans AC, Pruett JR, Botteron K, Zwaigenbaum L, Estes A, et al. Network inefficiencies in autism spectrum disorder at 24 months. Transl Psychiatry 2014;4:e388. doi:10.1038/tp.2014.24.

[284] Lisiecka DM, Holt R, Tait R, Ford M, Lai M-C, Chura LR, et al. Developmental white matter microstructure in autism phenotype and corresponding endophenotype during adolescence. Transl Psychiatry 2015;5:e529. doi:10.1038/tp.2015.23.

[285] Lai MC, Lombardo M V, Suckling J, Ruigrok AN V, Chakrabarti B, Ecker C, et al. Biological sex affects the neurobiology of autism. Brain 2013;136:2799–815. doi:10.1093/brain/awt216.

[286] Beacher FD, Minati L, Baron-Cohen S, Lombardo M, Lai MC, Gray MA, et al. Autism attenuates sex differences in brain structure: A combined voxel-based morphometry and diffusion tensor imaging study. Am J Neuroradiol 2012;33:83–9.

[287] Nordahl CW, Iosif A-M, Young GS, Perry LM, Dougherty R, Lee A, et al. Sex differences in the corpus callosum in preschool-aged children with autism spectrum disorder. Mol Autism 2015;6:1–11. doi:10.1186/s13229-015-0005-4.

[288] Kirkovski M, Enticott PG, Maller JJ, Rossell SL, Fitzgerald PB. Diffusion tensor imaging reveals no white matter impairments among adults with

autism spectrum disorder. Psychiatry Res Neuroimaging 2015;233:64–72. doi:10.1016/j.pscychresns.2015.05.003.

[289] Goch CJ, Stieltjes B, Henze R, Hering J, Poustka L, Meinzer HP, et al. Quantification of changes in language-related brain areas in autism spectrum disorders using large-scale network analysis. Int J Comput Assist Radiol Surg 2014;9:357–65. doi:10.1007/s11548-014-0977-0.

[290] Li H, Xue Z, Ellmore TM, Frye RE, Wong STC. Network-based analysis reveals stronger local diffusion-based connectivity and different correlations with oral language skills in brains of children with high functioning autism spectrum disorders. Hum Brain Mapp 2014;35:396–413. doi:10.1002/hbm.22185.

[291] Ray S, Miller M, Karalunas S, Robertson C, Grayson DS, Cary RP, et al. Structural and functional connectivity of the human brain in autism spectrum disorders and attention-deficit/hyperactivity disorder: A rich club-organization study. Hum Brain Mapp 2014;00. doi:10.1002/hbm.22603.

[292] Rudie JD, Brown JA, Beck-Pancer D, Hernandez LM, Dennis EL, Thompson PM, et al. Altered functional and structural brain network organization in autism. NeuroImage Clin 2013;2:79–94. doi:10.1016/j.nicl.2012.11.006.

[293] Lewis JD, Theilmann RJ, Townsend J, Evans AC. Network efficiency in autism spectrum disorder and its relation to brain overgrowth. Front Hum Neurosci 2013;7:845. doi:10.3389/fnhum.2013.00845.

[294] Kana RK, Libero LE, Hu CP, Deshpande HD, Colburn JS. Functional brain networks and white matter underlying theory-of-mind in autism. Soc Cogn Affect Neurosci 2014;9:98–105. doi:10.1093/scan/nss106.

[295] Constantino JN, and Todd RD. Autistic traits in the general population - a twin study. Arch Gen Psychiatry 2003;60:524–30.

[296] Robinson EB, Munir K, Munafò MR, Hughes M, McCormick MC, Koenen KC. Stability of autistic traits in the general population: further evidence for a continuum of impairment. J Am Acad Child Adolesc Psychiatry 2011;50:376–84. doi:10.1016/j.jaac.2011.01.005.

[297] Iidaka T, Miyakoshi M, Harada T, Nakai T. White matter connectivity between superior temporal sulcus and amygdala is associated with autistic trait in healthy humans. Neurosci Lett 2012;510:154–8. doi:10.1016/j.neulet.2012.01.029.

[298] Hirose K, Miyata J, Sugihara G, Kubota M, Sasamoto A, Aso T, et al. Fiber tract associated with autistic traits in healthy adults. J Psychiatr Res 2014;59:117–24. doi:10.1016/j.jpsychires.2014.09.001.

[299] Wechsler D. Wechsler abbreviated scale of intelligence (WASI) manual. San Antonio, TX: The Psychological Corporation; 1999.

[300] Clayden JD, Muñoz Maniega S, Storkey AJ, King MD, Bastin ME, and Clark CA. TractoR: Magnetic resonance imaging and tractography with R. J Stat Softw 2011;44.

[301] Smith SM, De Stefano N, Jenkinson M, and Matthews PM. Normalized accurate measurement of longitudinal brain change. J Comput Assist Tomogr 2001;25:466–75.

[302] Smith S, Zhang Y, Jenkinson M, Chen J, Matthews P, Federico A, et al. Accurate, robust, and automated longitudinal and cross-sectional brain change analysis. Neuroimage 2002;17:479–89. doi:10.1006/nimg.2002.1040.

[303] Patenaude B, Smith SM, Kennedy DN, Jenkinson M. A Bayesian model of shape and appearance for subcortical brain segmentation. Neuroimage 2011;56:907–22. doi:10.1016/j.neuroimage.2011.02.046.

[304] FMRIB. FSLutils n.d. http://fsl.fmrib.ox.ac.uk/fsl/fslwiki/Fslutils (accessed February 20, 2015).

[305] Novak MJU, Seunarine KK, Gibbard CR, Hobbs NZ, Scahill RI, Clark CA, et al. White matter integrity in premanifest and early Huntington's disease is related to caudate loss and disease progression. Cortex 2014;52:98–112. doi:10.1016/j.cortex.2013.11.009.

[306] Fischl B, Sereno MI, Tootell RB, Dale AM. High-resolution intersubject averaging and a coordinate system for the cortical surface. Hum Brain Mapp 1999;8:272–84.

[307] Fischl B. Automatically parcellating the human cerebral cortex. Cereb Cortex 2004;14:11–22. doi:10.1093/cercor/bhg087.

[308] Smith S, Jenkinson M, Woolrich M, Beckmann C, Behrens T, Johansen-Berg H, et al. Advances in functional and structural MR image analysis and implementation as FSL. Neuroimage 2004;23 Suppl 1:S208–19. doi:10.1016/j.neuroimage.2004.07.051.

[309] Smith S. Fast robust automated brain extraction. Hum Brain Mapp 2002;17:143–55. doi:10.1002/hbm.10062.

[310] Behrens TEJ, Berg HJ, Jbabdi S, Rushworth MFS, Woolrich MW. Probabilistic diffusion tractography with multiple fibre orientations: What can we gain? Neuroimage 2007;34:144–55. doi:10.1016/j.neuroimage.2006.09.018.

[311] Yendiki A, Koldewyn K, Kakunoori S, Kanwisher N, Fischl B. Spurious group differences due to head motion in a diffusion MRI study. Neuroimage 2013;88C:79–90. doi:10.1016/j.neuroimage.2013.11.027.

[312] Baron-Cohen S, Jolliffe T, Mortimore C, Robertson M. Another advanced test of theory of mind: evidence from very high functioning adults with autism or asperger syndrome. J Child Psychol Psychiatry 1997;38:813–22.

[313] Baron-Cohen S, Wheelwright S, Hill J, Raste Y, Plumb I. The "Reading the Mind in the Eyes" test revised version: A study with normal adults, and adults with Asperger syndrome or high-functioning autism. J Child Psychol Psychiatry 2001;42:241–51.

[314] Clayden JD, Jentschke S, Muñoz M, Cooper JM, Chadwick MJ, Banks T, et al. Normative development of white matter tracts: similarities and differences in relation to age, gender, and intelligence. Cereb Cortex 2012;22:1738–47.

doi:10.1093/cercor/bhr243.

[315] Kanaan RA, Allin M, Picchioni M, Barker GJ, Daly E, Shergill SS, et al. Gender differences in white matter microstructure. PLoS One 2012;7:e38272. doi:10.1371/journal.pone.0038272.

[316] Menzler K, Belke M, Wehrmann E, Krakow K, Lengler U, Jansen A, et al. Men and women are different: diffusion tensor imaging reveals sexual dimorphism in the microstructure of the thalamus, corpus callosum and cingulum. Neuroimage 2011;54:2557–62. doi:10.1016/j.neuroimage.2010.11.029.

[317] Gibbard CR, Ren J, Seunarine KK, Clayden JD, Skuse DH, Clark CA. White matter microstructure correlates with autism trait severity in a combined clinical-control sample of high-functioning adults. NeuroImage Clin 2013;3:106–14. doi:10.1016/j.nicl.2013.07.007.

[318] Dalgleish T. The emotional brain. Nat Rev Neurosci 2004;5:583–9. doi:10.1038/nrn1432.

[319] Rizzolatti G, Fogassi L, and Gallese V. Neurophysiological mechanisms underlying the understanding and imitation of action. Nat Rev Neurosci 2001;2:661–70.

[320] Catani M, Howard RJ, Pajevic S, Jones DK. Virtual in vivo interactive dissection of white matter fasciculi in the human brain. Neuroimage 2002;17:77–94. doi:10.1006/nimg.2002.1136.

[321] Rizzolatti G, and Craighero L. The mirror-neuron system. Annu Rev Neurosci 2004;27:169–92. doi:10.1146/annurev.neuro.27.070203.144230.

[322] Beaulieu C. The basis of anisotropic water diffusion in the nervous system - a technical review. NMR Biomed 2002;15:435–55. doi:10.1002/nbm.782.

[323] Hasan KM, Kamali A, Abid H, Kramer LA, Fletcher JM, Ewing-Cobbs L. Quantification of the spatiotemporal microstructural organization of the human brain association, projection and commissural pathways across the lifespan using diffusion tensor tractography. Brain Struct Funct 2010;214:361–73. doi:10.1007/s00429-009-0238-0.

[324] Lebel C, Gee M, Camicioli R, Wieler M, Martin W, Beaulieu C. Diffusion tensor imaging of white matter tract evolution over the lifespan. Neuroimage 2012;60:340–52. doi:10.1016/j.neuroimage.2011.11.094.

[325] Jones DK, Symms MR, Cercignani M, Howard RJ. The effect of filter size on VBM analyses of DT-MRI data. Neuroimage 2005;26:546–54. doi:10.1016/j.neuroimage.2005.02.013.

[326] Smith S, Johansen-Berg H, Jenkinson M, Rueckert D, Nichols T, Miller K, et al. Acquisition and voxelwise analysis of multi-subject diffusion data with tract-based spatial statistics. Nat Protoc 2007;2:499–503. doi:10.1038/nprot.2007.45.

[327] FSL. Templates and atlases included within FSL n.d. http://fsl.fmrib.ox.ac.uk/fsl/fslwiki/Atlases (accessed January 30, 2015).

[328] Takahashi M, Hackney DB, Zhang G, Wehrli SL, Wright AC, O'Brien WT, et al. Magnetic resonance microimaging of intraaxonal water diffusion in live excised lamprey spinal cord. Proc Natl Acad Sci U S A 2002;99:16192–6. doi:10.1073/pnas.252249999.

[329] Song S-K, Sun S-W, Ramsbottom MJ, Chang C, Russell J, Cross AH. Dysmyelination revealed through MRI as increased radial (but unchanged axial) diffusion of water. Neuroimage 2002;17:1429–36. doi:10.1006/nimg.2002.1267.

[330] Lau YC, Hinkley LBN, Bukshpun P, Strominger ZA, Wakahiro MLJ, Baron-Cohen S, et al. Autism traits in individuals with agenesis of the corpus callosum. J Autism Dev Disord 2012. doi:10.1007/s10803-012-1653-2.

[331] Kanwisher N. Functional specificity in the human brain: a window into the functional architecture of the mind. Proc Natl Acad Sci U S A 2010;107:11163–70. doi:10.1073/pnas.1005062107.

[332] Hampshire A, Highfield RR, Parkin BL, Owen AM. Fractionating human intelligence. Neuron 2012;76:1225–37. doi:10.1016/j.neuron.2012.06.022.

[333] Adolphs R, Tranel D, Damasio H, Damasio A. Impaired recognition of emotion in facial expressions following bilateral damage to the human amygdala. Nature 1994;372:669–72.

[334] Shaw P, Lawrence EJ, Radbourne C, Bramham J, Polkey CE, David AS. The impact of early and late damage to the human amygdala on "theory of mind" reasoning. Brain 2004;127:1535–48. doi:10.1093/brain/awh168.

[335] Baron-Cohen S, Ring HA, Bullmore ET, Wheelwright S, Ashwin C, Williams SC. The amygdala theory of autism. Neurosci Biobehav Rev 2000;24:355–64.

[336] Green SA, Rudie JD, Colich NL, Wood JJ, Shirinyan D, Hernandez L, et al. Overreactive brain responses to sensory stimuli in youth with autism spectrum disorders. J Am Acad Child Adolesc Psychiatry 2013;52:1158–72. doi:10.1016/j.jaac.2013.08.004.

[337] Schumann CM, Barnes CC, Lord C, Courchesne E. Amygdala enlargement in toddlers with autism related to severity of social and communication impairments. Biol Psychiatry 2009;66:942–9. doi:10.1016/j.biopsych.2009.07.007.

[338] Murphy ER, Foss-Feig J, Kenworthy L, Gaillard WD, Vaidya CJ. Atypical functional connectivity of the amygdala in childhood autism spectrum disorders during spontaneous attention to eye-gaze. Autism Res Treat 2012;2012:652408. doi:10.1155/2012/652408.

[339] von dem Hagen EAH, Stoyanova RS, Baron-Cohen S, Calder AJ. Reduced functional connectivity within and between "social" resting state networks in autism spectrum conditions. Soc Cogn Affect Neurosci 2013;8:694–701. doi:10.1093/scan/nss053.

[340] Radua J, Via E, Catani M, Mataix-Cols D. Voxel-based meta-analysis of regional white-matter volume differences in autism spectrum disorder versus

healthy controls. Psychol Med 2011;41:1539–50. doi:10.1017/S0033291710002187.

[341] Ecker C, Suckling J, Deoni SC, Lombardo M V, Bullmore ET, Baron-Cohen S, et al. Brain anatomy and its relationship to behavior in adults with autism spectrum disorder: A multicenter magnetic resonance imaging study. Arch Gen Psychiatry 2012;69:195–209.

[342] LeDoux JE. Emotion: clues from the brain. Annu Rev Psychol 1995;46:209–35. doi:10.1146/annurev.ps.46.020195.001233.

[343] LeDoux J. Fear and the brain: Where have we been, and where are we going? Biol Psychiatry 1998;44:1229–38.

[344] Saygin ZM, Osher DE, Augustinack J, Fischl B, Gabrieli JDE. Connectivity-based segmentation of human amygdala nuclei using probabilistic tractography. Neuroimage 2011;56:1353–61. doi:10.1016/j.neuroimage.2011.03.006.

[345] Johansen JP, Hamanaka H, Monfils MH, Behnia R, Deisseroth K, Blair HT, et al. Optical activation of lateral amygdala pyramidal cells instructs associative fear learning. Proc Natl Acad Sci U S A 2010;107:12692–7. doi:10.1073/pnas.1002418107.

[346] Kalin NH, Shelton SE, Davidson RJ. The role of the central nucleus of the amygdala in mediating fear and anxiety in the primate. J Neurosci 2004;24:5506–15. doi:10.1523/JNEUROSCI.0292-04.2004.

[347] Stefanacci L, Amaral DG. Topographic organization of cortical inputs to the lateral nucleus of the macaque monkey amygdala : A retrograde tracing study. J Comp Neurol 2000;421:52–79.

[348] Price JL, Amaral DG. An autoradiographic study of the projections of the central nucleus of the monkey amygdala. J Neurosci 1981;1:1242–59.

[349] Bach DR, Behrens TE, Garrido L, Weiskopf N, Dolan RJ. Deep and superficial amygdala nuclei projections revealed in vivo by probabilistic tractography. J Neurosci 2011;31:618–23. doi:10.1523/JNEUROSCI.2744-10.2011.

[350] Bauman M, Kemper TL. Histoanatomic observations of the brain in early infantile autism. Neurology 1985;35:866–74.

[351] Schumann CM, Amaral DG. Stereological analysis of amygdala neuron number in autism. J Neurosci 2006;26:7674–9. doi:10.1523/JNEUROSCI.1285-06.2006.

[352] Behrens TEJ, Johansen-Berg H, Woolrich MW, Smith SM, Wheeler-Kingshott CAM, Boulby PA, et al. Non-invasive mapping of connections between human thalamus and cortex using diffusion imaging. Nat Neurosci 2003;6:750–7. doi:10.1038/nn1075.

[353] Jenkinson M, Bannister P, Brady M, Smith S. Improved optimization for the robust and accurate linear registration and motion correction of brain images. Neuroimage 2002;17:825–41. doi:10.1006/nimg.2002.1132.

[354] Wang R, Wedeen VJ. TrackVis.org. Martinos Cent Biomed Imaging,

Massachusetts Gen Hosp 2007.

[355] Juranek J, Filipek PA, Berenji GR, Modahl C, Osann K, Spence MA. Association Between Amygdala Volume and Anxiety Level: Magnetic Resonance Imaging (MRI) Study in Autistic Children. J Child Neurol 2006;21:1051–8. doi:10.1177/7010.2006.00237.

[356] Schumann CM, Hamstra J, Goodlin-Jones BL, Lotspeich LJ, Kwon H, Buonocore MH, et al. The amygdala is enlarged in children but not adolescents with autism; the hippocampus is enlarged at all ages. J Neurosci 2004;24:6392–401. doi:10.1523/JNEUROSCI.1297-04.2004.

[357] Gläscher J, Adolphs R. Processing of the arousal of subliminal and supraliminal emotional stimuli by the human amygdala. J Neurosci 2003;23:10274–82.

[358] Skuse DH, Morris JS, Dolan RJ. Functional dissociation of amygdala-modulated arousal and cognitive appraisal, in Turner syndrome. Brain 2005;128:2084–96. doi:10.1093/brain/awh562.

[359] Creswell CS, Skuse DH. Autism in association with Turner syndrome: Genetic implications for male vulnerability to pervasive developmental disorders. Neurocase 1999;5:511–8. doi:10.1080/13554799908402746.

[360] Good CD, Lawrence K, Thomas NS, Price CJ, Ashburner J, Friston KJ, et al. Dosage-sensitive X-linked locus influences the development of amygdala and orbitofrontal cortex, and fear recognition in humans. Brain 2003;126:2431–46. doi:10.1093/brain/awg242.

[361] Skuse DH, Gallagher L. Dopaminergic-neuropeptide interactions in the social brain. Trends Cogn Sci 2009;13:27–35. doi:10.1016/j.tics.2008.09.007.

[362] Craig AD. How do you feel--now? The anterior insula and human awareness. Nat Rev Neurosci 2009;10:59–70. doi:10.1038/nrn2555.

[363] Bachevalier J. Medial temporal lobe structures and autism: a review of clinical and experimental findings. Neuropsychologia 1994;32:627–48.

[364] Goodale MA, Milner AD. Separate visual pathways for perception and action. Trends Neurosci 1992;15:20–5.

[365] Bullmore E, Sporns O. Complex brain networks: graph theoretical analysis of structural and functional systems. Nat Rev Neurosci 2009;10:186–98. doi:10.1038/nrn2575.

[366] Clayden JD. Imaging connectivity: MRI and the structural networks of the brain. Funct Neurol 2013;28:197–203. doi:10.11138/FNeur/2013.28.3.197.

[367] Sporns O. Graph theory methods for the analysis of neural connectivity patterns. In: Kötter R, editor. Neurosci. Databases A Pract. Guid., Dordrecht, Netherlands: Klüwer; 2002, p. 169–83.

[368] Papez JW. A proposed mechanism of emotion. Arch Neurol Psychiatry 1937;38:725–43.

[369] Nieuwenhuys R. The insular cortex. A review. vol. 195. 1st ed. Elsevier B.V.;

2012. doi:10.1016/B978-0-444-53860-4.00007-6.

[370] Chang LJ, Yarkoni T, Khaw MW, Sanfey AG. Decoding the role of the insula in human cognition: Functional parcellation and large-scale reverse inference. Cereb Cortex 2013;23:739–49. doi:10.1093/cercor/bhs065.

[371] Good M. Spatial Memory and Hippocampal Function: Where are we now? Psicológica 2002;23:109–38.

[372] Kesner RP, Lee I, Gilbert P. A behavioral assessment of hippocampal function based on a subregional analysis. Rev Neurosci 2004;15:333–51. doi:10.1515/REVNEURO.2004.15.5.333.

[373] Di Martino A, Ross K, Uddin LQ, Sklar AB, Castellanos FX, Milham MP. Functional brain correlates of social and nonsocial processes in autism spectrum disorders: An activation likelihood estimation meta-analysis. Biol Psychiatry 2009;65:63–74. doi:10.1016/j.biopsych.2008.09.022.

[374] Clayden JD, Dayan M, Clark CA. Principal Networks. PLoS One 2013;8:1–12. doi:10.1371/journal.pone.0060997.

[375] Jones DK. Challenges and limitations of quantifying brain connectivity in vivo with diffusion MRI 2010;2:341–55. doi:10.2217/iim.10.21.

[376] Reveley C, Seth AK, Pierpaoli C, Silva AC, Yu D, Saunders RC, et al. Superficial white matter fiber systems impede detection of long-range cortical connections in diffusion MR tractography. Proc Natl Acad Sci 2015:201418198. doi:10.1073/pnas.1418198112.

[377] Jakab A, Emri M, Spisak T, Szeman-Nagy A, Beres M, Kis SA, et al. Autistic traits in neurotypical adults: correlates of graph theoretical functional network topology and white matter anisotropy patterns. PLoS One 2013;8:e60982. doi:10.1371/journal.pone.0060982.

[378] Lai MC, Lombardo M V, Pasco G, Ruigrok AN V, Wheelwright SJ, Sadek S a., et al. A behavioral comparison of male and female adults with high functioning autism spectrum conditions. PLoS One 2011;6. doi:10.1371/journal.pone.0020835.

[379] Bejerot S, Eriksson JM, Bonde S, Carlström K, Humble MB, Eriksson E. The extreme male brain revisited: Gender coherence in adults with autism spectrum disorder. Br J Psychiatry 2012;201:116–23. doi:10.1192/bjp.bp.111.097899.

[380] Baron-Cohen S, Knickmeyer RC, Belmonte MK. Sex differences in the brain: Implications for explaining autism. Science 2005;310:819–23. doi:10.1126/science.1115455.

[381] Bloss CS, Courchesne E. MRI neuroanatomy in young girls with autism: a preliminary study. J Am Acad Child Adolesc Psychiatry 2007;46:515–23. doi:10.1097/chi.0b013e318030e28b.

[382] Tepest R, Jacobi E, Gawronski A, Krug B, Möller-Hartmann W, Lehnhardt FG, et al. Corpus callosum size in adults with high-functioning autism and the relevance of gender. Psychiatry Res - Neuroimaging 2010;183:38–43.

doi:10.1016/j.pscychresns.2010.04.007.

[383] Chou KH, Cheng Y, Chen IY, Lin CP, Chu WC. Sex-linked white matter microstructure of the social and analytic brain. Neuroimage 2011;54:725–33. doi:10.1016/j.neuroimage.2010.07.010.

[384] Robinson EB, Lichtenstein P, Anckarsäter H, Happé F, Ronald A. Examining and interpreting the female protective effect against autistic behavior. Proc Natl Acad Sci U S A 2013;110:5258–62. doi:10.1073/pnas.1211070110.

[385] Duvall JA, Lu A, Cantor RM, Todd RD, Constantino JN, Geschwind DH. A quantitative trait locus analysis of social responsiveness in multiplex autism families. Am J Psychiatry 2007;164:656–62. doi:10.1176/appi.ajp.164.4.656.

[386] Kaiser MD, Hudac CM, Shultz S, Lee SM, Cheung C, Berken AM, et al. Neural signatures of autism. Proc Natl Acad Sci U S A 2010;107:21223–8. doi:10.1073/pnas.1010412107.

[387] Pearson. Differential Ability Scales: DAS-II. 2nd Editio. 2007.

[388] Western Psychological Services. Social Responsiveness Scale. 2005.

[389] O'Donnell LJ, Westin CF. An introduction to diffusion tensor image analysis. Neurosurg Clin N Am 2011;22:185–96. doi:10.1016/j.nec.2010.12.004.

[390] Segovia F, Holt R, Spencer M, Górriz JM, Ramírez J, Puntonet CG, et al. Identifying endophenotypes of autism: a multivariate approach. Front Comput Neurosci 2014;8:60. doi:10.3389/fncom.2014.00060.

[391] Hazlett HC, Gu H, Mckinstry RC, Shaw DWW, Botteron KN, Dager S, et al. Brain volume findings in six month old infants at high familial risk for autism. Am J Psychiatry 2012;169:601–8. doi:10.1176/appi.ajp.2012.11091425.Brain.

[392] Martin JH. Neuroanatomy: Text and atlas. Amsterdam: Elsevier Science Publishing; 1989.

[393] Nolte J. The human brain: An introduction to its functional anatomy. 4th Editio. St Louis, USA: Mosby-Year Book; 1999.

[394] Tournier JD, Yeh CH, Calamante F, Cho KH, Connelly A, Lin CP. Resolving crossing fibres using constrained spherical deconvolution: Validation using diffusion-weighted imaging phantom data. Neuroimage 2008;42:617–25. doi:10.1016/j.neuroimage.2008.05.002.

[395] Zhang H, Schneider T, Wheeler-Kingshott CA, Alexander DC. NODDI: Practical in vivo neurite orientation dispersion and density imaging of the human brain. Neuroimage 2012;61:1000–16. doi:10.1016/j.neuroimage.2012.03.072.

[396] Rushton WAH. A theory of the effects of fibre size in medullated nerve This information is current as of August 30 , 2007 This is the final published version of this article ; it is available at : This version of the article may not be posted on a public website for 1 2007.

[397] Stikov N, Perry LM, Mezer A, Rykhlevskaia E, Wandell BA, Pauly JM, et al.

Bound pool fractions complement diffusion measures to describe white matter micro and macrostructure. Neuroimage 2011;54:1112–21. doi:10.1016/j.biotechadv.2011.08.021.Secreted.

[398] Stikov N, Campbell JSW, Stroh T, Lavelée M, Frey S, Novek J, et al. In vivo histology of the myelin g-ratio with magnetic resonance imaging. Neuroimage 2015;118:397–405. doi:10.1016/j.neuroimage.2015.05.023.

[399] Wedeen VJ, Hagmann P, Tseng WYI, Reese TG, Weisskoff RM. Mapping complex tissue architecture with diffusion spectrum magnetic resonance imaging. Magn Reson Med 2005;54:1377–86. doi:10.1002/mrm.20642.

[400] Tuch DS, Reese TG, Wiegell MR, Wedeen VJ. Diffusion MRI of complex neural architecture. Neuron 2003;40:885–95. doi:10.1016/S0896-6273(03)00758-X.

[401] Duyn JH. The future of ultra-high field MRI and fMRI for study of the human brain. Neuroimage 2012;62:1241–8. doi:10.1016/j.neuroimage.2011.10.065.

Appendix A: ICD-10 Diagnostic Criteria

F84 Pervasive developmental disorders

This group of disorders is characterized by qualitative abnormalities in reciprocal social interactions and in patterns of communication, and by restricted, stereotyped, repetitive repertoire of interests and activities. These qualitative abnormalities are a pervasive feature of the individual's functioning in all situations, although they may vary in degree. In most cases, development is abnormal from infancy and, with only a few exceptions, the conditions become manifest during the first 5 years of life. It is usual, but not invariable, for there to be some degree of general cognitive impairment but the disorders are defined in terms of *behaviour* that is deviant in relation to mental age (whether the individual is retarded or not). There is some disagreement on the subdivision of this overall group of pervasive developmental disorders. In some cases the disorders are associated with, and presumably due to, some medical condition, of which infantile spasms, congenital rubella, tuberous sclerosis, cerebral lipidosis, and the fragile X chromosome anomaly are among the most common. However, the disorder should be diagnosed on the basis of the behavioural features, irrespective of the presence or absence of any associated medical conditions; any such associated condition must, nevertheless, be separately coded. If mental retardation is present, it is important that it too should be separately coded, under F70-F79, because it is not a universal feature of the pervasive developmental disorders.

F84.0 Childhood autism

A pervasive developmental disorder defined by the presence of abnormal and/or impaired development that is manifest before the age of 3 years, and by the characteristic type of abnormal functioning in all three areas of social interaction, communication, and restricted, repetitive behaviour. The disorder occurs in boys three to four times more often than in girls.

Diagnostic guidelines

Usually there is no prior period of unequivocally normal development but, if there is, abnormalities become apparent before the age of 3 years. There are always qualitative impairments in reciprocal social interaction. These take the form of an inadequate appreciation of socio-emotional cues, as shown by a lack of responses to other people's emotions and/or a lack of modulation of behaviour according to social context; poor use of social signals and a weak integration of social, emotional, and communicative behaviours; and, especially, a lack of socio-emotional reciprocity.

Similarly, qualitative impairments in communications are universal. These take the form of a lack of social usage of whatever language skills are present; impairment in make-believe and social imitative play; poor synchrony and lack of reciprocity in conversational interchange; poor flexibility in language expression and a relative lack of creativity and fantasy in thought processes; lack of emotional response to other people's verbal and nonverbal overtures; impaired use of variations in cadence or emphasis to reflect communicative modulation; and a similar lack of accompanying gesture to provide emphasis or aid meaning in spoken communication.

The condition is also characterized by restricted, repetitive, and stereotyped patterns of behaviour, interests, and activities. These take the form of a tendency to impose rigidity and routine on a wide range of aspects of day-to day functioning; this usually applies to novel activities as well as to familiar habits and play patterns. In early childhood particularly, there may be specific attachment to unusual, typically non-soft objects. The children may insist on the performance of particular routines in rituals of a non-functional character; there may be stereotyped

preoccupations with interests such as dates, routes or timetables; often there are motor stereotypies; a specific interest in non-functional elements of objects (such as their smell or feel) is common; and there may be a resistance to changes in routine or in details of the personal environment (such as the movement of ornaments or furniture in the family home).

In addition to these specific diagnostic features, it is frequent for children with autism to show a range of other nonspecific problems such as fear/phobias, sleeping and eating disturbances, temper tantrums, and aggression. Self-injury (e.g. by wrist-biting) is fairly common, especially when there is associated severe mental retardation. Most individuals with autism lack spontaneity, initiative, and creativity in the organization of their leisure time and have difficulty applying conceptualizations in decision-making in work (even when the tasks themselves are well within their capacity). The specific manifestation of deficits characteristic of autism change as the children grow older, but the deficits continue into and through adult life with a broadly similar pattern of problems in socialization, communication, and interest patterns. Developmental abnormalities must have been present in the first 3 years for the diagnosis to be made, but the syndrome can be diagnosed in all age groups. All levels of IQ can occur in association with autism, but there is significant mental retardation in some three-quarters of cases.

Includes:

Autistic disorder; infantile autism; infantile psychosis; Kanner's syndrome.

Differential diagnosis:

Apart from the other varieties of pervasive developmental disorder it is important to consider: specific developmental disorder of receptive language (F80.2) with secondary socio-emotional problems; reactive attachment disorder (F94.1) or

disinhibited attachment disorder (F94.2); mental retardation (F70-F79) with some associated emotional/behavioural disorder; schizophrenia (F20.-) of unusually early onset; and Rett's syndrome (F84.2).

Excludes:

Autistic psychopathy (F84.5).

F84.1 Atypical autism

A pervasive developmental disorder that differs from autism in terms either of age of onset or of failure to fulfil all three sets of diagnostic criteria. Thus, abnormal and/or impaired development becomes manifest for the first time only after age 3 years; and/or there are insufficient demonstrable abnormalities in one or two of the three areas of psychopathology required for the diagnosis of autism (namely, reciprocal social interactions, communication, and restrictive, stereotyped, repetitive behaviour) in spite of characteristic abnormalities in the other area(s). Atypical autism arises most often in profoundly retarded individuals whose very low level of functioning provides little scope for exhibition of the specific deviant behaviours required for the diagnosis of autism; it also occurs in individuals with a severe specific developmental disorder of receptive language. Atypical autism thus constitutes a meaningfully separate condition from autism.

Includes:

Atypical childhood psychosis.

Mental retardation with autistic features

F84.2 Rett's syndrome

A condition of unknown cause, so far reported only in girls, which has been differentiated on the basis of a characteristic onset, course, and pattern of symptomatology. Typically, apparently normal or near-normal early development is followed by partial or complete loss of acquired hand skills and of speech, together with deceleration in head growth, usually with an onset between 7 and 24 months of age. Hand-wringing stereotypies, hyperventilation and loss of purposive hand movements are particularly characteristic. Social and play development are arrested in the first 2 or 3 years, but social interest tends to be maintained. During middle childhood, trunk ataxia and apraxia, associated with scoliosis or kyphoscoliosis tend to develop and sometimes there are choreoathetoid movements. Severe mental handicap invariably results. Fits frequently develop during early or middle childhood.

Diagnostic guidelines

In most cases onset is between 7 and 24 months of age. The most characteristic feature is a loss of purposive hand movements and acquired fine motor manipulative skills. This is accompanied by loss, partial loss or lack of development of language; distinctive stereotyped tortuous wringing or "hand-washing" movements, with the arms flexed in front of the chest or chin; stereotypic wetting of the hands with saliva; lack of proper chewing of food; often episodes of hyperventilation; almost always a failure to gain bowel and bladder control; often excessive drooling and protrusion of the tongue; and a loss of social engagement. Typically, the children retain a kind of "social smile", looking at or "through" people, but not interacting socially with them in early childhood (although social interaction often develops later). The stance and gait tend to become broad-based, the muscles are hypotonic, trunk movements usually become poorly coordinated, and scoliosis or kyphoscoliosis usually develops. Spinal atrophies, with severe motor disability, develop in adolescence or adulthood in about half the cases. Later, rigid spasticity

may become manifest, and is usually more pronounced in the lower than in the upper limbs. Epileptic fits, usually involving some type of minor attack, and with an onset generally before the age of 8 years, occur in the majority of cases. In contrast to autism, both deliberate self-injury and complex stereotyped preoccupations or routines are rare.

Differential diagnosis:

Initially, Rett's syndrome is differentiated primarily on the basis of the lack of purposive hand movements, deceleration of head growth, ataxia, stereotypic "hand-washing" movements, and lack of proper chewing. The course of the disorder, in terms of progressive motor deterioration, confirms the diagnosis.

F84.3 Other childhood disintegrative disorder

A pervasive developmental disorder (other than Rett's syndrome) that is defined by a period of normal development before onset, and by a definite loss, over the course of a few months, of previously acquired skills in at least several areas of development, together with the onset of characteristic abnormalities of social, communicative, and behavioural functioning. Often there is a prodromic period of vague illness; the child becomes restive, irritable, anxious, and overactive. This is followed by impoverishment and then loss of speech and language, accompanied by behavioural disintegration. In some cases the loss of skills is persistently progressive (usually when the disorder is associated with a progressive diagnosable neurological condition), but more often the decline over a period of some months is followed by a plateau and then a limited improvement. The prognosis is usually very poor, and most individuals are left with severe mental retardation. There is uncertainty about the extent to which this condition differs from autism. In some cases the disorder can be shown to be due to some associated encephalopathy, but

the diagnosis should be made on the behavioural features. Any associated neurological condition should be separately coded.

Diagnostic guidelines:

Diagnosis is based on an apparently normal development up to the age of at least 2 years, followed by a definite loss of previously acquired skills; this is accompanied by qualitatively abnormal social functioning. It is usual for there to be a profound regression in, or loss of, language, a regression in the level of play, social skills, and adaptive behaviour, and often a loss of bowel or bladder control, sometimes with a deteriorating motor control. Typically, this is accompanied by a general loss of interest in the environment, by stereotyped, repetitive motor mannerisms, and by an autistic-like impairment of social interaction and communication. In some respects, the syndrome resembles dementia in adult life, but it differs in three key respects: there is usually no evidence of any identifiable organic disease or damage (although organic brain dysfunction of some type is usually inferred); the loss of skills may be followed by a degree of recovery; and the impairment in socialization and communication has deviant qualities typical of autism rather than of intellectual decline. For all these reasons the syndrome is included here rather than under F00-F09.

Includes:

Dementia infantilis; disintegrative psychosis; Heller's syndrome; symbiotic psychosis.

Excludes:

Acquired aphasia with epilepsy (F80.3); elective mutism (F94.0); Rett's syndrome (F84.2); schizophrenia (F20.-)

F84.4 Overactive disorder associated with mental retardation and stereotyped movements

This is an ill-defined disorder of uncertain nosological validity. The category is included here because of the evidence that children with moderate to severe mental retardation (IQ below 50) who exhibit major problems in hyperactivity and inattention frequently show stereotyped behaviours; such children tend not to benefit from stimulant drugs (unlike those with an IQ in the normal range) and may exhibit a severe dysphoric reaction (sometimes with psychomotor retardation) when given stimulants; in adolescence the overactivity tends to be replaced by underactivity (a pattern that is not usual in hyperkinetic children with normal intelligence). It is also common for the syndrome to be associated with a variety of developmental delays, either specific or global.

The extent to which the behavioural pattern is a function of low IQ or of organic brain damage is not known, neither is it clear whether the disorders in children with mild mental retardation who show the hyperkinetic syndrome would be better classified here or under F90.-; at present they are included in F90-.

Diagnostic guidelines:

Diagnosis depends on the combination of developmentally inappropriate severe overactivity, motor stereotypies, and moderate to severe mental retardation; all three must be present for the diagnosis. If the diagnostic criteria for F84.0, F84.1 or F84.2 are met, that condition should be diagnosed instead.

F84.5 Asperger's syndrome

A disorder of uncertain nosological validity, characterized by the same kind of qualitative abnormalities of reciprocal social interaction that typify autism, together with a restricted, stereotyped, repetitive repertoire of interests and activities. The disorder differs from autism primarily in that there is no general delay or retardation in language or in cognitive development. Most individuals are of normal general intelligence but it is common for them to be markedly clumsy; the condition occurs predominantly in boys (in a ratio of about eight boys to one girl). It seems highly likely that at least some cases represent mild varieties of autism, but it is uncertain whether or not that is so for all. There is a strong tendency for the abnormalities to persist into adolescence and adult life and it seems that they represent individual characteristics that are not greatly affected by environmental influences. Psychotic episodes occasionally occur in

early adult life.

Diagnostic guidelines:

Diagnosis is based on the combination of a lack of any clinically significant general delay in language or cognitive development plus, as with autism, the presence of qualitative deficiencies in reciprocal social interaction and restricted, repetitive, stereotyped patterns of behaviour, interests, and activities. There may or may not be problems in communication similar to those associated with autism, but significant language retardation would rule out the diagnosis.

Includes:

Autistic psychopathy; schizoid disorder of childhood.

Excludes:

Anankastic personality disorder (F60.5); attachment disorders of childhood (F94.1, F94.2); obsessive-compulsive disorder (F42.-); schizotypal disorder (F21); simple schizophrenia (F20.6); F84.8 Other pervasive developmental disorders.

F84.9 Pervasive developmental disorder, unspecified.

This is a residual diagnostic category that should be used for disorders which fit the general description for pervasive developmental disorders but in which a lack of adequate information, or contradictory findings, means that the criteria for any of the other F84 codes cannot be met.

F88 Other disorders of psychological development

Includes: developmental agnosia.

F89 Unspecified disorder of psychological development

Includes: developmental disorder NOS.

Appendix B: DSM-5 Diagnostic Criteria

Diagnostic criteria

A. Persistent deficits in social communication and social interaction across multiple contexts, as manifested by the following, currently or by history (examples are illustrative, not exhaustive, see text):

1. Deficits in social-emotional reciprocity, ranging, for example, from abnormal social approach and failure of normal back-and-forth conversation; to reduced sharing of interests, emotions, or affect; to failure to initiate or respond to social interactions.

2. Deficits in nonverbal communicative behaviors used for social interaction, ranging, for example, from poorly integrated verbal and nonverbal communication; to abnormalities in eye contact and body language or deficits in understanding and use of gestures; to a total lack of facial expressions and nonverbal communication.

3. Deficits in developing, maintaining, and understanding relationships, ranging, for example, from difficulties adjusting behavior to suit various social contexts; to difficulties in sharing imaginative play or in making friends; to absence of interest in peers.

Specify current severity:

Severity is based on social communication impairments and restricted repetitive patterns of behavior (see Table A).

B. Restricted, repetitive patterns of behavior, interests, or activities, as manifested by at least two of the following, currently or by history (examples are illustrative, not exhaustive; see text):

1. Stereotyped or repetitive motor movements, use of objects, or speech (e.g., simple motor stereotypies, lining up toys or flipping objects, echolalia, idiosyncratic phrases).

2. Insistence on sameness, inflexible adherence to routines, or ritualized patterns or verbal nonverbal behavior (e.g., extreme distress at small changes, difficulties with transitions, rigid thinking patterns, greeting rituals, need to take same route or eat food every day).

3. Highly restricted, fixated interests that are abnormal in intensity or focus (e.g, strong attachment to or preoccupation with unusual objects, excessively circumscribed or perseverative interest).

4. Hyper- or hyporeactivity to sensory input or unusual interests in sensory aspects of the environment (e.g., apparent indifference to pain/temperature, adverse response to specific sounds or textures, excessive smelling or touching of objects, visual fascination with lights or movement).

Specify current severity:

Severity is based on social communication impairments and restricted, repetitive patterns of behavior (see Table A).

C. Symptoms must be present in the early developmental period (but may not become fully manifest until social demands exceed limited capacities, or may be masked by learned strategies in later life).

D. Symptoms cause clinically significant impairment in social, occupational, or other important areas of current functioning.

E. These disturbances are not better explained by intellectual disability (intellectual developmental disorder) or global developmental delay. Intellectual disability and autism spectrum disorder frequently co-occur; to make comorbid diagnoses of autism spectrum disorder and intellectual disability, social communication should be below that expected for general developmental level.

Note: Individuals with a well-established DSM-IV diagnosis of autistic disorder, Asperger's disorder, or pervasive developmental disorder not otherwise specified should be given the diagnosis of autism spectrum disorder. Individuals who have marked deficits in social communication, but whose symptoms do not otherwise meet criteria for autism spectrum disorder, should be evaluated for social (pragmatic) communication disorder.

Specify if:

With or without accompanying intellectual impairment.

With or without accompanying language impairment.

Associated with a known medical or genetic condition or environmental factor. (**Coding note:** Use additional code to identify the associated medical or genetic condition.)

Associated with another neurodevelopmental, mental, or behavioral disorder. (**Coding note:** Use additional code[s] to identify the associated neurodevelopmental, mental, or behavioral disorder[s].)

With catatonia (refer to the criteria for catatonia associated with another mental disorder, pp. 119-120, for definition). (**Coding note:** Use additional code 293.89 [F06.1] catatonia associated with autism spectrum disorder to indicate the presence of the comorbid catatonia.)

Table A Severity levels for autism spectrum disorder

	Social communication	Restricted, repetitive behaviors
Level 3 "Requiring very substantial support"	Severe deficits in verbal and nonverbal social communication skills cause severe impairments in functioning, very limited initiation of social interactions, and minimal response to social overtures from others. For example, a person with few words of intelligible speech who rarely initiates interaction and, when he or she does, makes unusual approaches to meet needs only and responds to only very direct social approaches	Inflexibility of behavior, extreme difficulty coping with change, or other restricted/repetitive behaviors markedly interfere with functioning in all spheres. Great distress/difficulty changing focus or action.
Level 2 "Requiring substantial support"	Marked deficits in verbal and nonverbal social communication skills; social impairments apparent even with supports in place; limited initiation of social interactions; and reduced or abnormal responses to social overtures from others. For example, a person who speaks simple sentences, whose interaction is limited to narrow special interests, and how has markedly odd nonverbal communication.	Inflexibility of behavior, difficulty coping with change, or other restricted/repetitive behaviors appear frequently enough to be obvious to the casual observer and interfere with functioning in a variety of contexts. Distress and/or difficulty changing focus or action.
Level 1 "Requiring support"	Without supports in place, deficits in social communication cause noticeable impairments. Difficulty initiating social interactions, and clear examples of	Inflexibility of behavior causes significant interference with functioning in one or more

	atypical or unsuccessful response to social overtures of others. May appear to have decreased interest in social interactions. For example, a person who is able to speak in full sentences and engages in communication but whose to- and-fro conversation with others fails, and whose attempts to make friends are odd and typically unsuccessful.	contexts. Difficulty switching between activities. Problems of organization and planning hamper independence

Recording procedures

For autism spectrum disorder that is associated with a known medical or genetic condition or environmental factor, or with another neurodevelopmental, mental, or behavioral disorder, record autism spectrum disorder associated with (name of condition, disorder, or factor) (e.g., autism spectrum disorder associated with Rett syndrome). Severity should be recorded as level of support needed for each of the two psychopathological domains in Table A (e.g., "requiring very substantial support for deficits in social communication and requiring substantial support for restricted, repetitive behaviors"). Specification of "with accompanying intellectual impairment" or "without accompanying intellectual impairment" should be recorded next. Language impairment specification should be recorded thereafter. If there is accompanying language impairment, the current level of verbal functioning should be recorded (e.g., "with accompanying language impairment no intelligible speech" or "with accompanying language impairment-phrase speech"). If catatonia is present, record separately "catatonia associated with autism spectrum disorder."

Specifiers

The severity specifiers (see Table A) may be used to describe succinctly the current symptomatology (which might fall below level 1), with the recognition that severity may vary by context and fluctuate over time. Severity of social communication difficulties and restricted, repetitive behaviors should be separately rated. The descriptive severity categories should not be used to determine eligibility for and provision of services; these can only be developed at an individual level and through discussion of personal priorities and targets. Regarding the specifier "with or without accompanying intellectual impairment," understanding the (often uneven) intellectual profile of a child or adult with autism spectrum disorder is necessary for interpreting diagnostic features. Separate estimates of verbal and nonverbal skills are necessary (e.g., using untimed nonverbal tests to assess potential strengths in individuals with limited language).

To use the specifier "with or without accompanying language impairment," the current level of verbal functioning should be assessed and described. Examples of the specific descriptions for "with accompanying language impairment" might include no intelligible speech (nonverbal), single words only, or phrase speech. Language level in individuals "without accompanying language impairment" might be further described by speaks in full sentences or has fluent speech. Since receptive language may lag behind expressive language development in autism spectrum disorder, receptive and expressive language skills should be considered separately.

The specifier "associated with a known medical or genetic condition or environmental factor" should be used when the individual has a known genetic disorder (e.g., Rett syndrome, Fragile X syndrome, Down syndrome), a medical disorder (e.g. epilepsy), or a history of environmental exposure (e.g., valproate, fetal alcohol syndrome, very low birth weight).

Additional neurodevelopmental, mental or behavioral conditions should also be noted (e.g., attentiondeficit/hyperactivity disorder; developmental coordination disorder; disruptive behavior, impulse-control, or conduct disorders; anxiety, depressive, or bipolar disorders; tics or Tourette's disorder; self-injury; feeding, elimination, or sleep disorders).

Diagnostic features

The essential features of autism spectrum disorder are persistent impairment in reciprocal social communication and social interaction (Criterion A), and restricted, repetitive patterns of behavior, interests, or activities (Criterion B). These symptoms are present from early childhood and limit or impair everyday functioning (Criteria C and D). The stage at which functional impairment becomes obvious will vary according to characteristics of the individual and his or her environment. Core diagnostic features are evident in the developmental period, but intervention, compensation, and current supports may mask difficulties in at least some contexts. Manifestations of the disorder also vary greatly depending on the severity of the autistic condition, developmental level, and chronological age; hence, the term *spectrum*. Autism spectrum disorder encompasses disorders previously referred to as early infantile autism, childhood autism, Kanner's autism, high-functioning autism, atypical autism, pervasive developmental disorder not otherwise specified, childhood disintegrative disorder, and Asperger's disorder.

The impairments in communication and social interaction specified in Criterion A are pervasive and sustained. Diagnoses are most valid and reliable when based on multiple sources of information, including clinician’s observations, caregiver history, and, when possible, self-report. Verbal and nonverbal deficits in social communication have varying manifestations, depending on the individual's age,

intellectual level, and language ability, as well as other factors such as treatment history and current support. Many individuals have language deficits, ranging from complete lack of speech through language delays, poor comprehension of speech, echoed speech, or stilted and overly literal language. Even when formal language skills (e.g., vocabulary, grammar) are intact, the use of language for reciprocal social communication is impaired in autism spectrum disorder.

Deficits in social-emotional reciprocity (i.e., the ability to engage with others and share thoughts and feelings) are clearly evident in young children with the disorder, who may show little or no initiation of social interaction and no sharing of emotions, along with reduced or absent imitation of others' behavior. What language exists is often one-sided, lacking in social reciprocity, and used to request or label rather than to comment, share feelings, or converse. In adults without intellectual disabilities or language delays, deficits in social-emotional reciprocity may be most apparent in difficulties processing and responding to complex social cues (e.g., when and how to join a conversation, what not to say). Adults who have developed compensation strategies for some social challenges still struggle in novel or unsupported situations and suffer from the effort and anxiety of consciously calculating what is socially intuitive for most individuals.

Deficits in nonverbal communicative behaviors used for social interaction are manifested by absent, reduced, or atypical use of eye contact (relative to cultural norms), gestures, facial expressions, body orientation, or speech intonation. An early feature of autism spectrum disorder is impaired joint attention as manifested by a lack of pointing, showing, or bringing objects to share interest with others, or failure to follow someone's pointing or eye gaze. Individuals may learn a few functional gestures, but their repertoire is smaller than that of others, and they often fail to use expressive gestures spontaneously in communication. Among adults with fluent language, the difficulty in coordinating nonverbal communication with speech may

give the impression of odd, wooden, or exaggerated "body language" during interactions. Impairment may be relatively subtle within individual modes (e.g., someone may have relatively good eye contact when speaking) but noticeable in poor integration of eye contact, gesture, body posture, prosody, and facial expression for social communication.

Deficits in developing, maintaining, and understanding relationships should be judged against norms for age, gender, and culture. There may be absent, reduced, or atypical social interest, manifested by rejection of others, passivity, or inappropriate approaches that seem aggressive or disruptive. These difficulties are particularly evident in young children, in whom there is often a lack of shared social play and imagination (e.g., age-appropriate flexible pretend play) and, later, insistence on playing by very fixed rules. Older individuals may struggle to understand what behavior is considered appropriate in one situation but not another (e.g., casual behavior during a job interview), or the different ways that language may be used to communicate (e.g., irony, white lies). There may be an apparent preference for solitary activities or for interacting with much younger or older people. Frequently, there is a desire to establish friendships without a complete or realistic idea of what friendship entails (e.g., one-sided friendships or friendships based solely on shared special interests). Relationships with siblings, co-workers, and caregivers are also important to consider (in terms of reciprocity).

Autism spectrum disorder is also defined by restricted, repetitive patterns of behavior, interests, or activities (as specified in Criterion B), which show a range of manifestations according to age and ability, intervention, and current supports. Stereotyped or repetitive behaviors include simple motor stereotypies (e.g., hand flapping, finger flicking), repetitive use of objects (e.g., spinning coins, lining up toys), and repetitive speech (e.g., echolalia, the delayed or immediate parroting of heard words; use of "you" when referring to self; stereotyped use of words, phrases,

or prosodic patterns). Excessive adherence to routines and restricted patterns of behavior may be manifest in resistance to change (e.g., distress at apparently small changes, such as in packaging of a favorite food; insistence on adherence to rules; rigidity of thinking) or ritualized patterns of verbal or nonverbal behavior (e.g., repetitive questioning, pacing a perimeter). Highly restricted, fixated interests in autism spectrum disorder tend to be abnormal in intensity or focus (e.g., a toddler strongly attached to a pan; a child preoccupied with vacuum cleaners; an adult spending hours writing out timetables). Some fascinations and routines may relate to apparent hyper- or hyporeactivity to sensory input, manifested through extreme responses to specific sounds or textures, excessive smelling or touching of objects, fascination with lights or spinning objects, and sometimes apparent indifference to pain, heat, or cold. Extreme reaction to or rituals involving taste, smelt texture, or appearance of food or excessive food restrictions are common and may be a presenting feature of autism spectrum disorder.

Many adults with autism spectrum disorder without intellectual or language disabilities learn to suppress repetitive behavior in public. Special interests may be a source of pleasure and motivation and provide avenues for education and employment later in life. Diagnostic criteria may be met when restricted, repetitive patterns of behavior, interests or activities were clearly present during childhood or at some time in the past, even if symptoms are no longer present.

Criterion D requires that the features must cause clinically significant impairment in social, occupational, or other important areas of current functioning. Criterion E specifies that the social communication deficits, although sometimes accompanied by intellectual disability (intellectual developmental disorder), are not in line with the individual's developmental level; impairments exceed difficulties expected on the basis of developmental level. Standardized behavioural diagnostic instruments with good psychometric properties, including caregiver interviews, questionnaires

and clinician observation measures, are available and can improve reliability of diagnosis over time and across clinicians.

Associated features supporting diagnosis

Many individuals with autism spectrum disorder also have intellectual impairment and/ or language impairment (e.g., slow to talk, language comprehension behind production). Even those with average or high intelligence have an uneven profile of abilities. The gap between intellectual and adaptive functional skills is often large. Motor deficits are often present, including odd gait, clumsiness, and other abnormal motor signs (e.g., walking on tiptoes). Self-injury (e.g., head banging, biting the wrist) may occur, and disruptive/challenging behaviors are more common in children and adolescents with autism spectrum disorder than other disorders, including intellectual disability. Adolescents and adults with autism spectrum disorder are prone to anxiety and depression. Some individuals develop catatonic-like motor behavior (slowing and "freezing" mid-action), but these are typically not of the magnitude of a catatonic episode. However, it is possible for individuals with autism spectrum disorder to experience a marked deterioration in motor symptoms and display a full catatonic episode with symptoms such as mutism, posturing, grimacing and waxy flexibility. The risk period for comorbid catatonia appears to be greatest in the adolescent years.

Prevalence

In recent years, reported frequencies for autism spectrum disorder across U.S. and non-U.S. countries have approached 1% of the population, with similar estimates in child and adult samples. It remains unclear whether higher rates reflect an expansion of the diagnostic criteria of DSM-IV to include subthreshold cases, increased awareness, differences in study methodology, or a true increase in the frequency of autism spectrum disorder.

Development and course

The age and pattern of onset also should be noted for autism spectrum disorder. Symptoms are typically recognized during the second year of life (12-24 months of age) but may be seen earlier than 12 months if developmental delays are severe, or noted later than 24 months if symptoms are more subtle. The pattern of onset description might include information about early developmental delays or any losses of social or language skills. In cases where skills have been lost, parents or caregivers may give a history of a gradual or relatively rapid deterioration in social behaviors or language skills. Typically, this would occur between 12 and 24 months of age and is distinguished from the rare instances of developmental regression occurring after at least 2 years of normal development (previously described as childhood disintegrative disorder).

The behavioral features of autism spectrum disorder first become evident in early childhood, with some cases presenting a lack of interest in social interaction in the first year of life. Some children with autism spectrum disorder experience developmental plateaus or regression, with a gradual or relatively rapid deterioration in social behaviors or use of language, often during the first 2 years of life. Such losses are rare in other disorders and may be a useful “red flag” for autism spectrum disorder. Much more unusual and warranting more extensive medical investigation are losses of skills beyond social communication (e.g., loss of self-care, toileting, motor skills) or those occurring after the second birthday (see also Rett syndrome in the section "Differential Diagnosis" for this disorder).

First symptoms of autism spectrum disorder frequently involve delayed language development, often accompanied by lack of social interest or unusual social interactions (e.g., pulling individuals by the hand without any attempt to look at them), odd play patterns (e.g., carrying toys around but never playing with them),

and unusual communication patterns (e.g., knowing the alphabet but not responding to own name). Deafness may be suspected but is typically ruled out. During the second year, odd and repetitive behaviors and the absence of typical play become more apparent. Since many typically developing young children have strong preferences and enjoy repetition (e.g., eating the same foods, watching the same video multiple times), distinguishing restricted and repetitive behaviors that are diagnostic of autism spectrum disorder can be difficult in preschoolers. The clinical distinction is based on the type, frequency, and intensity of the behaviour (e.g., a child who daily lines up objects for hours and is very distressed if any item is moved).

Autism spectrum disorder is not a degenerative disorder, and it is typical for learning and compensation to continue throughout life. Symptoms are often most marked in early childhood and early school years, with developmental gains typical in later childhood in at least some areas (e.g., increased interest in social interaction). A small proportion of individuals deteriorate behaviorally during adolescence, whereas most others improve. Only a minority of individuals with autism spectrum disorder live and work independently in adulthood; those who do tend to have superior language and intellectual abilities and are able to find a niche that matches their special interests and skills. In general, individuals with lower levels of impairment may be better able to function independently. However, even these individuals may remain socially naive and vulnerable, have difficulties organizing practical demands without aid, and are prone to anxiety and depression. Many adults report using compensation strategies and coping mechanisms to mask their difficulties in public but suffer from the stress and effort of maintaining a socially acceptable facade. Scarcely anything is known about old age in autism spectrum disorder.

Some individuals come for first diagnosis in adulthood, perhaps prompted by the diagnosis of autism in a child in the family or a breakdown of relations at work or home. Obtaining detailed developmental history in such cases may be difficult, and it is important to consider self-reported difficulties. Where clinical observation suggests criteria are currently met, autism spectrum disorder may be diagnosed, provided there is no evidence of good social and communication skills in childhood. For example, the report (by parents or another relative) that the individual had ordinary and sustained reciprocal friendships and good nonverbal communication skills throughout childhood would rule out a diagnosis of autism spectrum disorder; however, the absence of developmental information in itself should not do so.

Manifestations of the social and communication impairments and restricted/repetitive behaviors that define autism spectrum disorder are clear in the developmental period. In later life, intervention or compensation, as well as current supports, may mask these difficulties in at least some contexts. However, symptoms remain sufficient to cause current impairment in social, occupational, or other important areas of functioning.

Risk and prognostic factors

The best established prognostic factors for individual outcome within autism spectrum disorder are presence or absence of associated intellectual disability and language impairment (e.g., functional language by age 5 years is a good prognostic sign) and additional mental health problems. Epilepsy, as a comorbid diagnosis, is associated with greater intellectual disability and lower verbal ability.

Environmental. A variety of nonspecific risk factors, such as advanced parental age, birth weight, or fetal exposure to valproate, may contribute to risk of autism spectrum disorder.

Genetic and physiological. Heritability estimates for autism spectrum disorder have ranged from 37% to higher than 90%, based on twin concordance rates. Currently, as many as 15% of cases of autism spectrum disorder appear to be associated with a known genetic mutation, with different de novo copy number variants or de novo mutations in specific genes associated with the disorder in different families. However, even when an autism spectrum disorder is associated with a known genetic mutation, it does not appear to be fully penetrant. Risk for the remainder of cases appears to be polygenic, with perhaps hundreds of genetic loci making relatively small contributions.

Culture-related diagnostic issues

Cultural differences will exist in norms for social interaction, nonverbal communication, and relationships, but individuals with autism spectrum disorder are markedly impaired against the norms for their cultural context. Cultural and socioeconomic factors may affect age at recognition or diagnosis; for example, in the United States, late or underdiagnosis of autism spectrum disorder among African American children may occur.

Gender-related diagnostic issues

Autism spectrum disorder is diagnosed four times more often in males than in females. In clinic samples, females tend to be more likely to show accompanying intellectual disability, suggesting that girls without accompanying intellectual impairments or language delays may go unrecognized, perhaps because of subtler manifestation of social and communication difficulties.

Functional consequences of autism spectrum disorder

In young children with autism spectrum disorder, lack of social and communication abilities may hamper learning, especially learning through social interaction or in settings with peers. In the home, insistence on routines and aversion to change, as well as sensory sensitivities, may interfere with eating and sleeping and make routine care (e.g., haircuts, dental work) extremely difficult. Adaptive skills are typically below measured IQ. Extreme difficulties in planning, organization, and coping with change negatively impact academic achievement, even for students with above-average intelligence. During adulthood, these individuals may have difficulties establishing independence because of continued rigidity and difficulty with novelty.

Many individuals with autism spectrum disorder, even without intellectual disability, have poor adult psychosocial functioning as indexed by measures such as independent living and gainful employment. Functional consequences in old age are unknown, but social isolation and communication problems (e.g., reduced help-seeking) are likely to have consequences for health in older adulthood.

Differential diagnosis

Rett syndrome. Disruption of social interaction may be observed during the regressive phase of Rett syndrome (typically between 1-4 years of age); thus, a substantial proportion of affected young girls may have a presentation that meets diagnostic criteria for autism spectrum disorder. However, after this period, most individuals with Rett syndrome improve their social communication skills, and autistic features are no longer a major area of concern. Consequently, autism spectrum disorder should be considered only when all diagnostic criteria are met.

Selective mutism. In selective mutism, early development is not typically disturbed. The affected child usually exhibits appropriate communication skills in certain contexts and settings. Even in settings where the child is mute, social reciprocity is not impaired, nor are restricted or repetitive patterns of behavior present.

Language disorders and social (pragmatic) communication disorder. In some forms of language disorder, there may be problems of communication and some secondary social difficulties. However, specific language disorder is not usually associated with abnormal nonverbal communication, nor with the presence of restricted, repetitive patterns of behavior, interests, or activities.

When an individual shows impairment in social communication and social interactions but does not show restricted and repetitive behavior or interests, criteria for social (pragmatic) communication disorder, instead of autism spectrum disorder, may be met. The diagnosis of autism spectrum disorder supersedes that of social (pragmatic) communication disorder whenever the criteria for autism spectrum disorder are met, and care should be taken to enquire carefully regarding past or current restricted/ repetitive behavior.

Intellectual disability (intellectual developmental disorder) without autism spectrum disorder. Intellectual disability without autism spectrum disorder may be difficult to differentiate from autism spectrum disorder in very young children. Individuals with intellectual disability who have not developed language or symbolic skills also present a challenge for differential diagnosis, since repetitive behavior often occurs in such individuals as well. A diagnosis of autism spectrum disorder in an individual with intellectual disability is appropriate when social communication and interaction are significantly impaired relative to the developmental level of the individual's nonverbal skills (e.g., fine motor skills,

nonverbal problem solving). In contrast, intellectual disability is the appropriate diagnosis when there is no apparent discrepancy between the level of socialcommunicative skills and other intellectual skills.

Stereotypic movement disorder. Motor stereotypies are among the diagnostic characteristics of autism spectrum disorder, so an additional diagnosis of stereotypic movement disorder is not given when such repetitive behaviors are better explained by the presence of autism spectrum disorder. However, when stereotypies cause self-injury and become a focus of treatment, both diagnoses may be appropriate.

Attention-deficit/hyperactivity disorder. Abnormalities of attention (overly focused or easily distracted) are common in individuals with autism spectrum disorder, as is hyperactivity. A diagnosis of attention-deficit/hyperactivity disorder (ADHD) should be considered when attentional difficulties or hyperactivity exceeds that typically seen in individuals of comparable mental age.

Schizophrenia. Schizophrenia with childhood onset usually develops after a period of normal, or near normal, development. A prodromal state has been described in which social impairment and atypical interests and beliefs occur, which could be confused with the social deficits seen in autism spectrum disorder. Hallucinations and delusions, which are defining features of schizophrenia, are not features of autism spectrum disorder. However, clinicians must take into account the potential for individuals with autism spectrum disorder to be concrete in their interpretation of questions regarding the key features of schizophrenia (e.g., “Do you hear voices when no one is there?” “Yes [on the radio]”).

Comorbidity

Autism spectrum disorder is frequently associated with intellectual impairment and structural language disorder (i.e., an inability to comprehend and construct sentences with grammar), which should be noted under the relevant specifiers when applicable. Many individuals with autism spectrum disorder have psychiatric symptoms that do not form part of the diagnostic criteria for the disorder (about 70% of individuals with autism spectrum disorder may have one comorbid mental disorder, and 40% may have two or more mental disorders). When criteria for both ADHD and autism spectrum disorder are met, both diagnoses should be given. This same principle applies to concurrent diagnoses of autism spectrum disorder and developmental coordination disorder, anxiety disorders, depressive disorders, and other comorbid diagnoses. Among individuals who are nonverbal or have language deficits, observable signs such as changes in sleep or eating and increases in challenging behavior should trigger an evaluation for anxiety or depression. Specific learning difficulties (literacy and numeracy) are common, as is developmental coordination disorder. Medical conditions commonly associated with autism spectrum disorder should be noted under the "associated with a known medical/genetic or environmental/acquired condition" specifier. Such medical conditions include epilepsy, sleep problems, and constipation. Avoidant-restrictive food intake disorder is a fairly frequent presenting feature of autism spectrum disorder, and extreme and narrow food preferences may persist.

Appendix C: Publication Attributed to Thesis

NeuroImage: Clinical 3 (2013) 106–114

Contents lists available at ScienceDirect

NeuroImage: Clinical

journal homepage: www.elsevier.com/locate/ynicl

White matter microstructure correlates with autism trait severity in a combined clinical–control sample of high-functioning adults ☆

Clare R. Gibbard [a,*], Juejing Ren [b], Kiran K. Seunarine [a], Jonathan D. Clayden [a], David H. Skuse [b], Chris A. Clark [a]

[a] Imaging and Biophysics Unit, UCL Institute of Child Health, 30 Guilford Street, London WC1N 1EH, UK
[b] Behavioural and Brain Sciences Unit, UCL Institute of Child Health, 30 Guilford Street, London WC1N 1EH, UK

ARTICLE INFO

Article history:
Received 11 April 2013
Received in revised form 26 July 2013
Accepted 26 July 2013
Available online 2 August 2013

Keywords:
Autism spectrum disorder
Autism quotient
Diffusion tensor imaging
Tract-based spatial statistics
White matter

ABSTRACT

Diffusion tensor imaging (DTI) studies have demonstrated white matter (WM) abnormalities in tracts involved in emotion processing in autism spectrum disorder (ASD), but little is known regarding the nature and distribution of WM anomalies in relation to ASD trait severity in adults. Increasing evidence suggests that ASD occurs at the extreme of a distribution of social abilities. We aimed to examine WM microstructure as a potential marker for ASD symptom severity in a combined clinical–neurotypical population. SIENAX was used to estimate whole brain volume. Tract-based spatial statistics (TBSS) was used to provide a voxel-wise comparison of WM microstructure in 50 high-functioning young adults: 25 ASD and 25 neurotypical. The severity of ASD traits was measured by autism quotient (AQ); we examined regressions between DTI markers of WM microstructure and ASD trait severity. Cognitive abilities, measured by intelligence quotient, were well-matched between the groups and were controlled in all analyses. There were no significant group differences in whole brain volume. TBSS showed widespread regions of significantly reduced fractional anisotropy (FA) and increased mean diffusivity (MD) and radial diffusivity (RD) in ASD compared with controls. Linear regression analyses in the combined sample showed that average whole WM skeleton FA was negatively influenced by AQ ($p = 0.004$), whilst MD and RD were positively related to AQ ($p = 0.002$; $p = 0.001$). Regression slopes were similar within both groups and strongest for AQ social, communication and attention switching scores. In conclusion, similar regression characteristics were found between WM microstructure and ASD trait severity in a combined sample of ASD and neurotypical adults. WM anomalies were relatively more severe in the clinically diagnosed sample. Both findings suggest that there is a dimensional relationship between WM microstructure and severity of ASD traits from neurotypical subjects through to clinical ASD, with reduced coherence of WM associated with greater ASD symptoms. General cognitive abilities were independent of the relationship between WM indices and ASD traits.

1. Introduction

Autism spectrum disorder (ASD) is a neurodevelopmental condition characterised by impaired communication skills and poor social reciprocity in combination with repetitive and stereotypic behaviours (WHO, 1994). Recent estimates show that autism affects approximately 1 in 88 (Centers for Disease Control and Prevention, 2012). Symptoms are thought to arise from aberrant neurodevelopment in childhood. A recent report by Raznahan et al. (2013) has questioned the theory that this altered development is underpinned by early brain overgrowth, as previously found using magnetic resonance imaging (MRI) (Courchesne et al., 2001), suggesting that brain volume in ASD remains more similar to neurotypical controls than previously thought.

Consequently, ASD may be associated with subtle differences in brain structure, as opposed to abnormalities in overall volume. Social and communication functions, which are impaired in ASD, are mediated by specialised brain regions that are connected in complex networks, such as the limbic (Dalgleish, 2004) and mirror neuron systems (Rizzolatti et al., 2001). The limbic network is supported structurally by well-defined white matter (WM) tracts, including the cingulum, inferior longitudinal fasciculus (ILF) and arcuate fasciculus (Catani et al., 2002; Catani and Thiebaut de Schotten, 2008). The white matter connections underlying the mirror neuron system, which include the frontal motor areas, posterior parietal cortex and superior temporal sulcus (Rizzolatti and Craighero, 2004), are less-well defined. These are, however, likely to be connected by the cingulum and superior longitudinal fasciculus (SLF) (Catani et al., 2002; Catani and Thiebaut de Schotten, 2008).

Diffusion tensor imaging (DTI) provides information about WM microstructure using measures of water diffusion in tissue (Basser

* Corresponding author at: Imaging and Biophysics Unit, UCL Institute of Child Health, 30 Guilford Street, London WC1N 1EH, UK. Tel: +44 207 905 2192; fax: +44 207 905 2358.
E-mail address: c.gibbard@ucl.ac.uk (C.R. Gibbard).

2213-1582/$ – see front matter © 2013 The Authors. Published by Elsevier Inc. All rights reserved.
http://dx.doi.org/10.1016/j.nicl.2013.07.007

and Pierpaoli, 1996). DTI measures include: fractional anisotropy (FA), which represents the directional dependence of water diffusion (ranging from 0 to 1, with 0 representing no anisotropy, or isotropic diffusion, and 1 representing infinite anisotropy); mean diffusivity (MD), which measures the overall magnitude of diffusion; axial diffusivity (AD) which measures the magnitude of diffusion along the principal diffusion direction; and radial diffusivity (RD), which is the magnitude of diffusion perpendicular to the principal direction. Most previous DTI studies of ASD have been carried out in children and adolescents. The majority have reported decreases in FA and increases in MD compared to neurotypical controls (Barnea-Goraly et al., 2004; Groen et al., 2011; Pugliese et al., 2009; Shukla et al., 2011a). Such changes are indicative of aberrant WM and may represent irregular organisation of WM tracts, relatively low axon density and/or deficient axon myelination (Beaulieu, 2002).

Some DTI studies of ASD have been conducted with adults included in the cohort, but samples have often been heterogeneous in terms of age, which may confound their findings (Alexander et al., 2007; Keller et al., 2007; Kleinhans et al., 2012). Evidence shows that age and developmental stage contribute to DTI findings in ASD children and adolescents (Kleinhans et al., 2012). Further, DTI studies of WM maturation show that the majority of FA and MD changes occur prior to 30 years of age, though maturation trajectories differ in each white matter tract (Hasan et al., 2010; Lebel et al., 2012). Thus, heterogeneity in age may explain some apparently paradoxical reports that children with ASD have increased FA (Ben Bashat et al., 2007; Weinstein et al., 2011). The typical WM developmental process is non-linear (Yap et al., 2013) and is therefore difficult to control for by simply covarying age in a mixed adult–child sample. We considered a preferable approach to studying WM anomalies in ASD would be to select a sample of adults, rather than children, for this investigation.

Previous DTI investigations of samples containing ASD adults have usually employed voxel-based techniques, including statistical parametric mapping (SPM), or region of interest (ROI) techniques, such as deterministic tractography which follows pathways of maximal diffusion in order to trace WM tracts. One problem with techniques such as ROI-based deterministic tractography and other ROI methodologies is that their interpretation requires a prior hypothesis. Only those WM tracts pre-selected as regions of interest can be subjected to analysis, thus potential WM alterations in other tracts will not be measured. Previous voxel-based methodologies are limited by the partial volume effects of registration error and smoothing techniques (Jones et al., 2005; Smith et al., 2006). Findings in ASD adults using these techniques include reduced FA in the corpus callosum, which mediates cross-talk between the two cerebral hemispheres (Thakkar et al., 2008). Reduced corpus callosum FA was also reported in a combined sample of children and adults with ASD (Alexander et al., 2007). Reduced FA in adults with ASD has been further reported in the inferior fronto-occipital fasciculus (IFOF), uncinate fasciculus (UF) (Pugliese et al., 2009) and cerebellar WM tracts (Catani et al., 2008). Increased MD, another marker of altered WM microstructure, has been measured in the ILF and cingulum (Pugliese et al., 2009). Co-localised reductions in FA and increases in RD have been reported in frontal, medial, temporal and parietal brain regions (Bloemen et al., 2010). Alterations in the number of streamlines obtained using tractography have been reported in the ILF, IFOF, UF and corpus callosum (Thomas et al., 2010).

In contrast to the limitations of ROI and previous voxel-based techniques, there are advantages to employing tract-based spatial statistics (TBSS) (Smith et al., 2006) which is an automated method that enables voxel-wise comparison of WM parameters, including FA and MD. Like other voxel-based techniques, TBSS removes the requirement for prior determination of tracts of interest, but TBSS additionally moderates registration errors and reduces partial volume effects. It achieves this by aligning the FA data from each subject to a common space before extracting a WM skeleton comprising the core of the WM voxels, thus excluding the more variable voxels at the extremities of the WM (Smith et al., 2006; Smith et al., 2007). TBSS has been applied to DTI scans of ASD children and adolescents, and WM tract alterations have been reported compared to controls (Ameis et al., 2011; Barnea-Goraly et al., 2010; Bode et al., 2011; Cheng et al., 2010; Jou et al., 2011; Kumar et al., 2010; Noriuchi et al., 2010; Sahyoun et al., 2010; Shukla et al., 2011a; Shukla et al., 2011b; Weinstein et al., 2011). Recently, Kleinhans et al. (2012) applied TBSS to a combined adolescent–adult cohort, with findings showing widespread reductions in FA and increases in MD and RD. TBSS has not, to the best of our knowledge, yet been used to study brain structure in a purely adult cohort of ASD.

ASD clinical characteristics are often considered to be on a continuum with social and communication skills found in the general population (Baron-Cohen et al., 2001; Constantino and Todd, 2003; Robinson et al., 2011). Some evidence suggests that the severity of ASD traits correlates with WM microstructure in clinical populations. For example, a negative correlation has been shown between FA in the cingulum and restricted and repetitive behaviours (Autism Diagnostic Interview – Revised (ADI-R)) in adults with ASD (Thakkar et al., 2008). Catani et al. (2008) reported a negative correlation between ADI-R social score and FA of the left cerebellar peduncle in adults with Asperger syndrome. On the other hand, some studies have not found significant correlations between WM characteristics and measures of ASD severity in clinically defined groups (Barnea-Goraly et al., 2010; Kleinhans et al., 2012; Shukla et al., 2010). Others have investigated whether the presence of ASD traits in non-clinical populations is correlated with WM microstructure characteristics. Kumar et al. (2010) reported a positive correlation between ASD traits and tract volume of the left UF in neurotypical subjects. Iidaka et al. (2012) identified a positive correlation between ASD traits and the volume of WM tracts connecting the superior temporal sulcus and the amygdala in healthy individuals. Both studies suggest that larger WM tract volume is associated with more severe ASD-like symptoms in neurotypical subjects. Alexander et al. (2007) reported a negative correlation between abnormalities in corpus callosum FA and social responsiveness scale (SRS) scores in a heterogeneous sample of neurotypical and ASD children and adults. These findings indicate that the relationship between WM microstructure and ASD symptoms could extend beyond the clinical syndrome into the neurotypical population, but to date studies have either only investigated ASD and neurotypical subjects separately or have been confounded by the inclusion of both child and adult subjects.

Intelligence quotient (IQ) has been shown to correlate with WM microstructure (Alexander et al., 2007) and is likely to influence, or be influenced by, DTI parameters. We therefore selected high-functioning individuals in order to minimise this confound. This enabled us to investigate any ASD-specific effects whilst minimising any potential confound of low general cognitive ability.

To our knowledge no previous investigation has examined a high functioning adult cohort of clinical and non-clinical subjects in the type of analyses we present.

2. Material and methods

2.1. Participants

Twenty-six high-functioning young adults with ASD and 25 age-matched neurotypical controls were recruited locally. None of the subjects had a history of neuropsychiatric disorders including anxiety, attention deficit hyperactivity disorder, depression and epilepsy. All MRI scans were visually inspected for neurological abnormalities, with no irregularities observed. The study was approved by the local Ethics committee and each participant gave written informed consent. Full-scale, verbal and performance IQ were measured using the four-scale Wechsler Abbreviated Scale of Intelligence (WASI) (Wechsler, 1999). All subjects had an IQ >80. The autism quotient (AQ) self-report questionnaire was administered to all subjects.

The Autism Diagnostic Observation Schedule (ADOS) (Lord et al., 1989) semi-structured interview was conducted with the ASD subjects to confirm their diagnosis. One subject was subsequently excluded from the study as their diagnosis could not be re-confirmed, leaving a total of 25 in the ASD group. Two-tailed t-tests were used to compare demographic measures between groups.

2.2. Data acquisition and pre-processing

Whole-brain MRI was carried out on a 1.5 T Siemens Magnetom Avanto scanner (Siemens, Erlangen, Germany) with 40 mT/m gradients and a 12-channel receive head coil. A T_1-weighted three-dimensional fast low angle shot sequence was acquired with flip angle = 15°; TR = 11 ms; TE = 4.94 ms; voxel size = 1 mm isotropic; and slices = 176. The DTI protocol consisted of a twice-refocused spin echo diffusion-weighted echo planar imaging sequence with 60 unique gradient directions (b = 1000 s/mm^2). Three images without diffusion weighting (b = 0) were interleaved. The parameters were: TR = 7300 ms; TE = 81 ms; voxel size = 2.5 mm isotropic; and 60 axial slices. The protocol also included resting-state and task-based functional MRI (fMRI), and the results of which will be reported elsewhere. The total imaging protocol took 42 min.

All scans were visually inspected for abnormalities, motion and other artefacts. Plots of estimated head motion during the diffusion-weighted scan were visually inspected and rotation was found to be minimal. There was no appreciable evidence that motion or other artefacts varied between groups. The DTI data were pre-processed using TractoR version 2.1 (Clayden et al., 2011) and FMRIB Software Library (FSL) version 4.1 (Smith et al., 2004). Briefly, within a given subject, a reference b = 0 volume was brain-extracted (Smith, 2002) and the diffusion-weighted volumes were registered to this reference to correct for eddy current distortions. A diffusion tensor was derived at each voxel using a standard least-squares process to provide a voxel-wise calculation of FA, MD, RD and AD.

2.3. Whole brain volume measurements

Whole brain, total grey matter (GM) and total WM volumes, both raw and normalised for intracranial volume, were calculated on the T_1-weighted scans using the FSL tool SIENAX (Smith et al., 2001; Smith et al., 2002). Briefly, SIENAX brain extracts the images, affine-registers them to MNI152 space and then uses partial volume estimation to segment tissue types. The skull is used for normalisation. Group comparisons of normalised volumes were calculated using linear regression with age, gender and full-scale IQ as covariates.

2.4. Voxel-wise analysis of diffusion tensor imaging data

TBSS was carried out using FSL 4.1. All participants' FA data were projected onto a mean FA image using the non-linear registration tool FNIRT to register to the FMRIB58_FA template. The registered data was thinned to create a mean FA skeleton restricted to voxels with the highest FA at the centre of the major WM tracts. Following visual assessment of the optimal threshold value, the skeleton was thresholded at the recommended level of FA = 0.2 in order to remove confounding low-FA voxels, which may be caused by partial volume effects of GM or cerebrospinal fluid. Each participant's aligned FA data were projected onto the skeleton and voxel-wise cross-participant statistics was applied using non-parametric permutation testing within TBSS. Results were corrected for multiple comparisons using family wise error (FWE) and thresholded using threshold-free cluster enhancement (TFCE), as per the standard TBSS protocol. Only clusters surviving FWE $p < 0.05$ are reported. The locations of significant clusters were determined using the FSL atlas tools . This process was repeated for MD, RD and AD. TBSS fill was used for visualisation.

FSL tools were used to ascertain those WM regions that were most significantly different between the ASD and neurotypical groups. This was achieved by overlaying a skeleton of the John's Hopkins University (JHU) ICBM-DTI-81 atlas on the TBSS results. As delineated by the atlas, the number of voxels in particular WM tracts that had a significant group difference in FA and MD was recorded. To control for tract size, this was normalised as a percentage of the total number of voxels within the skeleton of the WM tract. Any WM regions in the skeleton which fell outside of the atlas were recorded as 'unclassified WM'.

2.5. Whole white matter skeleton analysis of diffusion tensor imaging data

The values for each DTI metric were averaged across the whole WM skeleton for each participant. Group comparisons of mean WM skeleton FA, MD, RD and AD were made using linear regression.

2.6. Relationship between structural measures and clinical scores

Linear regression was used to investigate the relationship between the DTI parameters averaged across the whole WM skeleton and AQ. AQ measures the extent of autistic traits in both neurotypical controls and individuals with ASD in social, communication, attention switching, attention to detail and imagination domains. This makes the AQ an ideal tool for assessing ASD-like symptoms in the whole study population. Regressions were carried out in a combined sample of all subjects in order to investigate whether any relationship between ASD traits and WM microstructure applied across the entire study population.

We carried out further analyses in order to confirm that the ASD and control group did not differ substantially in terms of their relationships with AQ, and hence that the study of the entire population as one continuum was reasonable. This was done through a standard statistical model comparison for each diffusion measure, where one model treats the data set as a whole (as was carried out previously), whilst the other includes separate AQ slope and intercept terms for each group. The latter model was fully flexible, allowing for any combination of relationships between diffusion parameters and AQ in the two groups. In addition, we plotted the regression slopes from each fit for comparison.

Linear regression was used to investigate the relationship between the whole WM skeleton diffusion parameters and each sub-domain of the AQ score across all participants. Multiple comparisons correction was applied to control the false discovery rate (FDR), and only p values <0.05 after correction were considered significant.

In order to visualise which WM voxels were contributing to these results, the relationships between DTI measures and AQ were estimated in each voxel across all subjects using TBSS. Only clusters surviving FWE $p < 0.05$ are reported.

2.7. Covariates

All DTI-based statistics included age, gender, full-scale IQ and unnormalised whole brain volume as covariates. These parameters were selected as covariates because they have previously been shown to influence DTI parameters (Alexander et al., 2007; Clayden et al., 2012; Kanaan et al., 2012; Menzler et al., 2011) and could thus confound findings.

3. Results

3.1. Demographics

Table 1 summarises participant demographics. Analysis with two-tailed t-tests showed no significant group differences in age, verbal IQ, performance IQ or full-scale IQ. AQ was significantly higher in the ASD group, with an overlap in scores between the groups.

Table 1
Participant demographics and cognitive test scores.

	Control (n = 25)[a]	ASD (n = 25)[a]	t-statistic	p value
Gender	20M:5F	21M:4F	–	–
Handedness	25R:0L	23R:2L	–	–
Age (years)	24.50 (4.02) [18.83–33.30]	23.22 (4.05) [18.31–31.90]	1.12	0.27
Full-scale IQ	122.08 (8.02) [94–138]	119.40 (11.59) [105–136]	0.95	0.35
Verbal IQ	120.44 (8.43) [106–136]	116.84 (12.56) [84–135]	1.19	0.24
Performance IQ	118.40 (7.01) [103–129]	117.36 (11.04) [88–135]	0.40	0.69
AQ	13.60 (7.86) [4–37]	36.60 (6.53) [22–49]	−11.23	<0.0001
ADOS[b]	–	9.22 (4.11) [3–20]	–	–

[a] Data are expressed as mean (SD) [range].
[b] Combined social and communication sub-scores.

Linear regression analysis controlling for age, gender and full-scale IQ showed no significant group differences in whole brain volume ($t = -0.69$; $p = 0.49$), total GM volume ($t = -0.80$; $p = 0.43$) or total WM volume ($t = -0.36$; $p = 0.72$).

3.2. Whole white matter skeleton diffusion measurements

FA values averaged across the whole WM skeleton in each subject were significantly lower in the ASD group compared to controls ($t = -3.54$; $p = 0.001$), whilst MD ($t = 2.78$; $p = 0.008$) and RD ($t = 3.32$; $p = 0.002$) were significantly elevated in the ASD group. There were no significant group differences in AD ($t = 0.98$; $p = 0.33$).

3.3. Voxel-wise diffusion measurements

The voxel-wise group comparison between ASD and controls showed widespread clusters of significantly reduced FA in the ASD group ($p < 0.05$; FWE-corrected) (see Fig. 1A). This included WM tracts bilaterally in the frontal, temporal, parietal and occipital lobes, in addition to the corpus callosum. The same group-wise comparison for MD showed similarly widespread increases of MD in the ASD group compared to controls (Fig. 1B). This was comparable to those seen in the FA comparison, though the fornix did not contain any significant clusters and affected voxels were more widespread in the temporal lobe and the right cingulum. Widespread significant increases in RD in the ASD group compared to controls were observed in a very similar pattern (Fig. 1C). No significant group differences in AD were detected.

Table 2 shows the 20 WM tracts, as outlined by the JHU-ICBM-DTI-81 atlas, which had the highest percentage of voxels showing significantly reduced FA and elevated MD in the ASD group in comparison to neurotypical controls. WM tracts key for long-range pathways in the brain, such as the corona radiata, SLF, and the corpus callosum, showed large areas with significant group differences in WM microstructure. Tracts involved in social processing, such as the fornix, ILF and IFOF, also presented with large proportions of affected WM microstructure in ASD. In WM not encompassed by the atlas, 29.69% had significantly reduced FA in ASD compared to neurotypical controls, whilst 30.27% showed significantly elevated MD.

3.4. Relationship between structural measures and clinical scores

In the entire study population, whilst controlling for age, gender, full-scale IQ and whole brain volume, FA averaged over the whole WM skeleton was negatively influenced by AQ ($t = -3.04$; $p = 0.004$). Highly significant positive relationships were observed between MD and AQ ($t = 3.24$; $p = 0.002$) and RD and AQ ($t = 3.42$; $p = 0.001$). A weaker positive influence was seen by AQ on AD ($t = 1.52$; $p = 0.14$). See Fig. 2 for plots of the regressions. One control participant had an outlying high AQ score. Results found when excluding this high outlier remained very similar to those found whilst including them.

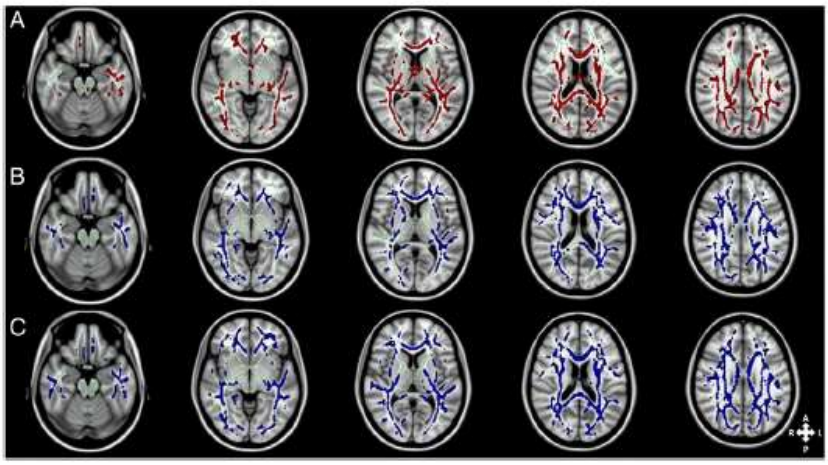

Fig. 1. Axial slices of the cohort's mean white matter skeleton (green) overlaid with (A) red clusters depicting white matter voxels with significantly lower fractional anisotropy (FA) in subjects with autism spectrum disorder (ASD) compared to healthy controls ($p < 0.05$; FWE-corrected). Tracts in all major lobes of the cerebrum (frontal, parietal, occipital and temporal lobes) and the corpus callosum connecting the two brain hemispheres are affected. (B and C) Blue clusters showing regions with significantly higher mean diffusivity (MD) (B) and radial diffusivity (RD) (C) in ASD compared to controls ($p < 0.05$; FWE-corrected). Similarly to the FA results, the clusters are widespread throughout the cerebrum. There were no significant differences in axial diffusivity (AD) between the two groups. TBSS fill was used for visualisation.

Table 2
The 20 WM tracts in the skeletonised JHU-ICBM-DTI-81 atlas which had the greatest proportion of voxels showing significantly reduced FA and significantly elevated MD in ASD compared to neurotypical controls.

WM tract	Proportion of voxels with significantly ($p < .05$) reduced FA in ASD (%)	WM tract	Proportion of voxels with significantly ($p < .05$) elevated MD in ASD (%)
L[a] Tapetum	100.00	CC – genu	80.25
R[a] Tapetum	100.00	L SFOF	79.49
L SFOF[a]	89.74	L Sagittal stratum[b]	77.55
R Retrolenticular IC[a]	80.84	R Sagittal stratum	75.17
R Superior CR[a]	79.97	L SLF	71.20
R PTR[a]	79.59	R Posterior CR	64.64
CC[a] – genu	76.99	L PTR	63.59
Fornix – column and body	76.61	L Retrolenticular IC	62.26
L Fornix stria terminalis	72.78	R Anterior CR	60.86
L PTR	72.39	L Anterior CR	60.04
L UF	68.85	R PTR	58.20
CC – splenium	68.40	R Retrolenticular IC	56.47
R Posterior CR	67.86	R SLF	55.59
R SLF[a]	67.02	L Superior CR	54.12
L Superior CR	62.21	R Superior CR	53.89
CC – body	58.62	L Posterior CR	51.20
R SFOF	58.57	L External capsule	47.19
L Posterior CR	57.28	L Fornix – stria terminalis	46.84
L SLF	56.90	CC – body	42.64
L Retrolenticular IC	56.29	R External capsule	40.58

[a] Abbreviations: CC (corpus callosum); CR (corona radiata); IC (internal capsule); L (left); PTR (posterior thalamic radiation); R (right); SFOF (superior fronto-occipital fasciculus); SLF (superior longitudinal fasciculus); UF (uncinate fasciculus).
[b] Sagittal stratum includes the inferior longitudinal fasciculus (ILF) and inferior fronto-occipital fasciculus (IFOF).

Results from the model comparison showed no significant improvement in explained variance observed when using a regression model allowing for any combination of different relationships between diffusion parameters and AQ in the two groups, as opposed to the regression model using the entire study sample (F statistics: FA = 2.74, MD = 0.44, RD = 0.77, AD = 1.07; all $p > 0.24$). Thus, the added complexity of the full model is not required to describe the data, and one fit line is sufficient to encapsulate all of the data. Plots of the regression slopes from these combined sample relationships are shown alongside regression slopes from within-group regressions in Fig. 3. The slopes of the regressions look similar, which once again indicates that the AQ–WM relationships are consistent across the spectrum from neurotypical controls through to autism. Some of the confidence intervals overlap zero. This may be because variance was higher in the individual groups, particularly the ASD group, as would be expected.

Voxel-wise analysis of relationships between the diffusion measures and AQ, controlling for age, gender, full-scale IQ and whole brain volume, indicated widespread clusters throughout the WM of the left hemisphere and bilaterally in the occipital lobe in which MD was positively influenced by AQ ($p < 0.05$; FWE-corrected) (Fig. 4A). There was a significant positive relationship between RD and AQ in a limited number of voxels from the SLF in the left hemisphere only (see Fig. 4B). There were no significant voxel-wise relationships between AQ and either FA or AD.

Linear regressions between sub-divisions of the AQ score and diffusion measures averaged across the whole WM skeleton, controlling for age, gender, full-scale IQ and whole brain volume, are summarised in Table 3. There were significant negative relationships between FA and the AQ social and communication and attention switching domains. MD and RD showed highly significant positive relationships with the AQ social, communication, attention switching and imagination domains. The only significant relationship for AD was with the imagination domain.

4. Discussion

Our study is the first to investigate the dimensional relationship between WM microstructure and ASD traits in an adult cohort of combined clinical and non-clinical cases. We found that WM characteristics, as evidenced by reduced FA and increased MD and RD, correlate with ASD symptom severity in the combined sample. Regressions between WM measures and ASD traits within each group were very similar in strength to the corresponding regression for all subjects. These results support the concept of a dimensional relationship between WM microstructure and ASD symptomatology in young adults. Group comparisons further support this finding, with more widespread WM disruption found in subjects diagnosed with clinical ASD in comparison to controls.

ASD, particularly in highly-functioning individuals, is often considered to be at the extreme of a continuum of social and communication skills (Baron-Cohen et al., 2001; Constantino and Todd, 2003; Robinson et al., 2011). Our findings provide support for the hypothesis that dimensionality of ASD traits, including social–communication ability and attention switching, is closely related to WM microstructure. The results we show across the whole WM skeleton are compatible with Alexander et al. (2007) who indicated that there was a dimensional relationship between corpus callosum microstructure and ASD traits in a combined clinical–control sample of adolescents and adults. Our finding is also consistent with previous studies which have reported correlations between ASD traits and WM tract volume in neurotypical young adults (Iidaka et al., 2012; Kumar et al., 2010). Further, our results are consistent with reports of correlations between ASD severity and greater WM disruption within adult ASD groups alone (Catani et al., 2008; Thakkar et al., 2008; Thomas et al., 2010). Our study investigated the relationship between WM microstructure and ASD traits more comprehensively across the entire WM skeleton in a combined clinical and non-clinical sample, and is thus able to show the extent of this relationship more clearly.

Reductions in FA and increases in MD are thought to reflect reduced organisation of the WM, reduced axonal density, and/or reduced myelination (Basser and Pierpaoli, 1996; Beaulieu, 2002), although the precise biology underpinning particular FA and MD values cannot be determined due to restrictions in the resolution of DTI. Elevated RD represents increased water diffusion perpendicular to axon bundles, which may reflect reduced axon density, increased axon diameter, increased membrane permeability (Takahashi et al., 2002) and/or reduced myelination (Song et al., 2002). Our results indicate that it is these types of WM characteristics which relate to ASD traits. Upon investigation of the specificities of each WM metric's relationship with ASD traits, we found that the relationship between FA and ASD traits was strongest for social, communication and attention switching domains and weakest for imagination and attention to detail. This supports the concept of distributed WM connectivity particularly influencing cognitive flexibility, social and communication ASD behaviours. MD and RD also showed strong associations with the core social and communication features of ASD as well as with attention switching and imagination. Interestingly, MD had a stronger relationship with imagination than with social ability. This is in contrast to FA and RD which were more strongly related to social skills. In summary, we found that MD is more strongly associated with a wider complement of ASD traits than FA, which is more closely linked to attention switching and the core social–communication ASD behaviours. A similar dissociation was also observed by Catani et al. (2008).

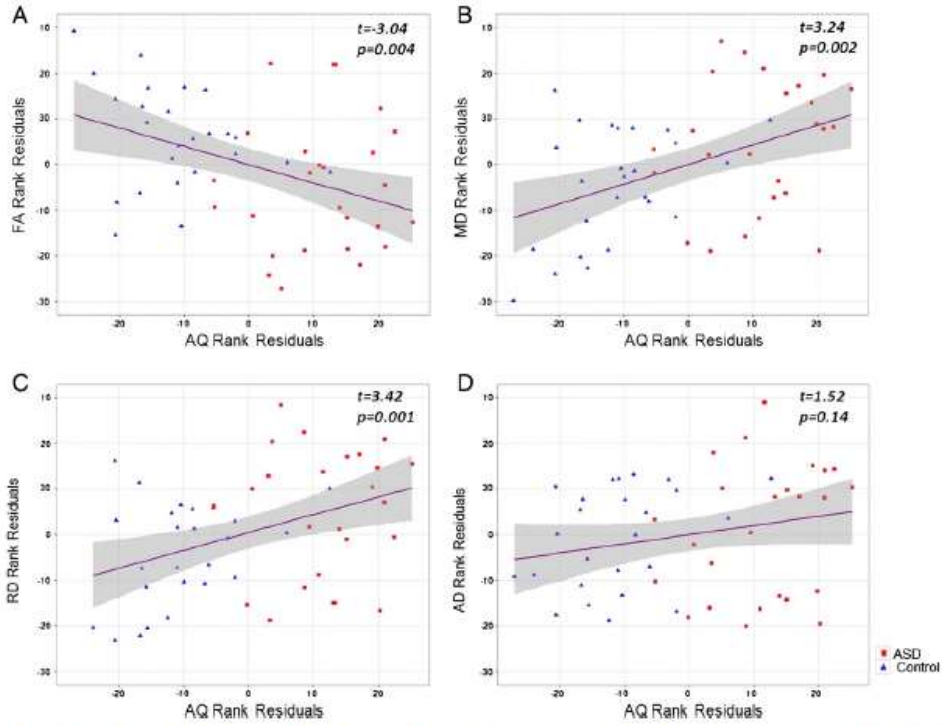

Fig. 2. Scatter plots showing results of linear regression controlling for age, gender, full-scale intelligence quotient (IQ) and whole brain volume. Red squares denote participants diagnosed with an autism spectrum disorder (ASD); blue triangles represent neurotypical controls. Grey shading shows the standard error of the fit. (A) A significant negative relationship between autism quotient (AQ) and fractional anisotropy (FA) ($t = -3.04$; $p = 0.004$) in addition to significant positive relationships for AQ with (B) mean diffusivity (MD) ($t = 3.24$; $p = 0.002$) and (C) radial diffusivity (RD) ($t = 3.42$; $p = 0.001$). (D) There was a weak positive influence of AQ on axial diffusivity (AD) ($t = 1.52$; $p = 0.14$).

Group comparisons using TBSS showed that WM characteristics were significantly altered in ASD compared to neurotypical controls. Specifically, we found significantly decreased FA in the ASD group, alongside increased MD and RD. We did not detect a significant difference in AD between the two groups. These results are compatible with Kleinhans et al.'s (2012) recent report of widespread WM anomalies in a heterogeneous cohort of adolescents and adults with ASD using TBSS. The results of the group comparison indicate that clinically-significant ASD is associated with a greater degree of WM abnormalities than is found in neurotypical controls. Coupled with the findings of the relationship with AQ, a spectrum of WM changes, with ASD at one extreme of a distribution, is supported. Maintenance of AD coupled with an increase in RD could signify reduced axon myelination (Song et al., 2002) or increased membrane permeability (Takahashi et al., 2002). These observations are suggestive of involvement of processes responsible for the myelination and preservation of axons in development of ASD, though elucidation of this is outside the remit of DTI.

Our finding of widespread WM aberrations in ASD adults are also consistent with the results of previous voxel-based and tractography studies in adults showing ASD-related WM anomalies in the temporal lobe and cortico-thalamic tracts (Lee et al., 2007); limbic tracts, such as the cingulum, fornix and UF (Pugliese et al., 2009); the arcuate fasciculus (Nagae et al., 2012); tracts of the mirror neuron system, such as the arcuate fasciculus and IFOF (Pugliese et al., 2009); and in the corpus callosum which connects the two cerebral hemispheres (Alexander et al., 2007; Thakkar et al., 2008; Thomas et al., 2010). Our analysis was not limited to prior regions of interest and so we were able to demonstrate the more widespread nature of WM anomalies in a group of ASD adults. We investigated the relative contributions of particular WM tracts to the group difference in WM microstructure. The results showed that tracts which link widespread regions of the brain were affected in ASD. These included the superior fronto-occipital fasciculus, corpus callosum, internal capsule and corona radiata. Tracts associated with social processing were also majorly affected, including the fornix and uncinate fasciculus, by changes in FA, and the ILF, IFOF, and to a lesser extent, the fornix, by changes in MD. However, we did not find that limbic tracts were singularly affected to a degree which would have been expected from previous ROI-based studies. This indicates that the structural deficits associated with ASD are more wide-reaching than previously reported, and appear to be related to ASD traits, such as imagination, repetitive behaviours and flexibility, which are likely to require the recruitment of several brain regions.

Despite the widespread nature of these WM changes our participants had relatively high IQs. The group comparisons and regressions between ASD traits and WM microstructure were independent of IQ, which was well matched between groups and controlled for in all statistical tests. The relationship between WM microstructure and severity of social and communication impairments is thus independent of general cognition. This implies that we are observing a relationship between WM microstructure and cognitive faculties that are specifically

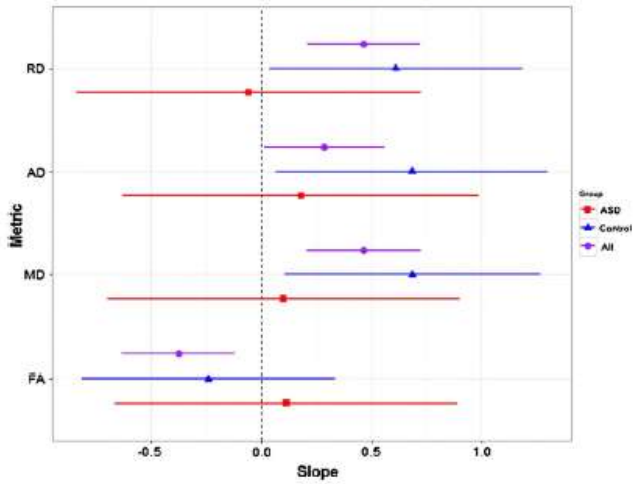

Fig. 3. Plots of the regression slopes between the DTI metrics and AQ across all participants (purple circle), and within ASD (red square) and neurotypical control (blue triangle) groups separately. All regressions controlled for age, gender, full-scale intelligence quotient (IQ) and whole brain volume. Points represent the value of the regression slope; lines show the 95% confidence interval of the fit. The plots show greater variance in the separate groups, particularly the ASD group. Slopes were similar for regression in the combined sample in comparison to regressions in the separate groups, particularly for MD and AD. Slopes for FA and RD were more different, but model comparison showed no significant difference in the fits (all $p > 0.24$).

linked to ASD behaviours, such as social cognition, as opposed to general cognitive ability. The finding of a close relationship between WM microstructure and social cognition independently from general cognition is consistent with evidence that corpus callosum agenesis is associated with increased incidence of ASD traits, but no significant difference in IQ scores (Lau et al., 2012). Evidence suggests that social and communication processing involve co-ordinated activation of a network of brain areas in both hemispheres (Dalgleish, 2004; Rizzolatti et al., 2001). This need for recruitment of widely dispersed brain regions during social processing means that WM abnormalities are particularly likely to exert a negative impact on effective communication between them. Kanwisher (2010) reviews evidence suggesting that several social functions, including face recognition and thinking about another person's thoughts, are localised to functionally specialised brain regions, each of which will need to communicate via WM tracts. Additional recent evidence indicates that intelligent cognition may occur via multiple networks (Hampshire et al., 2012), suggesting that some elements of duplication may provide a 'back-up' for functions tested by conventional measures of general intelligence.

We did not find a significant difference in whole brain volume, total GM volume or total WM volume between the groups. This is consistent with previous reports that brain volumes of adults with ASD are similar to those of neurotypical controls (Aylward et al., 2002; Courchesne et al., 2001; Raznahan et al., 2013), implying that alterations in the structural wiring of the brain underpin ASD symptomatology to a greater extent than brain volume itself.

Limitations of the study include the following issues: First, at present only post-mortem studies could confirm the exact nature of the WM changes we report, since DTI resolution is too low to allow evaluation of single axons. Second, the values of WM indices in our participants

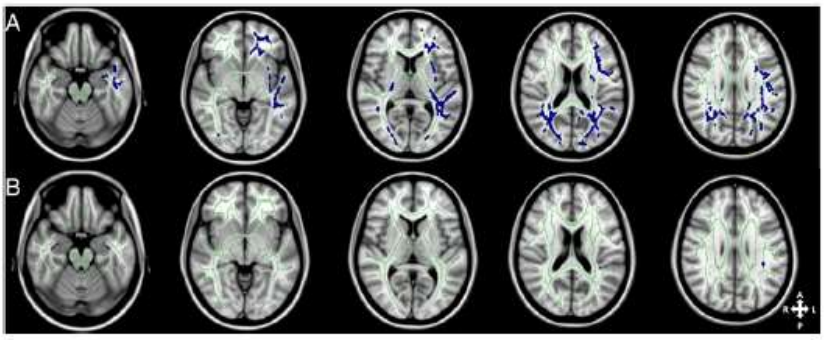

Fig. 4. Axial slices of the group white matter skeleton (green) overlaid with blue clusters showing white matter voxels in which autism quotient (AQ) is positively related ($p < 0.05$; FWE-corrected) with (A) mean diffusivity (MD) widespread through the left hemisphere and bilaterally in the occipital lobe and (B) with radial diffusivity (RD) in voxels of the left hemisphere forming part of the left superior longitudinal fasciculus (SLF). There were no significant relationships between AQ and fractional anisotropy (FA) or axial diffusivity (AD).

Table 3
Results of linear regressions across both groups between AQ sub-scores and DTI parameters averaged throughout the white matter skeleton.

AQ domain	DTI metric	Est	p value[a]
Social	FA	−0.38	**0.008**
	MD	0.38	**0.01**
	RD	0.41	**0.005**
	AD	0.13	0.34
Communication	FA	−0.44	**<0.001**
	MD	0.39	**0.006**
	RD	0.43	**0.003**
	AD	0.13	0.35
Attention switching	FA	−0.51	**<0.001**
	MD	0.40	**0.006**
	RD	0.47	**0.001**
	AD	0.06	0.66
Imagination	FA	−0.28	0.06
	MD	0.40	**0.006**
	RD	0.38	**0.009**
	AD	0.28	0.04
Attention to detail	FA	−0.24	0.11
	MD	0.31	0.04
	RD	0.29	0.06
	AD	0.22	0.12

[a] p values were adjusted for multiple comparisons using false discovery rate correction. Those p values remaining significant ($p < 0.05$) after correction are displayed in bold text.

are highly variable in both groups. Some of the within-group AQ–WM relationships had an estimated slope in the opposite direction compared to the analysis within the entire study sample. Although this was minor and we found no significant difference in the slopes, this finding highlights the variability in the relationship between WM microstructure and ASD symptom severity. Further studies on larger cohorts would be helpful to confirm the findings. Further, variability does currently limit the usefulness of DTI measures as biomarkers of change at an individual level. Third, we recognise that the AQ is not a 'gold standard' of ASD traits: it is a self-report measure, which may influence its validity. Finally, it would be valuable to conduct a further study that combines DTI with fMRI, which would enable analysis of the relationship between WM microstructure, brain activity, and the strength of ASD traits in a mixed neurotypical and clinical sample.

5. Conclusions

In conclusion, our findings indicate that the strength of ASD traits is related to WM microstructure in both neurotypical and clinically identified participants, but that WM anomalies are more severe in those diagnosed with ASD. Our findings are consistent with recent evidence from studies of separate neurotypical and ASD groups that the dimensional characteristics of the ASD phenotype reflect a distributed variability of WM microstructure affecting tracts involved in social and communication processing in addition to attention switching. IQ was maintained in these individuals, thus our findings imply that a dissociation exists between WM features linked to IQ-related abilities and WM characteristics associated with ASD traits.

Financial disclosures

CAC wishes to acknowledge European Union Grant FP7-2009-C 238292. CRG is funded by a UCL Grand Challenge studentship. JR is funded by an Erasmus Mundus Chinese Collaborative PhD studentship. The authors have no conflicts of interest.

Acknowledgements

We thank all participants who took part in the study as well as Tina Banks and Charlotte Sanderson for assistance in acquiring the data. We would also like to thank Martin King for helpful statistical discussions.

References

Alexander, A.L., Lee, J.E., Lazar, M., Boudos, R., DuBray, M.B., Oakes, T.R., Miller, J.N., Lu, J., Jeong, E.-K., McMahon, W.M., Bigler, E.D., Lainhart, J.E., 2007. Diffusion tensor imaging of the corpus callosum in autism. NeuroImage 34 (1), 61–73.
Ameis, S.H., Fan, J., Rockel, C., Voineskos, A.N., Lobaugh, N.J., Soorya, L., Wang, A.T., Hollander, E., Anagnostou, E., 2011. Impaired structural connectivity of socio-emotional circuits in autism spectrum disorders: a diffusion tensor imaging study. PLoS One 6 (11), e28044.
Aylward, E.H., Minshew, N.J., Field, K., Sparks, B.F., Singh, N., 2002. Effects of age on brain volume and head circumference in autism. Neurology 59 (2), 175–183.
Barnea-Goraly, N., Kwon, H., Menon, V., Eliez, S., Lotspeich, L., Reiss, A., 2004. White matter structure in autism: preliminary evidence from diffusion tensor imaging. Biological Psychiatry 55 (3), 323–326.
Barnea-Goraly, N., Lotspeich, L., Reiss, A., 2010. Similar white matter aberrations in children with autism and their unaffected siblings: a diffusion tensor imaging study using tract-based spatial statistics. Archives of General Psychiatry 67 (10), 1052–1060.
Baron-Cohen, S., Wheelwright, S., Skinner, R., Martin, J., Clubley, E., 2001. The autism-spectrum quotient (AQ): evidence from Asperger syndrome/high-functioning autism, males and females, scientists and mathematicians. Journal of Autism and Developmental Disorders 31 (1), 5–17.
Basser, P.J., Pierpaoli, C., 1996. Microstructural and physiological features of tissues elucidated by quantitative-diffusion-tensor MRI. Journal of Magnetic Resonance 213 (2), 560–570.
Beaulieu, C., 2002. The basis of anisotropic water diffusion in the nervous system — a technical review. NMR in Biomedicine 15 (7–8), 435–455.
Ben Bashat, D., Kronfeld-Duenias, V., Zachor, D.A., Ekstein, P.M., Hendler, T., Tarrasch, R., Even, A., Levy, Y., Ben Sira, L., 2007. Accelerated maturation of white matter in young children with autism: a high b value DWI study. NeuroImage 37 (1), 40–47.
Bloemen, O.J.N., Deeley, Q., Sundram, F., Daly, E.M., Barker, G.J., Jones, D.K., van Amelsvoort, T.A.M.J., Schmitz, N., Robertson, D., Murphy, K.C., Murphy, D.G.M., 2010. White matter integrity in Asperger syndrome: a preliminary diffusion tensor magnetic resonance imaging study in adults. Autism Research 3 (5), 203–213.
Bode, M.K., Mattila, M., Kiviniemi, V., Rahko, J., Moilanen, I., Ebeling, H., Tervonen, O., Nikkinen, J., 2011. White matter in autism spectrum disorders — evidence of impaired fiber formation. Acta Radiologica 52, 1169–1174.
Catani, M., Thiebaut de Schotten, M., 2008. A diffusion tensor imaging tractography atlas for virtual in vivo dissections. Cortex; a journal devoted to the study of the nervous system and behavior 44 (8), 1105–1132.
Catani, M., Howard, R.J., Pajevic, S., Jones, D.K., 2002. Virtual in vivo interactive dissection of white matter fasciculi in the human brain. NeuroImage 17 (1), 77–94.
Catani, M., Jones, D.K., Daly, E., Embiricos, N., Deeley, Q., Pugliese, L., Curran, S., Robertson, D., Murphy, D.G.M., 2008. Altered cerebellar feedback projections in Asperger syndrome. NeuroImage 41 (4), 1184–1191.
Centers for Disease Control and Prevention, 2012. Prevalence of autism spectrum disorders — Autism and Developmental Disabilities Monitoring Network, 14 sites, United States, 2008. Morbidity and Mortality Weekly Report. Surveillance Summaries 61 (3), 1–19.
Cheng, Y., Chou, K., Chen, I., Fan, Y., Decety, J., Lin, C., 2010. Atypical development of white matter microstructure in adolescents with autism spectrum disorders. NeuroImage 50 (3), 873–882.
Clayden, J.D., Muñoz Maniega, S., Storkey, A.J., King, M.D., Bastin, M.E., Clark, C.A., 2011. TractoR: magnetic resonance imaging and tractography with R. Journal of Statistical Software 44 (8).
Clayden, J.D., Jentschke, S., Muñoz, M., Cooper, J.M., Chadwick, M.J., Banks, T., Clark, C.A., Vargha-Khadem, F., 2012. Normative development of white matter tracts: similarities and differences in relation to age, gender, and intelligence. Cerebral Cortex 22 (8), 1738–1747.
Constantino, J.N., Todd, R.D., 2003. Autistic traits in the general population — a twin study. Archives of General Psychiatry 60, 524–530.
Courchesne, E., Karns, C.M., Davis, H.R., Ziccardi, R., Carper, R.A., Tigue, Z.D., Chisum, H.J., Moses, P., Pierce, K., Lord, C., Lincoln, A.J., Pizzo, S., Schreibman, L., Haas, R.H., Akshoomoff, N.A., Courchesne, R.Y., 2001. Unusual brain growth patterns in early life in patients with autistic disorder: an MRI study. Neurology 57 (2), 245–254.
Dalgleish, T., 2004. The emotional brain. Nature Reviews Neuroscience 5 (7), 583–589.
Groen, W.B., Buitelaar, J.K., van der Gaag, R.J., Zwiers, M.P., 2011. Pervasive microstructural abnormalities in autism: a DTI study. Journal of Psychiatry & Neuroscience 36 (1), 32–40.
Hampshire, A., Highfield, R.R., Parkin, B.L., Owen, A.M., 2012. Fractionating human intelligence. Neuron 76 (6), 1225–1237.
Hasan, K.M., Kamali, A., Abid, H., Kramer, L.A., Fletcher, J.M., Ewing-Cobbs, L., 2010. Quantification of the spatiotemporal microstructural organization of the human brain association, projection and commissural pathways across the lifespan using diffusion tensor tractography. Brain Structure & Function 214 (4), 361–373.
Iidaka, T., Miyakoshi, M., Harada, T., Nakai, T., 2012. White matter connectivity between superior temporal sulcus and amygdala is associated with autistic trait in healthy humans. Neuroscience Letters 510 (2), 154–158.

Jones, D.K., Symms, M.R., Cercignani, M., Howard, R.J., 2005. The effect of filter size on VBM analyses of DT-MRI data. NeuroImage 26 (2), 546–554.
Jou, R.J., Mateljevic, N., Kaiser, M.D., Sugrue, D.R., Volkmar, F.R., Pelphrey, K.A., 2011. Structural neural phenotype of autism: preliminary evidence from a diffusion tensor imaging study using tract-based spatial statistics. American Journal of Neuroradiology 32 (9), 1607–1613.
Kanaan, R.A., Allin, M., Picchioni, M., Barker, G.J., Daly, E., Shergill, S.S., Woolley, J., McGuire, P.K., 2012. Gender differences in white matter microstructure. PLoS One 7 (6), e38272.
Kanwisher, N., 2010. Functional specificity in the human brain: a window into the functional architecture of the mind. Proceedings of the National Academy of Sciences of the United States of America 107 (25), 11163–11170.
Keller, T.A., Kana, R.K., Just, M.A., 2007. A developmental study of the structural integrity of white matter in autism. NeuroReport 18 (1), 23–27.
Kleinhans, N.M., Pauley, G., Richards, T., Neuhaus, E., Martin, N., Corrigan, N.M., Shaw, D.W., Estes, A., Dager, S.R., 2012. Age-related abnormalities in white matter microstructure in autism spectrum disorders. Brain Research 1479, 1–16.
Kumar, A., Sundaram, S.K., Sivaswamy, L., Behen, M.E., Makki, M.I., Ager, J., Janisse, J., Chugani, H.T., Chugani, D.C., 2010. Alterations in frontal lobe tracts and corpus callosum in young children with autism spectrum disorder. Cerebral Cortex 20 (9), 2103–2113.
Lau, Y.C., Hinkley, L.B.N., Bukshpun, P., Strominger, Z.A., Wakahiro, M.L.J., Baron-Cohen, S., Allison, C., Auyeung, B., Jeremy, R.J., Nagarajan, S.S., Sherr, E.H., Marco, E.J., 2012. Autism traits in individuals with agenesis of the corpus callosum. Journal of Autism and Developmental Disorders 43 (5), 1106–1118.
Lebel, C., Gee, M., Camicioli, R., Wieler, M., Martin, W., Beaulieu, C., 2012. Diffusion tensor imaging of white matter tract evolution over the lifespan. NeuroImage 60 (1), 340–352.
Lee, J.E., Bigler, E.D., Alexander, A.L., Lazar, M., DuBray, M.B., Chung, M.K., Johnson, M., Morgan, J., Miller, J.N., McMahon, W.M., Lu, J., Jeong, E.-K., Lainhart, J.E., 2007. Diffusion tensor imaging of white matter in the superior temporal gyrus and temporal stem in autism. Neuroscience Letters 424 (2), 127–132.
Lord, C., Rutter, M., Goode, S., Heemsbergen, J., Jordan, H., Mawhood, L., Schopler, E., 1989. Autism diagnostic observation schedule: a standardized observation of communicative and social behavior. Journal of Autism and Developmental Disorders 19 (2), 185–212.
Menzler, K., Belke, M., Wehrmann, E., Krakow, K., Lengler, U., Jansen, A., Hamer, H.M., Oertel, W.H., Rosenow, F., Knake, S., 2011. Men and women are different: diffusion tensor imaging reveals sexual dimorphism in the microstructure of the thalamus, corpus callosum and cingulum. NeuroImage 54 (4), 2557–2562.
Nagae, L.M., Zarnow, D.M., Blaskey, L., Dell, J., Khan, S.Y., Qasmieh, S., Levy, S.E., Roberts, T.P.L., 2012. Elevated mean diffusivity in the left hemisphere superior longitudinal fasciculus in autism spectrum disorders increases with more profound language impairment. American Journal of Neuroradiology 1–6.
Noriuchi, M., Kikuchi, Y., Yoshiura, T., Kira, R., Shigeto, H., Hara, T., Tobimatsu, S., Kamio, Y., 2010. Altered white matter fractional anisotropy and social impairment in children with autism spectrum disorder. Brain Research 1362, 141–149.
Pugliese, L., Catani, M., Ameis, S., Dell'Acqua, F., Thiebaut de Schotten, M., Murphy, C., Robertson, D., Deeley, Q., Daly, E., Murphy, D.G.M., 2009. The anatomy of extended limbic pathways in Asperger syndrome: a preliminary diffusion tensor imaging tractography study. NeuroImage 47 (2), 427–434.
Raznahan, A., Wallace, G.L., Antezana, L., Greenstein, D., Lenroot, R., Thurm, A., Gozzi, M., Spence, S., Martin, A., Swedo, S.E., Giedd, J.N., 2013. Compared to what? Early brain overgrowth in autism and the perils of population norms. Biological Psychiatry 1–13.
Rizzolatti, G., Craighero, L., 2004. The mirror–neuron system. Annual Review of Neuroscience 27, 169–192.
Rizzolatti, G., Fogassi, L., Gallese, V., 2001. Neurophysiological mechanisms underlying the understanding and imitation of action. Nature Reviews Neuroscience 2, 661–670.
Robinson, E.B., Munir, K., Munafò, M.R., Hughes, M., McCormick, M.C., Koenen, K.C., 2011. Stability of autistic traits in the general population: further evidence for a continuum of impairment. Journal of the American Academy of Child and Adolescent Psychiatry 50 (4), 376–384.
Sahyoun, C.P., Belliveau, J.W., Mody, M., 2010. White matter integrity and pictorial reasoning in high-functioning children with autism. Brain and Cognition 73 (3), 180–188.
Shukla, D.K., Keehn, B., Lincoln, A.J., Müller, R.-A., 2010. White matter compromise of callosal and subcortical fiber tracts in children with autism spectrum disorder: a diffusion tensor imaging study. Journal of the American Academy of Child and Adolescent Psychiatry 49 (12), 1269–1278 (1278.e1–2).
Shukla, D.K., Keehn, B., Müller, R.-A., 2011a. Tract-specific analyses of diffusion tensor imaging show widespread white matter compromise in autism spectrum disorder. Journal of Child Psychology and Psychiatry 52 (3), 286–295.
Shukla, D.K., Keehn, B., Smylie, D.M., Müller, R.-A., 2011b. Microstructural abnormalities of short-distance white matter tracts in autism spectrum disorder. Neuropsychologia 49 (5), 1378–1382.
Smith, S., 2002. Fast robust automated brain extraction. Human Brain Mapping 17 (3), 143–155.
Smith, S.M., De Stefano, N., Jenkinson, M., Matthews, P.M., 2001. Normalized accurate measurement of longitudinal brain change. Journal of Computer Assisted Tomography 25 (3), 466–475.
Smith, S., Zhang, Y., Jenkinson, M., Chen, J., Matthews, P., Federico, A., De Stefano, N., 2002. Accurate, robust, and automated longitudinal and cross-sectional brain change analysis. NeuroImage 17 (1), 479–489.
Smith, S., Jenkinson, M., Woolrich, M., Beckmann, C., Behrens, T., Johansen-Berg, H., Bannister, P., De Luca, M., Drobnjak, I., Flitney, D., Niazy, R., Saunders, J., Vickers, J., Zhang, Y., De Stefano, N., Brady, J., Matthews, P., 2004. Advances in functional and structural MR image analysis and implementation as FSL. NeuroImage 23 (Suppl. 1), S208–S219.
Smith, S., Jenkinson, M., Johansen-Berg, H., Rueckert, D., Nichols, T., Mackay, C., Watkins, K., Ciccarelli, O., Cader, M., Matthews, P., Behrens, T., 2006. Tract-based spatial statistics: voxelwise analysis of multi-subject diffusion data. NeuroImage 31 (4), 1487–1505.
Smith, S., Johansen-Berg, H., Jenkinson, M., Rueckert, D., Nichols, T., Miller, K., Robson, M., Jones, D., Klein, J., Bartsch, A., Behrens, T., 2007. Acquisition and voxelwise analysis of multi-subject diffusion data with tract-based spatial statistics. Nature Protocols 2 (3), 499–503.
Song, S.-K., Sun, S.-W., Ramsbottom, M.J., Chang, C., Russell, J., Cross, A.H., 2002. Dysmyelination revealed through MRI as increased radial (but unchanged axial) diffusion of water. NeuroImage 17 (3), 1429–1436.
Takahashi, M., Hackney, D.B., Zhang, G., Wehrli, S.L., Wright, A.C., O'Brien, W.T., Uematsu, H., Wehrli, F.W., Selzer, M.E., 2002. Magnetic resonance microimaging of intraaxonal water diffusion in live excised lamprey spinal cord. Proceedings of the National Academy of Sciences of the United States of America 99 (25), 16192–16196.
Thakkar, K.N., Polli, F.E., Joseph, R.M., Tuch, D.S., Hadjikhani, N., Barton, J.J.S., Manoach, D.S., 2008. Response monitoring, repetitive behaviour and anterior cingulate abnormalities in autism spectrum disorders (ASD). Brain 131 (Pt. 9), 2464–2478.
Thomas, C., Humphreys, K., Jung, K.-J., Minshew, N., Behrmann, M., 2010. The anatomy of the callosal and visual-association pathways in high-functioning autism: a DTI tractography study. Cortex 47 (7), 863–873.
Wechsler, D., 1999. Wechsler Abbreviated Scale of Intelligence (WASI) Manual. The Psychological Corporation, San Antonio, TX.
Weinstein, M., Ben-Sira, L., Levy, Y., Zachor, D.A., Ben Itzhak, E., Artzi, M., Tarrasch, R., Eksteine, P.M., Hendler, T., Ben Bashat, D., 2011. Abnormal white matter integrity in young children with autism. Human Brain Mapping 32 (4), 534–543.
WHO, 1994. International Classification of Diseases, 10th ed. World Health Organization, Geneva.
Yap, Q.J., Teh, I., Fusar-Poli, P., Sum, M.Y., Kuswanto, C., Sim, K., 2013. Tracking cerebral white matter changes across the lifespan: insights from diffusion tensor imaging studies. Journal of Neural Transmission. (Epub ahead of print).

Appendix D: Presentations Attributed to this Thesis

Oral Presentations

C.R. Gibbard, J. Ren, D.H. Skuse, J.D. Clayden & C.A. Clark *'Altered amygdala nuclei projections in young adults with autism spectrum disorder'* International Meeting for Autism Research, May 2014, Atlanta, USA.

R.J. Jou, C.R. Gibbard, C. Pretzsch, D. Yang, I.Y. Murphy & K.A. Pelphrey *'White Matter Microstructure in Girls With Autism Spectrum Disorder: Comparison With Neurotypical Controls and Unaffected Siblings'* International Meeting for Autism Research, May 2014, Atlanta, USA.

C.R. Gibbard, J. Ren, D.H. Skuse, J.D. Clayden & C.A. Clark *'Altered amygdala nuclei projections in young adults with autism spectrum disorder'* International School of Clinical Neuroanatomy, May 2013, Bibione, Italy.

C.R. Gibbard, J. Ren, K.K. Seunarine, J.D. Clayden, D.H. Skuse & C.A. Clark *'Widespread white matter abnormalities in high-functioning adults with autism spectrum disorder correlate with symptom severity'* Annual Meeting of the British Chapter of the International Society of Magnetic Resonance Imaging in Medicine, September 2012, Cambridge, UK.

Poster Presentations

C.R. Gibbard, J. Ren, D.H. Skuse, J.D. Clayden & C.A. Clark *'Altered amygdala connectivity in young adults with autism spectrum disorder'* Annual Meeting of the British Chapter of the International Society of Magnetic Resonance Imaging in Medicine, September 2014, Edinburgh, UK.

C.R. Gibbard, J. Ren, D.H. Skuse, J.D. Clayden & C.A. Clark *'Altered amygdala nuclei projections in young adults with autism spectrum disorder'* Annual Meeting of the Organization for Human Brain Mapping, June 2013, Seattle, USA.

C.R. Gibbard, J. Ren, K.K. Seunarine, J.D. Clayden, D.H. Skuse & C.A. Clark *'White matter connectivity predicts autism spectrum disorder symptom severity in high-functioning young adults'*, Implications of Affect, Attachment and Social Cognition Meeting, May 2013, London, UK.

C.R. Gibbard, J. Ren, K.K. Seunarine, J.D. Clayden, D.H. Skuse & C.A. Clark *'White matter connectivity predicts autism spectrum disorder severity in high-functioning young adults'*, International Meeting for Autism Research, May 2013, San Sebastian, Spain.